Formulation Strategies and Engineering Processes for Orally Disintegrating Tablets – The Importance of Robustness and Disintegration

Jasdip Singh Koner

Doctor of Philosophy

Aston University

June 2017

Aston University

Formulation Strategies and Engineering Processes for Orally Disintegrating Tablets – The Importance of Robustness and Disintegration

Jasdip Singh Koner

Doctor of Philosophy

2017

Thesis Summary

Orally disintegrating tablets (ODTs) are a dosage form ideal for paediatric or geriatric patients as they disintegrate/disperse within the oral cavity. Direct compression manufacture of ODTs is increasing in popularity due to its cost effectiveness and use of traditional tableting equipment, however excipients are required to fulfil certain requirements to form robust, fast disintegrating tablets. Mannitol is a vital excipient for ODT manufacture due to its high palatability, however its fragmentation behaviour under compression leads to mechanically weak and friable tablets. The work in this thesis aimed to investigate the fragmentation behaviour of milled mannitol, followed by development of preblends to obtain ideal ODT properties without the use of any superdisintegrant. Development of a novel method for ODT disintegration testing was also conducted due to the lack of current techniques that are representative of oral conditions.

Mannitol fracture occurred primarily at the (011) crystal plane, which was the most hydrophilic, therefore increasing the wettability of milled mannitol. Resulting ODTs had a faster disintegration time than the unmilled equivalent, with enhancement in compressibility due to increased plastic deformation. Milled mannitol presented a suitable alternative for ODT production compared to current commercial grades, with high mechanical strength and improved disintegration time. Novel optimised ODT preblends were developed with milled mannitol incorporated alongside micro crystalline cellulose (MCC) and silica to aid powder flow.

Dry particle coating was also employed to develop an MCC/silica hybrid to enhance MCC properties. Silicified MCC had previously been shown to enhance MCC compression, whilst improving MCC powder flow and reducing lubricant sensitivity. Dry coated MCC was optimised with 1%w/w silica, with ODT disintegration being significantly lower than the spray dried alternative or uncoated MCC, whilst allowing a 40% drug load of a non-compressible API to be formed into a robust fast disintegrating ODT.

A novel ODT disintegration method was developed to mimic *In Vivo* oral conditions. A vastly improved correlation to *In Vivo* results was observed with the newly developed method, in comparison to the recommended USP tester, with a linear correlation obtained with the new test method compared to the curved dataset gathered with the USP test.

Novel preblends were developed utilising dry particle coating, with resultant ODTs showing improved ODT behaviour, with disintegration time being low even without the use of superdisintegrant. To supplement ODT disintegration, novel ODT disintegration time test method was developed and results indicated it was a superior alternative compared to the currently recommend USP test.

Acknowledgements

I would like to commence by thanking my supervisor Professor Afzal Mohammed for giving me the opportunity to undertake this PhD under his guidance. His support, advice and enthusiasm has been invaluable in allowing me to complete the project. His confidence and belief in my ability has allowed me to develop and grow as a researcher, whilst his passion for pharmaceutical research has helped drive my hunger in developing and growing new ideas. I will always be eternally grateful for his supervision. I would also like to thank my associate supervisors Dr Daniel Kirby and Professor Yvonne Perrie for their contribution towards my project. I would also like to extend my gratitude to Colorcon Inc., in particular Dr Ali Rajabi-Siahboomi and Dr Sharhzad Missaghi, and the Aston Research Centre for Children and Healthy Young People (ARCHY) for their financial support throughout the project.

I would like to thank the technical team members at Aston University, in particular Jiteen Ahmed and Christine Jakeman for their irreplaceable expertise and assistance throughout. I am also grateful to Dr James Bowen, from Open University for his help and expertise when performing the AFM and DVS analysis. I would also like express my gratitude to my colleagues in our research group, in particular; Tom Dennison, Eman Dahmash, Hamad Alyami, Habtom Ftuwi, Annsar Warraich, Abdul El-Ershad, Affiong Iyire and Ali Al-Khattawi.

I would like to dedicate this thesis to my mother, Sue Koner, and brother, Harry Koner for their unbelievable support throughout the last 3 years and for my whole life. I would not have been able to proceed with this PhD without their faith in me. I would like to especially thank my mom for everything she has done for me, I could not describe how grateful I am for all you have done throughout my life, and I would not be where I am today without you, I am truly blessed to have you as my parent.

Lastly I would like to dedicate this thesis to my partner (soon to be wife!) Bhavisha Patel. Your support and guidance over the past few years has been incredible. Your patience and understanding with me, particularly in the last few months has been amazing, when times were difficult I always had you to put a smile on my face and I am incredibly lucky to have you.

List of Contents

List of Abbreviations

AFM – Atomic Force Microscopy

ANOVA – Analysis of Variance

API – Active Pharmaceutical Ingredient

BET – Brunauer-Emmet-Teller

BP – British Pharmacopeia

BPR – Ball to Powder Weight Ratio

BR – Bounding Rectangular

DSC – Differential Scanning Calorimetry

FDA – Food and Drug Administration

ICH – International Conference on Harmonisation

MCC – Microcrystalline Cellulose

ODF – Orally Disintegrating Film

ODT – Orally disintegrating tablet

Ph.Eur – European Pharmacopeia

P_y – Yield pressure

rpm – Revolutions per Minute

SD – Standard Deviation

SEM – Scanning Electron Microscopy

SMCC – Silicified Microcrystalline Cellulose

TGA – Thermogravimetric Analysis

USP – United States Pharmacopeia

VMD – Volume Mean Diameter

WHO – World Health Organisation

XRD – X-ray Diffraction

List of Tables

List of Figures

Publication List

Peer Reviewed Articles:

Koner, J. S., Rajabi-Siahboomi, A., Bowen, J., Perrie, Y., Kirby, D. & Mohammed, A. R. (2015). A Holistic Multi Evidence Approach to Study the Fragmentation Behaviour of Crystalline Mannitol. *Sci Rep,* 5**,** 16352.

Al-Khattawi, A., Koner, J., Rue, P., Kirby, D., Perrie, Y., Rajabi-Siahboomi, A. & Mohammed, A. R. (2015). A pragmatic approach for engineering porous mannitol and mechanistic evaluation of particle performance. *European Journal of Pharmaceutics and Biopharmaceutics,* 94**,** 1-10.

Alyami, H., Koner, J., Dahmash, E. Z., Bowen, J., Terry, D. & Mohammed, A. R. (2016). Microparticle surface layering through dry coating: impact of moisture content and process parameters on the properties of orally disintegrating tablets. *J Pharm Pharmacol*, 69, 807-822.

Conference Proceedings:

Koner, J., Rajabi-Siahboomi, A., Perrie, Y., Kirby, D., Mohammed, A. R. A Systematic Investigation of Surface Properties and Compression Profiles of Milled D-Mannitol. UKPharmSci, Hertfordshire, September 2014.

Koner, J., Perrie, Y., Kirby, D., Rajabi-Siahboomi, A., Bowen, J., Mohammed, A. R. A Systematic Multi Evidence Investigation to Study the Fragmentation Behaviour and Compression Profiles of Milled D-Mannitol. CRS Edinburgh, July 2015.

Koner, J., Perrie, Y., Kirby, D., Rajabi-Siahboomi, A., Bowen, J., Mohammed, A. R. A Holistic Multi Evidence Approach to Study the Fragmentation Behaviour of Crystalline Mannitol. AAPS Denver, November 2016.

Chapter 1

Introduction and Literature Review

1.1 Paediatric Drug Delivery

Over the last decade, paediatric drug delivery has come to the forefront of pharmaceutical formulation due to the financial rewards and patent extensions offered to big Pharma from the regulatory bodies in the US and within the EU (Turner *et al*., 2014). The companies had previously focussed on making 'lower risk, higher reward' solid oral dosage forms targeted at adult populations, due to the increased financial reward and the development of fixed dose dosage forms required for a typical adult patient. This resulted in few paediatric friendly dosage forms being available, with liquids being the primary treatment option, and many treatments plans, especially in primary care, consisting of unlicensed and off label use of adult medicines for a paediatric patient (Ivanovska *et al*., 2014). Due to the clinical and safety issues arising from the limited research into drug treatment for paediatric patients, legislation was drawn up in the US and the EU, led by the World Health Organisation (WHO), which stated a need for more paediatric drug research, offering financial incentives and patent extensions (EU, 2006, FDA, 2007).

The paediatric age range varies significantly up to adulthood, with the first 18 years of life subdivided into different categories starting from Premature new-borns (<38 weeks gestational age); Term new-borns (>38 weeks gestational age); Neonate (0-30 days); Infant (1 month-2 years); Young child (2-6 years); Child (6-12 years) up to Adolescents (12-18years) (Kellie and Howard, 2008). Due to the rapid rate of development within paediatric patients, variations in pharmacokinetics and pharmacodynamics present a multitude of challenges, leading to different dosing requirements for different ages, as well as a preference for certain dosage forms, depending both on the patients capability to take the medicine, as well as their liking of the dosage form (EMA, 2006). Medication adherence is governed by the acceptability of the dosage form by the patient with taste, colour, shape and size of dosage form being very important (Alyami *et al*., 2016a). Liquid dosage forms were, and still are, the most common dosage form for paediatric patients, due to their ease of administration and ability to adjust doses according to the age of the patient (Nunn and Williams, 2005). However, due to the newer legislation and the subsequent increase in research into paediatric

pharmaceutics/formulation, the availability of newer, more suitable and advantageous dosage forms has also risen.

1.2 Types of Paediatric Dosage Form

The type of dosage form that a paediatric patient is capable of taking varies throughout the age range as the patient ages from 0-18 years. Thus there are a wide range of dosage forms used in paediatric drug delivery, and each of them have their own advantages and disadvantages. The key to paediatric drug development in the current climate is the manufacture of age appropriate formulations for paediatrics; as the child grows their needs and capabilities develop and thus the production of age appropriate formulations is vital for therapeutic effect and patient adherence to their medication regime (Lopez *et al*., 2015).

1.2.1 Liquid Oral Dosage Forms

Liquid dosage forms are currently the most popular type of dosage form utilised in paediatrics due to their favourable opinion amongst healthcare professionals and patients themselves, with liquids being acceptable from birth, throughout the whole paediatric age range and into adulthood (van Riet-Nales *et al*., 2013). Liquid formulations include solutions, suspensions, syrups and drops (Ivanovska *et al*., 2014). The key advantage to liquid dosage forms is that they can be easily administered to paediatric patients from birth, with good dose flexibility that is near to the required therapeutic amount, through either oral syringes or measuring spoons. The most common paediatric medicines are formulated as liquids for this precise reason, with paracetamol, ibuprofen and a wide range of antibiotics readily available as liquids (Ivanovska *et al*., 2014). However there are numerous disadvantages to liquid preparations which has resulted in current formulation efforts going towards developing more suitable dosage forms. Liquids have various stability issues related to highly moisture sensitive drugs, which often leads to formulations with short expiry dates and those that need to be reconstituted upon dispensing, this is especially evident for antibiotic formulations. Transportation of liquids can also be problematic as they come in bulky containers, and storage conditions often require liquids to

be refrigerated (Lopez *et al*., 2015, Ivanovska *et al*., 2014). Taste and palatability is a key disadvantage of liquid formulations as paediatric patients, especially those below 6 years will often spit out the medicine with unpleasant taste, thus affecting medication adherence. Most drugs have a bitter taste, therefore flavours and sweeteners need to be added to mask the taste which often leads to increased costs of liquid preparations (Mennella *et al*., 2013). From a formulation aspect, the limited availability of controlled release formulations amongst liquids also affects patient adherence, as liquids are often required to be administered numerous time throughout the day, and research efforts are ongoing towards developing a wider range of controlled release paediatric formulations (Cuna *et al*., 2000, Childress and Sallee, 2013).

1.2.2 Solid Oral Dosage forms

Solid oral dosage forms for paediatrics encompass a wide variety of dosage forms, including traditional tablets and capsules, chewable/crushable tablets, orally disintegrating tablets, orally disintegrating films and mini tablets. Traditional tablets and capsules have been the dosage form of choice for the pharmaceutical formulators/industry due to their high stability, ease of manufacture and low manufacture cost, whilst formulators have the ability to develop modified release formulations/fixed dose combinations that can increase medication adherence whilst reducing medication burden on the patient (EMA, 2006). Specifically for paediatrics, taste of the tablets doesn't become an issue as the tablet would be swallowed whole, or the drug would be incorporated within the capsule shell. However traditional tablets and capsules also present disadvantages for paediatrics that include limited dose flexibility, which is a necessity in paediatrics, risk of choking on the dosage form due to the sizes of dosage forms, and the fact that most tablets and capsules are manufactured and licensed only for adult patients (EMA, 2006, Ivanovska *et al*., 2014, Lopez *et al*., 2015).

Attempts have been made to improve solid oral dosage forms for paediatrics, with the development of mini tablets which are around 2mm in diameter. These have proved to be safer for paediatric patients, however dose flexibility becomes an issue due to the limited weight available to incorporate

the API (Lopez *et al*., 2015, Spomer *et al*., 2012). The development of chewable/crushable tablets and orally disintegrating films has also accelerated due to their benefits in paediatrics. Chewable/crushable tablets are designed to be chewed or crushed before administration, which reduces the safety risk/risk of choking of the dosage forms, however formulation of these can be complex and they often require special packaging due to the fragile nature of the tablets (Dahiya *et al*., 2015). Orally disintegrating films (ODF) are a fairly new innovation in pharmaceutics, which incorporate API within a hydrophilic polymer that forms a wafer thin film designed to disintegrate rapidly in the oral cavity. The advantage of ODFs is that it reduces the choking risk associated with traditional solid oral dosage forms, however they can be complex to formulate, whilst dose flexibility is also very limited (Irfan *et al*., 2016).

1.2.3 Parenteral Dosage Forms

Parenteral administration is a common dosing method in neonates as well as in emergency drug delivery. It bypasses first pass metabolism and makes the API readily available for therapeutic effect. Specifically in paediatrics its advantages lie in the absence of the need of complex formulation as there is no need for taste masking APIs, or formulating them into oral dosage forms. It also provides a rapid onset of action, and can be formulated as controlled release preparations. However the disadvantages do outweigh the advantages for paediatric drug delivery as the comfort aspect of injections is very low, often resulting in pain for the paediatric patient, with regular parenteral drug delivery causing high levels of discomfort (Vega *et al*., 2014, Ivanovska *et al*., 2014). Due to the limited acceptance by the paediatric patient, parenteral formulations are rarely used unless in emergency cases and for vaccination.

1.3 Orally Disintegrating Tablets (ODT)

Orally disintegrating tablets (ODTs) are a dosage form designed to disperse on the tongue when it comes into contact with saliva, thereby reducing the need for tablets to be swallowed whole with water. This makes them ideal dosage forms for paediatric and elderly populations who may have

difficulties swallowing conventional tablets (Sastry *et al*., 2000). The standards for a dosage form to be classed as an ODT are that 'it must disintegrate rapidly in the oral cavity, with an in-vitro disintegration time of approximately 30 seconds or less', and in general have a weight of no more than 500 mg (FDA, 2008). Although the USP states a disintegration time of 30 s the European Pharmacopoeia provides a much longer disintegration time of 180s (Ph.Eur, 2013). However it is more common to adhere to the 30 s disintegration time guidance as 180 s would be a very long time for a tablet to be present within the mouth, especially for paediatric patients. A study conducted by Alyami *et al*. (2016a) found that paediatric patients much preferred a fast disintegrating tablet that would disintegrate within the USP time of 30 s. This study also provided very interesting results, with the paediatric population giving an overwhelming positive attitude towards ODTs as a suitable dosage form, indicating that they would prefer an ODT compared to other commonly utilised paediatric dosage forms (Alyami *et al*., 2016a).

ODTs present many advantages over traditional dosage forms used in paediatric drug delivery, by combining the stability/suitability of a solid oral dosage form whilst possessing the safety profile and acceptability similar to a liquid formulation. Due to the rapid disintegration of the dosage form within the oral cavity, ODTs reduce the risk of choking as the dosage form is designed to disperse into a viscous semi-solid/liquid state upon contact with saliva. The manufactured formulation retains a high stability profile, especially for moisture sensitive drugs, as they are manufactured into a solid tablet and often stored in regular tablet blisters (McLaughlin *et al*., 2009, Hirani *et al*., 2009). They also provide a more palatable dosage form compared to liquids, as upon disintegration ODTs can provide a cooling effect in the mouth and with the use of solid taste masking techniques providing a more acceptable dosage form for the patient. ODTs also increase medication adherence compared to liquids, due to the less bulky nature of the tablets, and therefore transportability does not become an issue (Navarro, 2010). It can also be stated that increased bioavailability may be an advantage of ODTs as buccal absorption may occur, and upon swallowing the already disintegrated tablet would provide a faster onset of action compared to a traditional solid oral dosage form (Lopez *et al*., 2015).

As mentioned above, palatability of ODTs can be an advantage, but the use of sweeteners and flavourings can be limited in improving the taste of very bitter/bad tasting APIs. This will often require complex multiparticulate taste masking technologies, which will invariably lead to rises in formulation costs (Barra *et al*., 1999). Dose flexibility is also limited with ODTs, as with traditional solid oral dosage forms, ODTs are formulated in fixed strengths and the ability to alter the dosage form prior to administration is difficult, which may not be ideal for patients requiring tailored doses (Lopez *et al*., 2015) . Due to patient dosing capability it has been established that ODTs are only suitable for patients above the age of 6, as the size of tablets up to 500 mg may still present a hazard to younger patients (EMA, 2006). As the drug/tablet is designed to disintegrate rapidly in the mouth, highly soluble drugs may be absorbed through buccal or sublingual pathways, and therefore the patient may be exposed to very high doses as the drug would avoid first pass metabolism (Buck, 2013).

Table 1.1 provides a summary and comparison of all types of paediatric dosage form highlighting both the advantages and disadvantages of the different types.

Table 1.1: Table highlighting advantages and disadvantages of paediatric dosage forms

Formulation Type	Advantages	Disadvantages
ODT	• Can increase medication compliance • Safer to use than traditional tablets – low choking risk • Require no water • More stable / longer shelf life than liquid dosage forms • No transportability issues i.e. no bulky containers • Is perceived as acceptable by paediatric populations • Increased bioavailability	• Usually requires taste masking • Limited dose flexibility • Only suitable from 6 years onwards • Buccal/sublingual absorption may lead to too high dosing • Lack of availability of certain drugs
Liquids	• Ease of administration • Can be used from birth • Good dose flexibility – measuring spoons / syringes • Most commonly recognised / prescribed	• Require taste masking • Can be unstable – have short shelf life • May have to be stored in the fridge • Transportability issues • Lack of MR capability
Tablets / Capsules	• Cost effective • Palatability / taste not usually an issue • Controlled release capability • Large variety of drugs available	• Risk of choking – presents a safety risk to the paediatric patient • Dose flexibility • Doses usually too high for paediatrics
Chewable / Crushable tablets	• Can increase medication compliance • Present less of a safety risk	• May need to administer with water • Can be expensive to formulate • Require taste masking
ODF's	• Very safe to use – low choking risk • Rapid disintegration in the mouth • Increased bioavailability	• Require complex formulation • Limited dosing flexibility • Can only incorporate small amounts of API
Parenteral	• Provide rapid onset of action – useful in emergency • No first pass metabolism • No need to taste mask	• Can be painful / cause distress • Can be expensive • Hypersensitivity / extravasation risk is high

1.4 Manufacturing Methods for ODTs

1.4.1 Freeze Drying

Freeze drying/Lyophilisation is a process where a solution/suspension of excipients is formed with a suitable solvent and frozen. The solvent is then removed from the frozen formulation through the drying process. For ODTs, the drug/excipients str usually dissolved/dispersed in the solvent and poured into premanufactured blisters followed by freeze drying to produce the tablets. This results in highly porous, but fragile tablets that disintegrate rapidly on the tongue, and during the freezing process the drug may form into its amorphous state therefore enhancing dissolution rate (Fu *et al*., 2004). The freeze drying process is a fairly expensive method of ODT production as it requires specialised equipment, a complex manufacturing method and may not always be suitable for unstable drugs, such as those sensitive to moisture. The freeze drying of ODTs also requires specialised packaging which further fuels the cost of the manufacturing method (Yadav *et al*., 2012).

Zydis Technology (Catalent, NJ, USA) is the most common and widely used freeze drying technology employed for ODTs. It has a range of marketed ODTs, including Maxalt Melts (Rizatriptan), Zofran Zydis (Ondansetron) and Claritin Reditabs (Loratidine). The basic method consists of the drug trapped in a matrix of saccharide and polymer, which is then dispensed into the blisters and frozen in a liquid nitrogen tunnel. The solvent in its frozen state is then removed to form the highly porous tablets, which are then sealed into the blisters with a foil packaging, as part of the specialised Zydis production process. The resulting water content is very small, and so the tablets are considered to be self-preserving. However the ODTs are sensitive to moisture and can dissolve between the fingers, or degrade when exposed to moisture levels greater than 65% (Fu *et al*., 2004, McLaughlin *et al*., 2009).

1.4.2 Other Technologies/Manufacturing Methods

Flashdose (Bioavail, Mississauga, Canada) is an ODT production method that uses a sugar floss system. This method involves producing crystalline fibres, similar to candy floss, from molten saccharides using centrifugal force. The fibres are then formed into granules and subject to mixing with the API and

other tableting excipients and compressed to form the ODTs. This system requires complex formulation steps, and saccharides which are highly soluble and crystalline, which in turn increases production cost (Fu *et al*., 2004, McLaughlin *et al*., 2009).

Another process for ODT production is the manufacture of moulded tablets such as the WOWtab (Astellas Pharma, Yamanouchi, Japan). The technology uses water soluble excipients (such as saccharides) which allow the tablet to disintegrate rapidly. The powder blend is moistened with a solvent and then moulded into tablets under low pressures, and air dried to form porous dosage forms. The WOWtab method includes humidity conditioning, which increases robustness of the dosage form (Fu *et al*., 2004, McLaughlin *et al*., 2009).

1.4.3 Direct Compression

Direct compression is a method whereby powder blends are compressed to form tablets without the process of granulation (Thoorens *et al*., 2014). Manufacturing using direct compression is a cost effective method to produce ODTs, which are less inclined to damage upon handling and more mechanically robust, while still being able to disintegrate within the stipulated amount of time (Harmon, 2007). The cost effectiveness of the manufacturing method comes from the fact that traditional tabletting equipment can be used and no specialised processes are required for tablet formation (Gohel, 2009).

However with the advantages of direct compression also comes some disadvantages. As there is no pre-processing of the blend before compression, the blend is required to flow well, so that uniform tablets are produced with the absence of any capping or lamination, and a uniform weight throughout. Therefore the starting materials are required to have a similar particle size, and the bulk density of the starting materials should not be too low, as this directly impacts the flow of the resulting powder blend (McCormick, 2005). If poorly flowing APIs are used, this may also limit the proportion of API that can be employed in the blend, as the excipients and the mixing method would be required to enhance flow of the bulk powder. During mixing, static charges may also build up leading to aggregation and

increases in the amounts of cohesive and adhesive forces present within the blend, therefore ultimately worsening flow (Jivraj *et al*., 2000). The excipients toned to be highly compressible/compactible to allow the resulting tablet to retain its structure, as the use of a high proportion of fracturing or elastically deforming materials may lead to poor compression of the powder resulting in poor quality tablets with low mechanical strength (McCormick, 2005).

ODT manufacture using this method requires the inclusion of superdisintegrants/effervescent agents or high aqueous solubility ingredients to produce rapid disintegration. Direct compression of ODTs also requires the use of taste masking platforms which increases the palatability of the resulting dosage form, without compromising the resultant mechanical properties of the tablet. However the magnitude of the compression force needs to be balanced with the disintegration time of the tablet, and be low enough to allow the excipients to retain their integrity, particularly when taste masking technologies are used (McLaughlin *et al*., 2009). Another key advantage of direct compression ODTs over freeze drying is that there are usually no requirements for specialised packaging, which further fuels the cost effectiveness of this method of manufacture (Pabari and Ramtoola, 2012). There are several ODT direct compression platforms utilised in industry, which include Orasolv (CIMA Labs, PA, USA), Durasolv (CIMA Labs, PA, USA), Flashtab (Ethypharma, Saint Cloud, France) and Advatab (Eurand Pharmaceuticals, OH, USA). (McLaughlin *et al*., 2009).

1.5 Commonly used Materials in Directly Compressed ODTs

Commonly used excipients in ODTs fall under a few different categories. The three main excipient categories for directly compressed ODTs include; filler/binder, disintegrant/superdisintegrant and lubricant. Many excipients can fall under more than one category especially new co-processed excipients which are multi-functional (AlHusban *et al*., 2010).

Microcrystalline cellulose (MCC) is a very common excipient used as a binder-filler within ODTs that are directly compressed because it has very good binding properties when it is dry, and also acts as a

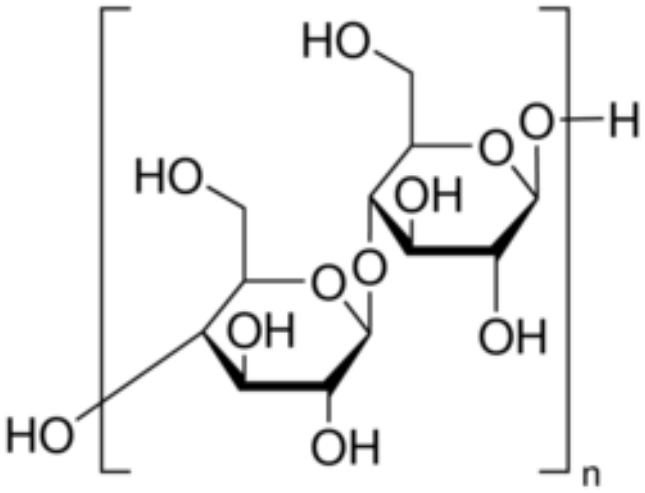

Figure 1.1: Chemical structure of the tablet binder MCC, with the chemical formula $(C_6H_{10}O_5)_n$,

disintegrant and low lubricant requirement. Figure 1.1 shows its chemical structure. It also has a high dilution potential which allows high quantity of API to be incorporated within an ODT (Bolhuis and Chowhan, 1996). An advantage of using MCC is that it plastically deforms which provides MCC with its highly compactable nature. The plastic deformation increases the surface area of the excipient which leads a higher rate of hydrogen bonding between hydroxyl groups on the adjacent cellulose particles (Bi *et al*., 1999), which in turn results in tablets of high mechanical hardness (Zhang *et al*., 2003). When the particle is compressed it forms several slip planes, which in turn exposes a larger proportion of the hydroxyl groups. The increasing proportion of exposed hydroxyl groups lead to a higher level of hydrogen bonding resulting in highly robust dosage form production (Hüttenrauch, 1971, Bolhuis and Chowhan, 1996, Thoorens *et al*., 2014). It can act as a disintegrant due to its capillary action and swelling ability, which in turn promotes disintegration of the ODT (Bi *et al*., 1999). However there are some disadvantages to MCC as it does come at a high cost compared to other binder-fillers and has a poor flowability, due to irregularly shaped particles which are fibrous and can interlock (Limwong *et al*., 2004). Also contributing to its poorly flowing nature is its low bulk density, partially attributed to the irregular shape of the particles within the powder (Bolhuis, 2011, Staniforth and Aulton, 2007). Also MCC is insoluble in water which can result in a gritty rough texture when the tablet disintegrates in the mouth (Bi *et al*., 1996).

Mannitol is a very popular excipient used as a filler in the manufacture of ODTs. It is a polyol isomer of sorbitol which is prepared by the catalytic reduction of different sugars (Bolhuis and Chowhan, 1996). Figure 1.2 shows the structure of D-mannitol, it is a sugar alcohol that has four chiral centres. The D form of mannitol is the most commonly occurring and is regularly used within the food and pharmaceutical industry (Kaminsky and Glazer, 1997). Mannitol is formed of crystalline needle shaped particles which have a glass transition temperature (T_g) below room temperature. It has three crystalline forms; α-polymorph, β-polymorph and δ-polymorph. The β-polymorph is the most stable, with δ being the least stable/metastable and α is a stable intermediate between the two (Willart *et al*., 2007). The advantages of using sugar based excipients like mannitol include pleasant mouth feel and taste. Mannitol has a negative heat of solution which produces a cooling effect in the mouth as the ODT disintegrates to form a gel, while also producing a sweet taste despite having a low sugar content. However mannitol has low compressibility, therefore producing weaker tablets when directly compressed. This is due to mannitol particles undergoing fragmentation under pressure which leads to tablets which are friable upon handling (Al-Khattawi *et al*., 2012).

Starch is one of the most common excipients used in tableting and can be classed as a multifunctional excipient in solid oral dosage forms, where it can act as a filler/binder as well as a disintegrant, in quantities of 3-25%w/w (Rowe *et al*., 2012, Zámostný *et al*., 2012, Ingram and Lowenthal, 1968). Its chemical structure is shown in Figure 1.3. It is made up of two molecules of glucose, amylopectin and

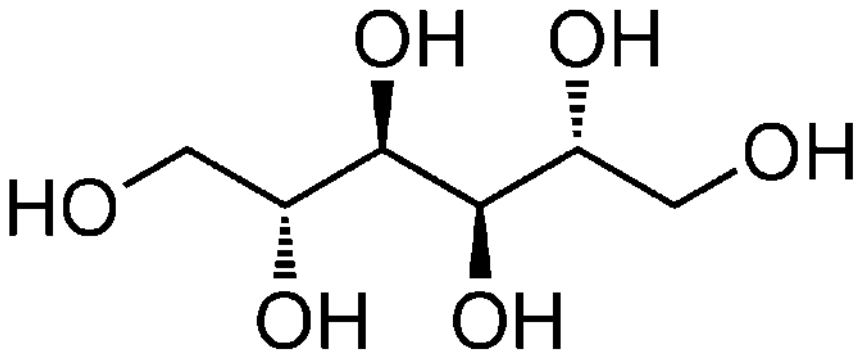

Figure 1.2: Chemical structure of the naturally occurring D-Mannitol, with the chemical formula $C_6H_{14}O_6$ and molecular mass of 182

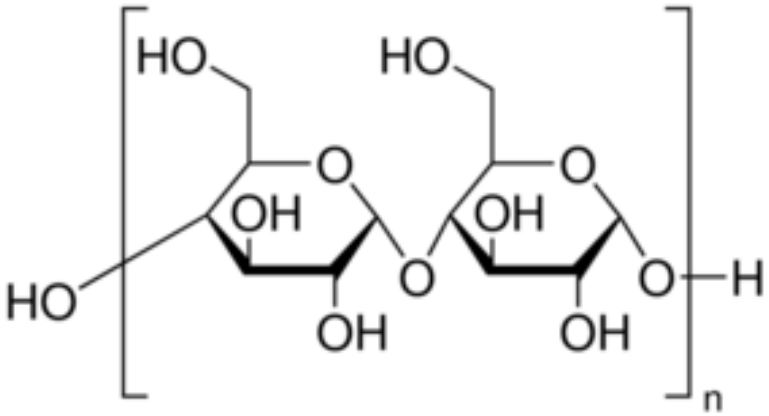

Figure 1.3: Chemical structure of starch, with the chemical formula $(C5H10O5)_n$.

amylose (Levina and Rajabi-Siahboomi, 2004). Although starch is a naturally sourced excipient it exhibits poor compactability, partially due to small levels of elastic deformation (Hong *et al*., 2016). This led to concerted efforts to produce processed starch excipients with improved properties and functionalities. Partially pregelatinised maize starch (PPMS), which is marketed as Starch 1500 by Colorcon Inc., is a relatively new excipient which increased the functionality of unprocessed starch, giving Starch 1500 improved binding properties and improvements in flowability, allowing it to be utilised in direct compression (Rowe *et al*., 2012). Rather than the elastic deforming properties of the native starch, it had been shown that starch 1500 undergoes higher levels of plastic deformation, giving it its improved compressibility profile (Colorcon, 2005). It also has the ability to act as a sustained release excipient partially due to different levels of cross linking within the starch, particularly with increased amylose branches, allowing it to swell in water and therefore retard drug release (Zámostný *et al*., 2012, Levina and Rajabi-Siahboomi, 2004). Starch 1500 is a model excipient for ODTs due to its highly compressible nature, whilst retaining some of the disintegrating properties of the native starch.

Lactose is a common diluent used in tablets, with the most common form being α-lactose monohydrate. It has good flow properties and compresses by plastic deformation and fragmentation, with fragmentation being more predominant (Bolhuis and Chowhan, 1996). However the fragmentation of lactose has been shown to increase the mechanical strength of tablets, as the

fracture of the particle into smaller parts increases the amount of bonding sites available, which in turn allows a stronger compact to be formed (Lerk *et al*., 1983).

Cross-linked polypryrrolidone (Crospovidone) is an excipient that acts as a superdisintegrant in ODT formulations. This is because crospovidone acts as a wicking agent and has a high swelling ability which contributes to its highly disintegrating nature when employed within tablet dosage forms (Desai *et al*., 2012). Crospovidone is a stable excipient that doesn't interact with many API's, however it does have small particles which contribute to poor bulk powder flow properties (Mohamed *et al*., 2012). Cross linked sodium carboxymethylcellulose (Ac-di-sol or crosscarmellose sodium) is another superdisintegrant used in ODTs. It has a fibrous structure which allows wicking of water, and has a high swelling ability allowing it to cause disintegration of tablet dosage forms quite rapidly (Bi *et al*., 1999).

Magnesium Stearate is the most common lubricant used in ODT formulations to prevent friction between the tablet and die wall during the ejection of the tablet in the direct compression process and to prevent the tablet sticking to the punch face. It is non-toxic and doesn't interact with many API's or excipients. However it does have a hydrophobic nature, which in the case of ODTs will cause disintegration time to be prolonged, whilst a high concentration or lengthy mixing time can lead to mechanically weak compacts being manufactured during direct compression (Carter, 2001). Sodium stearyl fumarate however is a more hydrophilic lubricant used, although not as widely employed as magnesium stearate due to its higher cost. It has been increasingly incorporated in ODTs as it shows better disintegrating properties than magnesium stearate, and overall aids the disintegration of the dosage form (Kuno *et al*., 2008).

Colloidal silicon dioxide (silica, fumed silica, SiO_2) is the most common glidant utilised in tabletting, with the powder possessing a high specific surface area due to nanosized particles. It is marketed as Aerosil by Evonik Industries (Essen, Germany), with different grades based on the specific surface area. This property is exploited during mixing to allow the highly charged silica particles to coat the main

constituent particles within the powder, reducing cohesive forces and interparticle friction between the bulk powder and therefore allowing an improvement in the flow of the particles (Rowe *et al*., 2012, Kojima and Elliott, 2013). This is essential for the direct compression tableting process as free flowing powder results in uniform and consistent dosage forms being produced (Staniforth and Aulton, 2007). It is insoluble in water, and thus high concentrations are avoided in ODTs as this can result in a gritty sensation within the oral cavity.

1.6 Factors affecting compressibility of excipients during Direct Compression

Direct compression is a method of tableting whereby the dosage form is compressed directly from the powder blend containing the API and excipients (Gohel, 2009). Due to the very small number of steps required in direct compression, the key requirements the powder blends are required to fulfil include good flow, good blending properties and high compressibility.

Powder flow is essential for compressibility of an excipient that undergoes direct compression. An excipient which exhibits good flow contributes to homogenous bulk powder flow, and allows uniform filling of the die, which in turn results in a uniform dosage form (Bolhuis and Chowhan, 1996). There are lots of factors which can affect the flow of an excipient powder which include; Particle size and size distribution, particle shape, particle density and friction and adhesion profiles (McCormick, 2005). Particle size is key for powder flow. Particles that are too small have poor flow properties compared to particles of a bigger size, as the smaller particles tend to stick together due to cohesive forces, meaning that the powder is unable to flow uniformly. A similar size distribution is also required for good flow. Also powders which have particles that are more spherical tend to flow better than irregularly shaped particles, as there is less chance of friction occurring between the spherical particles themselves, whereas if the particles were more irregularly shaped there is an increased risk of interlocking/cohesion between them (Limwong *et al*., 2004). Bulk density can also have an impact on flow, as low bulk density particles occupy a large volume, which results in them flowing relatively poorly compared to high bulk density particles which tend to flow a lot better, due to the improved

volume to weight ratio. Also cohesion can depend on moisture content, so excipients which have a high moisture content flow worse compared to excipients with low moisture content (Zhang *et al*., 2003, Staniforth and Aulton, 2007).

The compressibility of an excipient is also key in direct compression. An excipient needs to be highly compressible to allow it to form a suitable dosage form that remains intact after the compaction force has been applied. This is referred to as plastic deformation. Plastic deformation is when an excipient remains in its deformed/compacted state within the tablet after the compression force has been applied and subsequently retracted. If the excipient particles exhibited elastic deformation, they would rebound back to their original shape/form once the compression force is removed and exhibit large amounts of relaxation, whereby the thickness of the tablet increases post-compression. Also a material can be brittle and fragment under compression, where particles break and crack, but can still remain formed as a tablet (Gupta *et al*., 2006). Excipients that fragment under compression produce tablets with high porosity due to increased bonding within the fragments (Mattsson, 2000). An ideal excipient for direct compression would therefore undergo plastic deformation with little or no elastic deformation. In some cases, brittle materials can be used where the highly porous nature of the compressed dosage form could be utilised, such as in ODT formulations. The different types of compression behaviour are illustrated in Figure 1.4. Compressibility under pressure can also be determined by surface energy (Zhang *et al*., 2003). This is because energy is consumed when the pressure is applied resulting in loss of air between the particles, and allowing them to become compact. This compaction is due to the formation of bonds which results in a loss of energy within the system (Mattsson, 2000).

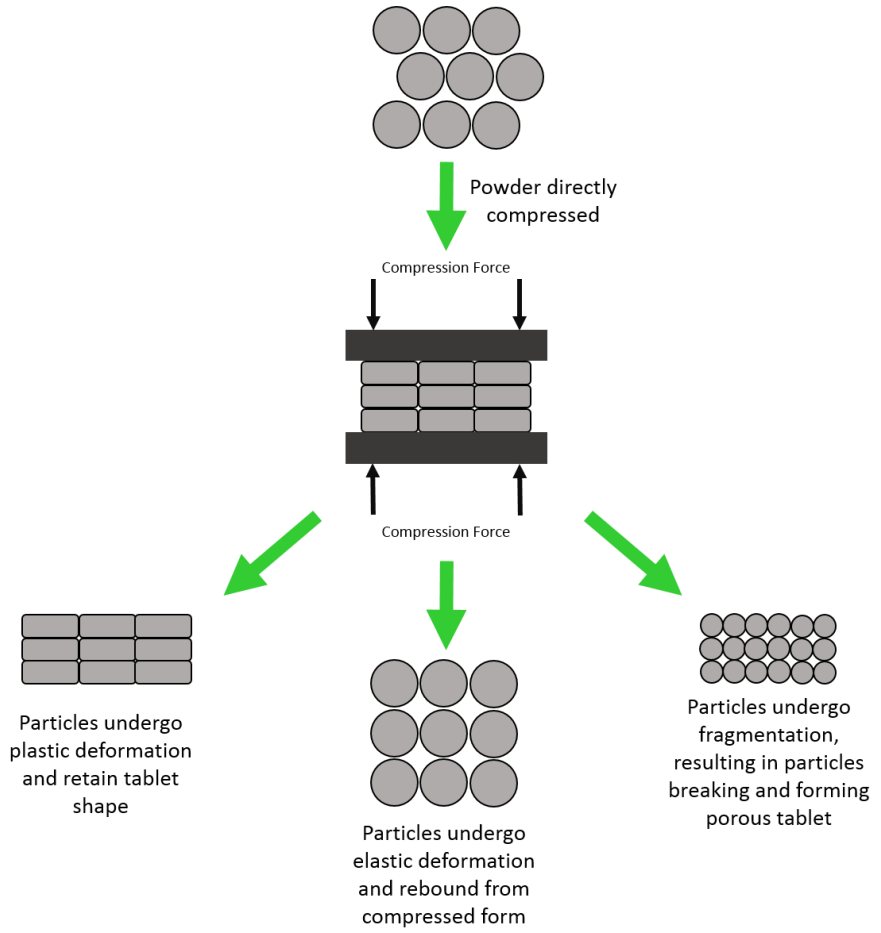

Figure 1.4: A schematic diagram highlighting the three main compression methods for excipients undergoing direct compression, with plastic deformation showing particle shape retention, elastic deformation indicating particle shape rebound and fragmentation deformation profile highlighting resulting in particle fracture and production of pores within the dosage form.

1.7 Processing of Materials prior to Direct Compression

1.7.1 Ball Milling and its impact on Powder and Material Characteristics

The basic principle of ball milling is to reduce the size of particles which may have a variety of chemical, physical and mechanical characteristics. Planetary ball mills operate with a rotating disk which spins in the opposite direction to the vials, as illustrated in Figure 1.5, generating high levels of energy/centrifugal force within the vial/balls, allowing grinding to take place. Ball mills reduce the size

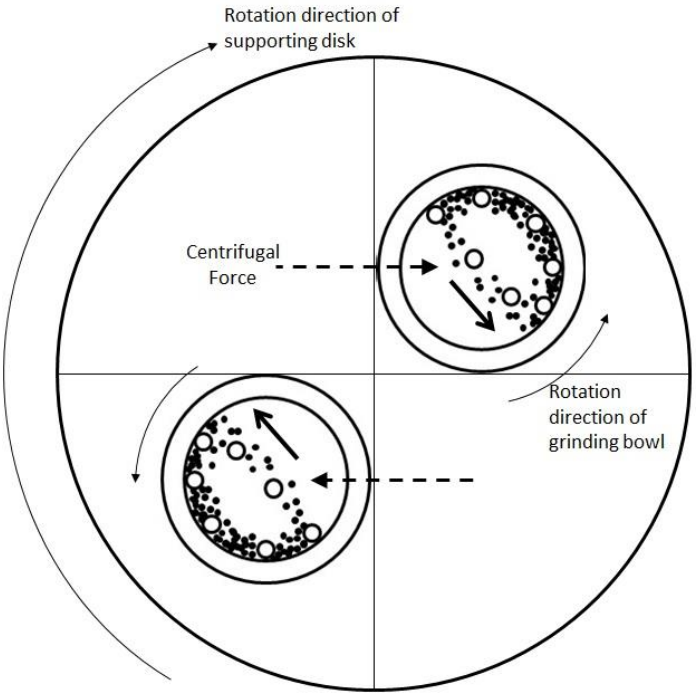

Figure 1.5: A diagram showing the motion of balls and powder through a planetary ball mill. Centrifugal force is produced through the opposite acceleration and velocity of the vial and supporting disk, causing high levels of energy within the moving balls, which come into contact with the powder, causing particle breakdown upon collision.

of particles through transfer of energy from the balls to the powder causing comminution, as well as mixing/blending/dispersing the powder. Particle size can depend on various parameters, including 1) Characteristics of the ball, including; mass, density, ball size distribution; 2) Characteristics of the powder, including; mass, volume, density, hardness, size, distribution of charge; and 3) The speed and time of rotation. The size reduction of particles also falls under three mechanisms; the first is abrasion where very fine particles are broken off the main particle due to low intensity stress. The second mechanism is cleavage where particles about 50-80% the size of the original are formed due to slow high intensity stresses and the final mechanism is fracture where rapid high intensity stress causes small size fragments to form with a high particle size distribution (Monov *et al*., 2012).

The particle size is reduced due to the breakage of bonds within the particle which alters the shape (Castricum *et al*., 1997). Milling can also result in a loss of energy in the particles due to the weaker

bonds, caused by repeated impact of the balls (Shabir *et al*., 2011). The breakage of bonds can also uncover parts of the particles exposing them to free radicals, and also allowing the formation of new chains and bonds, which could in some cases increase the molecular weight of the particles (Castricum *et al*., 1997), disputing the general principle of particle size reduction and reduction of molecular mass.

The surface characteristics of materials that have undergone ball milling are also altered. There is a larger surface area produced compared to the original powder as the particles are finer. Some studies have shown that the particles display nanoporous surface caused by the impact of the balls that have high energy, and the generation of heat due to friction between the particle and ball upon contact (Shabir *et al*., 2011). In the study by Shabir *et al*. (2011) the surface charge and hydrophobicity of the material had altered. The surface charge had become less negative due to a smaller particle size and increased drug loading, as the drug was positively charged, and the decrease in hydrophobicity was due to the increased surface area of the particles allowing more interaction with water. This increased hydrophilicity was also shown in another study by Jones *et al*. (2011), which was attributed to the increased surface area available to interact with water.

Ball milling can also alter the crystal form of certain powders, and change them to a more amorphous material. The loss of crystal structure is caused by the reduction in particle size, as a result of fracturing of the crystals along their slip planes. Milling can therefore result in a partial or total loss of crystal form as more amorphous domains are formed. Crystals with a more needle like morphology are more prone to loss of crystal structure than crystals with a plate like morphology (Ho *et al*., 2012). This loss of crystal form can in turn lead to changes in the hydrophilicity of a material as well as affecting the solubility and bioavailability of drugs (Jones *et al*., 2011).

1.7.1.1 Ball Milling in ODTs

Ball milling can be a method of modifying excipients to optimise them for use in ODTs. Excipients such as mannitol can be individually ground to improve its compressibility/compactability, or excipients can be co-ground to improve the characteristics of one or both the materials to optimise them for use in

ODTs. The co-milling method has been used in several studies to improve ODT properties, mainly employing a co-milled combination of mannitol with crospovidone.

A study by Katsuno *et al*. (2013) co-milled a mixture, of micronized crospovidone (m-cpvp) and mannitol to improve the stability of the powder blend. An SEM study to assess particle size and shape showed that the mannitol crystals within the co-ground mix had significantly reduced in size and changed shape to a more block like structure, with no large mannitol crystals contained in the co-ground mix. M-cpvp had a popcorn like shape with lots of cavities, which wasn't significantly different after milling. Post-compression, SEM also showed a significant difference between the surface of the tablet between co-milled and a physical mixture of the excipients, with the co-milled tablet having a surface that was a lot smoother than the tablet containing the physical mixture of the two. It was suggested that co-milling promoted inter particle bonding and fusion during compression. The study showed that a co-ground mix absorbed a lot less moisture than just the m-cpvp on its own and the physical mix of the two excipients, which meant that co-milling had led to a reduction in hygroscopicity of the m-cpvp. This was as a result of milling which had led to an aggregation between mannitol and m-cpvp, which prevented water absorption into the m-cpvp as mannitol is a non-hygroscopic excipient. This was confirmed by stability studies, which showed that a co-ground mix was much more stable in accelerated conditions (40˚C and 75% relative humidity) for 1 day/1 week, with strength remaining at 1.5MPa and disintegration below 30s. Storage of the co-milled powder for one month under accelerated conditions showed a slight decrease in strength, with disintegration remaining below 30s. In comparison the physical mixture and individual excipients displayed a worsening in tablet properties. Overall this study showed that co-milling was advantageous for preparing ODT formulations as it produced stable, mechanically robust and suitably disintegrating tablets compared to unmilled formulations.

A study by Shu *et al*. (2002) used a vibrational rod mill to produce a co-milled mix of regular crospovidone with mannitol to prepare directly compressed ODTs. In this study the use of a co-ground

mix showed an overall increase in hardness of the tablets as the amount of the co-ground mix within the formulation increased up to 30%, with the disintegration time remaining at around 60s for all of the formulations. Particle size reduction of crospovidone was evident in both co-grinding and individual grinding, whilst mannitol particle size also reduced in both cases. However co-grinding was found to decrease particle size more than individually ground material, which showed that crospovidone could act as a grinding assistant for mannitol. This study also looked at different excipients utilised in the co-ground mix, with the mannitol being substituted for other saccharides (erythritol, xylitol, lactose, glucose), and crospovidone substituted for other disintegrants (crosscarmellose sodium, L-HPC, sodium carboxymethyl starch, partially pre-gelatinzed starch). The relevant tests conducted showed that mannitol couldn't be substituted within the co-ground mix as tablets took too long to disintegrate, however they all had good mechanical hardness. The substitution of the crospovidone however produced tablets that were mechanically robust and disintegrated relatively quickly, with all formulations disintegrating within 30-45s.

Other studies have used milling to asses other properties surrounding ODTs. A study by Jones *et al*. (2011) looked at the impact of ball milling parameters on ODTs manufactured by freeze drying. Mixtures of gelatin and mannitol were milled in the frozen state before freeze drying. The milling parameters that were altered were milling time, rotation speed and ball to powder weight ratio (BPR). It showed that post milled powders had increased wettability due to the increased surface area of particles, and also porosity of the powders varied significantly depending on milling conditions.

From the above studies it can be deduced that milling can have a direct impact on the improvement in ODT properties, particularly those manufactured through direct compression. The one study by Jones *et al*. (2011) showed no improvement in ODT performance using freeze drying technology, whereas the other studies using direct compression all showed an improvement in the properties of ODTs. Of particular note was that studies generally found that milling time could be optimised at

around 20mins to produce ODTs that had a fast disintegration time as well as a good mechanical strength, and that co-milling of mannitol and crospovidone was a very popular combination.

1.7.2 Spray Drying

Spray drying is a process whereby a solution, usually containing API/excipients mixed with a suitable solvent, is atomised into a spray and dried rapidly within a heated chamber in a one step process, forming solid powder particles, which are spherical in shape (Wisniewski, 2015, Vehring, 2008). The advantages of spray dried particles is that they have a controlled particle shape and size, the spherical nature is obtained by the drying of the spherical droplets that are atomised into the chamber of the spray drier, with the particle size adjusted by the pump rate of the solution and the inlet/outlet temperatures of the equipment itself. This allows for a controlled manufacture of particles within the desired range (Vehring, 2008). The narrow size distribution along with the spherical shape also allows the powder to flow fairly well due to the reduction in segregation and mechanical interlocking occurring between the powder particles, meaning spray dried particles are ideal for direct compression (Staniforth and Aulton, 2007). However as with all processes there are some disadvantages to spray drying, which include the expensive nature of the process, the reduced capability to process heat/moisture sensitive materials and importantly the low yields that can be attributed to a spray drying process, as powders are usually lost on chamber walls as well as very fine powder particles being lost in the exhaust stream (Sosnik and Seremeta, 2015).

Spray drying has been utilised in previous research for the production of directly compressed ODTs, due to the many advantages it holds for pre-processing powders prior to direct compression. Work by Al-khattawi *et al*. (2015) showed that it was possible to engineer spray dried mannitol particles with a certain degree of porosity, which in the case of ODTs was advantageous, as this promoted rapid disintegration as well as a plastically deforming mannitol, due to the presence of α-mannitol within the spray dried excipient. Spray drying can also be useful for the preparation of co-processed excipients to reduce the individual disadvantages of the materials whilst trying to optimise and utilise

the advantages. A study by Mishra *et al*. (2006) showed that co-spray drying several common ODT excipients together, such as mannitol, MCC, aspartame and the superdisintegrant, prior to direct compression produced robust tablets that disintegrated within 20s. This showed that spray drying was a useful technique for producing rapidly disintegrating tablets whilst maintaining an acceptable mechanical strength.

1.7.3 Dry Powder Coating

Microencapsulation entails the formation of new particles that have a certain material as the core, with a surrounding coat composed of a distinctly different material. The core can be solid, liquid or gas, with the coat usually formed of a solid (Singh *et al*., 2010). Dry particle coating / hybrid mixing is an emerging process whereby fine guest particles are strongly adhered to the surface of a coarser host particle, forming new functionalised particles in the solid state (Dahmash, 2016). This form of mixing utilises the cohesive nature of the fine particles and attracts them to the surface of the host particle, as long as the difference in size is at least a magnitude of two. The coating of the fine particles is due to the cohesive forces that are present between the coarse particle and the fine particle, with surface energies also playing a part, and the fine particles not weighing a substantial amount. The weight plays a huge role in the adhesion of the fines as the coating only occurs if the weight of the fine particle is lower than the forces of attraction present between the guest and the host. The low weight of the guest causes the fine particle to be attracted and adhere to the surface of the coarse particle, producing a mechanically strong coating, leading to newly formed functionalised particles. This is very useful for fine particles, which usually would be difficult to process due to problems with agglomeration/segregation, as during dry particle coating they would be evenly dispersed upon the surface of the host particle, allowing a uniform blend to be produced. (Dahmash and Mohammed, 2015, Ishizaka *et al*., 1989, Honda *et al*., 1994, Alonso *et al*., 1990). During the dry particle coating mixing process the agglomerates of the fine powder would be uniformly dispersed prior to coating, therefore promoting attraction to the surface of the coarse particles and leading to production of either a discrete coat on the coarse particle or if highly successful, a continuous coat, as illustrated in

Figure 1.6. The level of coating would depend on the amounts of each excipient present within the blend, the particle size and true density of both and the levels of attractive forces generated between the two materials (Yang *et al*., 2005). Dry particle coating has several advantages over traditional mixing methods especially for powders utilised in direct compression. This processing method produces very flowable powders from excipients that are very fine and cohesive in nature, allowing the powder to flow freely during the tableting process (Han *et al*., 2013, Yang *et al*., 2005, Dahmash, 2016). The utilisation of two excipients to produce new functionalised particles is also advantageous, as the beneficial aspects of each of the excipients are maximised whilst reducing the negative aspects. This can lead to production of particles with not only an increased flowability but also for example, enhanced dissolution behaviour, a sustained release, an improved palatability or an increased wettability (Han *et al*., 2013, Dahmash, 2016). Dry particle coating is also a one-step, solvent free method of processing powders, which utilises widely available excipients to produce new functionalised particles, thereby providing not only an environmentally friendly mixing method, but also a very cost effective manufacturing process for new materials (Dahmash, 2016). As it is a relatively

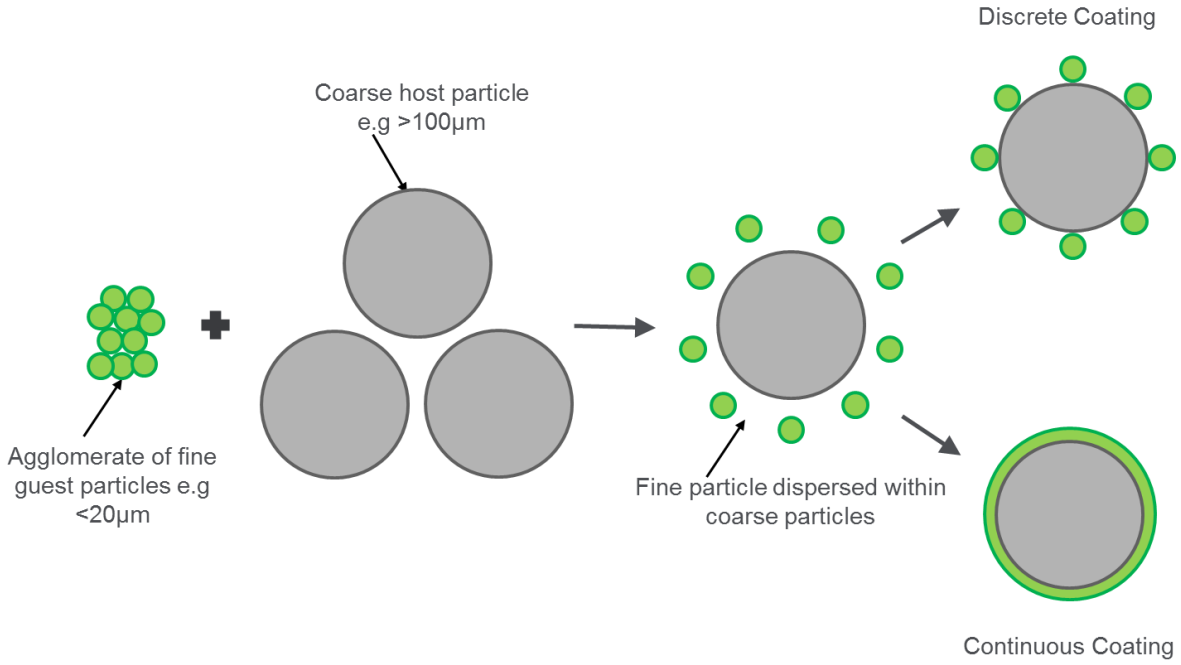

Figure 1.6: Figure showing the dry particle coating mixing process, whereby agglomerates of fine particles are dispersed prior to attraction and coating on to a coarse particle, levels of coating can vary between a discrete coat, where an element of the coarse particle surface is covered with the guest or a continuous coating where the whole host particle is encapsulated with particles of the fine guest particle.

new mixing concept, a multitude of dry coating devices have been developed over recent decades; with devices utilising high shear forces in a mechanofusion dry coating method (Yokoyama *et al*., 1987); devices utilising high shear in a hybridizer mixing method (Ishizaka *et al*., 1988); dry coating devices that utilise magnetic assistance (Beach, 2011) and dry particle coating using a fluidised energy mill (Han *et al*., 2013). With these methods particles may undergo some forms of chemical alteration and will often suffer attrition and damage during processing, therefore leading to changes in particle size and potential alterations in crystallinity and stability of the materials being processed. Also high levels of friction are generated in these processes which leads to a heating effect, meaning that heat sensitive materials may not be suitable for processing. With certain methods particles are required to be of a certain size, otherwise they cannot be processed, which does limit the materials that can be utilised for these particular dry coating methods.

A novel dry particle coating equipment developed by our research group was designed to overcome the limitations associated with previous devices (Dahmash, 2016). This dry particle coater provides a one-step, environmentally friendly process of producing functionalised particles, which utilises no solvents or generates no heat, with the particles not suffering any form of attrition during the mixing process. The device was able to produce materials with enhanced flowability, very high content uniformities, and able to produce particles with new functionalities such as modified release APIs (Dahmash, 2016), showing that the disadvantages associated with previous dry coating technologies could be minimised whilst enhancing the advantages of the process. The manufactured device was not only able to produce particles with new functionalities, but was able to enhance powder properties, with content uniformity and powder flow of blends produced in the mixer being superior to other mixing methods.

1.8 Characterisation techniques for Directly Compressed ODTs

Once the ODT has been manufactured using direct compression there are various techniques used to analyse its characteristics. The usual parameters that need to be investigated are; Uniformity of weight, uniformity of size (diameter and thickness), drug content, hardness, friability, disintegration time, dissolution studies, and in some cases wetting time and water absorption ratio (Srikar *et al*., 2013). These are very standard tests for oral dosage forms and some of them have certain limits the dosage form must meet for it to be suitably classed as an ODT.

Disintegration time of ODTs is one of the most crucial tests, as the tablet is required to disintegrate within 30s, according to the US FDA (FDA, 2008) or 180s according to European regulations (Ph.Eur, 2013). Other tablet tests, like hardness, friability, uniformity of weight/size, dissolution and drug content are relatively standard and the parameters are still the same and measured according to BP requirements for directly compressed tablets. For example the percentage friability still needs to be below 1%. Tablet porosity is another useful tablet property that can be assessed, as porosity of the ODTs is usually related to the disintegration time/hardness of the tablet. To calculate porosity the bulk density and true density of the ODT are required. The bulk density would be calculated using tablet weight, thickness and diameter measurements, and the true density would be calculated using helium pycnometry, and the values are put into an equation allowing the percentage porosity to be calculated (Jones *et al*., 2011).

1.9 Disintegration Testing for ODTs

Characterisation techniques used for testing orally disintegrating tablets are vital in ensuring that the manufactured dosage form is fit for purpose. Among the tests, disintegration time is one of the most essential testing methods to ensure that the ODT disintegrates within the recommended FDA time of 30 seconds (FDA, 2008) or European Pharmacopoeia time of 180 seconds (Ph.Eur, 2013).

The currently recommended test for ODT disintegration time from the US FDA is the standard disintegration test for oral dosage forms shown in Figure 1.7 (FDA, 2008). The test is comprised of a

basket rack attached to a rod which oscillates vertically, and a beaker filled with disintegration medium, is kept at around 37°C and placed beneath the basket. The basket is immersed into the disintegration medium at a frequency of between 29-32 cycles per minute through a distance of around 53mm to allow tablet disintegration to take place. The basket is made up of 6 disintegration vessels with a wire mesh at the bottom (with holes of between 1.8mm-2.2mm), and disintegration time is measured once all fragments of the tablet have passed through the wire mesh. A disk can be placed on top of the tablet, but for ODT testing this is not usually required (FDA, 2008).

However there are several limitations with this test for ODTs due to the vast differences between the in vivo and in vitro conditions. In vivo, an ODT would be placed on to the tongue of the patient and then subsequently dissolve/disintegrate through interaction with the saliva present within the oral cavity. As the ODT is placed on the tongue, there would also be an increase in the salivary flow rate, due to gustatory (taste) reflex in response to the taste of the ODT (Kerr, 1961). It has been shown

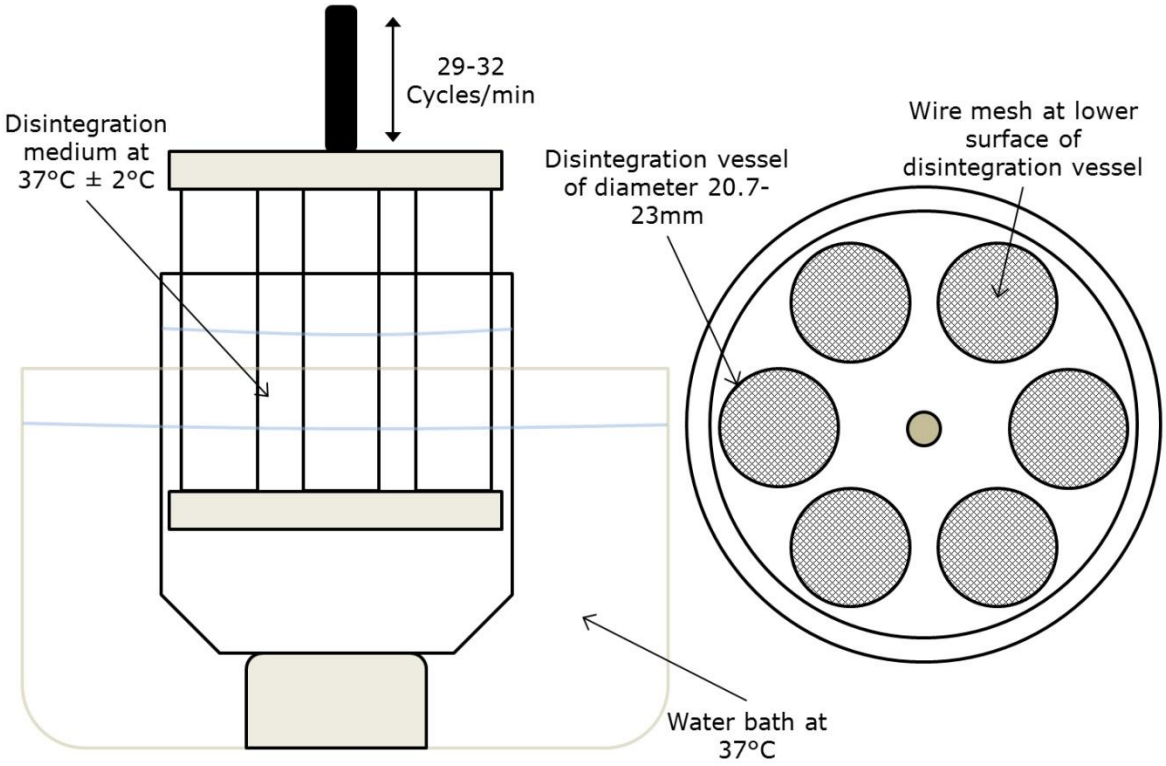

Figure 1.7: A diagram illustrating a typical set up for the standard USP disintegration test for oral dosage forms that is utilised for ODT disintegration testing. It shows how the basket would typically by placed within the beaker/water bath, and how the dissolution vessels are arranged within the basket.

that sour taste causes the highest increase in saliva flow rate, followed by salty, sweet and bitter taste (Jensen *et al*., 1998, Kerr, 1961). As the tablet is placed in the mouth, and the mouth closed, there would also be interactions between the ODT and upper palate, as well as a controlled temperature of around 37°C (Moore *et al*., 1999), and relative humidity of around 90-95% (Mathias *et al*., 2010). These conditions would also aid in the disintegration of the ODT, as the high humidity and temperature would promote saliva uptake into the tablet whilst the pressing of the upper palate would help manipulate and push the ODT towards the tongue as well as aiding in the breakdown of the tablet. The process of taking an ODT requires no water to be consumed as the dosage form disintegrates within the mouth allowing it to be swallowed easily. Having examined the in vivo conditions, it can be seen that the current recommended USP disintegration test does not bare many similarities to in vivo conditions. The standard test uses a large volume of disintegration medium, and the dosage form disintegrates within the oscillating vessel, which would be similar/correlate more to the disintegration of a conventional tablet, that is swallowed with water and disintegrates within the gastrointestinal tract. The significant differences between the conditions encountered by the ODT and the currently recommended USP disintegration test provide evidence that there is an opportunity to allow for development of a more representative ODT disintegration test. The USP guidance for orally disintegrating tablets stipulates that modified disintegration tests for ODTs can be developed (FDA, 2008).

Previous work has looked at improving the In Vivo in Vitro Correlation (IVIVC) for ODT disintegration time, and improvised tests, as well as actual testers have been developed to try and establish a comparable test. Table 1.2 contains information about a range of tests that have been reported after a thorough search through previous literature.

Table 1.2: Details of previous attempts in literature to produce disintegration tests for ODTs that give more comparable conditions to that encountered within the oral cavity. Each test has the details of how it works alongside the advantages and disadvantages of each test. R and R^2 values represent the IVIVC if it is available

Tests	Mechanism	Advantages	Disadvantages
Tricorptester **(Yoshita *et al*., 2013)** Manufactured equipment	• Uses two meshes – upper and lower, when they come into contact disintegration time (DT) ends • ODT place on lower mesh and time starts when upper mesh touches ODT • Upper mesh puts pressure on ODT (like upper palate) • Saliva kept at 37°C, and dripped from height of 80mm at 6ml/min • R^2= 0.79	• Saliva at 37°C • Automated measure of time • Force applied on ODT • Saliva flow can be varied	• Saliva dripped from above • Impact of water from 80mm height • Lack of humidity
KYO Method **(Kakutani *et al*., 2010)** Improvised Test	• Water permeability test prior to disintegration test (to decide whether 0.5ml/5ml of medium used) • Test tube contains predetermined volume of medium at 37°C • ODT placed on filter paper at bottom of tube	• Uses a weight to compress ODT • Filter paper as disintegration bed • Small volumes of disintegration medium (<5ml) • Disintegration medium at 37°C	• Stopwatch timer for disintegration • Double weight placed on ODT • Lack of humidity • Volume of medium varies according to pre-test

Tests	Mechanism	Advantages	Disadvantages
	• Double weight placed on ODT (acts as upper palate) • Time taken for weight to touch filter paper measured as DT • R^2=0.72		
ODT-101 **(Harada *et al*., 2006, Harada *et al*., 2010b, Narazaki *et al*., 2004)** Manufactured Equipment	• Weighted shaft places force on ODT and rotates at predetermined RPM • ODT placed on porous steel plates • Water bath contains 450ml of water at 37°C – level adjusted to just below plate, and level rises during test using a weight immersed in the water • Time measured when rotating shaft touches porous plate (shaft has conductive sponge on the bottom) • Several studies conducted; R^2=0.859, 0.610-0.701 and R=0.99	• ODT placed on a porous plate (allows it to disintegrate from below) • Automated measure of time • Disintegration medium at 37°C • Pressure placed on ODT	• Weighted shaft on top of ODT rotates • Uses a weight to raise water level • Lack of humidity • Large volume of disintegration medium (450ml)
Dissolution Apparatus	• 900ml of water at 37°C • Paddle rotated at 100rpm	• Disintegration medium at 37°C • Water agitated using paddle	• High volume of water (900ml) • Uses a basket submerged inside vessel

Tests	Mechanism	Advantages	Disadvantages
(Bi *et al*., 1996, Bi *et al*., 1999) Improvised Test	• Sinker placed at 8.5cm below water surface • DT taken as when the tablet has passed through the sinker screen		• Doesn't represent in vivo conditions • Not to dissimilar to current <701> test
Texture Analyser **(el-Arini and Clas, 2002, Abdelbary *et al*., 2005, Dor and Fix, 2000)** Improvised Test	• Flat faced probe with 1cm^3 surface area • Tablet attached to probe and probe moves down until trigger force detected • Predetermined weight (50g) is applied for a set amount of time (60s) • Artificial saliva used as disintegration medium – 2ml at 37°C • Measures a distance against time plot, where disintegration time can be calculated • Modified version of this test uses a sprung platform where ODT is placed instead of stuck to probe. • Perforated grid allows fragments to pass through during disintegration	• Automated measure of time (distance v time plot) • Constant load applied over given time • ODT place on mesh (allows it to disintegrate from below • Disintegration medium at 37°C	• Varied volumes of disintegration medium used (often too high e.g. 18ml) • Distance/time plot can complicate disintegration process • Lack of humidity

Tests	Mechanism	Advantages	Disadvantages
	• Uses 18ml artificial saliva at 37°C • Different R^2 values when parameters altered for different ODTs		
Simulated Wetting Test **(Park *et al*., 2008)** Improvised Test	• Used as a measure of DT • Whatman filter paper disk placed in each well of corning 12 well polystyrene microplate • Given volumes of Sensient blue #1 0.1% w/w dye added to each well based on ODT size • ODT added to well carefully and time for dye to diffuse through tablet and cover surface measured	• Die allows you to see when whole tablet has disintegrated • Small volume of disintegration medium (<1.75ml)	• Stopwatch timer for disintegration • Not much similarity to in vivo conditions • Uptake of dye doesn't necessarily indicate disintegration
OD Mate **(Haraguchi *et al*., 2014, Uchida *et al*., 2013)**	• ODT placed on trapezoidal mesh in flat bottomed test tube (acts as tongue) • Compressed by two weights (upper palate), 30g inner and 100g outer • Measurement starts when tube touches medium (20ml water at 37°C)	• Adjustable mesh/weight type • Automated measure of time • ODT placed on a mesh (allows it to disintegrate from below) • Uses a weight to compress ODT	• Uses two weights as compression force • Conditions are altered according to disintegration time of ODT • Lack of humidity

Tests	Mechanism	Advantages	Disadvantages
Manufactured Equipment	• Time taken for weight to touch test tube represents DT • Two studies with R^2=0.95 and 0.936	• Can adjust volume of test media	• 20ml water which can be stirred
CCD Camera **(Morita *et al*., 2002)** Improvised Test	• Two sections – disintegration component and measurement device • Measurement uses continuous pictures taken by a CCD camera to record disintegration – visualises tablet surface • Disintegration section has two components, inner tank with a stirring bar, steel grid and disintegration medium (200ml water at 37°C), grid has hollow areas for ODT placement. Outer tank is water bath kept at 37°C	• Can record disintegration • Disintegration medium at 37°C	• Time method calculation doesn't seem to work • Poor correlation with in vivo data • Large volume of medium
Electroforce **(BOSE)**	• Uses low force on the ODT (10mN or 1g) at 0.1N/s • Tablet placed in lower platform and force applied • 5ml water at 37°C added when 10mN force reached	• Small volume of medium (5ml) at 37°C • Very small force applied on ODT • Constant load applied over given time	• Distance/time plot can complicate disintegration process • Water added after force has been applied to ODT • Lack of humidity

Tests	Mechanism	Advantages	Disadvantages
Manufactured Equipment used for improvised test	• Disintegration plot drawn up as distance against time, and max distance reached is end of DT		
Prototypical ODT disintegration tester **(Kondo *et al*., 2012)** Improvised Test	• Tablet placed on centre of mesh and acrylic board acts as upper palate – rotates via attached motor at 25rpm • Test medium added to tank beneath mesh using a syringe until it makes contact with tablet (at 37°C) • Water level maintained by sink of tablet fragments into tank • CCD camera placed above tablet to record disintegration process, and is played back to calculate DT	• Camera replay system allows multi views of the disintegration process meaning that disintegration time can be calculated repeatedly from one film • Disintegration medium at 37°C • Uses a weight to apply a load to tablet	• Disintegration medium volume will vary as a specific amount isn't always added, and would be more than present in the oral cavity • Lack of humidity • Rotation of board doesn't simulate oral conditions
Test for Orally Disintegrating Mini Tablets **(Hermes, 2012)**	• Measures the electrical resistance of a gap where the sample tablet is placed • Uses a plunger with an adjustable weight to correspond the force to the force of the tongue	• Uses very small amounts of disintegration medium which are similar to that within oral cavity	• Study states an absolute disintegration could not be achieved • Does not take into account humidity

Tests	Mechanism	Advantages	Disadvantages
Manufactured Equipment	• Disintegration medium is added to the measuring cell – volume is small to allow complete wetting of the sample (can be <1ml)	• Disintegration medium used for testing was artificial saliva, which disintegrated tablet similar to in vivo conditions • Non-subjective measure of disintegration time • Assessment of tongue force in vivo to gather data for plunger weights	• Only appears to apply to mini tablets • Takes 40% loss in tablet structure to be the end of disintegration
Other Tests	• 100x10mm petri dish with 90mm filter paper and 9-10ml disintegration medium – solution of 10% w/w cobalt II 6 hydrate, DT taken as when tablet appears fully wet (Segado, 2003) • ODT placed on No.10 wire cloth and water dripped on to ODT at 4ml/min, DT taken as when all of ODT has passed through the wire (Ohta *et al*., 2001) • ODT placed in measuring cylinder with 10mesh base along with 1ml water.	• Disintegration medium at 37°C • Simple to do easy tests	• Don't really represent in vivo condition • Lack of humidity • No automatic recording can still be subjective

Tests	Mechanism	Advantages	Disadvantages
	Cylinder placed in water bath and shaken at 150rpm, and maintained at 37°C (Fu *et al*., 2006).		

From the literature review it was seen that extensive work had gone into trying to develop an ODT specific disintegration test, with some tests such as the Tricorptester, ODT-101 and OD Mate being specifically developed with the purpose of measuring ODT disintegration time.

1.10 Research Aims and Objectives

Orally disintegrating tablets are a key dosage form for paediatric drug delivery. They possess many advantages over traditional dosage forms, however the complex and expensive freeze drying process can lead to dosage forms that are mechanically weak and costly to produce. Utilising the traditional direct compression technique to manufacture ODTs yields tablets with impressive mechanical properties whilst maintaining low disintegration times and minimising manufacturing costs. However for direct compression a more in depth understanding of the materials is needed, as compression/compaction properties of excipients are key in providing a suitable dosage form.

The principal aim of this thesis is to produce materials that are highly compressible/compactable for ODT/solid oral dosage forms, whilst keeping disintegration times low, as this is essential for producing successful directly compressed ODTs. It is highly advantageous to produce compressible preblends that are 'ready to use' powders alongside an API and a suitable lubricant. This negates the needs for lengthy formulation processes as the preblends are able to produce robust/fast disintegrating tablets without the need for excessive alteration of the formulation.

The objectives of the work in this thesis include:

1. Evaluate the fragmentation behaviour of crystalline mannitol using a wide range of characterisation techniques and relate this to the performance of mannitol as a filler/binder, utilising particle size reduction through mechanical fracture
2. Investigate the possibility of milled mannitol as an alternative mannitol product for use in directly compressed tablets, comparing it to commercially available grades

3. Utilising a novel dry particle coating technique to produce several preblends for use in ODT/solid oral dosage forms, using hydrophobic and non-compressible APIs
4. Development of a novel disintegration method for testing ODTs due to the current limitations with the USP recommended method. Key aspect is to gather IVIVC to assess the suitability of the improvised test in its ability to obtain accurate and suitable disintegration times

Chapter 2

A Holistic Multi Evidence Approach to Study the Fragmentation Behaviour of Crystalline Mannitol

2.1 Introduction

The high patient compliance for orally disintegrating tablets (ODTs) among paediatric and geriatric populations, as well as patients with dysphagia, has led to a surge in the popularity of these dosage forms, as well as an increased number of licensed formulations becoming available on the market (Al-khattawi and Mohammed, 2013, AlHusban *et al*., 2010, Seager, 1998). Owing to the disintegration of the dosage form within the oral cavity, the formulation, and in particular the excipients used to formulate the ODT, are key to manufacturing a palatable, robust and fast disintegrating tablet. For the manufacture of ODTs, direct compression (DC) is an advantageous method as it utilises traditional tableting equipment and is able to produce tablets that have high mechanical strength, whilst being able to disintegrate within the recommended US FDA guidelines of 30 seconds (FDA, 2008), compared to freeze drying technology where tablets are mechanically weak and friable (Parkash *et al*., 2011, Harmon, 2007).

Mannitol, a polyol isomer of sorbitol, is one of the most widely used fillers/diluents in ODTs as it has sweet taste and cooling effect within the mouth upon its disintegration, whilst also being non-hygroscopic, minimising moisture uptake into the tablet during storage (Yoshinari *et al*., 2002). Although it is widely employed within ODT formulations in high concentrations (Jung *et al*., 2012), its primary disadvantage is that it fragments under compaction resulting in mechanically weak and friable tablets (Carlson and Hancock, 2006, Westermarck *et al*., 1998). Mannitol has a needle shaped crystal particle with very little or no amorphous regions (Campbell Roberts *et al*., 2002, Yu *et al*., 1998, Ho *et al*., 2009). Kaminsky and Glazer (1997) identified that mannitol exhibited five crystal planes; (011), (010), (120), (110) and (210). Similarly, a study by Ho. *et al*. (2012) identified that large recrystallised mannitol needles tended to fracture at the (010) and (011) planes, as shown in Figure 2.1, with the lowest attachment energy and shortest dimensions across all axis respectively. The particle shape of mannitol contributes to its increased fracture behaviour and low plastic deformability, as the crystal tends to break into smaller fragments. These smaller fragments then interact with the dies causing high friction (Abdel-Hamid and Betz, 2011), subsequently inhibiting strong bond formation between

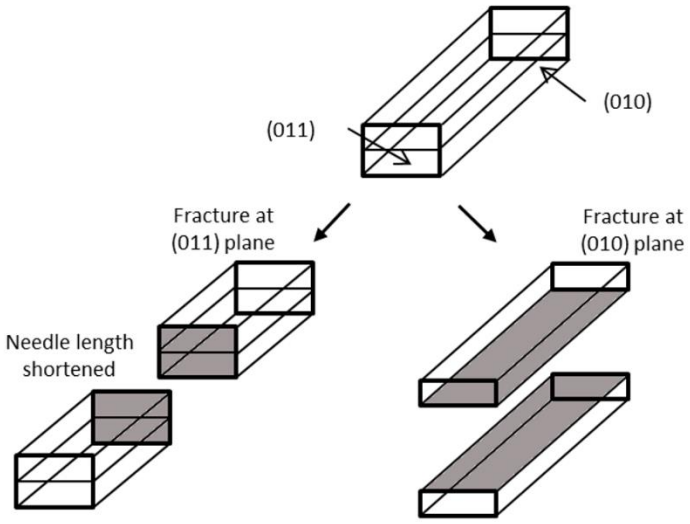

Figure 2.1: Diagram illustrating the fracture planes for mannitol crystals along with the two most common fracture processes; cleavage at (011) where needle length is shortened and cleavage at (010) where needle width is reduced.

the particles (Carlin, 2008). It has been reported that fragmentation can be advantageous for certain excipients, particularly lactose, as the increased number of particles leads to a larger number of bonding sites during compression (Vromans *et al*., 1987). However with mannitol, the high die wall friction, due to the interaction of the needle fragments with the dies, leads to poorly formed compacts. Mannitol has three polymorphic forms; alpha (α), beta (β) and delta (δ), with β being the most stable, δ being the least stable and α exhibiting intermediate stability between the two (Willart *et al*., 2007). It has been shown that the β polymorph exhibits the highest die wall friction, which in turn reduces compressibility, forming mechanically weak tablets (Burger *et al*., 2000), but is the widely available form due to its highly stable nature.

The aim of this study was to assess the fracture behaviour of unmodified crystalline mannitol using ball milling as a method of energy input into the particles. Particle size reduction during tableting occurs between the punches as the upper and lower punches exert energy into the powder and cause subsequent fracture of the mannitol crystals. Particle size reduction through high energy input was used to assess the fracture behaviour of mannitol and to develop an understanding of the fragmentation of the excipient during the tableting process. The morphology and powder

characteristics of the milled powders were assessed using multiple techniques such as; scanning electron microscopy; atomic force microscopy; dynamic vapour sorption and differential scanning calorimetry, to determine the exposed plane after particle size reduction. It was hypothesised that X-ray diffraction could be used as a novel method to predict energy input during milling, as the increased number of particles alongside a loss in their crystallinity during the milling process presented an overall reduction in the intensity of diffracted x-rays. In addition, compressibility was evaluated, with a view to investigating a pragmatic strategy to overcome the limitation of particle breakdown and widen the use of mannitol in various solid dosage forms.

2.2 Methods

2.2.1 Materials

D-Mannitol (≥98% purity) was obtained from Sigma-Aldrich (Dorset, UK) and magnesium stearate was obtained from Fischer Scientific (Loughborough, UK). Both powders were used as received.

2.2.2 Preparation of Ball Milled Powders

Milled samples were prepared using a Fritsch Pulverisette 7 planetary ball mill (Idar-Oberstein, Germany) according to parameters shown in Table 2.1. Powders were accurately weighed according to the ball to powder weight ratio (BPR) stated for each powder. The weighed samples were transferred into agate vials (45 cm^3 volume) along with 13 agate balls (diameter 10 mm). The vials were sealed with a plastic ring to prevent atmospheric contamination. Non-milled mannitol (F0) was used as a control.

2.2.3 Energy Involved in Ball Milling

The energy input into the powder during milling was calculated based on the hypothesis developed by Burgio *et al*. (1991), Maurice and Courtney (1990), and Abdellaoui and Gaffet (Abdellaoui and Gaffet, 1994, Abdellaoui and Gaffet, 1995). The calculated values were an estimation of the overall energy input per unit mass, into the system as it was virtually impossible to view what was happening

Table 2.1: The milling parameters used to prepare the different powders tested in this study, with varying milling times, rotation speed and ball:powder weight ratio. Non-milled mannitol (F0) was used as a control

Powder	Milling Time (min)	Rotation Speed (RPM)	BPR
F1	30	200	10
F2	30	200	5
F3	30	400	10
F4	30	400	5
F5	15	200	10
F6	15	200	5
F7	15	400	10
F8	15	400	5

inside the vials to enable an exact calculation of the energy input. However it was assumed milling was conducted under ideal conditions, therefore the equations provided an estimation of the energy input per unit mass into the powder bed upon altering the milling parameters. Figure 2.2 shows a schematic diagram of some of the parameters of the ball mill system that were used as integral parts of the energy calculation equations.

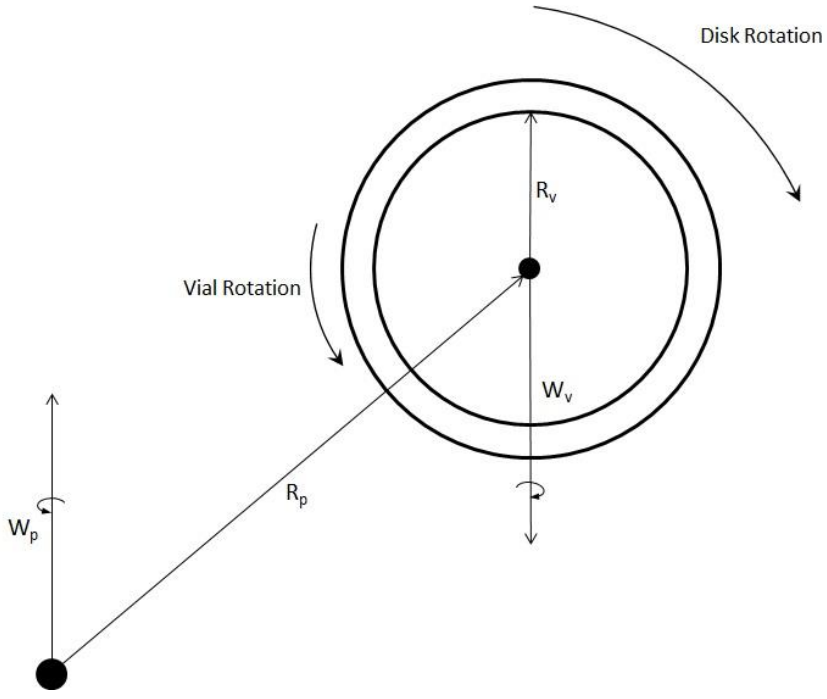

Figure 2.2: A schematic diagram of some of the mill parameters used in the calculation for energy input. This includes angular velocity of the disk (W_p) angular velocity of the vial (W_v), disk radius (R_p) and vial radius (R_v)

The speed of the mill was firstly converted from RPM to radians to allow angular velocity to be calculated with the equations:

$$\text{Radians} = \left(\frac{RPM}{60}\right) \times 2\pi \quad \text{(Eq. 2.1)}$$

$$\text{Angular Velocity} = Radians \times R_p \; or \; R_v \quad \text{(Eq. 2.2)}$$

With R_p representing the radius of the disk (distance from centre of disk to centre of vial), and R_v representing the radius of the vial (distance from centre of vial to vial wall). This enabled the angular velocity of the disk (W_p) and vial (W_v) to be calculated. The angular velocity of the vial was negative as the vial movement was in the opposite direction to the movement of the disk.

Once angular velocities had been calculated the absolute velocity of one ball detaching from the vial wall (V_b) was given by:

$$V_b = [\ (W_p\ R_p)^2 + W_v^2\ (R_v - d_b/2)^2\ (1 - 2W_v/W_p)\ ]^{1/2} \quad \text{(Eq. 2.3)}$$

With d_b representing the diameter of the ball. The velocity of the ball after the collision with the powder/inner wall (V_s) was given by:

$$V_s = [\ (W_p\ R_p)^2 + W_v^2\ (R_v - d_b/2)^2\ + 2W_pW_vR_p\ (R_v - d_b/2)\ ]^{1/2} \quad \text{(Eq. 2.4)}$$

Once the velocity of the ball was calculated, it enabled the kinetic energy of that ball to be worked out. When the ball was launched from the vial wall the kinetic energy (E_b) was given by:

$$E_b = (1/2)\ m_b V_b^2$$

With m_b being the mass of one ball. During the collision of the ball with the powder/inner vial wall only a small amount of the kinetic energy of the launched ball was released, which was the energy imparted to cause particle fracture/deformation within the milling system. The residual energy of the ball after the collision event (E_s) was calculated with the equation:

$$E_s = (1/2)\ m_b V_s^2$$

This allowed the total energy released by that single ball to be calculated:

$$\Delta E_b = E_b - E_s = -m_b\ [\ W_v^3(R_v - d_b/2)\ /\ W_p\ +\ W_pW_vR_p\ ]\ (R_v - d_b\ /\ 2) \quad \text{(Eq. 2.5)}$$

For the theoretical energy value to be a more accurate estimation, the degree of filling of the vial by the balls had to be considered, as the balls inevitably collided and hampered each other's movement. The vial filling factor (φ_b) had two limiting factors, φ_b=1 for only one or very few balls in the vial or

φ_b=0 for when the vial was completely full and no movement possible. In the experiment the amount of free space within the vial was calculated using measurements of the empty and filled vial, and the vial filling factor worked out as a percentage. The adjusted equation became:

$$\Delta E_b^* = \varphi_b \Delta E_b \quad \text{(Eq. 2.6)}$$

With ΔE_b^* representing the energy release of one ball within a system containing a certain number of balls (N_b).

The value for total energy transfer per unit mass from the mill into the powder (E/m_p) was calculated using the equation:

$$\frac{E}{m_p} = -\varphi_b N_b m_b t\left(W_p - W_v\right)\left[W_v^3\left(R_v - d_b/2\right)/W_p + W_p W_v R_p\right]\left(R_v - d_b/2\right)/2\pi m_p \quad \text{(Eq. 2.7)}$$

The equation included all variables that were altered during the milling process; time (t); the mill speed/angular velocities of the disk and vial (W_p and W_v respectively); and the powder weight (m_p). Values such as vial filling factor (ϕ_b), number of balls (N_b), the mass of a ball (m_b) and the ball diameter (d_b) were all kept constant. The radius of the vial (R_v) and disk (R_p) were also constant according to the manufacturers design.

2.2.4 Scanning Electron Microscopy (SEM)

SEM micrographs were obtained using a Phillips XL-30 FEG ESEM (Eindhoven, Netherlands) to allow an exploration of particle shape/size and fracture behaviour. Approximately 1mg of each sample was adhered to a double-sided adhesive strip and placed on to an aluminium stub. The samples were coated with a thin layer of gold using an Emscope SC500 sputter coater (Quorum Technologies, Lewes, UK) at 20 mA for 1 minute. After gold coating each sample was examined using SEM, with the acceleration voltage (kV) and magnification stated on each monograph.

2.2.5 Atomic Force Microscopy (AFM)

Acquisition of topographical data was performed using a NanoWizard II AFM (JPK Instruments, Cambridge, UK) operating in force scan mapping mode under ambient conditions (18 ^{o}C, 50 % relative

humidity). This involved the use of a scanner with a maximum lateral range of 100×100 µm and a maximum vertical range of 15 µm. Data acquisition was performed using rectangular Si cantilevers (HQ:CSC17/noAl, MikroMasch, Sofia, Bulgaria) having pyramidal tips with 10nm nominal radii of curvature. Cantilever spring constants were of the order 0.3 N/m, calibrated according to the method reported by Bowen *et al.* (Bowen *et al*., 2010). Topography was assessed over a 2x2 µm area using a grid of 128x128 pixels. Data was acquired by driving the fixed end of the cantilever at a velocity of 50 µm/s towards the sample surface, whilst monitoring the deflection of the free end of the cantilever using a laser beam. Upon making contact with a surface feature, the height of the contact point was recorded, representing one pixel in the image, which was converted into a map of surface topography. A maximum compressive load of 10nN was applied to the surface during data acquisition.

2.2.6 X-ray Diffraction (XRD)

XRD was performed using a Bruker D2 Phaser (Massachusetts, USA) equipped with a Co-Kα tube (1.78896 Å). Approximately 1g of each powder was analysed across an angular range (2Θ) of 10-50° in steps of 0.02° every 0.25 s. A rectangular beam of size 0.6mm was used for measurement and the sample spun at 15rpm to allow maximum surface analysis. XRD patterns were obtained in counts per second (cps) and analysed using Eva 18.0 software. To quantify the polymorphic composition a Rietveld refinement was performed using MAUD software 2.49 (Luca Luterotti, University of California, USA) (Lutterotti, 2010). Calculated patterns for the mannitol polymorphs were obtained from the Cambridge Crystallographic Data Centre and imported into MAUD. The XRD patterns were then fitted to the calculated patterns and percentages of each polymorph generated using MAUD.

2.2.7 Particle Size analysis

Laser diffraction was employed to measure particle size using a Sympatec HELOS/BR equipped with a RODOS dry dispersing system with VIBRI/I feeder (Clausthal-Zellerfeld, Germany). Around 1 g of sample was placed on the VIBRI/I feeder and dispersed through the RODOS with 2 bars of pressure.

The volume mean diameter (VMD) of each sample was detected on the HELOS/BR set at a measuring range of 0-175 µm. All powders were analysed in triplicate and presented as mean ± SD.

2.2.8 Powder Flow analysis

A Sotax tap density tester USP II apparatus (Allschwil, Switzerland) was used to measure the bulk (ρ_{bulk}) and tapped density (ρ_{tapped}) of each sample following the test parameters set out in the USP monograph <616> (USP37, 2014a). A 50 mL cylinder was used for measurement as there was a limited quantity of sample available. Powder flow was analysed using the Carr's index/Hausner ratio equations.

$$Carr's \quad Index = \frac{\rho_{tapped} - \rho_{bulk}}{\rho_{tapped}} \times 100 \qquad \text{(Eq. 2.8)}$$

$$Hausner \quad Ratio = \frac{\rho_{tapped}}{\rho_{bulk}} \qquad \text{(Eq. 2.9)}$$

2.2.9 Differential Scanning Calorimetry (DSC)

DSC was undertaken on a TA Instruments DSC Q200 (Delaware, USA) using nitrogen as purge gas to analyse thermal properties of powders post-milling. DSC heat flow was calibrated using indium (melting point 156 °C), and samples weighing 3±0.1mg were sealed inside Tzero pans. A sealed empty Tzero pan was used as a reference, and each sample was ramp heated at 10 °C/min from 30 °C to 180 °C to detect for thermal differences. Analysis of the thermographs was performed using TA Universal Analysis 2000 software v4.5A. Each powder was analysed in triplicate.

2.2.10 Dynamic Vapour Sorption (DVS)

Specific surface area (SSA) and surface energy measurements were performed using a Dynamic Vapour Sorption instrument (DVS Advantage, Surface Measurement Systems, London, UK). Samples of powder in the range 20-60 mg were dried for a minimum of 4 hours using oxygen-free nitrogen, before being subjected stepwise to increasing partial pressures of octane (HPLC grade, Sigma-Aldrich,

Dorset, UK) from 0-90 % in 5 % increments. The chamber temperature was kept constant at 25±0.1 °C. Samples were allowed to reach a near-equilibrium state (%dm/dt = 0.0005 % min^{-1}) at each partial pressure step before progressing to the next stage. Application of the Brunauer-Emmett-Teller (BET) theory (Brunauer *et al*., 1938) was employed for calculation of the SSA, fitting data in the partial pressure range 5-60 %. Surface energies were calculated using the Advanced Analysis Suite in the DVS software.

2.2.11 Compressibility analysis using Heckel Profiling

To analyse compressibility differences between milled and non-milled powders, in-die/out-of-die Heckel analysis were performed (Heckel, 1961a). A Hounsfield Test Equipment H10K (Tinius Olsen, Pennsylvania, USA) equipped with 13 mm flat faced punches, a compression range of 0-40 MPa and upper punch speed of 400 mm/min was used to compress the powders into ODTs for in-die Heckel analysis. Dies and punches were externally lubricated using a 5 % magnesium stearate in acetone solution before each measurement. An accurately weighed sample of 500 mg of each powder was filled into the dies for each test run. A Heckel plot follows first order kinetics and is a model that represents densification of solids under pressure.

$$Heckel \quad Equation = \ln\left[\frac{1}{1-D}\right] = P \times K + A \qquad \text{(Eq. 2.10)}$$

Where (ln[1/1-D]) is plotted against compaction pressure (P), with K being the gradient from the linear portion of the plot. K was obtained above 30 MPa i.e. the linear region with R^2>0.98, with the reciprocal of K representing the in-die yield pressure (P_y). All powders were repeated for triplicate measurements.

An out-of-die Heckel analysis was performed to supplement in-die Heckel data. 500 mg samples of each powder were weighed and compressed using a Specac semi-automatic hydraulic press (Slough, UK) equipped with 13mm flat faced dies at compression forces ranging from 75-300 MPa. Dies and punches were externally lubricated with a 5 % magnesium stearate in acetone solution. Porosity of

the tablets was assessed post ejection, true volume was obtained using a Quantachrome Helium Multipycnometer (Florida, USA), and bulk volume taken using tablet diameter and thickness measured with a digital calliper. The Heckel plot was drawn up as -ln(porosity) against compaction pressure and the reciprocal of the gradient taken as the out-of-die yield pressure (P_y).

2.2.12 Tableting Studies

ODTs were prepared using a blend of 99.5 % mannitol and 0.5 % magnesium stearate mixed for one minute. Tablets were compressed using a Specac semi-automatic hydraulic press (Slough, UK) equipped with 13mm flat faced punches at compression forces of 75/225 MPa. ODTs were analysed immediately after manufacture to reduce storage effects.

2.2.12.1 Hardness

Hardness of the tablets was measured using a Copley TBF 100 Hardness tester (Nottingham, UK). Tensile strength (σ) was then calculated using the equation:

$$\sigma = \frac{2\,H}{\pi\,D\,T} \qquad \text{(Eq. 2.11)}$$

Where H is the hardness, D is the diameter and T is the thickness of the tablet. All readings were taken in triplicate and displayed as mean ± SD.

2.2.12.2 Disintegration Time

The standard USP disintegration method was used to assess disintegration time of the tablets (USP37, 2014b). A Copley ZT41 disintegration apparatus (Nottingham, UK) was used, with a single tablet being tested each time for accuracy. Each tablet was placed in the vessel (without a disk) and oscillated at 30 cycles per minute. A dissolution medium of 800ml distilled water was maintained at 37 °C, and disintegration time measured when all of the fragments of tablet had passed through the mesh at the bottom of the vessel. All readings were taken in triplicate and represented as mean ± SD.

2.2.12.3 Porosity

Porosity of the tablets was assessed using a Quantachrome Helium Multipycnometer (Florida, USA). Diameter and thickness of the ODT's was measured using a digital calliper, and the weight of individual ODT's taken using an electronic balance. The bulk volume (V_B) and bulk density (ρ_{bulk}) of the tablets were then calculated using the following equations:

$$V_B = \frac{\pi R^2}{T} \quad \text{(Eq. 2.12)}$$

$$\rho_{bulk} = \frac{Tablet\ weight}{V_B} \quad \text{(Eq. 2.13)}$$

The true volume (V_t) of the tablet was calculated using the pycnometer, which applies the theory of gas displacement allowing the porous nature of the tablet to be assessed. The true volume was calculated using the equation:

$$V_t = V_c - V_r \left(\frac{P1}{P2} - 1\right) \quad \text{(Eq. 2.14)}$$

Where V_C is the volume of the sample cell, V_r is the volume of the reference cell, P1 and P2 are the atmospheric pressure and pressure change during the measurement respectively. The true volume was then used to calculate true density in the equation:

$$\rho_{true} = \frac{Tablet\ weight}{V_t} \quad \text{(Eq. 2.15)}$$

The final step to calculate porosity (ε) of the ODT used the following equation:

$$\varepsilon = 1 - \frac{\rho_{bulk}}{\rho_{true}} \quad \text{(Eq. 2.16)}$$

All results were taken in triplicate and presented as mean ± SD.

2.2.13 Stability Study

Stability testing of three of the milled mannitol powders was conducted. Powders F1, F2 and F8 were chosen based on their favourable powder and ODT characteristics due to the optimum levels of energy

input per unit mass into the powder during the milling process. Stability testing was conducted according to ICH guidelines, (ICH, 2003). Powders were freshly milled and placed inside opaque plastic containers and sealed with a twist lid. Each formulation was tested in ambient and accelerated conditions, with humidity cabinets (Fraiolabo, Meyzieu, France) set at 25 °C with 60 % relative humidity (RH) and 40 °C with 75 % RH. Powders were tested over a 6 month period, with testing occurring at 2 weeks, 4 weeks, 2 months, 3 months, 4 months and at the 6 month end. Powders were tested for melting point using DSC to establish crystal state, alongside XRD analysis, and degradation and moisture content of the powders tested using thermogravimetric analysis (TGA). TGA analysis was conducted on a Perkin Elmer Pyris 1 TGA (Massachusetts, USA). Approximately 5 mg of each sample was carefully weighed into the sample pan and tested over a temperature range of 30-300 °C, with a heat ramp of 10 °C/min. Moisture content was measured between the range of 70-130 °C, and degradation temperature taken when the % loss of material started to rapidly decrease towards 0 %.

2.2.14 Flow Improvement Study

To assess the possibilities of mannitol being used in a commercial formulation a flowability study was conducted to see if it was possible to tablet milled mannitol through an auto tablet press (Riva MII Minipress, Hampshire, UK). Materials assessed for flow improvements, alongside milled mannitol, included varying concentrations of Starch 1500® (4-20 %) (Colorcon Inc, Pennsylvania, USA) and 0.5 % fumed silica (Aerosil 200, Evonik Industries, Essan, Germany). To investigate flow two mixing methods were assessed, standard cube mixing in an Erweka AR403s (Heusenstamm, Germany) with the cube mixer attachment; and novel composite mixing using a novel blender developed in our laboratory. Cube mixing was conducted for 10 mins at a speed of 250 rpm. Composite blending was conducted at speeds from 1500-2000 rpm for 10-30 mins, with and without air pressure. Angle of repose was used as the method of choice for assessing powder flow of the investigated blends. For angle of repose the method outlined in the USP monograph <1174> (USP37, 2014c) was followed, and the height and diameter of the pile measured. This was then added to the equation, $\tan(\Theta) = \text{height}/0.5\text{diameter}$,

where Θ was the angle of repose. All powders were analysed in triplicate and results displayed as mean ± SD.

Tablets of approximately 500 mg weight and of 13 mm diameter were compressed on a Riva MII Minipress (Riva, Hampshire UK), at a compression force 10 KN. MCC (Avicel PH102, FMC Biopolymer, Philadelphia, USA) was used as a comparison to Starch 1500® as it is a popular dry binder used in ODT formulations. Magnesium stearate (Fischer Scientific, Loughborough, UK) 1 % was used as a lubricant. A powder preblend of milled mannitol 87.5 %, Starch 1500®/MCC 12 % and silica 0.5 % was produced, the preblend (99 %) was then mixed with magnesium stearate (1 %) to be tableted. Tablets were assessed for hardness, disintegration time (as above) and friability using a Sotax F2 Friabilitor (Allschwil, Switzerland). Ten tablets were brushed off and weighed altogether for the initial weight, they were then inserted friabilitor. The test was conducted for a total time of 4 minutes at 25 rpm, with 100 revolutions in total. The tablets were then brushed off and reweighed to get the final weight. Percentage friability was calculated using the equation:

$$\%\ Friability = \frac{Initial\ weight - Final\ weight}{Intial\ weight} \times 100 \qquad \text{(Eq. 2.17)}$$

Uniformity of weight was conducted according to BP requirements (BP, 2015), with 20 tablets weighed at random and the % deviation from the mean calculated.

2.2.15 Statistical Analysis

One way ANOVA followed by a Tukey's multiple comparison post-hoc test / Two way ANOVA followed by a Sidaks multiple comparison post hoc test were performed using GraphPad Prism 6 software (California, USA). For statistical significance a p-value <0.05 was used, and all data was presented as mean ± standard deviation.

2.3 Results and Discussion

2.3.1 Milling Energy Input and Crystal State

The first set of investigations were focused on evaluating the energy input on various processing parameters such as ball-to-powder weight ratio (BPR), speed of rotation and duration of milling.

Theoretical energy calculations showed that mill speed was the most influential factor in increasing the energy input during each milling cycle, with powders processed at 400 rpm experiencing an eight fold increase in energy input compared to 200 rpm; whereas doubling the milling time and BPR resulted in doubling of the theoretical energy input. Results, presented in Table 2.2, indicated that powder F3 had the highest amount of energy input per unit mass, as expected, as it had all three of the highest parameters, and that powder F6 had the lowest amount of energy input per unit mass due to it having all of the lowest values for all the variables. However from the theoretical calculations it was seen that there was an overlap for the calculated energy between powders F2/F5, and F4/F7. This was because the theoretical calculations included limitations in that they were calculated based on ideal conditions, where it had to be assumed that the heating of the vial was negligible; the powder was only affected by energy transfer from the balls to the grinding media and that the majority of energy input occurred during the collision of the balls against the powder along the wall of the vial.

In order to overcome the limitations presented with theoretical calculation of energy, it was hypothesised that XRD patterns could be investigated as a novel tool for prediction of energy input, on the premise that the increased number of particles combined with a loss in crystallinity of the material would impact on peak intensity of the diffraction pattern, provided the polymorphic form of the material remained unchanged. To evaluate our hypothesis, initial investigations were aimed at studying peak intensity changes of the diffracted x-rays between non-milled and milled powders of mannitol. The XRD patterns for F0 and the subsequent milled powders represented strong fits for β-D-mannitol, as shown in Figure 2.3 (Hulse *et al*., 2009, Kim *et al*., 1998). XRD data showed that milling had caused a reduction in peak intensities along the patterns obtained for all milled powders as

Table 2.2: A table showing the theoretical energy inputs into the milled powders (F1-F8), along with the reduction in peak intensities observed upon XRD analysis with a subsequent energy ranking according to XRD data. Percentage of alpha mannitol within the powders is also included as obtained through Rietveld refinement. Morphological and topographical characteristics of the mannitol particles are also included for all powders; Data indicates particle size/surface area and flowability, alongside the surface roughness and surface energy of the powders. Data marked with a single asterisk (*) indicates results that are significantly different from the control (ANOVA $p<0.05$ when compared to F0). (**) indicates the rank order of energy input according to XRD peak intensity reduction data.

Powder	Theoretical energy input per unit mass (J/kg)	% reduction in peak intensity in comparison to F0**	% Alpha Mannitol present	Particle Size VMD (µm)	BET Surface Area (m^2/g)	Carr's Index	Hausner Ratio	AFM average surface area roughness Ra (nm)	DVS Surface Energy (mN/m)
F0	-	-	0.00	36.54 ± 0.28	0.261	38.91 ± 1.38	1.64 ± 0.04	20.39	73.37
F1	3.42	47.59 [5]	0.70	10.46 ± 2.51*	2.183	39.89 ± 1.03	1.67 ± 0.03	51.59	67.45
F2	1.71	44.83 [6]	0.26	11.76 ± 1.58*	1.585	38.85 ± 2.04	1.64 ± 0.06	188.8	63.79
F3	27.37	68.97 [1]	0.54	20.00 ± 1.61*	3.302	33.33 ± 2.08*	1.50 ± 0.05*	90.28	65.27
F4	13.69	60.00 [3]	0.24	14.51 ± 1.91*	3.173	34.03 ± 1.20*	1.52 ± 0.03*	163.4	64.74
F5	1.71	33.03 [7]	0.38	11.14 ± 0.38*	1.633	39.12 ± 1.06	1.64 ± 0.03	110.8	66.75
F6	0.86	15.17 [8]	0.40	16.96 ± 0.18*	1.068	37.50 ± 1.79	1.60 ± 0.05	131.0	63.96
F7	13.69	62.76 [2]	0.19	14.38 ± 1.81*	3.486	38.61 ± 1.36	1.63 ± 0.04	115.5	64.07
F8	6.84	58.62 [4]	0.24	11.46 ± 0.44*	2.826	41.83 ±1.78	1.72 ± 0.05	162.8	63.14

illustrated in Figure 2.3. The process of milling had produced particles of reduced crystal size, leading to increased numbers of particles under examination by the x-ray beam, this lead to differences in orientation of the sample which therefore affected the intensity of the diffracted x-rays (Baerlocher and McCusker, 1994). Additionally, a reduction in the crystallinity within the particles, from continued

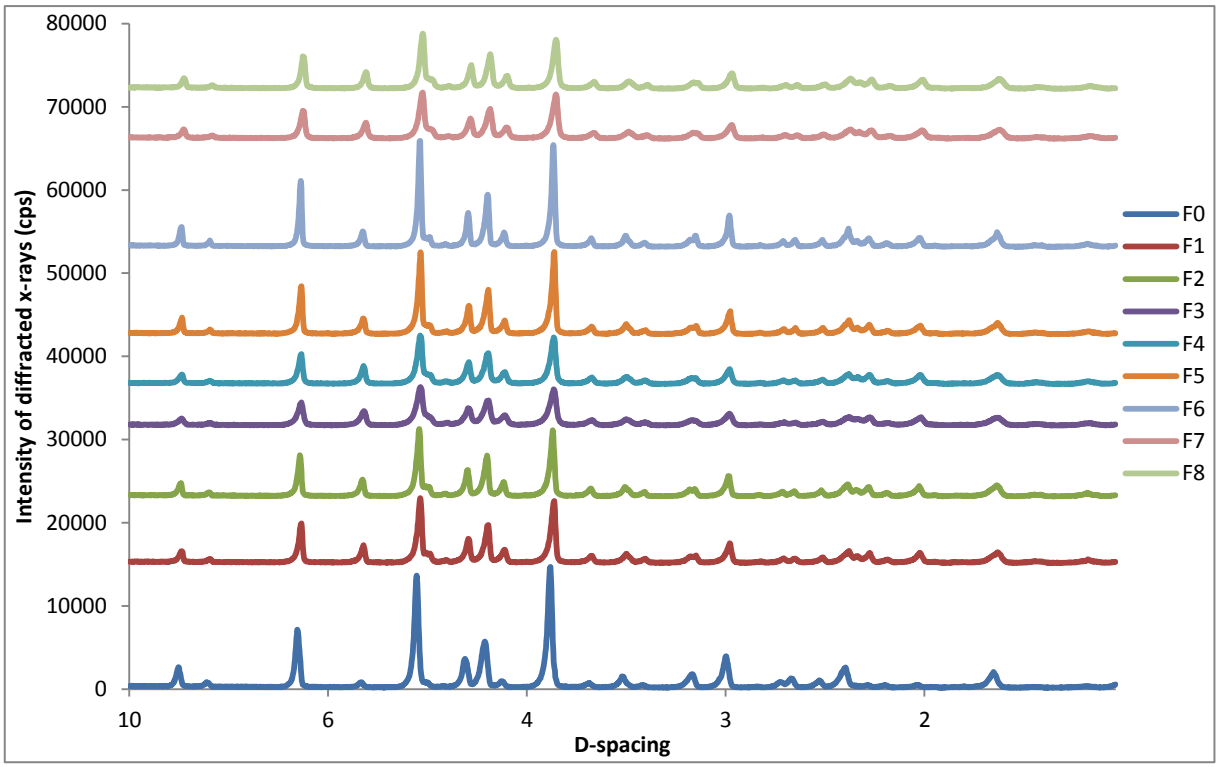

Figure 2.3: X-ray diffraction patterns showing that all powders tested represent a strong fit for β-D-Mannitol. The patterns for milled mannitol (F1-F8 (F0 line at bottom to F8 line at top)) also indicate the extent of peak intensity reduction across all milled powders compared to unmilled mannitol (F0), with Table 1.2 showing the corresponding percentage of peak intensity reduction.

collisions with the milling media, resulted in further lowering of peak intensity observed on XRD data(Rao *et al*., 2011, Tan *et al*., 2012).

The extent of peak reduction on the XRD patterns correlated well with the theoretical energy calculations, as shown in Table 2.2. For the peak intensity reduction calculations, the large right hand side peak at a d-spacing of 3.82 was used as this was the most prominent peak in β mannitol, and is almost 0 counts per second in α mannitol (Hulse *et al*., 2009, Kim *et al*., 1998). The results from the XRD patterns showed that powder F3 exhibited the sharpest peak intensity reduction at around 69 %, whereas F6 had the lowest peak intensity reduction at around 15 %. This was related to the increased number of particles and their crystallinity, as the higher amount of energy input into the milling system caused a larger number of collisions between the balls and powder. Therefore a greater level of strain was placed upon crystal lattice, whilst milling also cleaved and refined the crystal to a higher extent, reducing the peak intensities along the XRD plots (Rao *et al*., 2011, Tan *et al*., 2012). The XRD data therefore provided a good model to define the exact order of energy input, as each separate powder

had different degrees of peak reduction. This allowed an order to be distinguished between powders F2/F5, and F4/F7; with F2 having a higher energy input than F5 and F7 having a higher energy input than F4.

Equation 2.18 was developed according to the data obtained, and expresses peak intensity reduction (*I*) as a function of energy input per unit mass (E/m_p), where I_{max} is the maximum peak reduction, *a* is a constant and *b* is an exponent. Measured and calculated results were compared in Figure 2.4, and the model suggested that as the energy input was increased the value of $[1-(a/(E/m_p)^b]$ decreased, which in turn resulted in a larger *I* value. However the peak intensity reduction plateaued as energy input was increased towards the higher values.

$$\Delta I = \Delta I_{\max}\left[1-\left(\frac{a}{(E/m_p)}\right)^b\right] \qquad \text{(Eq. 2.18)}$$

Previous work had suggested that milling mannitol resulted in a transformation from the β to the α-

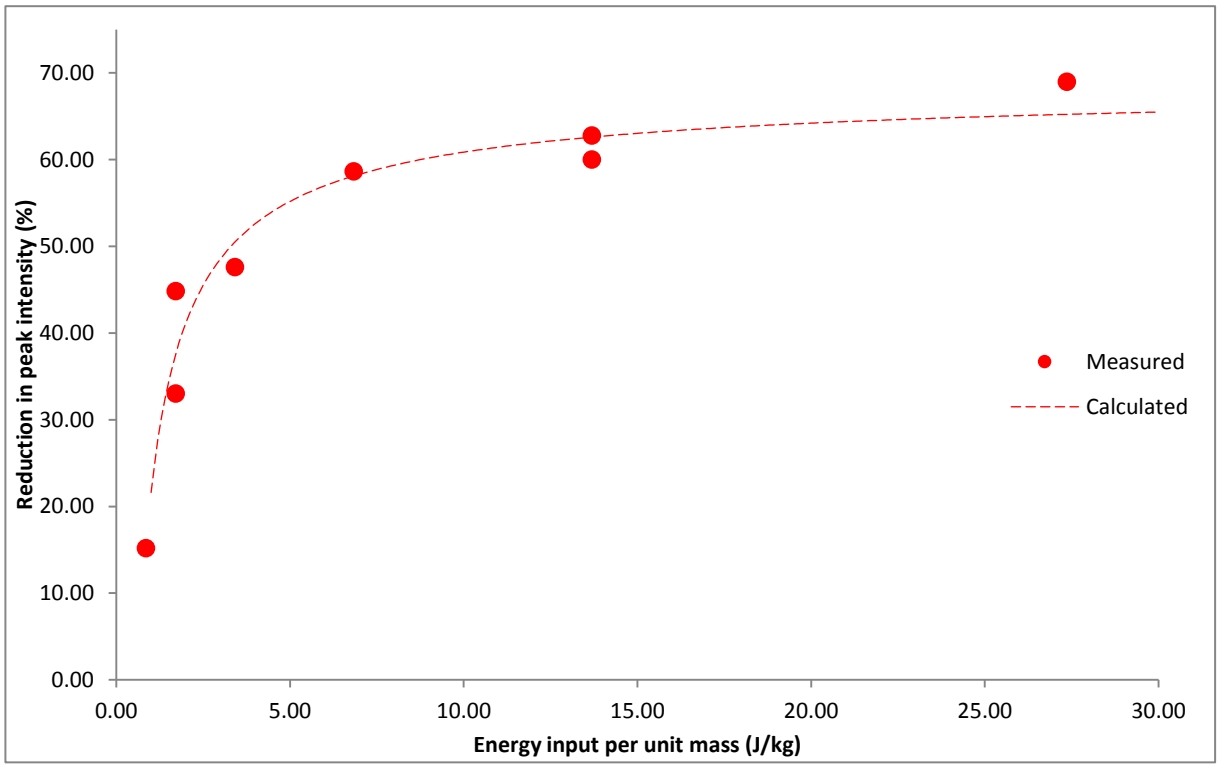

Figure 2.4: A graph comparing measured values of peak intensity reduction to the values calculated using Equation 2.18, against energy input per unit mass, showing that this model represents a good fit and provides a novel method of calculating energy input during milling.

polymorph after a three hour cycle (Descamps *et al*., 2007). In the current study a Rietveld refinement (Lutterotti, 2010) was conducted to quantify the polymorphs of mannitol present in all of the samples. The refinement indicated a very small/negligible amount of α mannitol present in the milled powders, as shown in Table 2.2, with the samples being composed of >99 % β mannitol. This very small percentage of α mannitol may have been due to contamination, or polymorphic transformation as the peak at a 2Θ of 27° reduced down towards zero, as would be observed on a typical plot for α mannitol. Additionally, the milling time employed in this study was very short compared to the previous study and as such it was likely that higher energy input was needed to witness a greater percentage of the alpha polymorph within the milled samples. However DSC thermal profiling, as shown in Figure 2.5, also suggested that there was little difference in the crystal state post-milling, as the thermal profiles had remained very similar to F0. This suggested that there were no amorphous regions in the milled samples and they were composed of the β polymorph.

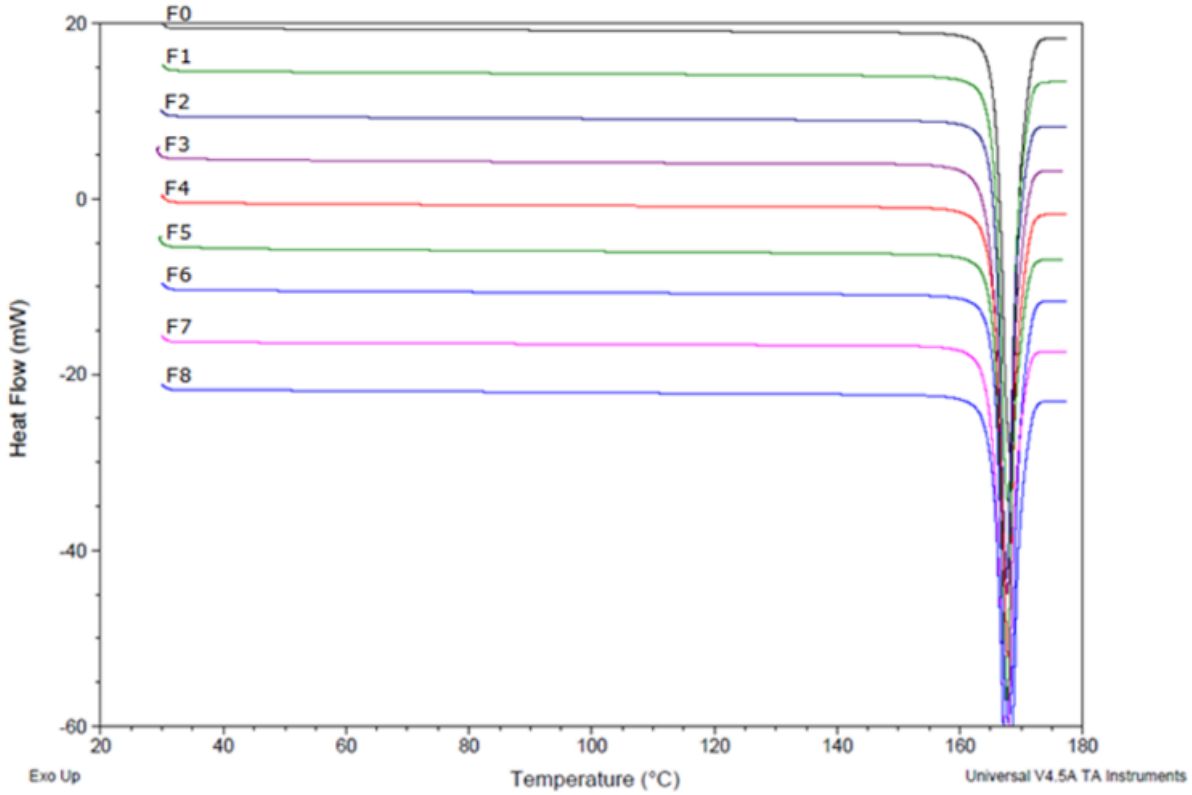

Figure 2.5: DSC scan of non-milled mannitol (F0) compared to milled powders (F1-F8) showing no difference in melting point, enthalpy of fusion or onset of melting, indicating there was no alteration in crystal state or structure.

2.3.2 Powder Properties and Morphology

It was evident from SEM images, as seen in Figure 2.6 that milling had caused a drastic alteration in the particle morphology of the mannitol crystals. It was observed that the control, F0, had the characteristic needle shape of mannitol, with a varied particle size on the SEM images, some being as large as 50 µm, and other particles around 37µm, as found during particle size analysis (Table 2.2). It was also recorded that the particles were fairly smooth, and results from AFM surface roughness analysis also confirmed that the non-milled mannitol had a roughness (Ra) of around 20.39 nm (Table 2.2). From the SEM it was observed that milling had modified most of the needle like structure of the original crystal to more globular structures, with maximum particle size reduction down to a size of around 10-11 µm, as observed in powders F1, F2, F5 and F8. However, the powders with higher energy input displayed an increased particle size VMD, with powder F3 having a VMD of 20 µm and powders F4 and F7 having a VMD of around 14 µm. This wasn't expected as it was anticipated that the highest energy powders would have had the most particle size reduction. However due to the high level of energy input, the particle size reduction of the mannitol crystals had reached its maximum and subsequent agglomeration had started to occur. This was evident on the SEM images, as the white arrows on powder F3 and F7 indicated the presence of large agglomerates (Balaz, 2008). As the particles were reduced in size, they started to become more cohesive possibly due to the increased surface area which subsequently, through larger van der Waals forces and electrostatic interactions produced larger agglomerates. It was proposed that the small particles produced during the milling process had aggregated due to the high levels of cohesion and large amounts of dispersion between the particles. However as the levels of dispersion reached zero, where no further particle size reduction was possible, the repeated impact of the balls upon the aggregates induced strong bond formation between the aggregated particles, which consequently produced larger more spherical shaped mannitol agglomerates (Balaz, 2008). Conversely powder F6 had a large particle size of around 17 µm, but in this case there wasn't enough energy input into the powder to allow a substantial reduction in particle size; therefore particle sizing data indicated that an ideal energy input for

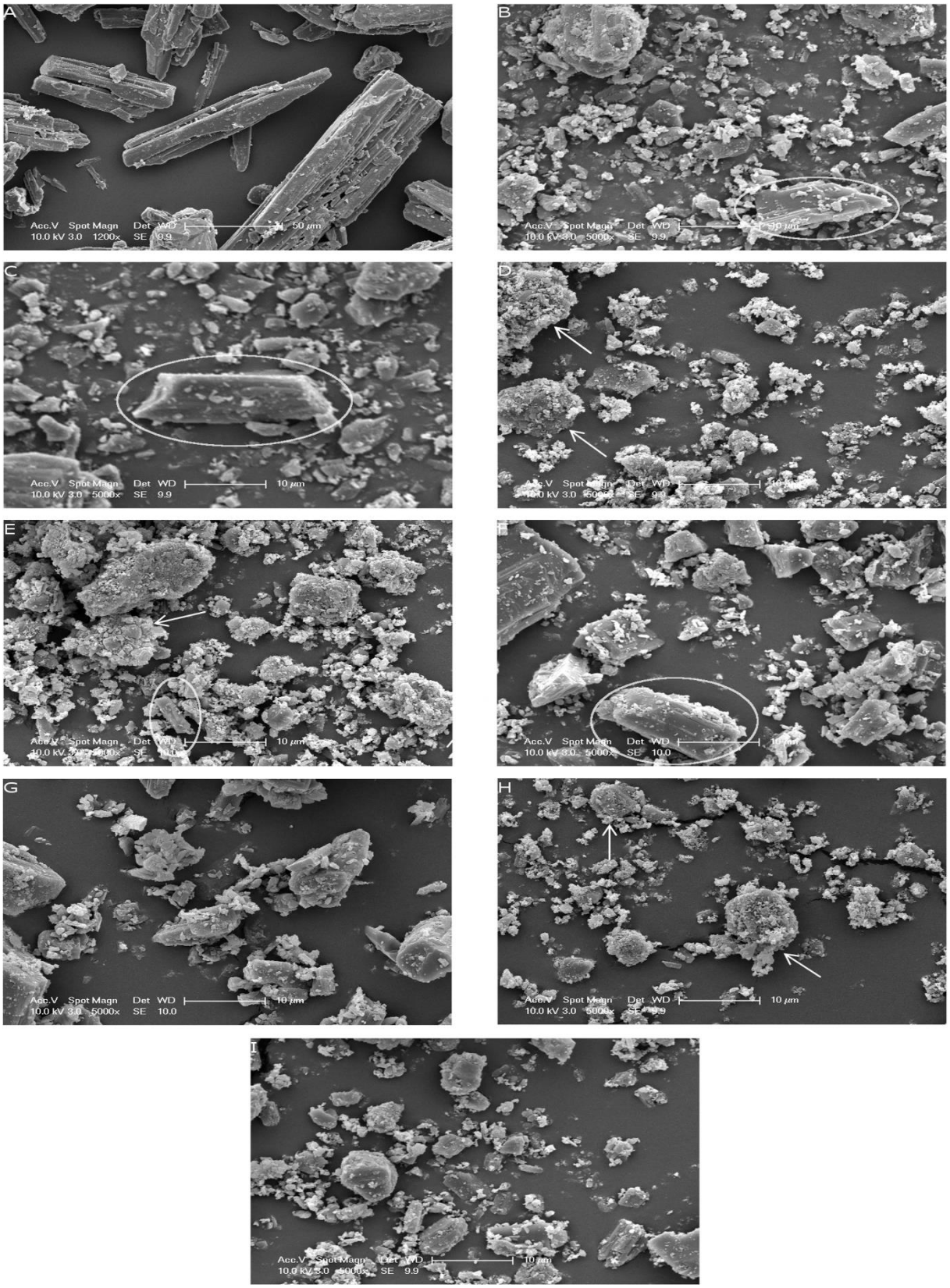

Figure 2.6: SEM images showing the morphology of the mannitol powders; A - F0 (control) showing needle like morphology at x1200 magnification (all milled samples are at x5000 magnification); B - F1, with circle indicating particle fracture at the (011) plane; C - F2, with circle indicating particle fracture at the (011) plane; D - F3, with arrows indicating agglomeration of particles; E - F4, with circle indicating particle fracture at the (010) plane, and arrow indicating agglomeration of particles; F - F5, with circle indicating particle fracture at (011) plane; G - F6; H - F7, with arrows indicating agglomeration of particles and I - F8.

maximum particle size reduction of mannitol was between 1.71-6.84 J/kg. BET surface area analysis, also confirmed that milling had caused a big shift in the powder morphology and size with an increase in the surface area from 0.2618 m^2/g up to 3.4865 m^2/g (Table 2.2). This was due to the large decrease in particle size of the powders, as was evidenced by SEM. AFM topographical analysis (Table 2.2) also indicated that milling resulted in rougher particle surfaces which gave rise to a larger surface area, due to the indentations on the milled particles. The high roughness was also an indicator that there would have been increased amounts of adhesion between the particles (Flament *et al*., 2004). SEM images also supported this theory as there was visible aggregation of the milled mannitol particles. Powder flow analysis, shown in Table 2.2 using Carr's index/Hausner ratio, indicated a very poor flow of all the milled samples. Powder flowability is essential for pharmaceutical tableting, and it was seen that the control, F0, also had very poor flow, largely due to the needle shape and the large particle size range, which promoted interlocking and segregation of the particles. However with the milled samples a more uniform shape was observed with a reduction in particle size. For most of the milled powders, the flow remained in a similar category to the control, due to the high levels of adhesion between the particles owing to increased roughness and small particle size, which also promoted interlocking and segregation. An improved flow was observed in powders F3 and F4, where the largest amount of agglomeration was produced. It can be hypothesised that the larger agglomerated particles lose the needle shaped feature of non-milled mannitol and have reduced levels of segregation and cohesive forces, due to the slightly enlarged agglomerated particles, which resulted in slightly improved powder flow, although it remained very poor.

2.3.3 Fracture Properties of Milled Mannitol

From morphological analysis of the SEM images (Figure 2.6), it was seen that the predominant plane of fracture for the crystalline mannitol was the (011) plane, as powder F2 showed a defined fracture plane parallel to the direction of growth for the crystal, and shortened the length of the particle. This was also evident in other powders, such as F1 and F5, as needle length was shorter than that observed in the control powder F0, whilst the width of the particles tended to remain at around 10 µm,

indicating that predominant fracture occurred at the (011) plane. The SEM images also showed that there was extensive particle size reduction, with particles visible within the nanometre range, which indicated high levels of cleavage at the fracture planes of the mannitol crystals. Due to this high level of particle size reduction there was likely to be some fracture at the (010) plane, where the width of the crystal had reduced due to the low attachment energy of the (010) plane, as evident on SEM for F4 in Figure 2.6. This was in agreement with work by Ho. *et al* (2012), who found that milling a large recrystallised mannitol crystal caused fracture at the (010) and (011) plane.

DVS analysis was employed to measure surface energy using octane as an organic vapour probe. The amount of adsorbed octane was calculated as a function of the partial pressure, which allowed the spreading pressure of the octane to be obtained. The spreading pressure of the probe molecule was then used in a combination of the Young's equation/Fowke's Theory to calculate the work of adhesion and therefore dispersive surface energy, as the adhesion forces between the solid and liquid probe were related to the surface energy of the mannitol powders. DVS analysis is able to measure all of the exposed crystal planes within the powder sample, thereby identifying a change in the overall dispersive surface energy. The surface energy results indicated that there was a reduction in the overall dispersive surface energy of all the milled powders (Table 2.2), which indicated that it was the low dispersive surface energy plane, (011), that was increasing in exposure. Work by Ho *et al*. (Ho *et al*., 2010) suggested that the (011) plane had the lowest dispersive surface energy of 39.5 mJ/m^2, compared to the higher dispersive surface energy of the (010) plane, at 44.1 mJ/m^2. If the (010) plane was increasing in exposure there would have been expected to be an increase in the overall dispersive surface energy of the powder, however due to the reduction in dispersive surface energy of all the powders tested, compared to F0, it was concluded that (along with SEM analysis) the predominant plane of fracture for the unmodified crystalline tableting grade of mannitol was the (011) plane, where the needle length was shortened.

To further evaluate the plane of fracture, disintegration times of ODT's prepared from different milled powders were evaluated and shown in Table 2.3 and Figure 2.7. The results indicated that at 75 MPa compression force, disintegration times tended to increase alongside the improved hardness of the tablets (Table 2.3); this was expected as the harder tablets resulted in less water being able to wick into the dosage form. However at 225 MPa, where large improvements in hardness were also observed, the disintegration time of the ODTs was generally lower than the control formulation, F0. Significant improvements in disintegration was seen in all powders, except F3 and F7 which both displayed significant improvements in hardness over the control. This indicated that the tablets had an improved wetting time, which was likely to be a contribution between the small particle size of the mannitol making up the ODT and the increased exposure of the (011) plane, which is the most hydrophilic plane

Table 2.3: A table showing the compressibility of the powders as analysed through out-of-die and in-die Heckel Analysis, with yield pressures giving an indication to the compression mechanism of the powder bed. Also displayed are the hardness and disintegration time of ODTs manufactured from milled mannitol powders (F1-F8) compared to the control (F0) at compression forces of 75 and 225 MPa. Data marked with a single asterisk (*) indicates results that are significantly different from the control (ANOVA $p<0.05$ when compared to F0).

Powder	Out-of-die Yield Pressure (MPa)	In-Die Yield Pressure (MPa)	Disintegration Time (s)		Hardness (N)	
			7 5MPa	225 MPa	75 MPa	225 MPa
F0	3333.33	144.47 ± 8.02	35.67 ± 2.08	280.00 ± 8.54	45.70 ± 5.61	120.47 ± 6.59
F1	1250.00	156.19 ± 17.35	52.33 ± 4.16	133.00 ± 6.08*	63.40 ± 10.13	161.80 ± 17.41
F2	714.29	280.88 ± 15.07*	34.33 ± 2.08	125.33 ± 7.51*	52.03 ± 8.79	148.83 ± 5.69
F3	833.33	380.37 ± 38.95*	283.00 ± 8.00*	281.67 ± 6.03	113.00 ± 18.49*	320.53 ± 45.76*
F4	1666.67	229.62 ± 15.20*	126.67 ± 37.90*	190.67 ± 13.61*	93.27 ± 10.17*	243.00 ± 13.95*
F5	1666.67	240.10 ± 31.98*	35.33 ± 2.89	119.00 ± 6.24*	51.13 ± 2.32	155.93 ± 11.16
F6	1250.00	324.26 ± 17.44*	36.67 ± 2.08	128.67 ± 3.51*	47.20 ± 6.68	142.53 ± 7.91
F7	1250.00	202.85 ± 43.75	154.67 ± 10.07*	249.67 ± 6.81	107.10 ± 11.44*	238.10 ± 24.21*
F8	1250.00	226.85 ± 43.21*	57.67 ± 4.73	169.67 ± 23.59*	87.80 ± 0.70*	181.93 ± 44.00

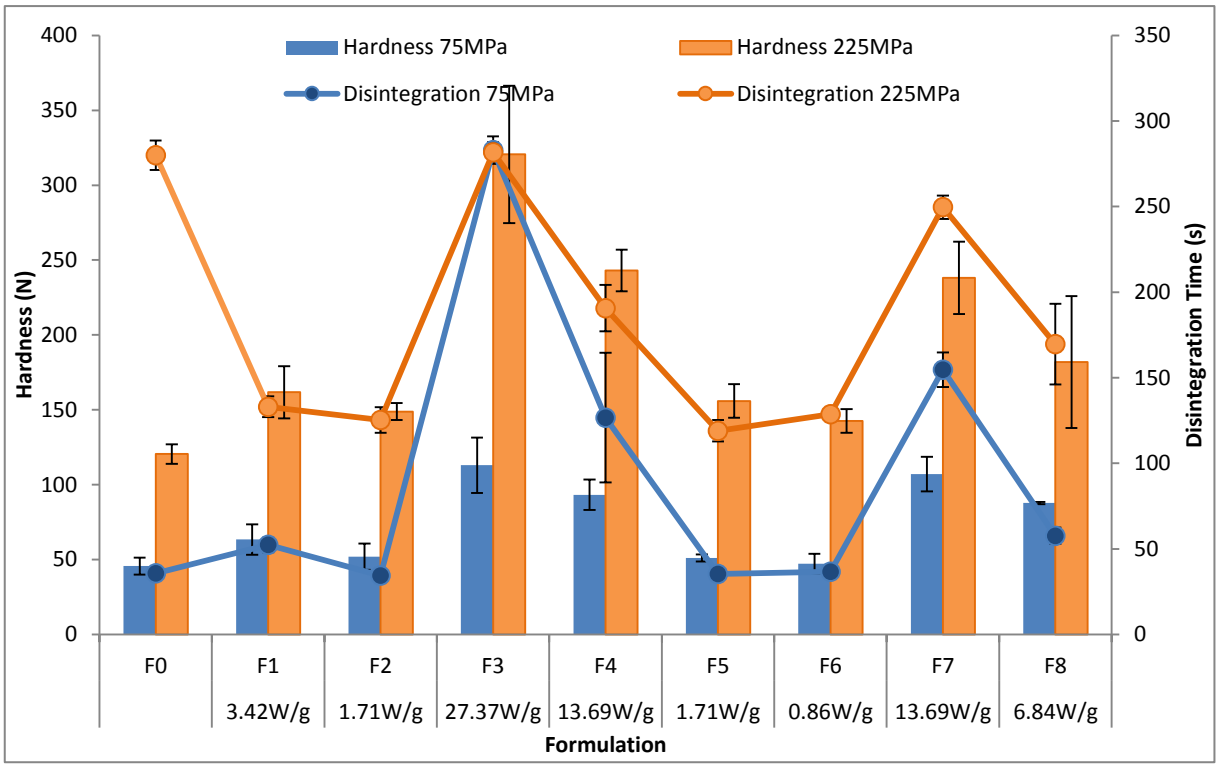

Figure 2.7: A graph showing the hardness and disintegration of the manufactured ODTs at a compression force of 75 and 225 MPa. At 75 MPa hardness of the milled ODTs has improved indicating improved compressibility of the milled mannitol. At 225 MPa disintegration time has improved for milled ODTs even with the increased mechanical strength of the tablets, indicating improved wettability of the milled powders ($p<0.05$). Data presented as mean ± SD.

on the crystal (Ho *et al.*, 2010). The improved disintegration time indicated that the ODTs had a higher affinity for water, which was an additional evidence for increased fracture at the (011) plane, as opposed to the hydrophobic (010) plane.

2.3.4 Compressibility

Compressibility of the powders was assessed using both in-die Heckel/out-of-die Heckel plots, as in-die equipment was limited to a maximum compaction force of 40 MPa. Out-of-die Heckel data (Figure 2.8), showed a typical plot for a brittle fragmenting material for non-milled mannitol (F0), whereby there was an initial sharp rise representing particle rearrangement, followed by a plateau region which indicated that the material was densifying largely through fragmentation as compression force was increased (Paronen and Ilka, 1996). However results for the milled mannitol showed a more linear compression profile, indicating an improvement in compressibility of the powder bed, possibly due to the lower degree of fragmentation under compression and a more plastic deformation profile. This

may have been because the particles within the milled powders underwent fragmentation/cleavage during the milling process therefore reducing the levels of fracture during tablet compression. The more linear profiles displayed steeper gradients, giving much lower yield pressures in comparison to powder F0, as seen in Table 2.3. This indicated that milling had reduced the levels of fragmentation during compression, and the compacts were formed through increased plastic deformation. To further support the out-of-die Heckel data, an in-die Heckel analysis was conducted over the initial compaction force range.

In-die Heckel results (Figure 2.9), displayed a different pattern to that of the out-of-die results, as this was a real time simulation of the compaction rather than an analysis of the ejected compacts. For non-milled mannitol (F0) it was seen that there was the characteristic rearrangement stage followed by densification, where the profile had become linear and the yield pressure was 145 MPa, similar to that reported in previous literature (Gharaibeh and Aburub, 2013, Klevan *et al.*, 2010). The milled powders showed a clear difference in the compression profiles within the rearrangement stage, as the data

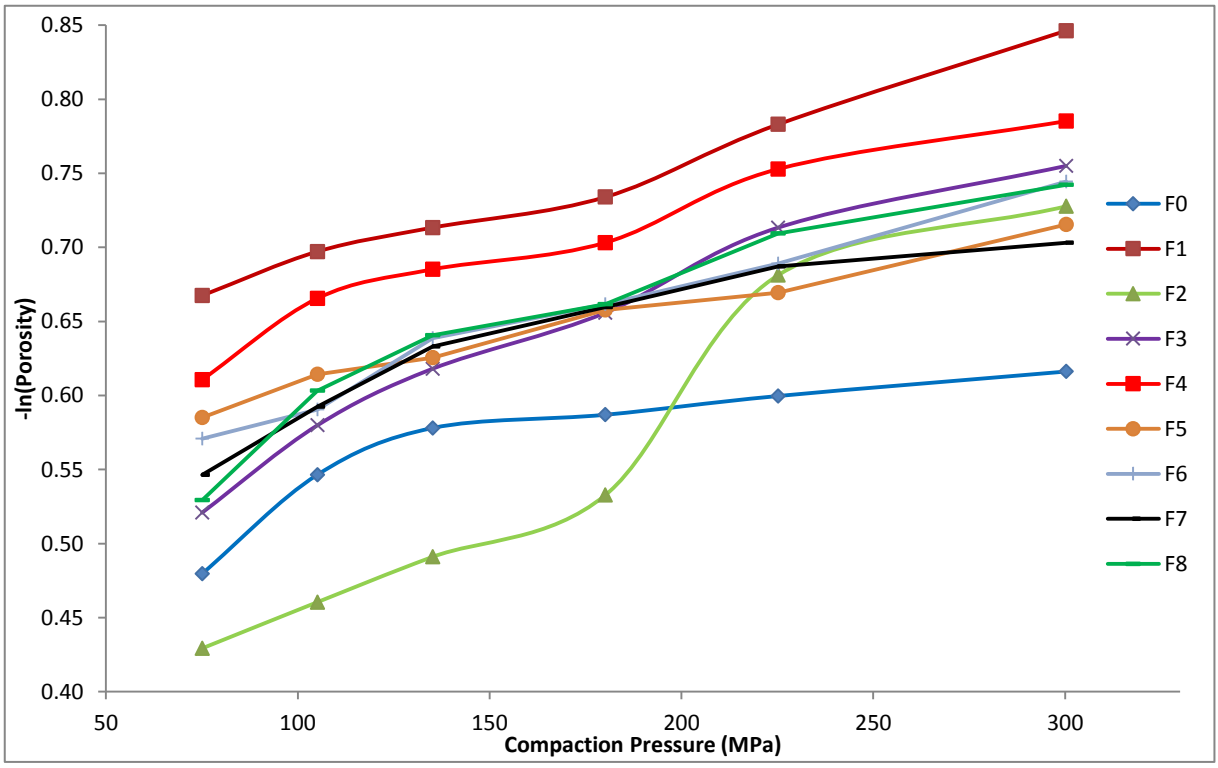

Figure 2.8: An out-of-die Heckel plot of the milled powders (F1-F8) compared to non-milled mannitol (F0) indicating a decreased yield pressure post-milling as seen through a steeper gradient.

revealed that they underwent lower degrees of rearrangement within the dies, shown by the faster onset of densification. This was due to the milled particles being smaller in size along with being very cohesive, prompting the particles to fall into the smaller voids amongst the packed powder within the dies, therefore leading to less rearrangement being required during the initial stage of compaction (Roberts and Rowe, 1986). However the yield pressures obtained appeared to be larger for the milled powders compared to the control (Table 2.3), which would have indicated that the milled powders were densifying through brittle fragmentation to a larger extent. However, these results revealed that there was less fragmentation occurring during compression, as when the particle size of a brittle material was reduced through milling, the larger yield pressures obtained indicated that the material was fragmenting to a lesser extent, and that the ductile behaviour of the milled powders had increased due to the less brittle nature of the material (Bolhuis and Chowhan, 1996, Hersey *et al*., 1973, Roberts and Rowe, 1985, Roberts and Rowe, 1986). This was because the particles had been previously fractured during the milling process, which imparted stress and cracks upon the crystal. This therefore increased the stress/force required to further fracture the particles during compression, which

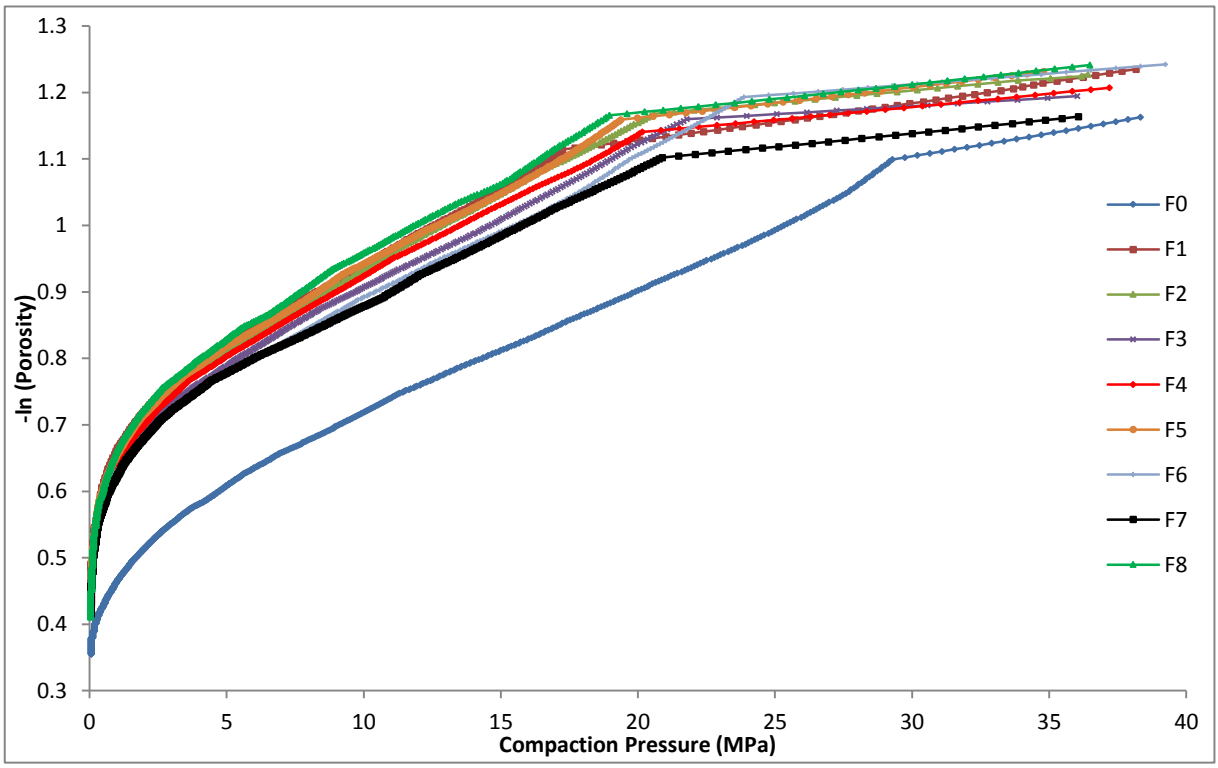

Figure 2.9: An in-die Heckel plot of the milled powders (F1-F8) compared to non-milled mannitol (F0) indicating an increased yield pressure post-milling as shown by a smaller gradient.

subsequently led to higher yield pressures being obtained on the in-die Heckel plot. This study therefore agreed with previous findings where it was stated that the reduction of particle size of a brittle fragmenting material had reduced fragmentation during compaction (Hersey *et al*., 1973, Roberts and Rowe, 1985, Roberts and Rowe, 1986) and in the current study, mannitol being a material that densifies largely through fragmentation also had enhanced compression behaviour after particle size reduction.

As most of the fracture on the mannitol particle was occurring prior to the material being tableted, the particles were less likely to fracture during the compaction process. This therefore led to less fracture at the (011) plane between the dies, which in turn was likely to lower the amount of die wall friction occurring during compression, as there would be an absence of newly fractured surfaces interacting with the dies. This was shown by the production of more robust, mechanically stronger ODTs manufactured from the milled samples, as shown in Figure 2.7 and Table 2.2. The fracture at the (011) plane during milling and prior to tableting led to an improvement in compressibility, as the reduction in die wall friction allowed the particles to interact and bond more tightly together. It can also be concluded that a larger proportion of the compression energy applied into the material would have been used to bond the particles together as opposed to causing the particles to break/fragment (Coffin-Beach and Gary Hollenbeck, 1983), which was shown by the improvement in hardness of the tablets at both compression forces.

2.3.5 Long Term Physical Stability Study

To establish the long term stability of milled mannitol three of the most favourable powders, with the optimum powder and ODT characteristics, were taken forward. These formulations had the ideal energy input during milling, with the energy input per unit mass being 1.71-6.84 J/kg. The selected powders were F1, F2 and F8. Figure 2.10 and 2.11 indicate the DSC melting point and the % of β-mannitol present in the powder respectively. It was seen that the melting point (Figure 2.10) remained very close to the literature reported value and the value tested immediately post milling, of around

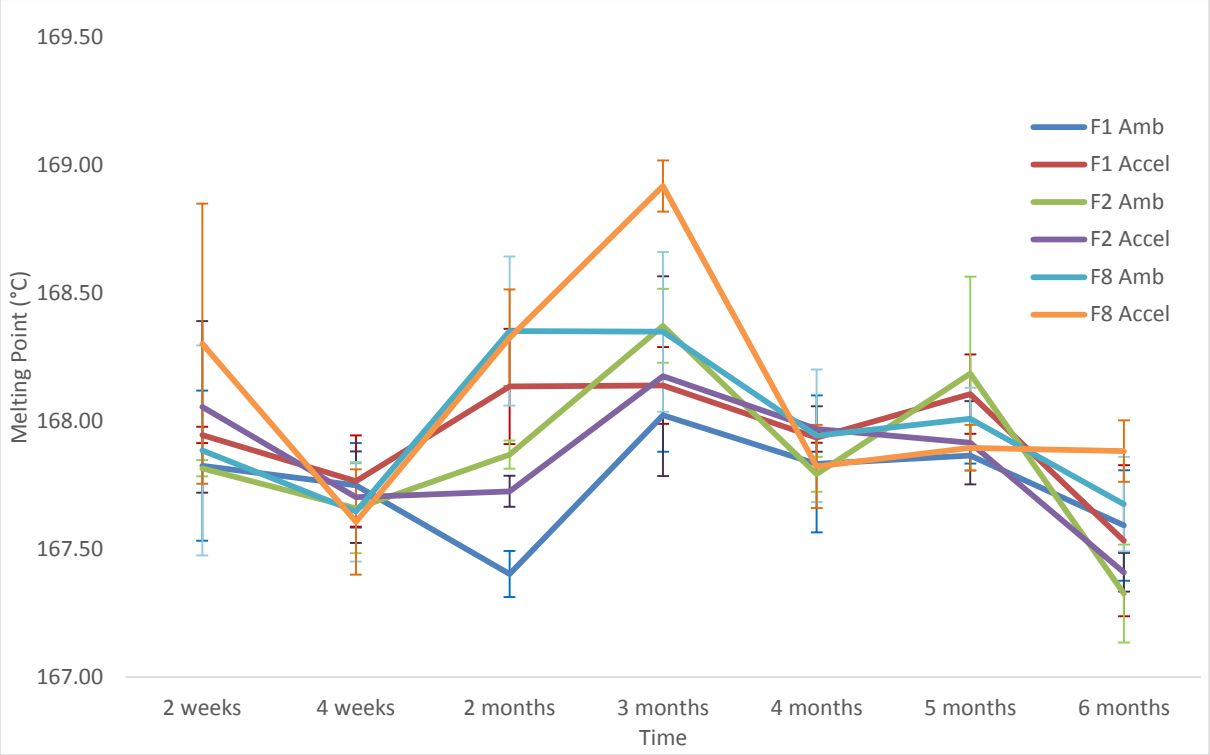

Figure 2.10: DSC melting point of the three milled mannitol powders tested at ambient and accelerated storage conditions over 6 months. Gives a clear indication that the melting point remained very consistent between 167-169°C, indicating a stable crystal form. Data presented as mean ± SD.

167°C (Rowe *et al*., 2012). In Figure 2.11 it was seen that the percentage amount of β-Mannitol also remained consistent throughout the testing period, with the amount in the powder constantly above 98 %, although a slight reduction from the first few weeks, and a plateau was observed. This gave an indication that the milling process had very little effect on the stability of the mannitol crystal, and that it remained crystalline material with little or no amorphous regions. The XRD patterns produced very sharp peaks indicating high crystallinity, and the high percentage of β-mannitol indicated that no polymorphic transformation was taking place, due to the high stability of the β-polymorph (Willart *et al*., 2007). The negligible amount of α-mannitol (<1.5 %) observed upon Rietveld refinement may have been due to impurities within the material or due to the reduction in peaks across the pattern, that was characteristically observed after the milling process. With the accelerated study at a high temperature and humidity, it was observed that the crystal properties of mannitol remained very stable for long periods of time, and that storage did not result in a reduction in the crystallinity of the material.

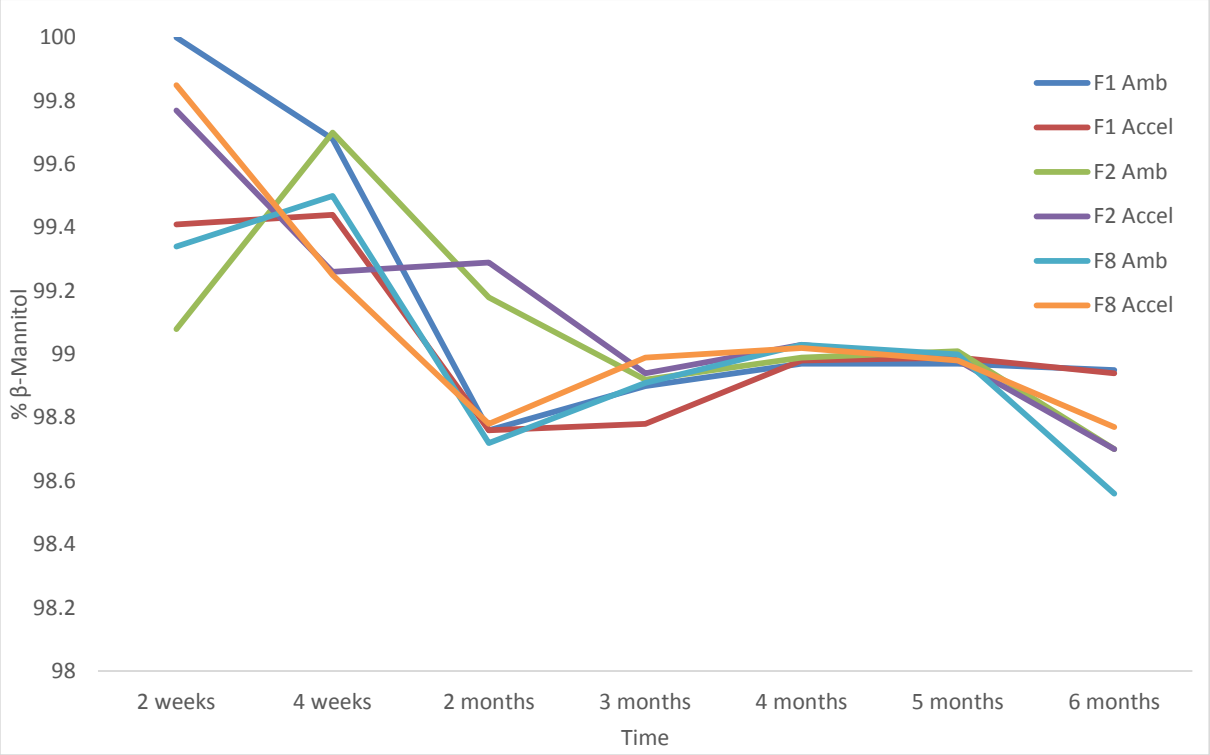

Figure 2.11: A graph indicating the % β-mannitol, through Rietveld refinement of the XRD patterns, of the milled powders stored at ambient and accelerated conditions over the 6 month stability testing period. In all cases the amount of β-Mannitol remains >98 % indicating that the polymorphic form remains stable post milling during storage in ambient and accelerated conditions.

Figures 2.12 and 2.13 indicate the degradation temperature and moisture content of the milled mannitol that was stored at ambient and accelerated condition over the 6 month period respectively, which was measured using TGA analysis. It was observed that over the 6 months, at both ambient and accelerated conditions, the degradation temperature remained very similar, with degradation occurring at around 235-245 °C, in one large mass loss, similar to what was observed in literature (Tong *et al*., 2010). This consistent degradation temperature, with very similar patterns observed throughout the stability study, indicated that the mannitol was remaining fairly stable, and there was very little production of by-products occurring during the storage of the milled mannitol. Along with DSC analysis, where no other transitions or melting points were observed, the data clearly showed that milled mannitol was chemically stable, and that there were no reactions of the material that led to the formation of by-products during storage. Also in Figure 2.13, it was seen that the moisture content of the milled mannitol remained similar throughout the study, and more importantly during accelerated storage conditions where RH is at 75 %, there was very little/no water uptake into

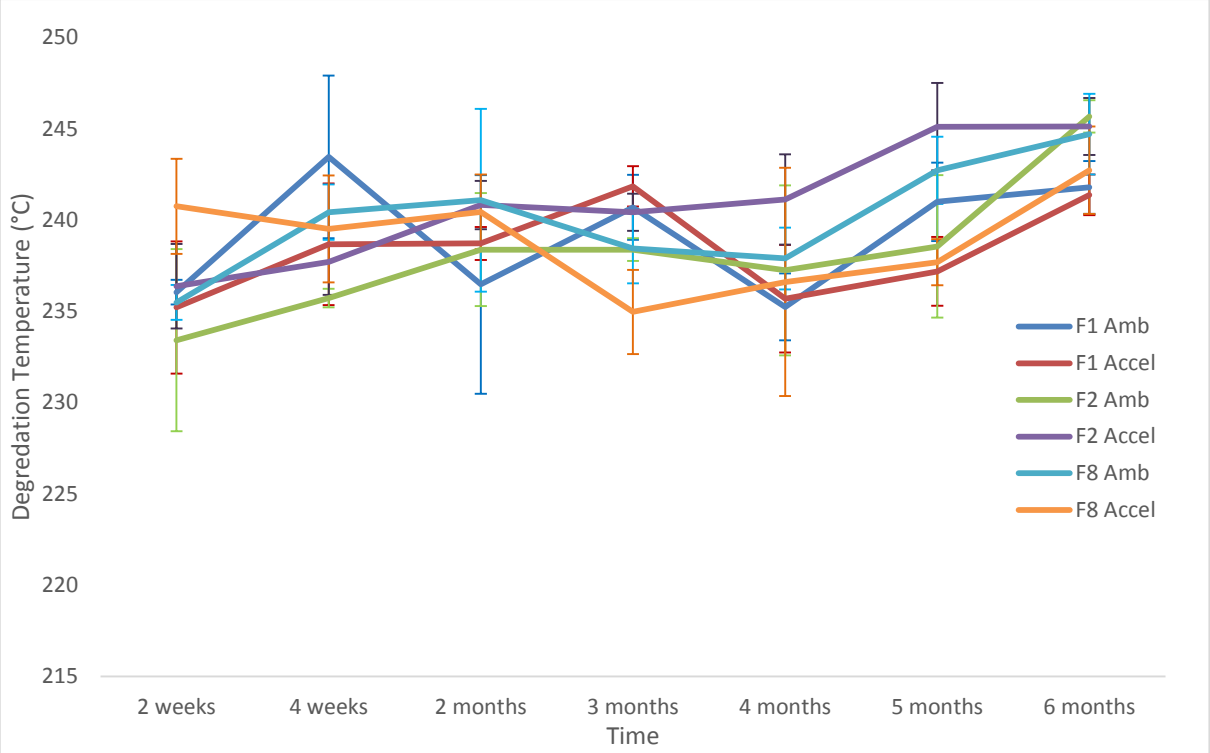

Figure 2.12: A graph showing the TGA degradation temperature of the milled mannitol powders stored at ambient and accelerated conditions over a 6 month period Degradation remains fairly constant at around 235-240 °C, indicating very little/no formation of by products during storage, and that post milling, mannitol remained stable. Data presented as mean ± SD.

the milled mannitol. As was mentioned previously mannitol is a non-hygroscopic material, which gives it one of its key advantages for employment in ODTs. In this study it was seen that milling exposed the hydrophilic (011) crystal plane, and therefore it was necessary to test moisture uptake during storage as the wettability of the powder had increased when it came into contact with water. However upon storage at a high relative humidity it was seen that there was no increase in moisture within the milled mannitol, with moisture levels remaining below 1 % at both ambient and accelerated conditions, indicating that the milled mannitol still had the advantage of being a non-hygroscopic material.

From the stability study it was concluded that across the 6 month period, at both ambient and accelerated conditions, very little change in any of the milled mannitol formulations (F1, F2 and F8) was observed and the properties of the material remained consistent throughout. This indicated that the material would be suitable as a long term alternative to regular mannitol, as the milling did not affect the crystallinity, polymorphic form, melting point, degradation temperature or moisture content during long term storage, and in fact the material remained very stable.

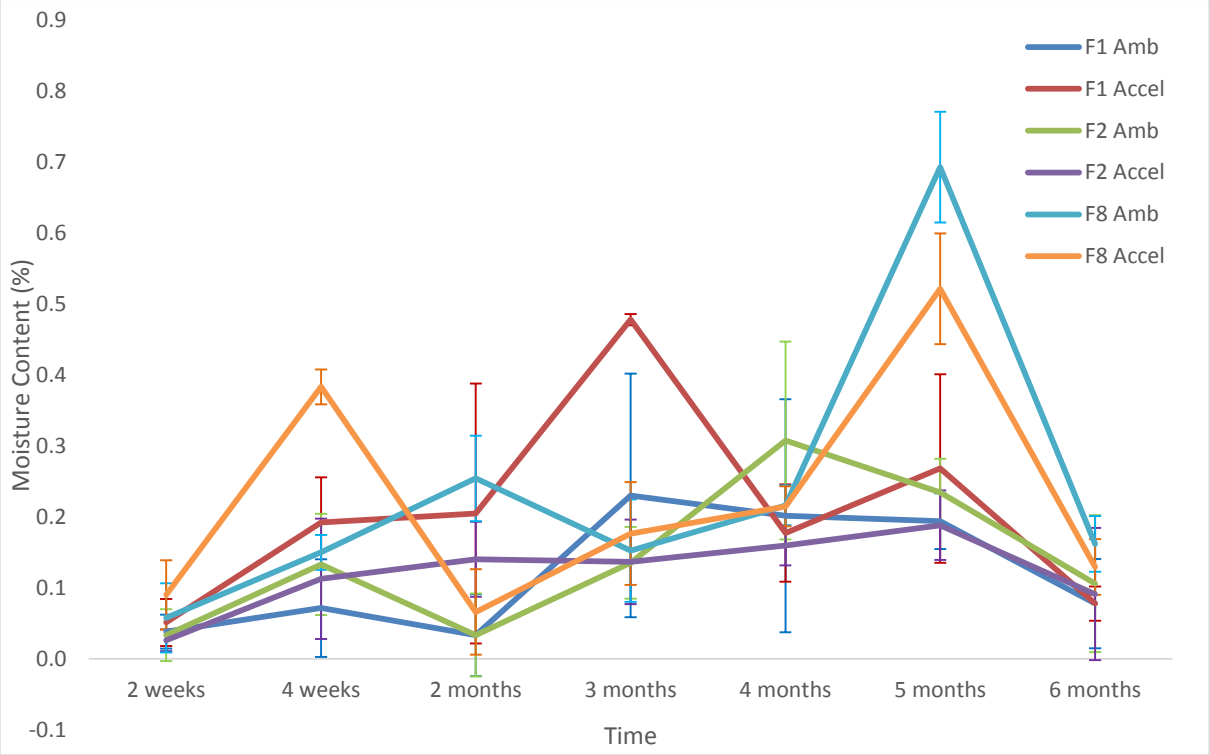

Figure 2.13: A graph indicating the moisture content of the milled mannitol powders stored at ambient and accelerated conditions over a 6 month period, measured using TGA analysis. The moisture content remained very low (<1 %) in all cases, even when stored in accelerated conditions at 75%RH, indicating that the milled mannitol did not become susceptible to moisture uptake during storage. Data presented as mean ± SD.

2.3.6 Milled Mannitol Flow Improvement

From the above work it was concluded that milled mannitol provided a pragmatic strategy to overcome the inherent poor compression properties it displays during direct compression, and was advantageous for ODT production. However the unaided mannitol powder had an extremely poor flow due to its highly cohesive nature, which was due to its very small particle size of around 10-11 µm. Good bulk flow characteristics are essential for large scale manufacture of tablets during direct compression as this results in a uniformly weighted dosage form, with the absence of any capping or lamination, as well as having a consistent drug content (Abe *et al.*, 2009, Thoorens *et al.*, 2014). With the milled mannitol having a small particle size, it led to a high surface area to volume ratio, which resulted in the cohesive Van der Waals forces increasing and therefore when the powders were poured it was more inclined to resist bulk flow (Mullarney and Leyva, 2009). Also as a result of milling the particle size distribution was wide which also contributed to the poor flow behaviour; segregation would be prevalent as the smaller particles aggregated due to their highly cohesive nature, separating

from the larger particles; there would also be high incidences of interlocking, as the smaller particles were able to pack in between the voids between the large particles, and along with their highly cohesive nature reduce the bulk flow behaviour. Powder F2 was taken forward for flow investigation due to its advantageous ODT properties and because of its highly stable nature. It had an ideal energy input per unit mass, being 1.71 J/kg, which would also be the least labour intensive if translated to larger scale production.

2.3.6.1 Optimising Flowability with Starch 1500®/Silica in the Cube Mixer

Figure 2.14 indicates a graph comparing varying concentrations of Starch 1500® (4-20 %) against the F2 mannitol control, with and without the use of silica as a flow aid, with all powders blended in the cube mixer at 250 rpm for 10 mins. The angle of repose data showed that adding starch (Span – 2.44 µm) to the milled mannitol tended to improve the flow of the milled mannitol, with statistical significance seen at concentrations of 8 % and above, from an angle of repose of 48.75° (poor flow) to

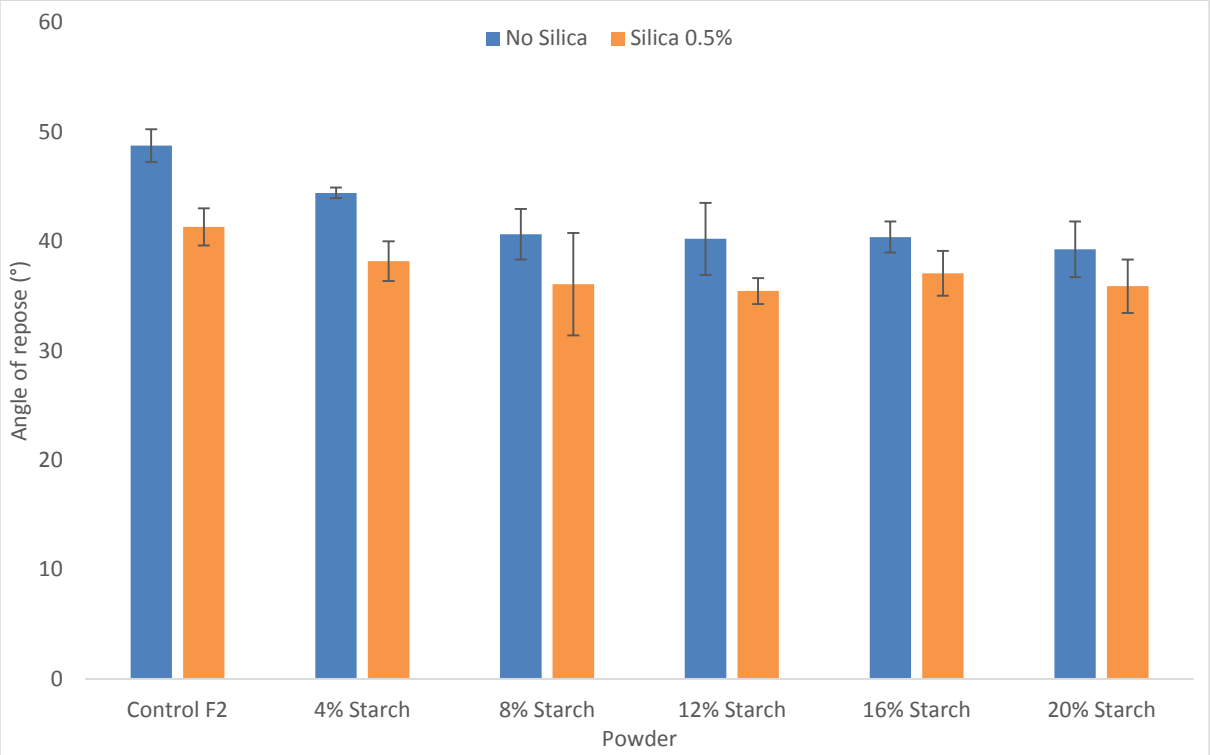

Figure 2.14: A graph showing the angle of repose of the milled powders, indicating that addition of Starch 1500® is advantageous in improving flow characteristics of the milled powders, with concentrations above 4 % being statistically significant. However it was also shown that addition of silica significantly improved flow compared to the control, similar to starch at high concentrations, with further improvement in flow seen at all starch concentrations (only 4 % starch showed statistical significance. Data presented as mean ± SD (n=3, $p<0.05$).

39.26° (Fair) when 20 % starch was incorporated. Starch 1500® had a larger particle size compared to mannitol, around a VMD of 60 µm according to laser diffraction data. These larger particles therefore flowed better than the milled mannitol, and once added to the mannitol helped to aid the flow, as the cohesive mannitol particles had been attracted to the larger starch particle, which resulted in lower cohesion between the mannitol particles. However when silica was incorporated into the powder blend the flow was further improved compared to adding the starch on its own (with statistical significance seen with the F2 control and 4 % starch). This was because silica is designed as a flow aid, so it was expected that the addition of silica would increase the flowability of the powder. The very small silica particles were able to coat the milled mannitol particles, which consequently would have reduced interparticle cohesion and friction between the mannitol, and improved flow (Kojima and Elliott, 2013, Zimmermann *et al*., 2004, Zhou *et al*., 2010). This was shown by the F2 formulation which displayed a significant decrease in angle of repose between the unaided mannitol and mannitol containing 0.5 % silica. When the starch was added further improvements in flow were seen, and it was observed that an optimum concentration of Starch 1500® was 12 %, as this displayed the best angle of repose at 35.45° (Good). The angle of repose with 20% starch + 0.5 % silica was also low at 35.89°, however a worsening in angle was observed in the results for starch 16 % + 0.5 % silica, with an angle of 37.07° (passable). This may have been attributed to the packing geometry of that particular powder, as having the larger starch particles may have allowed the small milled mannitol to pack within the voids of the starch particles, which subsequently inhibited the bulk flow of that powder, and cause a reduction in flowability of the bulk powder blend. From these results the powder taken forward to investigate for further flow improvement in the composite mixer was the 12 % starch formulation, with 0.5 % silica, as it displayed the best flowability according to angle of repose.

2.3.6.2 Optimisation of composite blender parameters

Figure 2.15 shows the angle of repose of milled mannitol with 0.5 % silica mixed in the novel composite mixer at speeds of 1500 rpm compared to 2000 rpm, with and without the use of 1 bar of air to help disperse and mix the powder. From Figure 2.15 it was seen that the angle of repose tended to decrease

as the speed of the mixer was increased, with the angle of repose with 1 bar air at 1500 rpm being 39.59° (Fair) compared to at 2000 rpm where the angle was 34.48° (Good). This was because at a higher mixing speed the particles were able to disperse more readily through the powder blend as higher shear forces were applied to the mannitol aggregates, which essentially broke them up (Le *et al*., 2012, Kale *et al*., 2009, de Villiers, 1997). This allowed the silica flow aid to then coat the cohesive mannitol particles more effectively, rather than coating the aggregated particles, and produced a more uniform particle size distribution, with a lower range of large agglomerates. From Figure 2.15 it was seen that there was statistical significance (ANOVA $p<0.05$) when the speed was increased from 1500 to 2000 rpm with 1bar of air, which also showed that increasing mixing speed allowed further improvements in flow categories. From this it was concluded that using a 2000 rpm speed with the composite mixer with 1 bar of air produced the most favourable flowing powder, and was therefore used for further investigation of the composite blender.

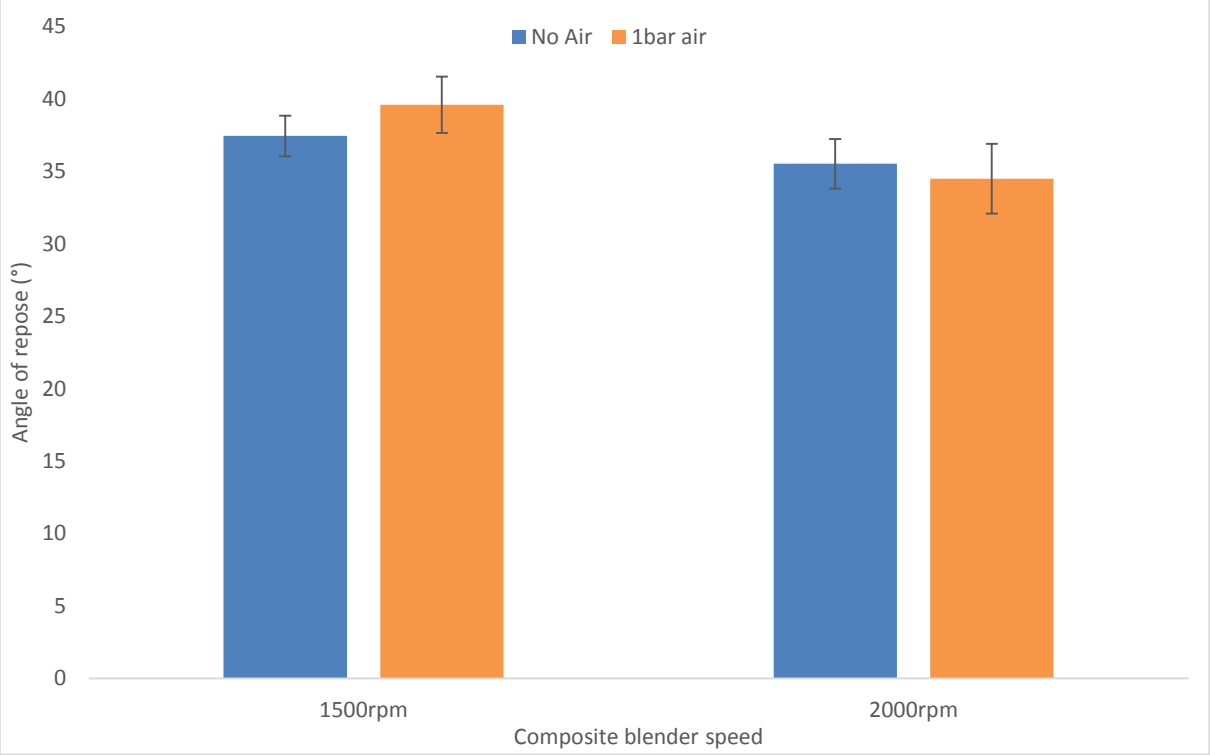

Figure 2.15: A graph showing the angle of repose of the milled mannitol + 0.5 % silica mixed in the novel composite blender at different parameters. It shows that increased speed does help in improving the flow behaviour of the powder, with a significant improvement seen between the powder tested at 1500 rpm and 2000 with 1 bar of air pressure. Data presented as mean ± SD (n=3, $p<0.05$).

2.3.6.3 Comparison of the Cube and Composite mixer

Figure 2.16 shows a graph of the angle of repose of milled mannitol mixed in different powder blends containing 0.5 % silica, 12 % starch and a combination of both. It was seen that the formulation containing 0.5 % silica mixed in the composite blender had the best flowability with an angle of repose of 34.48° (Good), compared to the cube mixer with just 0.5 % silica which had an angle of 41.319° (Passable), which was statistically significant (ANOVA $p<0.05$) . It was seen that in all cases adding 0.5 % silica did improve the flow, as it was utilised as a flow aid, and was able to reduce the cohesiveness of mannitol, therefore allowing the particles to flow better due to the lower Van der Waals forces. When 12 % starch was used, it was observed that there was very little difference in the angle of repose, as both were around 35° (Good). It may have been that for milled mannitol it was difficult to improve the flow further, as it appeared that, alongside the 0.5 % silica blend in the composite mixture, the lowest angle achieved was 34-35°. This was as a result of the cohesive nature of the powder, as the particles of mannitol were very small, and interparticle/electrostatic forces would have inhibited the

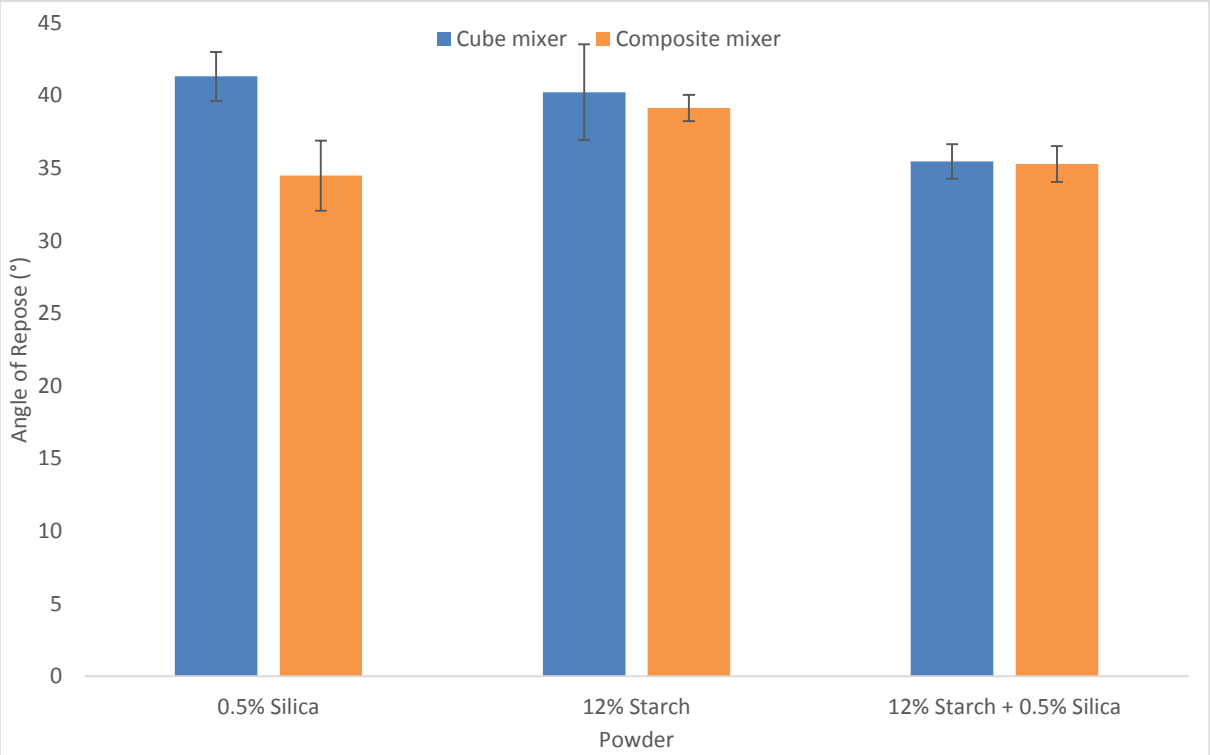

Figure 2.16: A graph showing the angle of repose of the various milled mannitol powders comparing cube mixing and composite mixing for 10 minutes. It can be seen in general that composite mixing proves advantageous in improving flow, with significant flow improvement observed with 0.5% silica. Data presented as mean ± SD (n=3, $p<0.05$).

flow behaviour of the bulk powder, even with the presence of silica which was acting as a lubricant. It was seen that including starch had little benefit in improving the flow properties of the powder, unless it was included with silica. The angle of repose tended to be around 40°, which in the case of the cube mixer was comparable to the silica blend. However in the composite mixer the flow of the starch blend was much higher than the mannitol with the silica alone. This may have been because in the composite mixer, which was able to dry coat smaller particles onto larger coarse particles, the mannitol may have coated on to the surface of the starch. The blends tested for angle of repose were not sieved to remove the finer particles, so in this particular batch there would have been a wide particle size distribution, therefore leading to particle segregation, and a more closely packed particle geometry, which would have therefore inhibited the flow further. Including starch with silica provided the best option for flow improvement at a concentration of 12 % starch, with the angle being around 35°, as the cohesive nature of the mannitol would have been reduced due to the presence of silica, whilst the good flowability of the starch would have also contributed to the better flowing nature of the bulk powder. It was shown here that the composite mixer presented a better option for flow improvement rather than the standard cube mixer, as the presence of high shear forces during the mixing process would help deagglomerate the cohesive milled mannitol particles, allowing it to coat the surface of larger particles, therefore reducing overall cohesivity of the powder blend. The ability of silica to coat the surfaces of mannitol was also increased as a larger surface area of mannitol was exposed due to the deagglomeration of the particles, allowing a larger area for the silica to coat (Dahmash and Mohammed, 2015). Work in the group had shown optimisation of the composite mixer parameters were needed for peak powder performance. Therefore the composite mixer was taken forward for further flow improvement assessment.

2.3.6.4 Assessing the effect of mixing time during Composite blending on Milled Mannitol flow

Figure 2.17 shows the differences observed between composite and cube mixing over a 30 min time period. It was seen that over the 30 min period the flow of the milled mannitol with silica was further enhanced, with composite blending proving more advantageous than cube mixing. This was down to the longer duration of powder mixing, which enabled the high shear forces within the composite mixer to break down aggregates of both silica and mannitol, and therefore the small silica particles were able to coat the milled mannitol more thoroughly. This would have led to lower cohesive forces being present in the powder blend as the silica was effectively coating a larger proportion of the mannitol and inhibiting the cohesive forces between adjacent mannitol particles. A statistically significant difference was seen at the 10 min mixing time (ANOVA<0.05), but not at 20 or 30 mins, however it was still seen that composite mixing gave a more flowable powder than cube mixing, with the lowest angle of repose being 32.53° (good), which was mixed for 30 mins in the composite blender. The corresponding cube mixed value was 34.56° (good), indicating a difference of approximately 2°, which

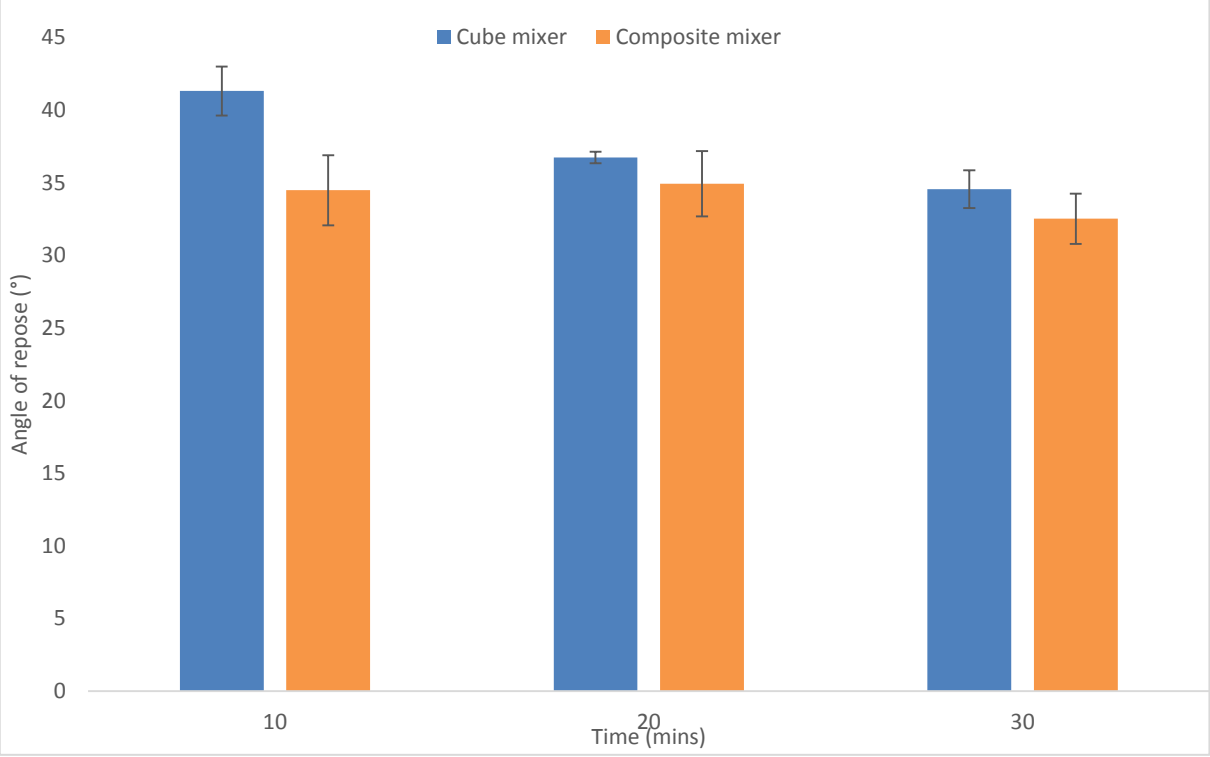

Figure 2.17: A graph showing the angle of repose of milled mannitol + 0.5 % silica comparing cube and composite blending over a 30 min period, highlighting that composite blending is advantageous over cube mixing as flow improvements are evident, with mixing at 10 mins being statistically significant. Data presented as mean ± SD (n=3, p<0.05).

was also similar for the 20 min time interval where the composite mixed powder had an angle 34.94° (good) as opposed to the cube blended powder at 36.75° (fair). With flow the USP gives guidelines on powder flow classification (USP37, 2014c), and in the case of the 20 min mixed powder, although statistical significance wasn't observed a flow category difference was observed, showing that the composite powder would be more flowable and actually be classed as a lower risk powder. Therefore in terms of the angle of repose it could be said that a 2° difference could be significant and therefore composite blending represented a more advantageous method for flow improvement over cube mixing, with a 30 min time giving the most flowable powder with a 2° improvement seen between the composite mixed powders at 30 mins compared to 20 mins.

2.3.7 Scale Up Study

To assess the suitability of milled mannitol as a viable option to unmilled mannitol, a scale up study was conducted, whereby a preblend of milled mannitol had undergone flow enhancement with an ideal blend from the flow investigation above. It was established that flow improvements could be seen when milled mannitol was dry coated on to a host particle, in the above case 12 % Starch 1500®, and used in combination with the flow aid, fumed silica. MCC was used as an alternative to the Starch 1500®, with a slightly larger particle size of 100 µm, to enable a different loading capacity of the guest mannitol on to the host particle. The powder blends were mixed in the composite mixer and compared to cube mixed blends. Table 2.4 shows results for the uniformity of weight test carried out according to BP specification (BP, 2015). BP requirements indicate that no tablet should fall outside of the range of 10 % from the mean of that batch, and no more than two should fall outside of 5 % from the mean. The composite blended starch passed the uniformity of weight test as no tablets fell outside the 5 % range, and provided a flowable powder that was easily tableted. The compositely blended MCC powder also gave fairly good results with tablets only varying in the 5-10 % range, although this test did fail with six falling within that range. Cube blended results however had tablets in both batches falling outside the 10 % variation parameter (13 for starch and 2 for MCC), indicating poor flowability and tableting capability of that powder. The results gave an indication that composite blending was

providing more uniformly weighted dosage forms, as the standard deviations observed were much tighter than those of the cube blended tablets. Twenty tablets were tested, and as was seen with the cube blending, massive variations in weight were seen, with SD being 79.59 and 33.16 mg, for starch and MCC respectively, compared to the composite blended SD being 11.88 and 23.67 mg, for starch and MCC respectively. The above results showed that the flow of the compositely blended powders proved advantageous, however with the use of angle of repose as the primary measure of flow this could been classed as subjective.

Table 2.4: A table showing the uniformity of weight of the four powder blends tested in the auto tablet press, with the amount of tablets falling between 5-10 % and greater than 10 % of the mean highlighted as per BP requirements (BP, 2015). Results show that composite blending provided more uniform dosage forms and in the case of compositely blended starch passed the compendial test. Results are displayed as mean ± SD (n=20)

	Starch Cube	**MCC Cube**	**Starch Composite**	**MCC Composite**
Mean Weight (mg)	467.65 ± 79.59	498.89 ± 33.16	536.31 ± 11.88	503.02 ± 23.67
5-10 %	1	3	0	6
>10 %	13	2	0	0

To provide evidence that the flowability of the composite blended powders was superior to the cube blended the tableting study was essential to provide actual practical evidence that the composite blended starch and MCC were giving powders that were able to flow down the hopper, into the dies and produce uniform dosage forms successfully. Figure 2.18 shows images of the produced tablets. Again this, alongside the uniformity of weight test showed that the composite blender provided far superior tablets compared to traditional cube blending, as the cube blended tablets had evidence of capping and lamination, due to the poor flowability of the powder, whereas the composite blended tablets looked more uniform, with much less imperfections. With cube blending the starch/MCC and silica were not being evenly dispersed throughout the milled mannitol, which was the largest constituent of the blend. Whereas in the composite blender the milled mannitol would have started

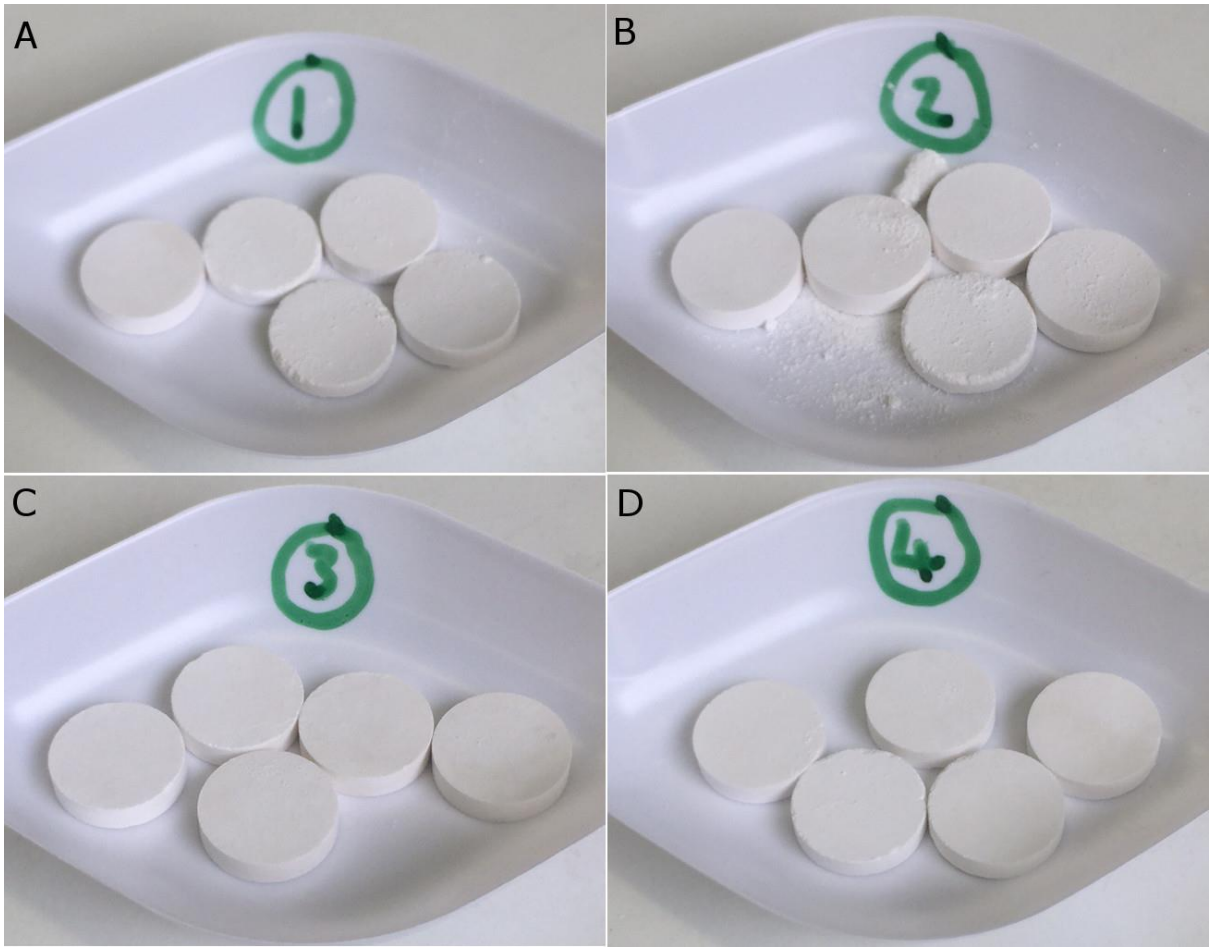

Figure 2.18: A picture showing tablets produced from the auto tablet press for the 4 powder milled mannitol blends test; 1 – Cube blended with starch, 2 – Cube blend with MCC, 3 – Composite blend with Starch and 4 – Composite blend with MCC. Observed that tablets made from cube blended powder were prone to capping and lamination, and the quality of the tablets were very poor compared to compositely blended powders which provided uniform tablets with very little/no imperfections.

to coat the surface of the large starch/MCC particles, whilst the silica would have been more likely to coat the mannitol surface and reduce the cohesiveness. The flow of the cube blended powders would have been inhibited due to the large particle size range, increasing the amounts of segregation in the blend, whilst also being more cohesive due to the increased surface electrostatic forces. This led to the powder flowing very poorly down into the dies during the automated process, which led to trapped air during the compression cycle, whilst the segregation caused excess fine particles within the powder which would have increased die wall friction, and therefore lead to dusty surfaces on the tablet, as was clear in Figure 2.18 (Staniforth and Aulton, 2007). However in the composite blender, the dry particle coating would have negated excess surface charges on the milled mannitol as the mannitol was able to utilise its cohesive nature to coat on to the surface of the starch/MCC, whilst also attracting larger quantities of silica, which helped improves it flow behaviour (Dahmash and Mohammed, 2015). This also produced particles of a more uniform size as the levels of small milled mannitol particles were reducing due to their coating on the larger particles. This therefore led to a more uniformly dispersed powder and improved bulk flow into the dies during tableting allowing the automated tablet process to produce tablets of a uniform weight and of good quality.

Tablet 2.5 shows the tablet test results of the tablets produced from the auto tablet press from the four blends investigated. The results indicated that the mechanical strength of the composite blended

Table 2.5: A table showing the tablet test results for the ODTs produced using the auto tablet press for the four different powder blends tested. Results indicated improved mechanical properties of the compositely blended ODTs alongside improved disintegration times, with hardness of composite blended ODTs being significantly better than the cube blended alternatives. Results are presented as mean ± SD (n=3, $p<0.05$). Data marked with an asterisk (*) indicates statistically significant results compared to the cube blended alternative.

	Starch Cube	**MCC Cube**	**Starch Composite**	**MCC Composite**
Disintegration time (s)	52.7 ± 18.4	43.7 ± 19.0	34.0 ± 17.3	41.0 ± 7.9
Hardness (N)	71.40 ± 2.31	99.70 ± 14.90	136.17 ± 11.64*	146.70 ± 16.74*
Friability (%)	2.23	1.67	0.77	0.76

powders was improved compared to the cube blended powders, with the improvement in hardness being statistically significant (ANOVA $p<0.05$). The primary reason for this would have been due to the poor quality of the cube blended dosage forms, as observed in Figure 2.18, with tablets displaying capping and lamination, alongside a dusty exterior. During auto tablet manufacture the powder is only within the dies for a matter of a few seconds at most, the reduced flow capability of the cube blended powder would have resulted in an incomplete filling of the dies and therefore poor compression of the powder, which resulted in weak dosage form production. This was reflected with the friability results, as excess dust was lost during the test, and the weaker cube blended tablets were more inclined to damage during the test. The hardness of the composite blended tablets was high, which resulted in the friability being below the 1 % standard.

Interesting results were observed for disintegration time. Although statistical significance was not evident, possibly due to a slightly high standard deviation, it was seen that the compositely blended tablets had an improved disintegration time, even with the higher mechanical strength. During disintegration testing it was seen that the cube blended tablets would disintegrate at a fast rate, however large pieces were left to disintegrate over the longer duration, whereas with the composite blended tablets a uniform disintegration of the tablet was observed. This again pointed to the poorly flowing nature of the cube blended tablets, as segregation would have been more prevalent (Staniforth and Aulton, 2007). This meant that during flow into the dies, and compression, the larger starch/MCC particles were more closely packed and bonding together, rather than with the other powder constituents, leading to the noticeable long disintegrating pieces observed during testing. Whereas the more uniform distribution of the starch/MCC through the composite powder, as well as the surface coating of mannitol, led to a tablet with a uniform composition of excipients throughout and therefore complete disintegration in a faster time, with disintegration occurring almost within USP ODT disintegration time standards even with the absence of any disintegrant.

2.4 Conclusion

Ball milling resulted in an alteration in the powder morphology of mannitol, with little of the original crystal structure remaining due to the high levels of energy input during the milling process. It was observed that optimisation of energy input is essential to overcome particle agglomeration post-milling, and that x-ray diffraction provides a useful model to predict energy input during milling. Additionally, the crystal structure remained stable as there were no amorphous regions formed with negligible polymorphic transformation. The main plane of fracture for mannitol during the milling process was the (011) plane as visualised on the SEM images and subsequent evaluation of surface energy analysis and disintegration time profiles. It can be concluded that inclusion of fractured mannitol in tableting would result in an improvement in the compressibility of the excipient as more of the compaction energy would be utilised in the bonding of the compact as opposed to fragmentation of the excipient. ODT properties were also improved when milled mannitol was used, with disintegration times being shorter at higher compaction forces, as the mannitol particles had increased wettability due to the exposure of the (011) plane. The hardness of the ODTs also improved due to the increased compressibility of the mannitol.

The scale up study provided evidence that the newly developed composite blender provided clear advantages for producing a flowable powder that was capable of being compressed in an auto tablet press. In fact without the composite blender, milled mannitol would not have been suitable for tableting on a larger scale due to the poorly flowing nature of the powder that was produced. The composite blender gave a powder that flowed well into the dies during auto-compression, and provided uniformly weighted tablets of a high quality, that were mechanically sound and disintegrated rapidly.

It can be concluded that particle size reduction is a pragmatic strategy to overcome the inherent poor compression properties of mannitol, and dry particle coating can be utilised as a novel method to

provide a scalable powder capable of providing tablets of a high mechanical strength as well as fast disintegrating properties.

Chapter 3

An Investigation into the Powder and ODT Properties of Commercially available Grades of Mannitol in Comparison to Ball Milled Mannitol

3.1 Introduction

The milled mannitol tested in the previous chapter provided interesting results in terms of ODT characteristics. The ODT's manufactured with the milled mannitol generally had very good mechanical properties with relatively low disintegration times, which confirmed that milling the mannitol prior to compression can improve ODT characteristics. However the main drawback of milling was the poor flowability of the powder due to the very small particle size, which increased cohesiveness and electrostatic forces between the individual particles. The wide particle size distribution also resulted in segregation which in turn inhibited powder flow. This poor flowability will cause the powder particles to not travel uniformly into the dies and can affect the uniformity of content and weight of the final dosage form, whilst also causing sticking and capping during the tabletting process (Rasenack and Müller, 2002, Sandler *et al*., 2010, Staniforth and Aulton, 2007). This was addressed with the flowability study whereby the milled mannitol was compositely blended in the dry particle coater alongside the glidant, fumed silica, and a larger particle, either Starch 1500® or MCC. The promising results achieved with dry coating of milled mannitol indicated that flow could be improved to acceptable levels, resulting in a powder that could be successfully tableted on a large scale automated tablet production process, giving tablets of an acceptable quality and rapid disintegration.

Mannitol is available commercially in two main modified forms, spray dried and granular powders. These are designed to overcome the inherent poor flow properties of crystalline mannitol, which due to its needle shape and small particle size, has high levels of cohesiveness and increased interlocking. Granulation is a process which is designed to increase particle size by fusing the mannitol particles together to form larger agglomerates/particles (Shanmugam, 2015), which in the case of mannitol will reduce the levels of needle shaped particles within the powder. This increase in size and alteration of particle shape leads to an improvement in powder flow by reducing the cohesiveness of the powder and lowering the levels of interlocking (Summers and Aulton, 2007). Also the introduction of more uniformly shaped particles reduces levels of segregation, and provides a more uniform bulk flow (Shanmugam, 2015). Spray drying is a process by which a solid excipient, for example mannitol, is

dissolved to form a solution. This solution is pumped into an atomiser on the spray dryer and sprayed into the chamber whereby the hot air evaporates the solvent and causes rapid drying of the droplets. The solid particles are then collected at the end of the process, with particle size of the solid powders controlled by the pump rate, which affects the droplet size, and the drying temperature of the device (Wisniewski, 2015). This forms particles which are spherical in shape, and have a uniform size distribution, with the size often described by the diameter of the particle (Vehring, 2008), which in turn increases powder flowability by reducing the interlocking and electrostatic forces between mannitol particles (Aulton, 2007).

The aim of this study was to assess powder characteristics and ODT properties of commercially available mannitol grades, and compare this to the milled mannitol that was prepared in the previous study. Processing of mannitol through milling provides a much more cost effective alternative to spray drying and granulation of crystalline mannitol. The powder doesn't have to be modified into a solution before production, as is the case with spray drying, and doesn't have to undergo the granulation process. Results for powder F2 were taken from the previous study and brought forward for comparison as it provided the ideal ODT properties (energy input per unit mass being around 1.71 J/kg) and allowed a true comparison to the commercially available grades. This will highlight any advantages and disadvantages that current commercial grades hold over the milled mannitol samples prepared, whilst showing areas where milled mannitol may actually perform similarly to the commercial grades.

3.2 Materials and Methods

3.2.1 Materials

Several different grades of D-Mannitol were investigated from two different suppliers. Mannogem powder, Mannogem 2080, Mannogem Granular and Mannogem EZ SD were provided by SPI Pharma (Wilmington, USA), and Pearlitol 50C, Pearlitol 500DC and Pearlitol 200SD were provided by Roquette (Lestrem, France). Milled mannitol results from the previous chapter were used as a reference point

for comparison in this study. Magnesium stearate was used as a tablet lubricant and was obtained from Fischer Scientific (Loughborough, UK).

3.2.2 Methods

3.2.2.1 Scanning Electron Microscopy (SEM)

SEM monographs were obtained using a Zeiss Supra 55-VP (Oberkochen, Germany) scanning electron microscope, allowing an analysis of the particle morphology of the graded mannitol products. A few milligrams of each sample was adhered to a separate double sided strip and then fixed on to an aluminium stub which was subsequently attached to the SEM holder. Each stub was then gold coated using an Emscope SC500 Sputter Coater (Quorum Technologies, Lewes, UK) at a current of 20 mA and acceleration voltage of 1.5 KV for 40 seconds. Each sample was the placed in the SEM and analysed under vacuum conditions, the magnification and acceleration voltage are on each of the monographs presented.

3.2.2.2 X-Ray Diffraction (XRD)

XRD was performed to detect the polymorphic form present in the samples of different grades of mannitol. A Bruker D2 Phaser (Massachusetts, USA) equipped with a lynxeye detector comprising of a Co-Kα tube, with a wavelength of 1.79026 Å, was used for the analysis of mannitol across a 2Θ range of 10-50 in steps of 0.02 every 0.25 seconds. A rectangular beam of size 0.6 mm was used for measurement and the sample spun at 15 rpm to allow maximum surface analysis. Around 1 g of each sample was poured into the centre of a grooved plastic disk and lightly flattened to obtain an even surface for the analysis; the sample disk was then inserted into the diffractometer. Eva 18.0 software was used for analysis of the obtained patterns.

To quantify the polymorphic phases within the commercially available grades a Rietveld Refinement was conducted using Material Analysis by Diffraction (Maud) software v2.49 (Luca Luterotti, University of California, USA) (Lutterotti, 2010). The obtained patterns for each of the grades was individually imported into the programme, whilst a calculated ideal pattern for both the α and β polymorphs,

obtained from the Cambridge Database, were imported as a .cif file into Maud. The software was then able to fit the obtained pattern from XRD analysis to the calculated patterns, and the refinement calculated as percentage quantity of each of the polymorphic forms.

3.2.2.3 Powder Flow

Powder flow was assessed using the Hausner ratio and Carr's index equation.

$$Carr's \quad Index = \frac{\rho_{tapped} - \rho_{bulk}}{\rho_{tapped}} \times 100 \qquad \text{(Eq. 3.1)}$$

$$Hausner \quad Ratio = \frac{\rho_{tapped}}{\rho_{bulk}} \qquad \text{(Eq. 3.2)}$$

With ρ_{tapped} being tapped density and ρ_{bulk} being bulk density. These were calculated as follows:

$$\rho_{bulk} = \frac{M}{V0} \qquad \text{(Eq. 3.3)}$$

With M being mass of powder, and V_0 being bulk volume.

$$\rho_{tapped} = \frac{M}{V_f} \qquad \text{(Eq. 3.4)}$$

With V_f being tapped volume.

A known weight of sample was poured into a measuring cylinder to allow a bulk/true volume to be taken. The measuring cylinder was tightly fastened in a Sotax TD2 tap density tester (Allschwil, Switzerland), using a foam ring to get an extra tight seal, and tapped 1250 times. A reading for tapped volume was taken at 10 taps, 500 taps and 1250 taps, and value for 1250 taps, i.e. with no further volume reduction, taken as the tapped volume.

3.2.2.4 Particle Size analysis

A Sympatec Helos detector equipped with a Rodos dry disperser and Vibri vibratory feeder (Clausthal-Zellerfeld, Germany) was used to analyse particle size of Mannogem powder and Pearlitol 50C to assess particle size in terms of contribution to powder flow. Other powders exceed the maximum measuring range of 175 µm, therefore particle size was observed on SEM images. All readings were taken in triplicate, and volume mean diameter (VMD) obtained and presented as ± SD.

3.2.2.5 Heckel Analysis

An in-die Heckel analysis was performed on all samples to assess the compressibility of the modified forms of mannitol compared to the crystalline powder (Heckel, 1961a). ODT's were manufactured using 100 % mannitol, so only the compressibility of the sole excipient was tested; 500 mg of mannitol was weighed out and poured into the punch containing the lower die. The tablet was compressed using a Hounsfield Test Equipment H10K (Horsham, USA) equipped with 13 mm flat faced punches up to a compression force of 5000 N, at a upper punch speed of 400 mm/min. This allowed a force over distance plot to be formed, and this data was transformed to calculate true and bulk densities of the tablet, which allowed a subsequent calculation of the porosity (ε) of the tablet over the force range of 0-5000 N. A plot of –ln(ε) against compaction force was then plotted, and the reciprocal of the gradient was taken as the yield pressure (P_Y). All readings were repeated in triplicate and P_Y displayed as mean ± SD. Both dies were externally lubricated using 5 %w/v magnesium stearate in acetone solution.

3.2.2.6 Tabletting Studies

A powder blend containing 99.5 % of mannitol and 0.5 % magnesium stearate was mixed for 1 minute, and individual 500 mg powder portions were weighed out. This was repeated for each of the mannitol grades analysed. ODT's were prepared by compressing 500 mg powder with a Specac semi-automatic hydraulic press (Slough, UK) equipped with 13 mm flat faced punches at a compression force of 75 MPa and 225 MPa. Analysis of the ODT's was conducted immediately after manufacture to reduce any storage effects on the tablet properties.

3.2.2.6.1 Hardness

Hardness of the tablets was established using a Copley TBF 100 Hardness tester (Nottingham, UK). The hardness was then converted to tensile strength using the equation:

$$\sigma = \frac{2\,H}{\pi\,D\,T} \qquad \text{(Eq. 3.5)}$$

Where H is the hardness, D is the diameter and T is the thickness of the tablet. All readings were taken in triplicate and displayed as mean ± SD.

3.2.2.6.2 Friability

ODT friability was measured using a Sotax F2 Friabilitor (AllSchwill, Switzerland). Six tablets were dusted off using a small soft brush and an initial weight taken, the ODT's were subsequently placed in the friabilitor, which was rotated for 100 revolutions at 25 rpm for 4 minutes. The tablets were then dusted off again and a final weight taken. The percentage friability was taken as:

$$\%\ Friability = \frac{Initial\ weight - Final\ weight}{Intial\ weight} \times 100 \qquad \text{(Eq. 3.6)}$$

3.2.2.6.3 Disintegration

The standard USP disintegration test was used to analyse the disintegration times of the manufactured ODT's. A single ODT was placed inside the vessel of a Copley ZT41 disintegration apparatus (Nottingham, UK) without a disk and oscillated at 30 cycles per minute. A single tablet at a time was analysed for accuracy of the timings. 800ml distilled water kept at 37 °C was used as the disintegration medium, and disintegration time was recorded when all fragments of ODT had passed through the mesh at the bottom of the vessel. Disintegration time was conducted in triplicate and displayed as mean ± SD.

3.2.2.6.4 Porosity

Porosity of the powders was assessed using a Quantachrome Helium Multipycnometer (Florida, USA). All measurements were carried out in triplicate and displayed as mean ± SD. Diameter and thickness

of the ODT's was taken using a digital calliper, and the weight of individual ODT's was measured using an electronic balance. The bulk volume (V_B) and bulk density (ρ) of the tablets were then calculated using the following equations:

$$V_B = \frac{\pi R^2}{T} \quad \text{(Eq. 3.7)}$$

$$\rho_{Bulk} = \frac{Tablet\ weight}{V_B} \quad \text{(Eq. 3.8)}$$

The true volume (V_t) of the tablet was calculated using the pycnometer, which applies the theory of gas displacement allowing the porous nature of the tablet to be assessed. The true volume is calculated using the equation:

$$V_t = V_C - V_r \cdot \left(\frac{P1}{P2} - 1\right) \quad \text{(Eq. 3.9)}$$

Where V_C is the volume of the sample cell, V_r is the volume of the reference cell, P1 and P2 are the atmospheric pressure and pressure change during the measurement respectively. The true volume is then used to calculate true density in the equation:

$$\rho_{true} = \frac{Tablet\ weight}{V_t} \quad \text{(Eq. 3.10)}$$

The final step to calculate porosity (ε) of the ODT uses the following equation:

$$\varepsilon = 1 - \frac{\rho_{bulk}}{\rho_{true}} \quad \text{(Eq. 3.11)}$$

3.2.2.7 Statistical Analysis

One way ANOVA was used to statistically analyse data from the different powders in all the tests that they underwent, using GraphPad Prism 6. The F2 milled mannitol powder was used as a control to compare the commercial powders to and a Tukey's multiple comparison post hoc test was used to

analyse the significant differences among powders. For statistical significant a p value <0.05 was used. All data was presented as mean ± SD.

3.3 Results and Discussion

3.3.1 Powder Morphology and Characteristics

Figure 3.1 displays SEM monographs for the Mannogem and Pearlitol grades compared to the F2 milled mannitol. From image (B) on Figure 3.1 it was evident that the Mannogem powder was not the characteristic needle shape of mannitol, although it appeared as a crystalline material with a slight longitudinal shape and grooves following the direction of growth for the crystal. With the Mannogem on all SEM monographs (Figure 3.1 (B-E)) the usual long needle shape wasn't observed, with most of the particles tending to be quite short and wide. This was related to the particle size, as the particle size was quite small (VMD - 37 µm, span – 3.27 µm), although the Sigma Aldrich brand tested in a previous chapter also had a similar particle size, the characteristic needle shape was observed, however the particles with the sigma brand tended to be a lot thinner and more needle like. The Pearlitol 50C, seen in Figure 3.1 (F), represented the typical structure for crystalline mannitol, with a long needle shape, and particles around 50 µm in size. In comparison to the Mannogem powder the Pearlitol crystalline powder had a similar particle size and was visibly similar to what was expected from a mannitol crystal (Ho *et al*., 2012, Koner *et al*., 2015). Figure 3.2 shows the graph of flowability of the graded mannitol powders tested; Mannogem powder and Pearlitol 50C clearly had the worst flowability, with the Carr's index above 40 and Hausner ratio above 1.6 which indicated a very, very poor flow. This was expected from the crystalline powder as they had a relatively small particle size which in turn promoted cohesiveness between the particles (Benedetti *et al*., 2007, Rowe *et al*., 2012). The crystalline mannitol had a more needle like shape, as observed in the SEM images, which could have promoted interlocking between particles and in turn may have contributed to a poorly flowing material. Figures 3.3 and 3.4 show particle size graphs for the Mannogem powder and Pearlitol 50C

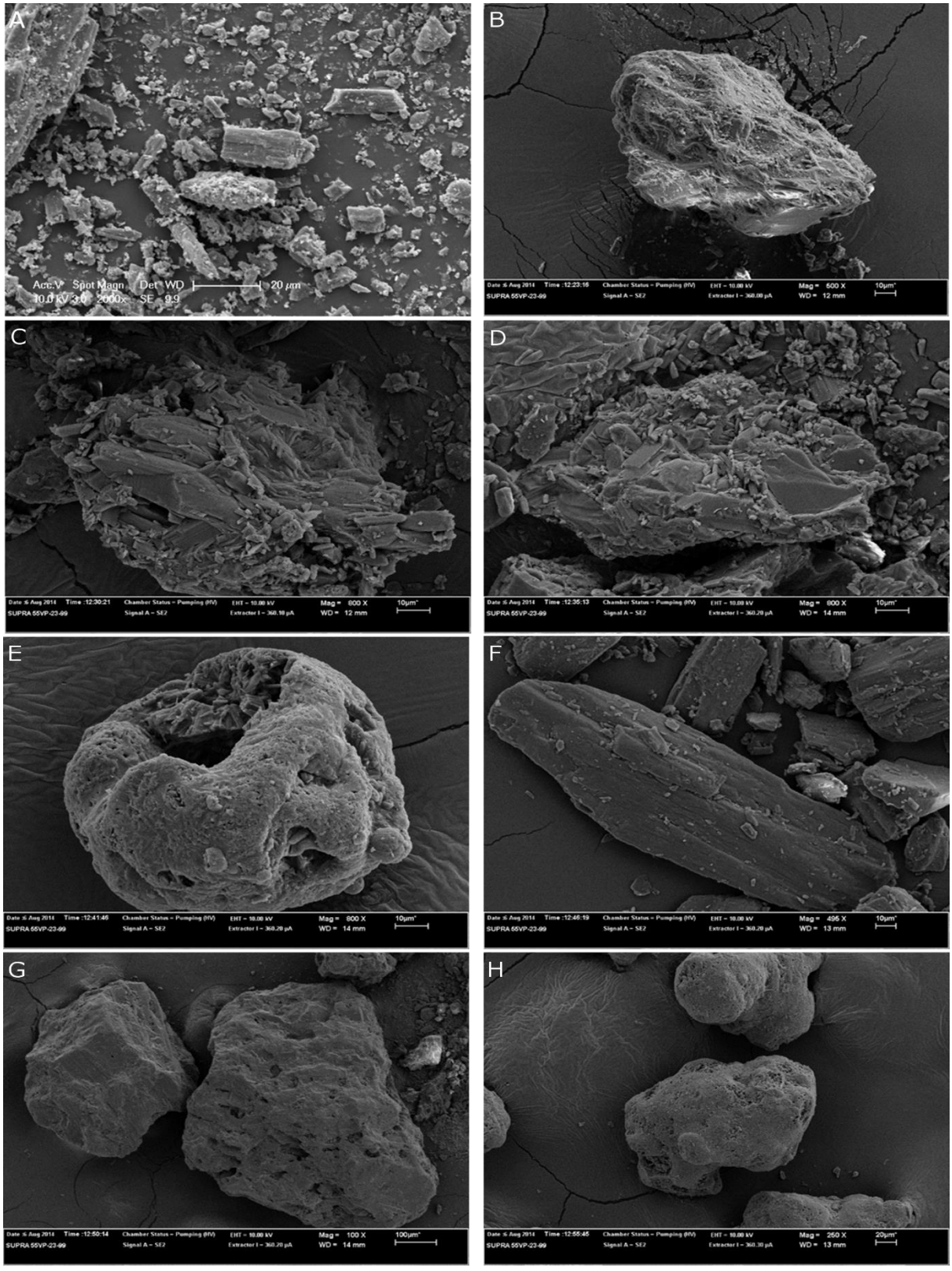

Figure 3.1: SEM images showing the morphology of the graded mannitol products compared to milled mannitol (F2); A – F2 Milled mannitol showing very small particle size at x2000 magnification; B – Mannogem powder showing crystalline structure at 500x magnification; C – Mannogem 2080 and D – Mannogem Granular highlighted granulated mannitol both at 800x magnification; E – Mannogem EZ illustrating a porous spray dried mannitol at 800x magnification; F – Pearlitol 50C showing a crystalline mannitol powder with needle like structure at 500x magnification; G – Pearlitol 500DC highlighting granular mannitol at 100x magnification and H – Pearlitol 200SD showing a spray dried mannitol at 250x magnification

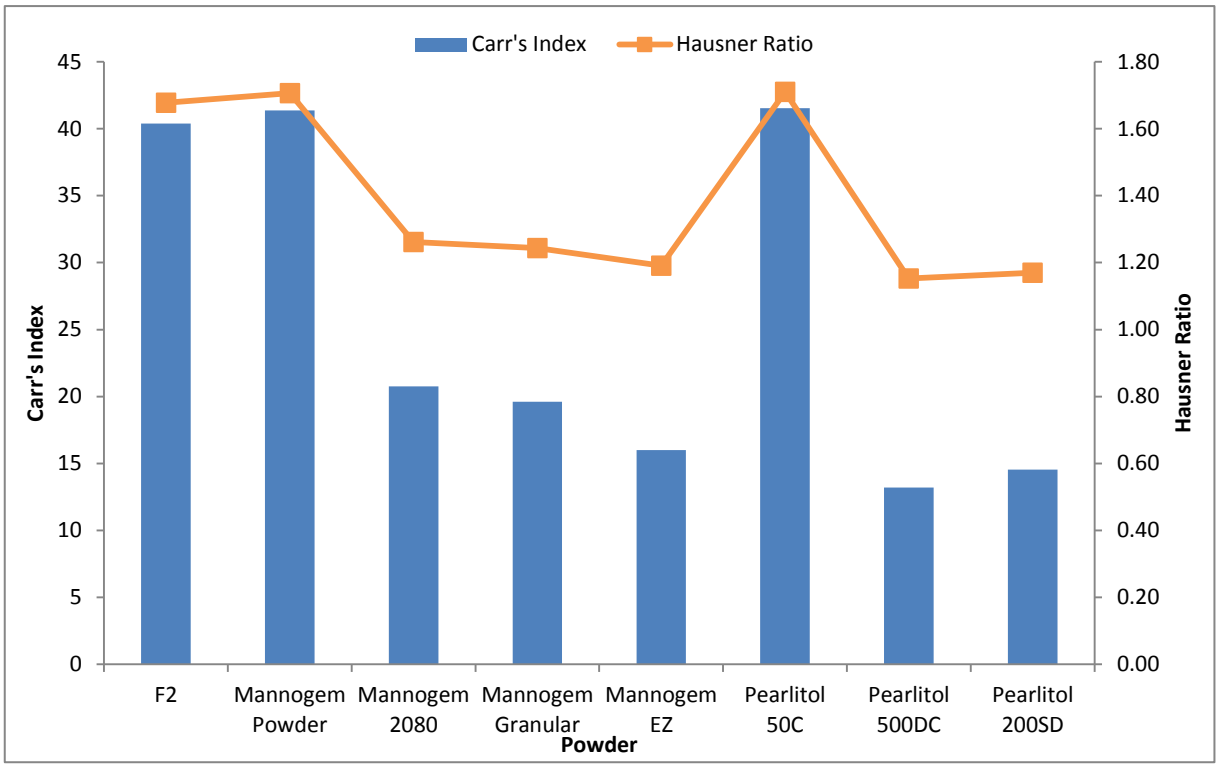

Figure 3.2: A graph showing the flowability of the graded mannitol powders compared to the ideal milled powder, F2, through Carr's Index and Hausner Ratio. Results show that the crystalline mannitol forms have very poor flow alongside the F2 control. All graded powders display an improved flow as expected due to the physical modifications to the mannitol particle, leading to an enhanced particle size and more uniform shape.

respectively, it was observed that there was a wide range of particle sizes within the samples that lead to increased segregation amongst the powder, further inhibiting powder flow, as the larger particles tended to bunch together while the smaller fines started to aggregate due to increased Van Der Waals forces present between the smaller particles of mannitol (Staniforth and Aulton, 2007). Interestingly these results were very similar to those observed with the milled mannitol F2, which also had a very poor flow due to the very small and cohesive particles, observed in Figure 3.1 (A), with particle size data shown in Figure 3.5. However with cohesive powders, like the crystalline Mannogem and Pearlitol grades, as well as the milled mannitol, tap density may not be the most accurate representation of powder flow. This is because the cohesiveness of the powders could lead to entrapped air within the sample and provide incorrect starting bulk volumes, which would in turn influence the final Carr's index and Hausner ratio.

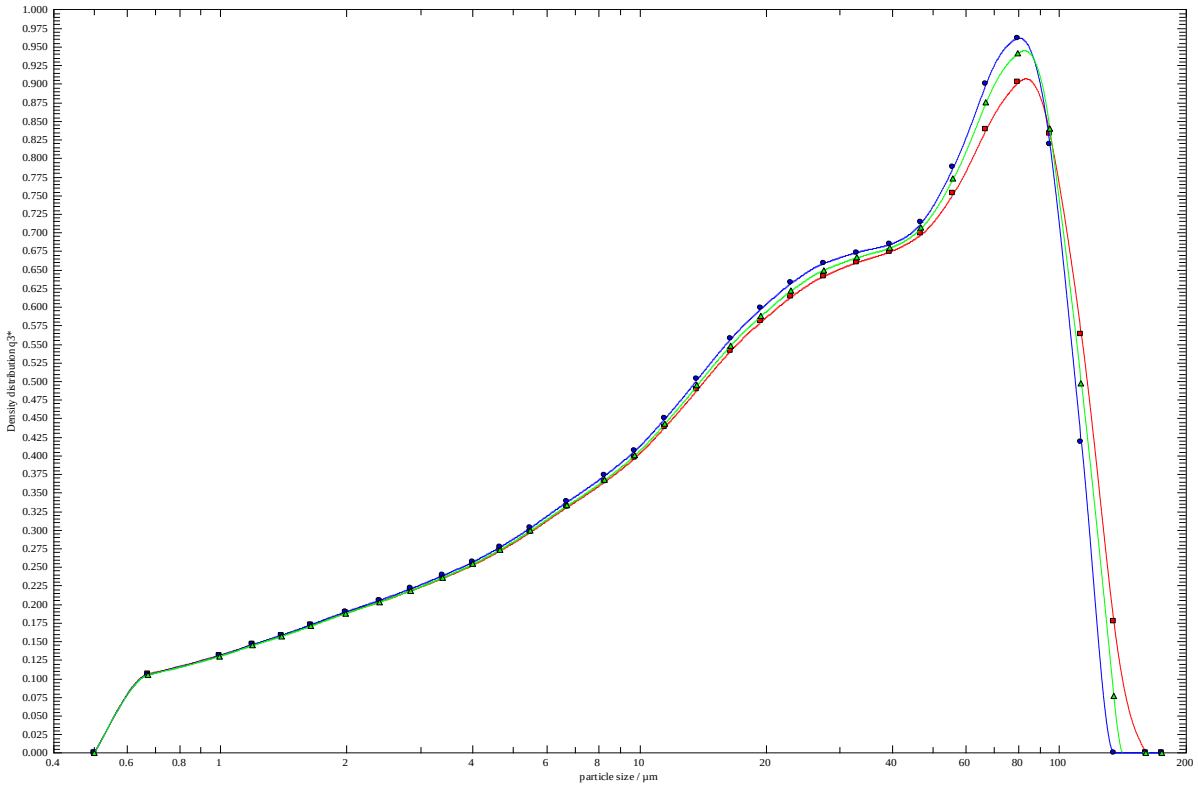

Figure 3.3: Particle sizing graph for the crystalline Mannogem powder indicating a wide particle size range within the powder, with sizes varying from 0.6-100µm, with VMD being 36.97 µm and span 3.27 µm (n=3).

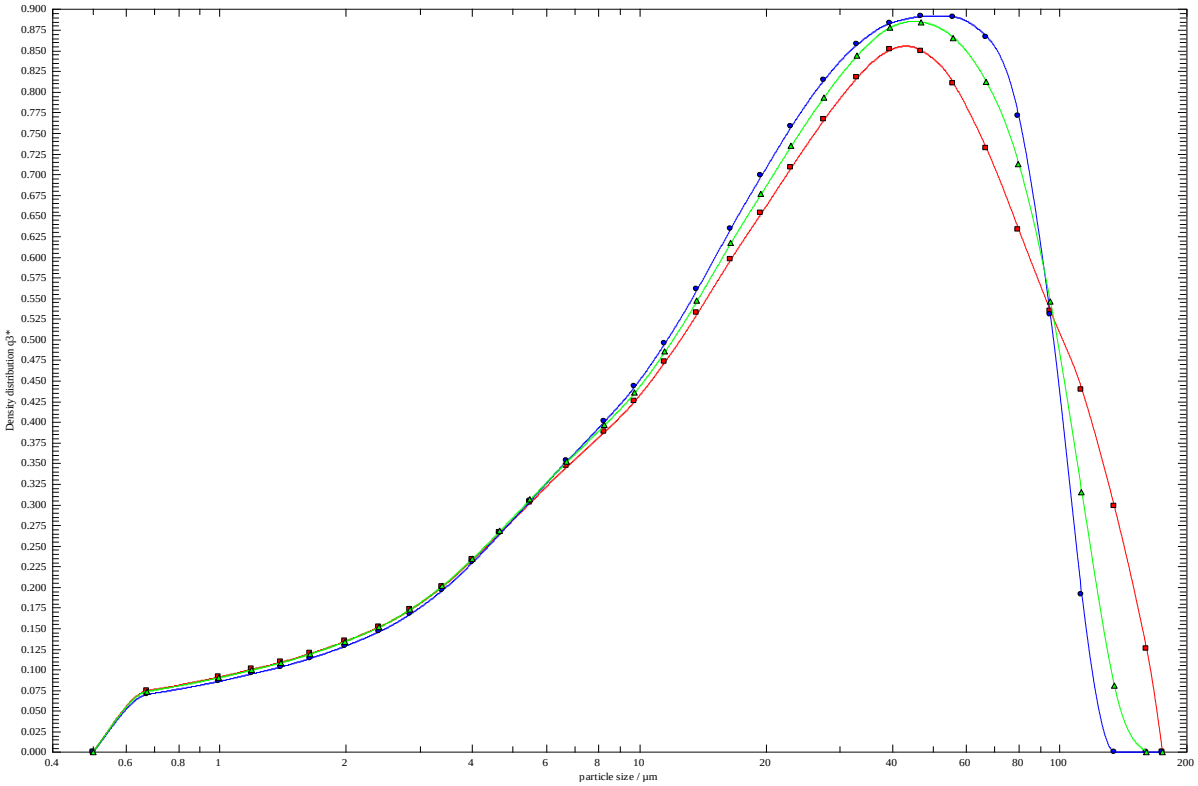

Figure 3.4: Particle sizing graph for the crystalline Pearlitol 50C powder indicating a slightly narrower particle size range within the powder compared to Mannogem Powder, with sizes varying from 0.6-80µm, with VMD being 35.33 µm and span 2.92 µm (n=3), although SEM showed particles of around 50µm (Figure 3.1 (F)).

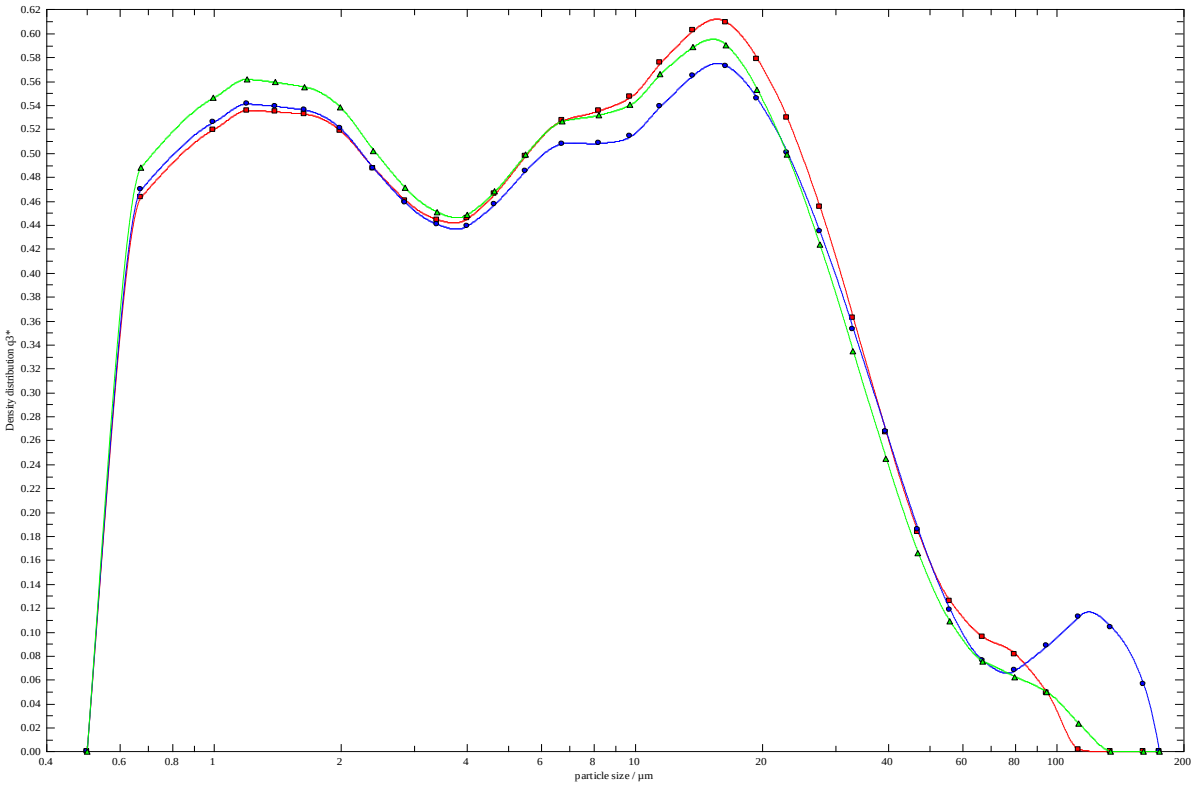

Figure 3.5: Particle sizing graph for the Milled mannitol powder (F2) with a very small particle size range with a bimodal distribution, with a high proportion of particles within the 1-2 µm size range and a high proportion in between the 10-20 µm size range, with the VMD being 11.76 µm and span 5.51 µm (n=3).

Figures (C) and (D) on Figure 3.1 represent Mannogem 2080 and Mannogem granular respectively, and are both granulated forms of crystalline mannitol. The foremost difference between the two in terms of physical properties was the particle size, as the Mannogem granular had a much wider particle size range of between 170-1190 µm (SPI-Pharma, 2012), which was evident on the SEM monographs as lots of different sized particles of different shapes were observed. The SEM monographs of Mannogem 2080 displayed a more of a uniform particle size distribution as was expected, as the particle size was between 300-590 µm (SPI-Pharma, 2012). The granulated forms of mannitol, as seen Figure 3.1 (C), showed the presence of needle shaped, crystalline grains within the granule. It was also clear that these granules were made up of agglomerated particles of crystalline mannitol, which were fused together through the granulation process. The Pearlitol 500DC (Figure 3.1 (G)) had an image at 100x magnification, as this was the only magnification whereby the whole particle could be visualised. This confirmed the manufacturer stated particle size of around 500 µm. In comparison to the granulated Mannogem grades, the Pearlitol grade displayed much less graininess

on the surface, and the presence of fine particles was reduced. Although it was expected that the granulated Pearlitol was also made up agglomerated crystals of the regular crystalline mannitol, the particle surface was much more smooth and regular. The particle size distribution in the Pearlitol sample was also much more uniform compared to both the samples of Mannogem which may explain better powder flowability results. From Figure 3.2 it was observed that the two Mannogem granulated grades did have the worst flow out of the five modified forms; however both had a fair flow which indicated that the powders would be suitable for tabletting. They didn't have as good flowability as the other grades, particularly the Pearlitol 500DC alternative, because of the wide particle size range indicated by the manufacturer. This wide particle size range would therefore have inevitably led to certain levels of segregation amongst the particles which in turn decreased the flowability of the powder. However this was overcome with the large particle size of these granulated form, which would have led to low levels of cohesiveness and promoted a homogenous bulk flow. The Pearlitol 500DC appeared to have the best flow properties of all the powders tested, with a Carr's index of 13.21 and Hausner Ratio of 1.15, which both indicated a good flowing powder. This was because this sample had a large particle size which negated any cohesive forces between the individual particles, and also the particle size distribution was narrower than what was observed with the Mannogem grades, which reduced the levels of segregation and promoted a better bulk flow of the powder.

Figure 3.1 (E) shows an image of Mannogem EZ, which is the spray dried grade of mannitol from SPI Pharma. From this diagram it was observed that the particles had a very uniform spherical shape, and had a narrow particle size range, which is a key advantage of spray drying (Hulse *et al*., 2009, Vehring, 2008). It was also evident from the SEM that there appeared to be pores present within the structure of the spherical mannitol particle, which may hold a key advantage for use in ODT's as it could help promote disintegration by having a more porous tablet, which would allow a faster influx of water/saliva into the tablet (Parkash *et al*., 2011). Pearlitol 200SD, Figure 3.1 (H), was the spray dried mannitol grade from Roquette. Similar to the Mannogem it had uniform sized spherical particles, however the key difference between the two brands was that the Pearlitol appeared to be much less

porous compared to Mannogem. Pearlitol had a smooth all round surface, whereas the Mannogem had large pores visible on the particle surface. Both spray dried forms of mannitol also had good powder flow properties, as would be expected from a spray dried formulation. This was because the spray drying process controlled particle size and shape, which in turn helped to improve powder flow by producing spherical particles with a narrow size distribution (Hulse *et al*., 2009, Lee *et al*., 2011). Both spray dried powders also had particle size of around 150-200 µm, which would have reduced the cohesiveness between the particles, thus helping to promote good bulk flow of the powder. Overall it was seen that the Pearlitol brand did appear to have better flow properties than the Mannogem grade, as there was a flow category difference between the granulated forms, possibly due to the wider particle size distribution.

In comparison to the milled samples the modified grades were all larger in size, and tended to have a more uniform particle size distribution. The milled powder was very small, on average around 11µm, and the shape varied on how the particles had interacted with the grinding media during the milling process, as seen in Figure 3.1 (A). This in turn led to poor flowability of the milled samples, with the modified grades of mannitol (excluding Mannogem powder and Pearlitol 50C, which are both regular crystalline mannitol powders) displaying a much improved powder flow, as would be expected as they had been manufactured with the main purpose of increasing powder flow (Rowe *et al*., 2012). However the crystalline powder displayed a similar flow to the milled mannitol, as this was unmodified and still had the small needle shaped particles, leading to poor flow. The difference with the milled mannitol and crystalline form of Mannogem and Pearlitol was that there were high levels of cohesiveness in the milled sample as the particle size was very small, around 11 µm, but there would have been lower levels of interlocking as the particle shape had been altered to become more uniform, and the needle shape was less evident. However there was a large particle size distribution within all the milled samples (as shown in Figure 3.5) which would have led to high levels of segregation and in turn decreased the flow properties further. The particle shape of the milled powder appeared to be more rounded / popcorn shape, as the particles had been fractured during milling, which was similar

to the granulated and spray dried grades which also had more rounded shapes as opposed to the needle shape of unmodified crystalline mannitol. With the milled powder that had undergone flow improvement through dry coating, powder flowability was substantially improved to allow for its use as a preblend in ODT development.

3.3.2 XRD and Polymorphic Form

Figures 3.6 and 3.7 represent the XRD patterns for the Mannogem and Pearlitol powders respectively. The Mannogem powder displayed a typical β-polymorph pattern, with two large peaks in the middle at 2-theta of 22 and 27, with the larger of the two peaks at 27. There were also two β-polymorph only peaks at a 2-theta of 17 and 34, and the three peaks of the fork at a 2-theta of around 24. The XRD peaks were slightly shifted to the right due to the utilisation of a cobalt x-ray source as opposed to a copper x-ray source, however the pattern remained similar (Hulse *et al*., 2009, Kim *et al*., 1998). From analysing the data, there were no significant differences between the Mannogem crystalline powder and the granulated Mannogem grades. The peaks all followed the same pattern, as seen in Figure 3.6, which indicated that the crystals within the granulated form were still predominantly of the β-polymorph, although there was a slight reduction of the large right peak at 2-theta of 27, which could have changed due to the agglomeration of the crystals within the granulated particles structure. Table 3.1 shows the results of the Rietveld refinement that quantified the phases present within the powder mix, and it was observed that there were very small amounts of the α polymorph within the crystalline and granulated forms, although this may possibly be attributed to the impurities within the powder. However there were also slight reductions of the peak intensities across the whole pattern for both Mannogem 2080 and Mannogem Granular, which may suggest the presence of the α-polymorph, but it was more likely due to the change in shape and size of the particles, as the whole pattern represented a strong fit for β-mannitol. The granulated forms on the SEM displayed a much more uniform shape with the loss of the characteristic needle form of mannitol. This in turn would have affected the way that the X-rays diffracted off the crystal due to the alteration of the particle shape and surface, and the fact that the granulated particle was now made up of agglomerated needle

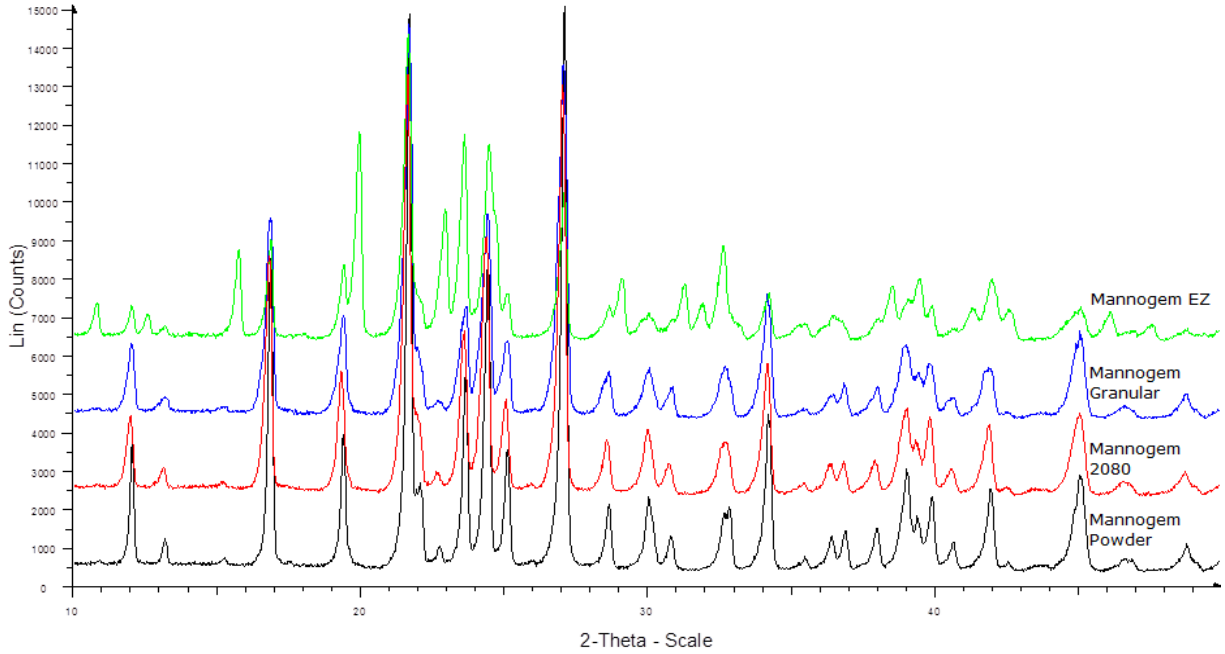

Figure 3.6: XRD patterns for the different Mannogem grades tested in this study. The Mannogem powder and the two granulated forms represented very crystalline powders with a strong fir for the β polymorph, however the Mannogem EZ, the spray dried form, showed peaks that are clearly representative of the α polymorph as well as for the β polymorph.

particles of mannitol (Scardi and Leoni, 2001). This was also evident with Pearlitol grade, as Pearlitol 50C and 500DC displayed a strong β-polymorph pattern, but Pearlitol 500DC had a reduction in intensity of the peaks across the XRD plot due to the alteration of particle shape, and increase in particle size. Again very small amounts of α-mannitol were detected on the refinement, however for the granulated form it was insignificant, suggesting that this powder was composed of the β-polymorph. The reduction of the peaks across the pattern may have been due to the enlarged particles and the inability of the x-rays to penetrate to the different crystal planes, as may have been possible with a single small mannitol crystal, which would have led to a higher intensity of diffracted x-rays. The XRD pattern for the spray dried forms, Mannogem EZ and Pearlitol 200SD, suggested that a polymorphic transformation had occurred during the spray drying process as both of the patterns showed the strong presence of the α-polymorph, with some peaks also indicating the presence of the β-polymorph. The appearance of a peak at 2-theta of 15.5, the alteration of the peaks within the fork at 2-theta of 24, the reduction of the peak at a 2-theta of 27 and the change of the pattern after a

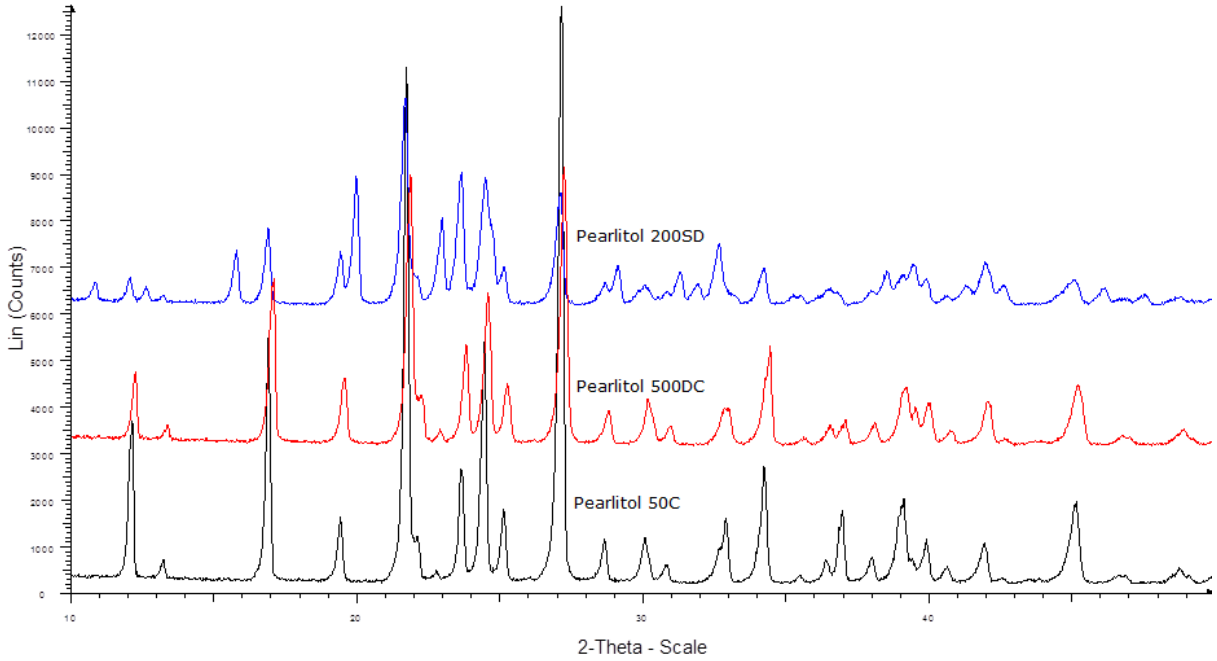

Figure 3.7: XRD patterns for the different Pearlitol grades tested in this study. The Mannogem powder and the granulated form represented very crystalline powders with a strong fir for the β polymorph, however the Pearlitol 200SD, the spray dried form, showed peaks that were clearly representative of the α polymorph as well as for the β polymorph.

2-theta of 40 all indicated that there was a strong presence of the α-polymorph within the samples. The presence of other peaks at a 2-theta of 21, 24 and 27 also indicated the presence of β-mannitol, with large parts of the plot between a 2-theta of 30-40 being typical of the β polymorph. This was confirmed through the Rietveld refinement, which indicated that Mannogem EZ had around 57% of the α polymorph present in the mixture, and Pearlitol 200SD had around 49% of α polymorph present. This was similar to previous findings (Hulse *et al*., 2009, Lee *et al*., 2011, Littringer *et al*., 2011), who all found that the spray drying induced a polymorphic change, although a quantification of the amount of polymorph present wasn't conducted, with process parameters in particular controlling the extent of polymorphic transformation. This is because the spray drying process rapidly forms a solid mannitol particle from a liquid solution, so the orientation of the atoms within the newly formed crystal would determine the polymorph present within the spray dried sample, and the results indicated that spray drying was likely to induce the formation of both α and β polymorphic crystals. The strong presence

Table 3.1: A table showing the polymorphic composition of the commercially available mannitol grades, as well as the milled mannitol tested in the previous chapter. The regular crystalline mannitol grades, alongside the granulated grades and milled mannitol provide a clear β polymorphic composition with very little α mannitol present, however spray dried forms give an almost 50:50 split for each of the β and α polymorph, indicating that spray drying clearly has an effect on the polymorphic form of mannitol.

Powder	% β-Mannitol	% α-Mannitol
F2	99.81	0.19
Mannogem Powder	99.74	0.26
Mannogem 2080	99.83	0.17
Mannogem Granular	99.98	0.02
Mannogem EZ SD	43.45	56.55
Pearlitol 50C	99.46	0.54
Pearlitol 500DC	99.96	0.04
Pearlitol 200SD	51.01	48.99

of α-mannitol suggested that the spray dried mannitol would be highly compressible, as Burger *et al*. (2000) showed that the α form was the most compressible/compactable polymorph of mannitol. The milled mannitol represented a strong fit to the β mannitol polymorph, similar to the granulated and crystalline grades, as shown in Table 3.1, indicating that it was composed of the most stable polymorph of mannitol, however the spray dried grades represented a clearly different composition which, in the case of the α polymorph, should give the spray dried powders a compressibility advantage (Burger *et al*., 2000).

3.3.3 Compressibility

Figure 3.8 represents a Heckel plot of the branded mannitol tested in this study. A clear pattern could be established between all powders, except Mannogem 2080 which followed a completely different pattern, with no visible plateau seen on the plot. This compaction simulation was conducted over a range of 0-5 KN, so a full range of compaction couldn't be studied due to a limitation with the equipment available.

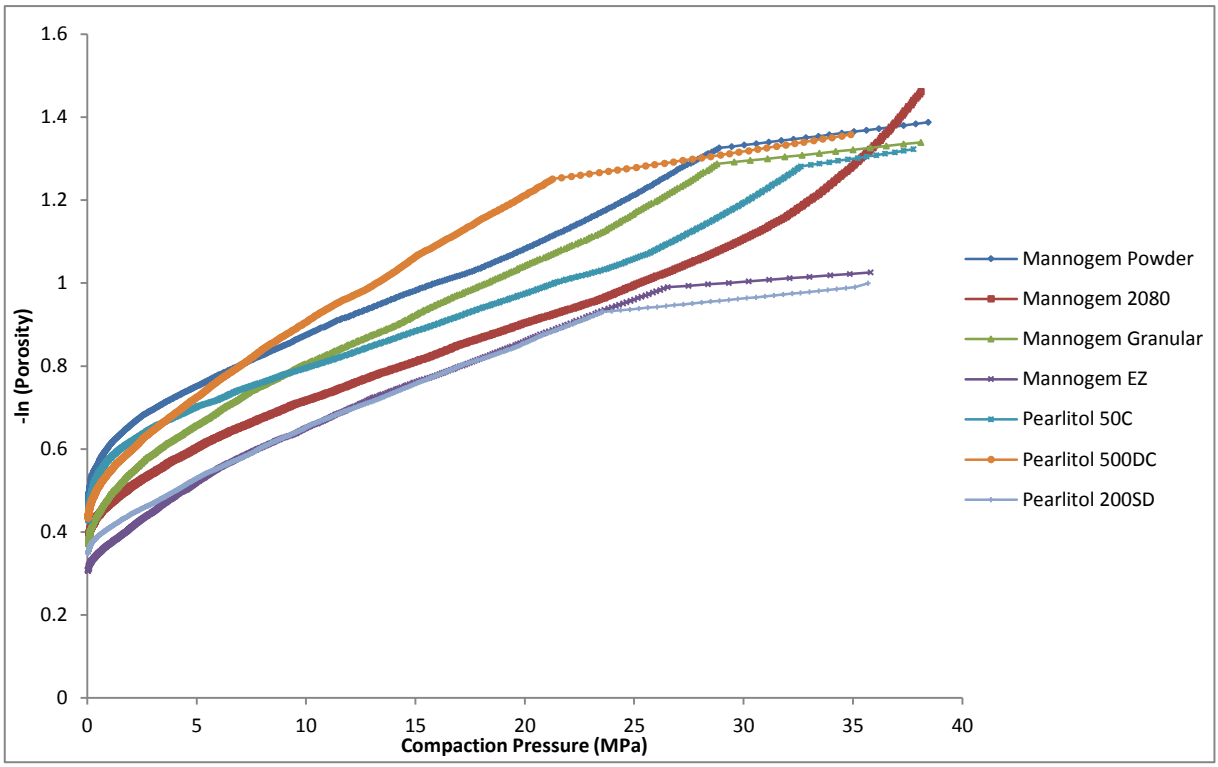

Figure 3.8: A graph showing the in die Heckel profile of the commercial mannitol grades tested in this study, with all powders, with the exception of Mannogem 2080, compressing through brittle fragmentation, as highlighted by obtained yield pressures shown in Table 3.2.

From these results it could be observed that all three Pearlitol powders, Mannogem powder, Mannogem Granular and Mannogem EZ compressed through brittle fragmentation. This was seen by the initial rearrangement stage where the line of the graph had an initial sharp rise and curved over towards the linear region, whereby the line reached a plateau and the linear part of the line indicated that further densification of the material was through fragmentation of the mannitol (Paronen and Ilka, 1996). The fragmentation of mannitol had been seen in previous studies (Ho *et al.*, 2012, Gharaibeh and Aburub, 2013), where it had been described as a brittle material. Other studies (Klevan *et al.*, 2010), described mannitol as a plastic, ductile material, but in the same study had a high yield pressure of around 132 MPa. This did however suggest that the material was compacting through fragmentation, due to the high yield pressure (>100 MPa), with plastic ductile materials usually having a yield pressure below 50 MPa (Gharaibeh and Aburub, 2013). Table 3.2 shows the graph of the calculated yield pressures of the powders tested, alongside the milled mannitol (F2) from the previous chapter, with six of the seven commercial grades having yield pressures above 100, indicating a brittle

fragmenting material, which was in agreement with previous literature (Gharaibeh and Aburub, 2013, Klevan *et al*., 2010). However, an interesting pattern emerged with Mannogem 2080, as it had a yield pressure of 17.04 ± 1.46 MPa, which indicated that this powder displayed plastic compression behaviour. The standard deviation was very small, and this material was tested on several different occasions to ensure that this was a true representation of this material, and each time a similar Heckel plot was observed, with a low yield pressure of below 20 MPa. This wasn't expected as mannitol is a fragmenting material and as seen in the previous work (Koner *et al*., 2015), and with the other six powders tested here, each different mannitol had fractured during applied pressure. The X-ray diffraction didn't indicate a high presence of the α-polymorph, which would increase plastic behaviour, whilst other powder properties were not significantly different to the Mannogem granular or Pearlitol 500DC. However in the tablet studies, ODT's made with the Mannogem 2080 displayed better hardness (Figure 3.9) than the other granulated mannitol powders tested, and friability was also low, which also led to the suggestion that this mannitol grade promoted plastic deformation rather than the fragmentation usually observed with mannitol. However because of the small compaction range analysed due to the equipment's limitation (0-5000 N), this may not have been high enough to allow the fragmentation pattern of the granular mannitol to become apparent. In comparison to the milled mannitol, which was established as a less brittle fragmenting material, likely to promote plastic compression behaviour, the yield pressures of the commercial grades were lower. However as particle size reduction of the original mannitol had occurred, the larger yield pressure indicated that mannitol was fragmenting to a lower extent and had increased ductile behaviour (Koner *et al*., 2015, Bolhuis and Chowhan, 1996, Hersey *et al*., 1973, Roberts and Rowe, 1986, Roberts and Rowe, 1985), as opposed to the brittle fragmenting mannitol observed with the commercial grades.

Table 3.2: A table showing the yield pressures of the commercial grades of mannitol obtained through in die Heckel analysis, compared to the milled mannitol (F2), showing brittle fragmentation is prevalent in most grades. Also displayed are friability/porosity results are displayed as an indicator of mechanical properties of the tablets, showing that spray dried powders are advantageous in reducing friability, with milled mannitol having quite a high friability. Data highlighted with an asterisk (*) indicates statistically significant data compared to F2 ($p<0.05$)

Powder	Yield Pressure (MPa)	Friability		Porosity	
		75 MPa	225 MPa	75 MPa	225 MPa
F2	280.88 ± 15.07	2.647	1.674	0.651 ± 0.013	0.506 ± 0.036
Mannogem Powder	156.79 ± 9.35	1.310	0.801	0.576 ± 0.012*	0.509 ± 0.012
Mannogem 2080	17.04 ± 1.46	1.702	1.345	0.602 ± 0.011*	0.530 ± 0.019
Mannogem Granular	174.93 ± 5.01	2.239	1.341	0.577 ± 0.016*	0.528 ± 0.007
Mannogem EZ	252.06 ± 6.29	1.275	0.676	0.579 ± 0.018*	0.512 ± 0.002
Pearlitol 50C	124.38 ± 0.23	4.982	1.740	0.604 ± 0.011*	0.527 ± 0.013
Pearlitol 500DC	119.33 ± 8.72	1.354	1.084	0.594 ± 0.014*	0.540 ± 0.007
Pearlitol 200SD	175.60 ± 13.80	0.865	0.675	0.616 ± 0.018*	0.544 ± 0.001

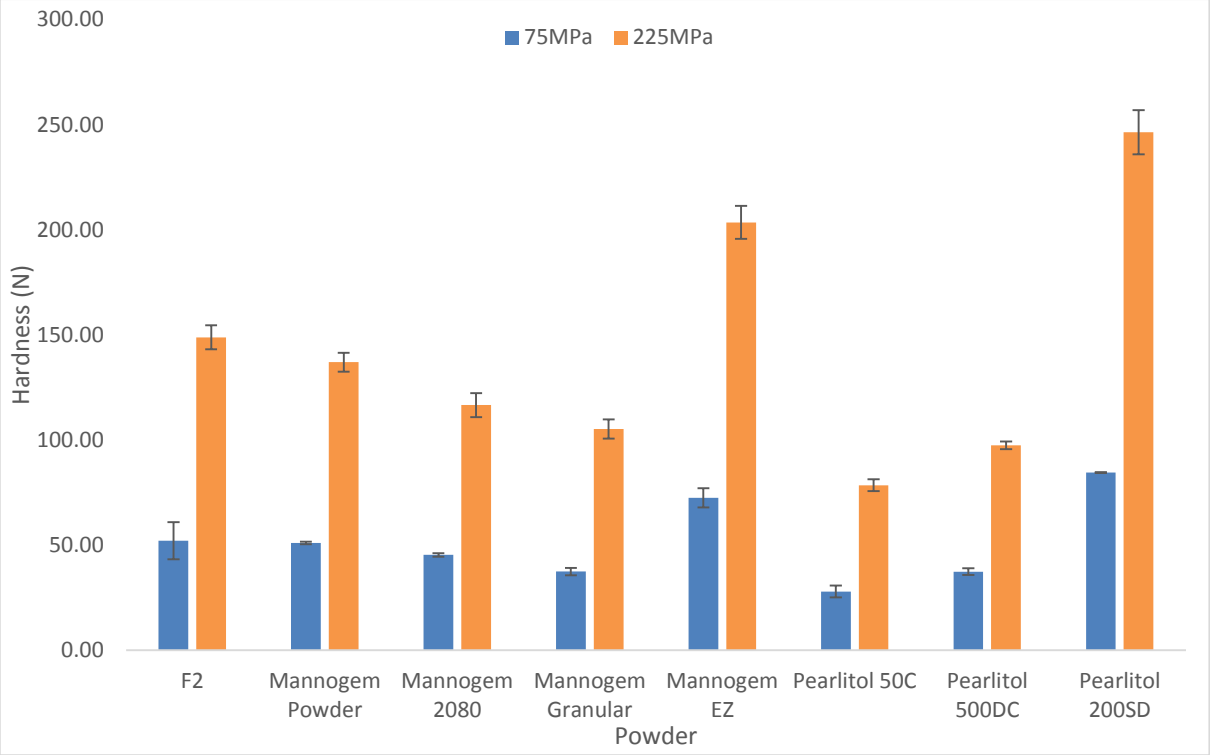

Figure 3.9: A graph showing the hardness of the commercially available mannitol grades compared to milled mannitol F2. Significant improvements in hardness were observed with the milled mannitol compared to the Mannogem 2080 (only at 225 MPa), Mannogem Granular, Pearlitol 50C and Pearlitol 500DC. However both spray dried grades (Mannogem EZ and Pearlitol 200SD) were significantly higher in mechanical strength compared to the milled mannitol. Data presented as mean ± SD ($p<0.05$, $n=3$).

An interesting pattern observed from these results was that the spray dried forms of mannitol, Mannogem EZ and Pearlitol 200SD, produced significantly harder ODT's compared to all other grades as well as the milled mannitol (ANOVA $p<0.05$), indicating improved compressibility, as shown in Figure 3.9. This was due to the presence of the α polymorph within these samples, as shown in the XRD data (Table 3.1), which had a better compressibility than the β polymorph (Burger *et al.*, 2000), thus allowing a better, more robust tablet to be formed. The Heckel analysis showed that fragmentation of the material was still occurring and that the high yield pressure was still indicative of a fragmenting material, due to the presence of 50% of the β polymorph within the powder; however the presence of the alpha polymorph in the mixture allowed an increased level of bonding within the compact, which increased the strength of the ODT. This was similar to α-lactose monohydrate in a previous study, which also showed high levels of fragmentation, but increased hardness due to the

higher level of bonding sites becoming available through the brittle fracture of the material during compression (Lerk *et al*., 1983, Vromans *et al*., 1985).

The crystalline powders displayed low hardness, with Pearlitol 50C showing significantly lower hardness than the milled mannitol (ANOVA $p<0.05$). From the SEM of Pearlitol 50C it was observed that this powder had more profound needle shaped particles than Mannogem. As can be seen with the Heckel analysis, this powder also had high levels of fragmentation during compression, coupled with the long needle shaped particles, possibly led to tablets of a lower mechanical strength. This was because during compaction the needle may have fragmented along the (011) plane (Ho *et al*., 2012), which increased the levels of die wall friction during the compression cycle. This high die wall friction was then inhibiting the levels of bonding within the compact leading to a weak ODT being formed. This was evident between Mannogem powder and Pearlitol 50C, which had significantly different hardness, as the Mannogem powder had much smaller particles that were quite wide, which then reduced the levels of die wall friction and allowed a stronger compact to be formed.

All the granulated grades didn't show very good hardness at 75 MPa, with the hardness being below 50 N, although at 225 MPa the hardness did get to an acceptable level. The hardness of the Mannogem granular forms were both reduced compared to the crystalline powder, although the Mannogem 2080 was not statistically significant at 75 MPa. This was unexpected as the yield pressure of the Mannogem 2080 was very low and even indicated a shift to a more plastic like behaviour during compression which in turn should have led to a stronger compact. The Pearlitol 500DC however did display a statistically significant improvement over the Pearlitol 50C as expected by a granular formulation, this would have been due to the granular powders being made up of less needle shaped particles, and instead having a more uniform particle shape which in turn led to lower die wall friction and a higher binding energy allowing stronger compact formation.

In comparison to the milled powders the granular and powdered mannitol's didn't fare too well, as the milled powders had a significantly higher hardness in all cases (except with Mannogem 2080 at 75

MPa). The spray dried grades represented a much better comparison to the milled powder as they had slightly improved hardness at both compaction forces compared to the F2 milled mannitol. This indicated that (for mechanical strength) the milled powders represented a good step forward in improving ODT robustness as they were high in strength, slightly lower than commercially available spray dried powders, whilst displaying a superior hardness than the crystalline and granulated grades.

3.3.3.1 Friability

Table 3.2 also shows the friability of the various mannitol grades tested in this study alongside the milled mannitol (F2). The results followed a very similar pattern to the hardness of the ODT's as described above. It was clear that the Pearlitol 50C had the worst friability at both compaction forces, which correlated with the lowest hardness as shown in Figure 3.9. This was due to the needle shape of the particle which inhibited strong compact formation and the high die wall friction during compression which possibly led to a highly friable dosage form due to the weaker bonds. It was observed that the spray dried grades also offered an advantage in terms of friability for ODT's, as they showed very low friability at both compaction forces, with Pearlitol 200SD showing below the specified 1% friability at 75 and 225 MPa. This indicated that these two forms were very useful in producing ODT's with good mechanical properties. The Mannogem powder again displayed a fairly low friability, even lower than the Mannogem granulated forms, which may have been due to the lack of long needles within the powder which allowed a stronger tablet to be formed, due to the reduction in die wall friction. The Pearlitol 500DC however displayed a massive improvement over the Pearlitol 50C, due to the granulated particles having no needle particles present within the powder blend, and also having a uniform particle size and shape.

In comparison to the milled powders, the spray dried grades and granulated forms were advantageous in reducing friability of the tablets. This was because the milled powders were made up of very small particles which were more inclined to come apart from the surface of the main compact during the friability test and therefore a higher weight loss would have been observed post friability test (Eiche

and Kudehinbu, 2009, Santl *et al*., 2012). This meant that the friability did come out higher for the milled powder, although at 225 MPa it was almost acceptable at 1.674%, which was similar to all of the granulated grades tested, showing that milling could produce ODT's with an acceptable friability if slight changes in compaction force or formulation were undertaken, although the spray dried mannitol appeared to be the best grade available for producing the least friable tablets.

3.3.4 ODT Disintegration

Figure 3.10 shows a graph of the mean disintegration times of three ODT's tested for each grade of mannitol, compared to milled mannitol (F2). From the results it was observed that the spray dried grades, Mannogem EZ and Pearlitol 200SD, produced ODTs with fast disintegration time. Upon statistical analysis it was also seen that the spray dried grades were significantly better disintegrating than both the crystalline powders and granulated forms of mannitol tested. This was because the spray dried powders had a fairly small particle size of between 150-200 µm as well as pores on the surface as seen in SEM images which may have helped increase the water uptake into the ODT, leading to faster disintegration. At 75 MPa the crystalline powders also had relatively low disintegration times of around 50 seconds, which wasn't statistically different from the spray dried grades, however there was a big increase in disintegration time at 225 MPa compared to the spray dried grades. At 75 MPa the ODTs composed of the crystalline powder disintegrated quite quickly as it had a relatively small particle size which allowed wetting of the tablet, and as the hardness was fairly low, water was able to penetrate the tablet structure more rapidly, allowing a fast disintegration of the ODT. At 225 MPa there would have been significant fragmentation occurring in the crystalline powder tablet, and as hardness was high, the subsequent disintegration time of the tablet was also high. However the granulated forms showed high disintegration time at both 75 MPa and 225 MPa. At 75 MPa the

Figure 3.10: A graph showing the disintegration times of the commercial mannitol grades compared to the milled mannitol. The results clearly show that milled mannitol provides advantages for tablet disintegration with the milled mannitol being significantly better than all grades at both compaction forces (except for the Mannogem Powder and Pearlitol 50C at 75 MPa. Data is presented as mean ± SD (n=3, $p<0.05$).

granulated forms had a significantly higher disintegration time than all the other commercial grades, and at 225 MPa the disintegration time was only significantly higher when compared to the spray dried forms, with the crystalline form having similar times at this compaction force. The high disintegration time of the granulated powders may have been due to the large particle size of the mannitol, the highest disintegration time observed was with the Pearlitol 500DC which had the largest mean size of particle, which in turn led to a slower disintegration time as the large particles took longer to break down within the disintegration medium (S Velmurugan and Vinushitha, 2010). This would have been due to the agglomeration of the mannitol crystals into one large particle, which would have resulted in large particles with the absence of pores, meaning it would have been more difficult for water to penetrate the particle and allow subsequent disintegration. Both Mannogem grades also displayed long disintegration times due to the very large particles present within the powder.

The clear advantage of milled mannitol compared to the commercial grades was its improved disintegration time. Statistical analysis showed that disintegration times with the milled mannitol was significantly lower than all the commercial grades at the 225 MPa compaction force, and all commercial grades at 75 MPa, except the crystalline powders (Mannogem powder and Pearlitol 50C). The poor disintegrating qualities of the granulated grades was due to the very large sized agglomerated particles, which led to significantly longer disintegration. Although the spray dried grades presented advantages in terms of disintegration compared to the granules, possibly due to the spherical smaller sized particles which contained pores, the milled mannitol was still clearly advantageous. This was due to the very small particle size of the milled powders (approximately 11 μm) and increased wettability of the mannitol crystal. This increased wettability of the powder particles was due to a higher exposure of the (011) plane, established as the most hydrophilic plane on the mannitol crystal, which led to an improved wetting of the ODT and therefore a faster disintegration of the dosage form (Koner *et al*., 2015).

Table 3.2 shows the porosities of the ODT's manufactured from the different grades of mannitol tested in this study. Statistical analysis showed that at 75 MPa, the milled mannitol was more porous than the commercial grades, which also gave further evidence for the faster disintegration of the ODTs. The spray dried form was expected to be more porous than the granulated grades as there were visible pores within the particles on the SEM monographs obtained, with significant pores visible on the Mannogem EZ (Figure 3.1 (E)). It can be said that the porosity differences between the graded mannitol was negligible, with all powders displaying a high porosity. The high porosity of the crystalline powder was due to the fragmentation of the needle shaped particles which led to a more porous structure, and it was seen that the Pearlitol 50C did have a slightly higher porosity than Mannogem powder due to more profound needle shaped crystals present within the powder blend. The granulated forms also formed highly porous ODT's as the large particles were unable to fill in the voids between the individual particles during packing resulting in more open pores within the tablet (Mattsson, 2000).

However the F2 milled powder tended to show a lower porosity at 225 MPa compared to all of the grades of mannitol tested in this study. This was due to the fact that the milled powders contained very small particles, which when poured into the die before compaction, and during rearrangement within the dies, could fill any small spaces of air and allow a more solid compact to be formed with a less porous structure. Compared to the 75 MPa ODTs, where the compaction force wasn't high enough to force the small voids to be filled, the 225 MPa tablets presented a less porous structure than the commercial grades. However, for milled mannitol, disintegration of the ODTs at 225 MPa was massively improved compared to the commercial grades, largely due to the increased hydrophilicity and wettability of the dosage forms.

3.4 Conclusion

In conclusion it can be seen that the spray dried mannitol had the best mechanical properties for utilisation as a binder within ODT tablets. This study indicated that it forms ODT's that have very high hardness and low friability, whilst also giving the lowest overall disintegration times of all the commercial brands tested. This was due to the presence of the alpha polymorph within the powder, which, as previously shown in literature, had the highest compressibility of all the mannitol polymorphs. The granulated forms however didn't display any significant improvements in tablet properties. This was due to the lack of α-mannitol present within the powder. The granulated forms did display a significant improvement in flow which is a key component for tabletting. If the excipient flows well it will promote the uniform flow of the bulk powder blend into the dies before compression, which is the key advantage of using granulated mannitol as opposed to the crystalline mannitol powder.

The key advantage of the milled mannitol was its very low disintegration time due to the increased wettability of the powder, providing ODTs that disintegrated rapidly, much faster than any of the commercial grades. Although mechanical strength and the friability of the milled mannitol ODT's was slightly worse than the spray dried grades the vast improvement in disintegration time provided a key

difference and upgrade compared to the commercial powders. The main disadvantage of the milled powders was the flowability which was very, very poor. As mentioned above, good powder flow is key in tableting to allow homogenous bulk powder movement into the dies, which produces a uniform and reproducible tablet. The flowability of the milled mannitol, as seen in the previous chapter, was capable of being enhanced to suitable levels, and therefore the milling of mannitol provided a suitable alternative to the commercial grades for the production of ODTs.

Chapter 4

Development of Novel Dry Coated Mannitol/MCC composite Powder for Utilisation in Orally Disintegrating Tablets

4.1 Introduction

Throughout the first two chapters of this thesis the advantages of milled mannitol have been clearly established, with the milling of commercially available crystalline mannitol producing a vastly superior tableting excipient over the unmilled equivalent. The inherent poor compressibility properties of crystalline mannitol were effectively reduced through the milling process, with the post milled mannitol presenting a more plastically deforming material as opposed to the usual fragmentation compression profile that mannitol undergoes (Koner *et al*., 2015). The hardness of the milled mannitol was also found to be superior compared to the unmilled mannitol, largely down to its superior compressibility, which upon Heckel analysis showed a reduction in the fragmentation behaviour. With this increased mechanical strength it was expected that the disintegration properties of the resulting tablets would worsen substantially, however the opposite pattern was attained. Due to the predominant fracture of the crystal at the hydrophilic (011) plane, the milled mannitol displayed increased wettability, producing tablets that were not only of superior mechanical strength, but disintegrated rapidly even in the absence of any disintegrants, making milled mannitol an ideal excipient for use in ODTs.

In comparison to the currently available commercial mannitol products, including the popular spray dried and granulated grades, milled mannitol presented a viable alternative. In terms of the tablet properties of the resulting ODTs, milled mannitol had many advantages over the granulated forms, with hardness being higher and disintegration of the tablets being lower. The mechanical properties of the tablets produced from the spray dried powders were impressive, whilst disintegration times were also low. This was due to the highly porous nature of the particles, whilst the presence of the α-polymorph gave spray dried mannitol an increased plastic deformability, resulting in the high mechanical strength (Hulse *et al*., 2009, Lee *et al*., 2011, Littringer *et al*., 2011, Burger *et al*., 2000). Yet milled mannitol gave very similar properties to the spray dried product, with mechanical strength being similarly high, whilst disintegration times of the tablets were low. However, the very small sized particles (<11µm) resulted in poor powder flow. Particles of this size are highly cohesive due to the

large degree of electrostatic/Van der Waals forces, leading to a poor homogenous bulk flow of the powder (Staniforth and Aulton, 2007, Mullarney and Leyva, 2009).

Powder flow is a major factor in the industrial scale processing of tablets, as the flow can impact on the tableting machines ability to produce a uniformly weighted tablet with a uniform dose, whilst the quality of the tablet surface can also be affected (Staniforth and Aulton, 2007, Sun, 2010). Preliminary flow optimisation studies were conducted in Chapter 2 whereby it was established that the flow of the milled mannitol could be optimised using a standard tableting excipient alongside the flow aid, colloidal silicon dioxide. The novel composite blender designed in the laboratory was the most effective at producing a flowable powder, whilst the industry standard cube mixing method was not able to replicate the same results. The powders were processed on a larger scale auto tablet press, whereby the composite blender produced dosage forms of a higher quality, whilst the uniformity of the cube blended tablets were poor. This gave a clear indication that milled mannitol could be used in scale up processes, however further optimisation was required.

The aim of this study was to utilise the novel composite blender to produce an optimised powder blend containing a large proportion of the milled mannitol. It was important that mannitol was the largest proportion of the blend due to the advantages it possessed in producing fast disintegrating, robust ODTs. The novel composite blender possesses unique qualities in its method of mixing powders. The utilisation of high speed and air pressure in the mixing vessel allows the powders to undergo a dry coating process (Dahmash, 2016). Due to the relatively small particle size of milled mannitol, it presented an ideal candidate for dry coating as a guest particle. MCC was chosen as the host particle for milled mannitol, as it is a commonly used excipient for direct compression (Thoorens *et al*., 2014). The overall aim of this study was to develop an optimised ODT blend capable of incorporating high payload of insoluble drug without compromising mechanical properties and disintegration time of the resultant ODT.

4.2 Materials and Methods

4.2.1 Materials

D-Mannitol (≥98% purity) was obtained from Sigma-Aldrich (Dorset, UK), MCC as Avicel PH102 and PH101 were used for this study and was obtained from FMC Biopolymer (Philadelphia, USA) and colloidal silicon dioxide (Aerosil 200) was obtained from Evonik Industries (Essan, Germany). For tableting studies magnesium stearate was obtained from Fischer Scientific (Loughborough, UK) and the API Ibuprofen was purchased from Shasun Chemicals (Tamil Nadu, India). Glyceryl Behenate (Compritol 888 ATO) was obtained from Gattefossé (St-Priest, France) and Ethocel HP was obtained from Colorcon Inc (Harleysville, USA) and were utilised as glidants.

4.2.2 Composite Blending

In total, 4 powder blends were manufactured as shown in Table 4.1. The blends were predominantly composed of 87.5% D-mannitol, (unmilled or milled), (F2 formulation taken from a previous study (Koner *et al*., 2015), as it was found to provide tablets with the most promising ODT characteristics) along with the addition of other excipients. The energy input into this powder was 1.71 J/kg, with the powder being milled for 30 mins at a speed of 200 rpm, with the ball to powder weight ratio (BPR) at 5. 12% w/w of MCC was added to the milled mannitol for preblend mixing, as this was the concentration that gave the most beneficial flow results from Chapter 2. Colloidal silicon dioxide was used as a flow aid. These powders were treated as premixes, as a powder blend which could be added to varying concentrations of API to manufacture an ODT. The composite blender is a lab scale device built and manufactured in the laboratory and uses a novel one step dry coating process to adhere small guest particles on to larger host particles to enable functionalised particles to be manufactured (Dahmash, 2016). All powders were accurately weighed according to the specifications outlined in Table 4.1, and added to the coater. The coater was then sealed and run for 30 mins at 2000 rpm with 1 bar of air pressure to aid the coating process.

4.2.3 Cube mixing

To analyse effects of composite blending, cube mixing was also used as a control to mix the preblends to allow assessment of any differences between the resulting powders from the two processes. Powders were weighed and added to the standard cube mixer, part of the Erweka AR403s Multi-Lab (Heusenstamm, Germany), and mixed for 30 mins at 250 rpm. Details are outlined in Table 4.1.

4.2.4 Investigation of Powder Flow

Angle of repose was used as the method of choice for assessing powder flow. For angle of repose the method outlined in the USP monograph <1174> (USP37, 2014c) was followed, and the height and diameter of the pile measured. This was then added to the equation, $\tan(\Theta)$ = height/0.5diameter, where Θ was the angle of repose. All values were analysed in triplicate and displayed as mean ± SD. This was conducted on the preblends only to allow the effects of processing methods to be assessed.

4.2.5 Blending with an API

Ibuprofen was used as a model low solubility, BCS class II drug (Alvarez *et al*., 2011, Rinaki *et al*., 2004), which is also poorly compressible at high doses (Nada *et al*., 2005, Patel and Bansal, 2011, More *et al*., 2013). Ibuprofen was added in concentrations varying between 10-50% to the each of the premix blends and mixed for 10 mins at 250 rpm in the cube mixer (Erweka Ar403s, Heusenstamm. Germany). 1% w/w magnesium stearate was added to lubricate the powder ready for tableting.

Table 4.1: A table outlining the powder compositions and blending process for each of the preblends investigated in this study.

Powder	Mannitol (87.5%)	Excipient (12%)	Mixing Method
1	Milled	MCC	Cube
2	Milled	MCC	Composite
3	Unmilled	MCC	Cube
4	Unmilled	MCC	Composite

4.2.6 Tableting and tablet properties

Individual 500 mg portions of powder from each of the blends were weighed and compressed using a Specac semi-automatic hydraulic press (Slough, UK) equipped with 13 mm flat faced punches. An initial compression force of 150 MPa was chosen to manufacture robust tablets at 10% w/w ibuprofen concentration and 75 MPa for tablets ≥30% w/w ibuprofen.

4.2.6.1 Hardness

Hardness of the all the tablets was measured using a Copley TBF 100 Hardness tester (Nottingham, UK). Tensile strength (σ) was then calculated using the equation:

$$\sigma = \frac{2\,H}{\pi\,D\,T} \qquad \text{(Eq. 4.1)}$$

Where H is the hardness, D is the diameter and T is the thickness of the tablet. All readings were taken in triplicate and displayed as mean ± SD.

4.2.6.2 Friability

The standard USP friability test was used for the assessment of the percentage friability of the manufactured tablets (USP37, 2014d). Six tablets were brushed off and weighed altogether for the initial weight, they were then inserted into a Sotax F2 Friabilitor (Allschwil, Switzerland). The test was conducted for a total time of 4 minutes at 25 rpm, with 100 revolutions in total. The tablets were then brushed off and reweighed to get the final weight. Percentage friability was calculated using the equation:

$$\%\,Friability = \frac{Initial\ weight - Final\ weight}{Intial\ weight} \times 100 \qquad \text{(Eq. 4.2)}$$

4.2.6.3 Disintegration Time

The standard USP disintegration method was used to assess disintegration time of the tablets (USP37, 2014b). A Copley ZT41 disintegration apparatus (Nottingham, UK) was used, with a single tablet being tested each time for accuracy. Each tablet was placed in the vessel (without a disk) and oscillated at

30 cycles per minute. A dissolution medium of 800 ml distilled water was maintained at 37 °C, and disintegration time measured when all of the fragments of tablet had passed through the mesh at the bottom of the vessel. All readings were taken in triplicate and represented as mean ± SD.

4.2.6.4 Porosity

Porosity of the tablets was assessed using a Quantachrome Helium Multipycnometer (Florida, USA). Diameter and thickness of the ODT's was measured using a digital calliper, and the weight of individual ODT's taken using an electronic balance. The bulk volume (V_B) and bulk density (ρ_{bulk}) of the tablets were then calculated using the following equations:

$$V_B = \frac{\pi R^2}{T} \quad \text{(Eq. 4.3)}$$

$$\rho_{bulk} = \frac{Tablet\ weight}{V_B} \quad \text{(Eq. 4.4)}$$

The true volume (V_t) of the tablet was calculated using the pycnometer, which applies the theory of gas displacement allowing the porous nature of the tablet to be assessed. The true volume was calculated using the equation:

$$V_t = V_c - V_r \left(\frac{P1}{P2} - 1\right) \quad \text{(Eq. 4.5)}$$

Where V_C is the volume of the sample cell, V_r is the volume of the reference cell, P1 and P2 are the atmospheric pressure and pressure change during the measurement respectively. The true volume was then used to calculate true density in the equation:

$$\rho_{true} = \frac{Tablet\ weight}{V_t} \quad \text{(Eq. 4.6)}$$

The final step to calculate porosity (ε) of the ODT used the following equation:

$$\varepsilon = 1 - \frac{\rho_{bulk}}{\rho_{true}} \quad \text{(Eq. 4.7)}$$

4.2.7 Optimisation of Silica Addition

Optimisation studies for silica included evaluation of concentration, time and stage of addition into the preblend. For addition stage, the aliquots of milled mannitol and MCC were mixed for the first 30mins, silica at a concentration of 0.5% was then added to the powder and mixed for a further 5mins and compared to when silica was added at the start of processing alongside both the mannitol and MCC. To gather data for the optimal mixing time of silica, an initial mixture of milled mannitol and MCC was compositely mixed for 30 mins, with 0.5% silica being added after this initial mixing step. Portions of powder were removed at 10 mins, 20 mins and 30 mins and analysed for angle of repose. The final stage of silica optimisation was the amount of silica added into the preblend. Several concentrations including 0.5%, 1%, 1.5% and 2% w/w were investigated. The silica was added after initial preblend mixing of 30 mins and blended for a further 20 mins. These blends were analysed for powder flow according to the angle of repose.

4.2.8 Surface Coverage Optimisation of the Preblend

For dry particle coating, there is a critical concentration of guest particle which results in full surface coverage of the host particle. This could be used to optimise the process of dry coating to allow one or more layers of coated particles on the host if the guest particle is added in separate stages, with the first stage involving the addition of the required amount of mannitol for full surface coverage, and the second stage whereby a second quantity of mannitol is added according to blend requirements. This percentage of mannitol was calculated using equations and methods developed by Yang *et al*. (2005). The equation found that 36% w/w of mannitol was needed for full surface coverage, with 64% MCC (Avicel PH102) as the carrier particle.

An additional investigation conducted was the effect of particle size of the host MCC. A comparison of the initially studied Avicel PH102 and Avicel PH101 was undertaken, with particle sizes being 100 µm and 50 µm respectively (FMC-Biolpolymer, 2016). The use of a smaller sized host particle resulted in the surface coverage calculations giving a 58% w/w of mannitol and 42% w/w of the MCC (Avicel

PH101), showing that the smaller sized particles were capable of hosting more of the guest mannitol. Blends were tested for flow followed by the addition of ibuprofen as outlined above.

4.2.9 Assessment of Alternative Glidants

An investigation into the type of glidant in the powder blends was undertaken to assess if there could be a suitable alternative to colloidal silicon dioxide. Glyceryl Behenate (Compritol 888 ATO) and Ethocel HP were investigated. The same concentration and mixing time/method as silica was used to allow a direct comparison between the properties of these three excipients (1% added post MCC/mannitol mixing and mix for 20mins). Blends were analysed for flow and Ibuprofen added at the same concentrations as above. 500 mg tablets were manufactured at 75 MPa and tested for their properties.

4.2.10 Statistical Analysis

One/Two-way ANOVA followed by a Tukey's/Sidak's multiple comparison post-hoc test were performed using GraphPad Prism 6 software (California, USA). For statistical significance a p-value <0.05 was used, and all data was presented as mean ± standard deviation.

4.3 Results and Discussion

4.3.1 Milled vs Non Milled Mannitol

The first set of investigations focussed on assessing the difference between employing milled and non-milled mannitol with the model API ibuprofen. In terms of powder flow, data from the previous chapters showed that milled mannitol flowed very poorly due to its very small particle size, resulting in cohesive powders when compared to unmilled mannitol. This was also evident with the angle of repose results generated in this study (Figure 4.1). Unmilled mannitol was several flow categories below that of milled mannitol for both cube and composite mixing indicating it was superior. This was attributed to the larger particles, resulting in lower Van der Waals and electrostatic forces.

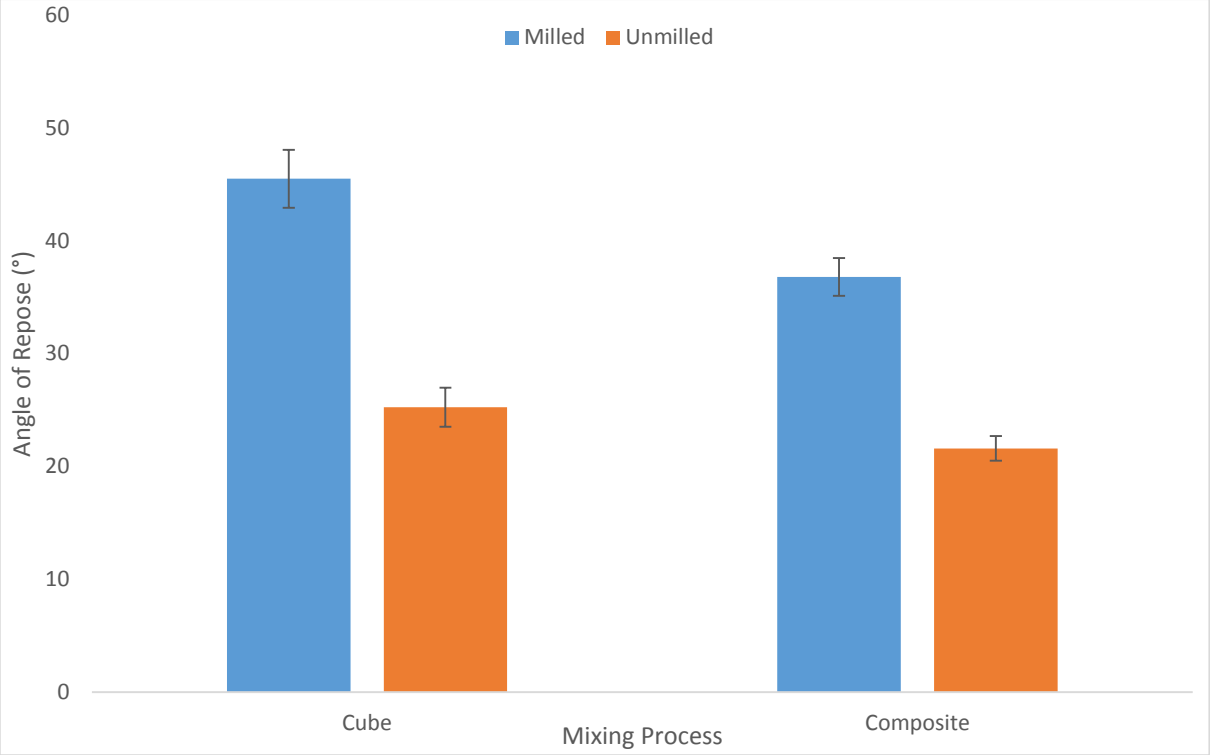

Figure 4.1: A graph showing the powder flow of the MCC/mannitol preblends, comparing the difference between milled and unmilled mannitol in the two different mixing processes, through the angle of repose. Results indicated that unmilled mannitol had a superior flow ($p<0.05$), whilst composite blending was also beneficial in reducing the angle of repose ($p<0.05$) for milled mannitol. Data is presented as mean ± SD (n=3).

As highlighted in the previous chapter milled mannitol presented several advantages over its unmilled counterpart, especially when employed in ODTs (Koner *et al*., 2015), with mechanical strength being higher and disintegration times being lower regardless of the improved strength of the tablet. Figure 4.2 and 4.3 shows the comparison of milled and unmilled mannitol in terms of the disintegration time and hardness respectively. From Figure 4.2 it was seen that the disintegration time with milled mannitol, even when employed with the poorly soluble drug ibuprofen, remained low. Compared to unmilled mannitol a significant improvement in disintegration time was observed at Ibuprofen concentrations of 30 and 50% w/w ($p<0.05$). When unmilled mannitol was used at the 50% w/w concentration the tablets could not be classed as an ODT, even within EU guidelines due to the tablets disintegrating beyond 30 mins. However when the milled mannitol was used, disintegration time remained below 80 s, highlighting the superiority of milled mannitol for ODT production, due to the increased wettability of the excipient, attributed to the increased exposure of the hydrophilic (011) crystal plane and small particle size (Koner *et al*., 2015, Ho *et al*., 2009).

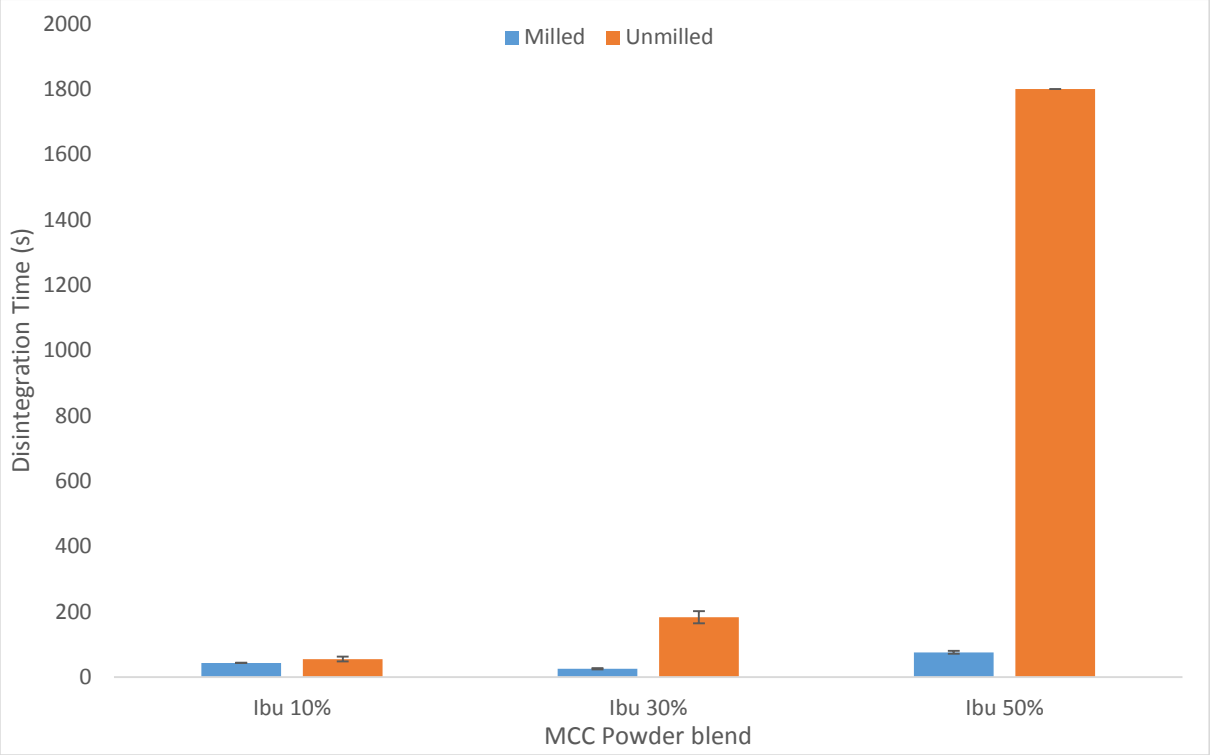

Figure 4.2: A graph showing the disintegration times of manufactured ODTs containing the model API ibuprofen at concentrations varying from 10-50% comparing milled and unmilled mannitol. Only compositely blended tablet data is shown on the graph. Results indicated that at concentrations of 30% ibuprofen and above tablets containing milled mannitol had significantly lower disintegration times than tablets containing unmilled mannitol. Data is presented as mean ± SD (n=3, $p<0.05$ at all concentrations except 10% ibuprofen).

Including milled mannitol was key in keeping disintegration times low, even in the presence of a low-soluble API at a high drug load. This study gave clear indication that milled mannitol was very beneficial in improving the wettability and disintegration profile of the dosage form as a whole. The small sized particles making up the milled powder would have been able to distribute themselves throughout the ibuprofen powder more uniformly than the larger unmilled particles. This would have resulted in not only the outer layer of the tablet having higher affinity for water, but the inner structure of the tablet having a higher affinity for water, resulting in a quicker breakdown of the whole table structure and resultant faster disintegration of the tablet.

However in terms of mechanical strength, shown in Figure 4.3, an opposite pattern was observed from the previous study; here it appeared that although mechanical strength was within acceptable levels for milled mannitol it was actually lower than the unmilled alternative. It was possible that the inclusion of ibuprofen had actually affected the bonding mechanism of the milled mannitol, as in the

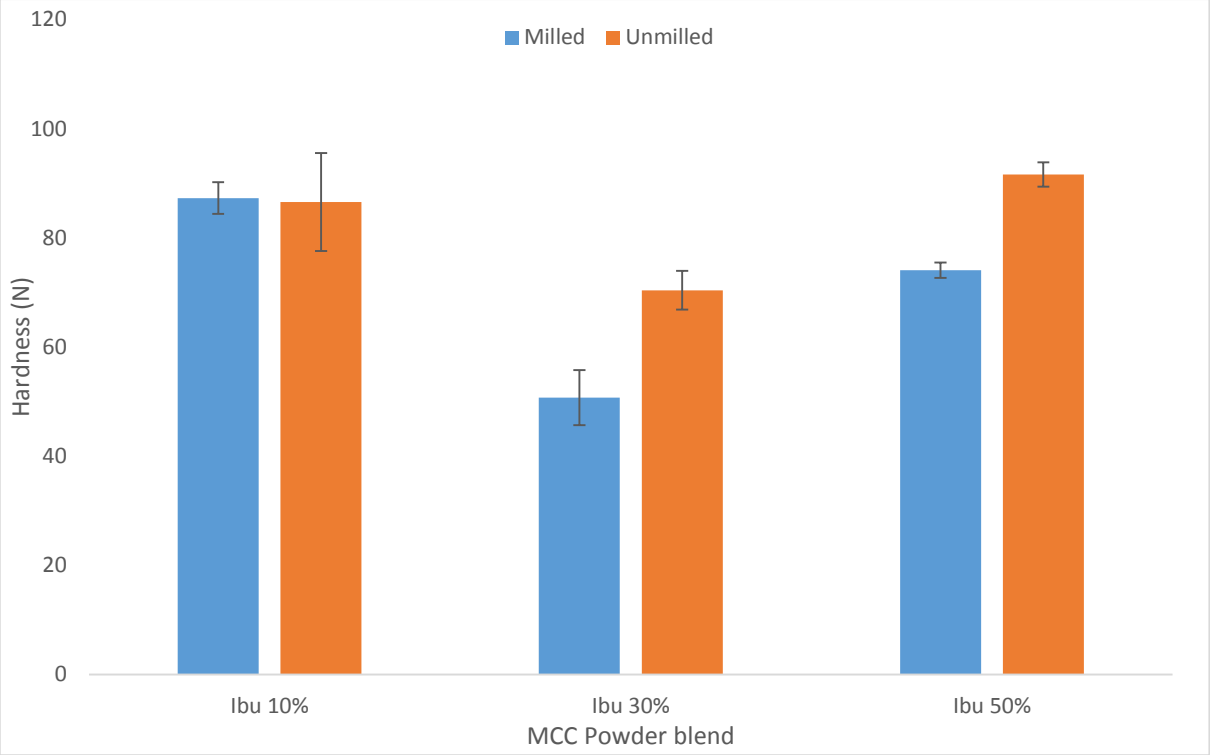

Figure 4.3: A graph showing the hardness of manufactured ODTs containing the model API ibuprofen at concentrations varying from 10-50% comparing milled and unmilled mannitol. Only compositely blended tablet data is shown on the graph. Data is presented as mean ± SD (n=3, $p<0.05$ for all conditions except MCC/Ibu 10%).

previous study milled mannitol had improved mechanical strength compared to the unmilled control, at a compression force of 225 MPa (Koner *et al*., 2015). This could have been due to the addition of the silica during the initial 30 min mix of the preblends. The milled mannitol was far more cohesive than the unmilled alternative due to its very small particle size. This could have led to the silica particles that were added at the start of mixing being more inclined to coat on to the milled mannitol as a result of the high interparticulate forces attracting the surrounding particles within the powder blend. Due to the mixing time of 30 mins, it provided a sufficient time for the silica to largely coat the surface of the milled mannitol. The coating of the silica on the milled mannitol would have therefore reduced the ability of the mannitol to form strong bonds with adjacent mannitol particles during tablet compression and therefore reduced the strength of the resulting compacts (Chowhan and Yang, 1983, Ohta *et al*., 2003). The unmilled mannitol was far less cohesive and there were less surface attractive forces present within the powder, therefore promoting a more even distribution of the silica throughout the powder blend, resulting in less disruption between the bonding of the mannitol

particles. Another key difference in this study compared to the previous study was that lower compression forces were used. Therefore it was possible that in this study the compression force was lower than that needed to induce levels of plastic deformation with the milled mannitol resulting in tablets of a slightly lower mechanical strength.

In terms of the friability of the ODTs, as shown in Figure 4.4, it was previously found that friability of the milled ODTs was generally similar to the unmilled tablets. This was primarily due to the very small mannitol particles making up the bulk of the tablet, which were more inclined to come apart from the surface of the tablet during the friability test. In this study the reduced interparticulate binding capability of the mannitol particles due to the lower compression force and presence of silica was expected to slightly increase the friability of the tablets made of milled mannitol. It was observed that the friability did vary between the powders, some indicating that milled mannitol had improved

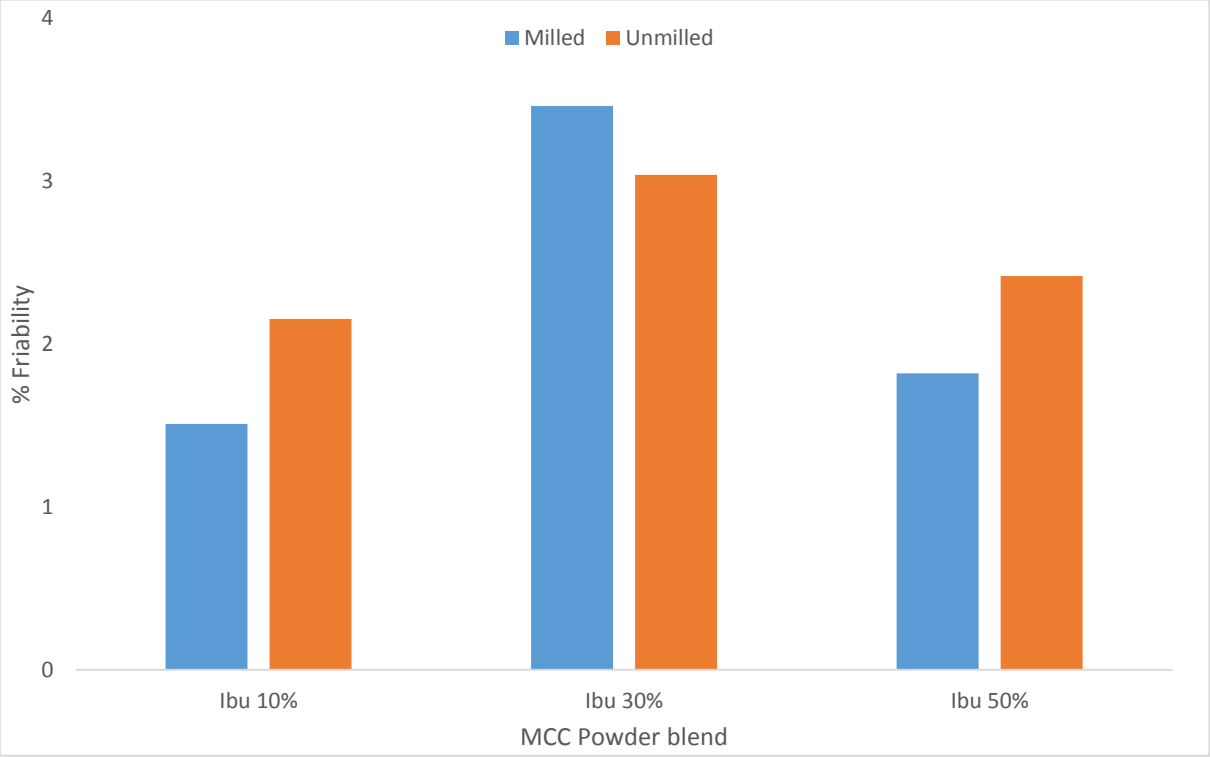

Figure 4.4: A graph showing the friability of manufactured ODTs containing the model API ibuprofen at concentrations varying from 10-50% comparing milled and unmilled mannitol, showing a mixed pattern with friability for both unmilled and milled mannitol being similar, ranging from 1.5-3.5%. Only compositely blended tablet data is shown on the graph.

friability and others indicating an increased friability. Overall it could be concluded that friability of the tablets wasn't distinctly different between the milled and unmilled mannitol.

4.3.2 Composite Mixing vs Cube Mixing

The next set of investigations were designed to assess the differences between the composite and cube blending processes. The composite blender was utilised as a method for dry particle coating whereby small guest particles adhere to a larger host particle to form new functionalised particles. Whereas the cube mixer is an industry standard mixing process that uses much lower speeds in a larger mixing volume. Figure 4.1 shows the flowability of the premix powder blends and allows a comparison of the two mixing processes. From the angle of repose it was evident that the composite blender was beneficial in providing a more flowable powder with both unmilled and milled mannitol, with an approximate reduction of 4° and 8° for the powders respectively. The key advantage with composite blending was evident with the milled mannitol, as a several category flow improvement was observed, from a poor flowing powder to a fair flowing powder, where no flow aid was needed, therefore being acceptable for use in an auto-tablet press (as highlighted in Chapter 2) (USP37, 2014c). There was also an improvement in flow observed with the unmilled powder, although both the cube and composite mixer provided powders that flowed well.

The improvement in flow with the composite blender was attributed to the dry coating process, whereby the highly cohesive small mannitol particles were coated on to the surface of the larger MCC particles as observed in the SEM images (Figure 4.5). It was observed that the milled mannitol composite blend (Figure 4.5(C)) resulted in more surface coating of the MCC, as small mannitol particles were clearly visibly adhered to large areas of the MCC surface. The surface layering was not as evident with both the unmilled mannitol (Figure 4.5(B) and (D)) and to the cube mixed powder

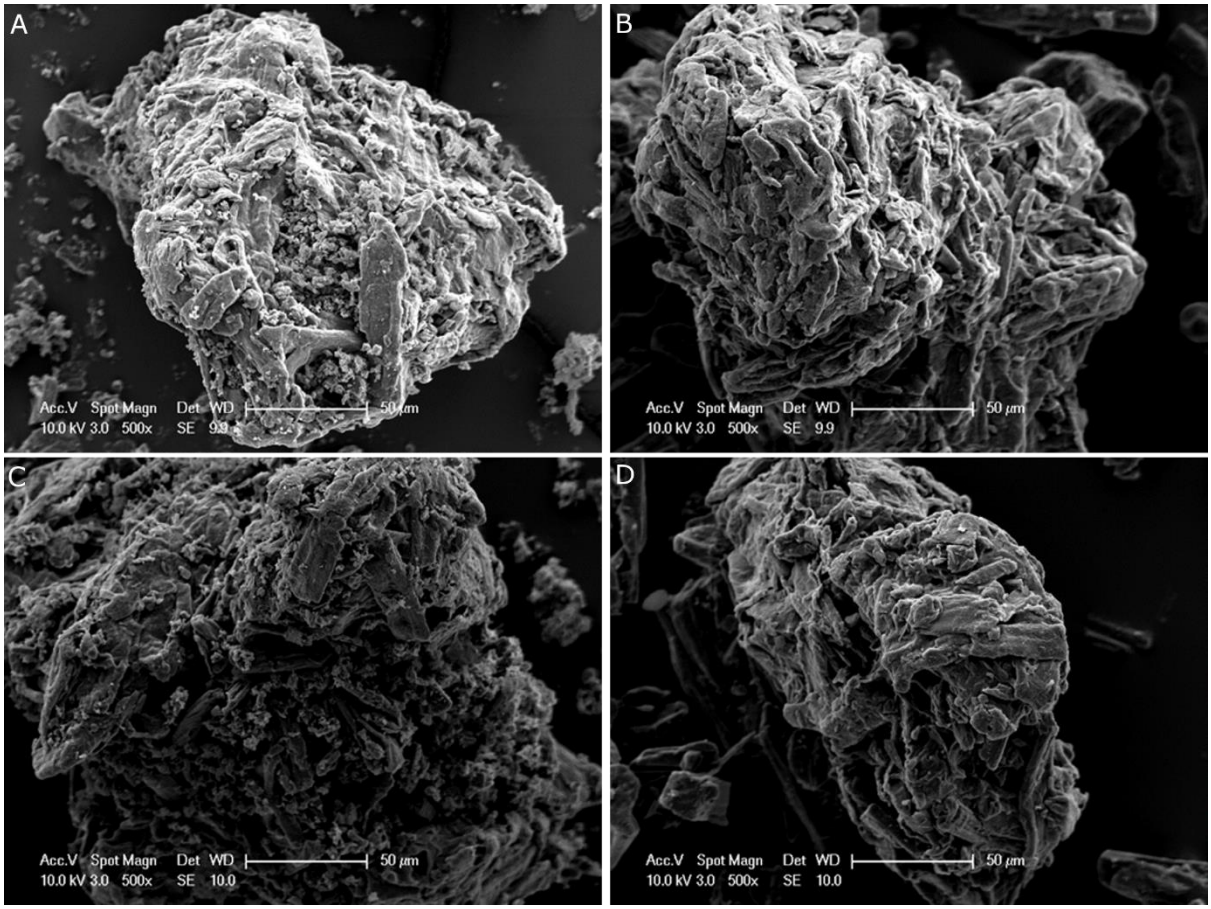

Figure 4.5: SEM images showing images of a typical MCC particle within the investigated preblends. A – Cube mixed milled mannitol/MCC; B – Cube mixed unmilled mannitol/MCC; C – Compositely mixed milled mannitol/MCC and D – Compositely mixed unmilled mannitol/MCC, with compositely mixing milled mannitol resulting in higher levels of dry coating.

(Figure 4.5(A)). The milled mannitol was on average around 11 µm, with particles observed in the nanorange, which led to the particles being highly cohesive. The dry coating process was a high shear procedure employing high speed and an air blade, through the introduction of 1 bar of air pressure. This produced deagglomeration of the cohesive mannitol particles, followed by deposition on to the surface of the much larger MCC particles. Compared to cube mixing, where the physical method of deagglomeration was absent, the composite blender resulted in more mannitol particles being available to adhere to the larger MCC particles. There would have been high levels of attractive forces between the milled mannitol and the MCC due to the large difference in the particle size between the leading to robust new particles being formed (Dahmash and Mohammed, 2015). The resulting powder therefore had less free milled mannitol within the blend and therefore overall cohesivity of the powder would have been reduced, allowing an improvement in powder flow compared to the cube

mixed alternative. The cube mixer didn't employ these high shear forces, and the process would have provided an interactive mix, whereby no/low levels of coating would occur, as seen in Figure 4.5. Due to the large particle size difference, leading to increased segregation, and high cohesivity, the powder would have flowed very poorly, as indicated by the high angle of repose (He *et al*., 2013).

In terms of tableting properties, graphs comparing disintegration time, hardness and friability are shown in Figures 4.6-4.8 respectively. The general consensus was that there wasn't a vast variation between the ODT properties in terms of the method required to produce the premix powder blend. Most of the disintegration times for ODTs (Figure 4.6) were lower for the composite mixer, however a significant difference was only observed with the MCC/Ibu 50% w/w blend. The advantage of using the composite mixer for disintegration time was that it provided a more uniform/homogenous mix, as the mannitol coated the larger MCC particles. This allowed water to be attracted to within the inner structure of the tablet to a higher extent, as the mannitol was more uniformly distributed throughout the tablet.

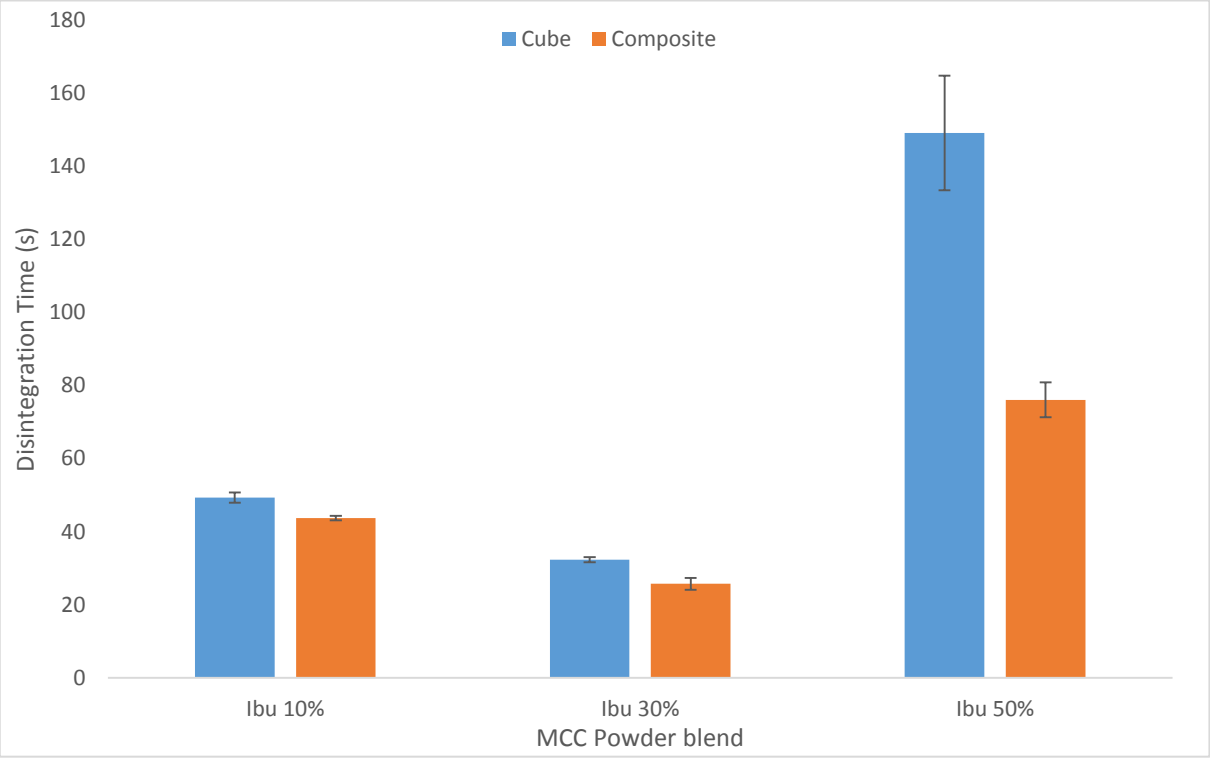

Figure 4.6: A graph showing the disintegration time of manufactured ODTs containing the model API ibuprofen at concentrations varying from 10-50%, comparing the cube and composite mixing methods, with statistically significant results only observed at MCC/Ibu 50%. Only milled mannitol results are shown in the graph. Data is presented as mean ± SD (n=3, $p<0.05$).

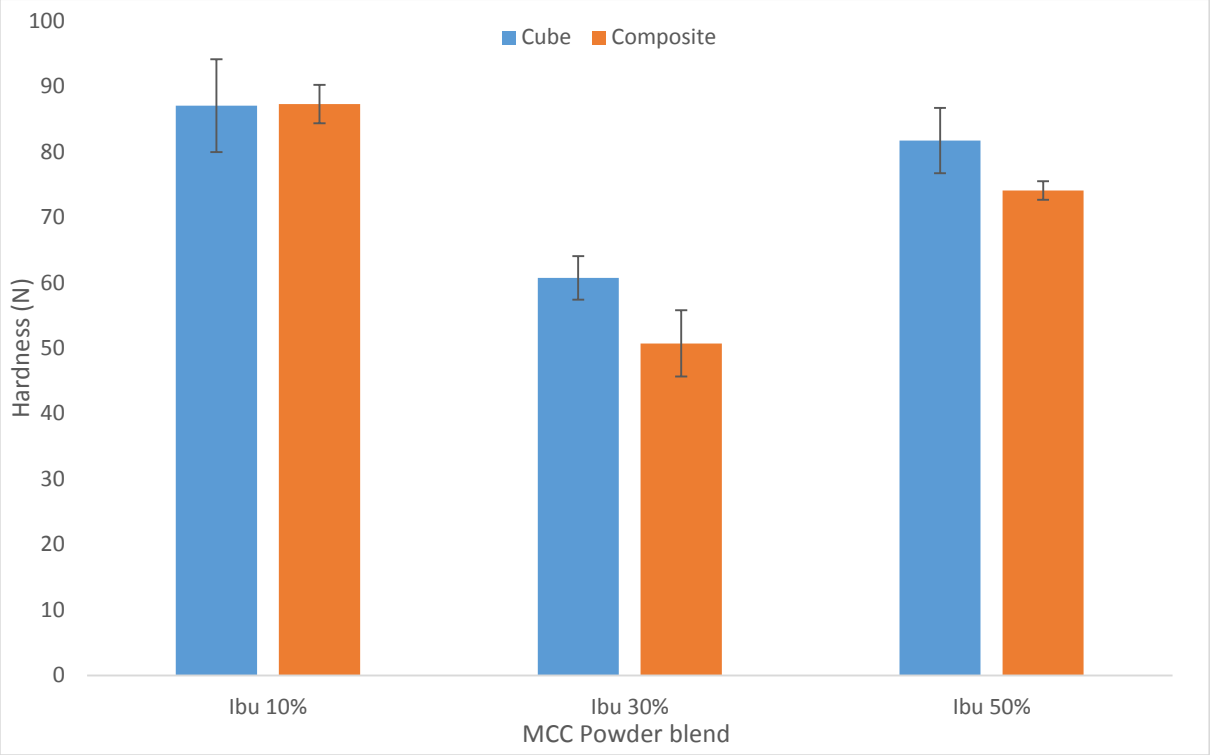

Figure 4.7: A graph showing the hardness of manufactured ODTs containing the model API ibuprofen at concentrations varying from 10-50% comparing the cube and composite mixers, with no statistically significant results observed between the methods. Only milled mannitol data is shown on the graph. Data is presented as mean ± SD (n=3, p>0.05).

The mechanical strength and friability (Figure 4.7 and 4.8 respectively) of dosage forms was very similar for both mixing methods and no statistical difference was observed in terms of hardness when the two methods were compared. This could have been due to the preblends mixing process, where silica was added during the beginning of the blending process. With composite mixing, this could have led to the silica coating a vast amount of the other excipient particles in the powder blend, resulting in lower levels of binding between these adjacent particles, in turn influencing the final mechanical strength and friability of the tablets. This was further investigated below by taking the silica out of the initial mixing process and adding it in at the end of the initial mixing stage. The results in this section indicated the beneficial use of composite mixing for preblend production as it provided a superior flowing powder, which for large scale processing would be key to allow tableting in auto-tableting machine. The properties of the resulting tablets through the composite blending process were also passable, with an acceptable robustness and disintegration times being improved when milled mannitol was utilised.

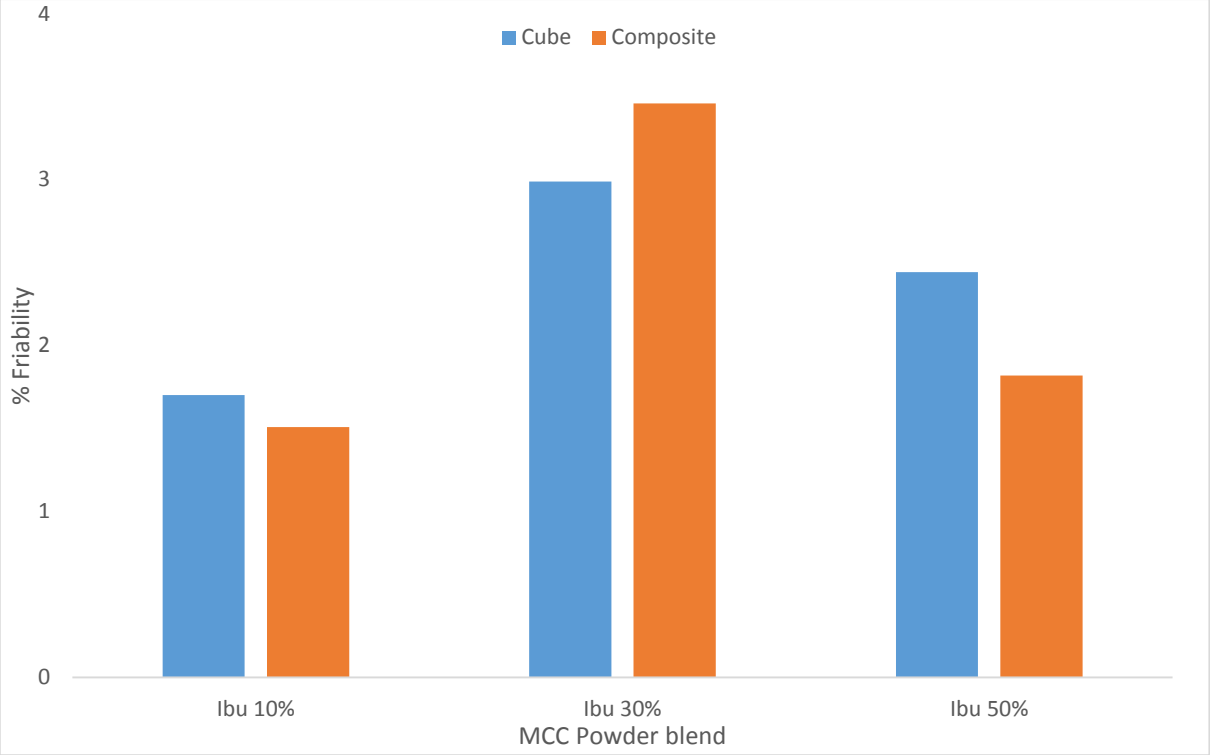

Figure 4.8: A graph showing the friability of manufactured ODTs containing the model API ibuprofen at concentrations varying from 10-50% comparing the cube and composite mixer. Results indicated no clear pattern in friability for the mixing methods, and friability was varied according to a particular blend. Only milled mannitol data is shown on the graph.

4.3.3 Effect of Ibuprofen Concentration

From Figures 4.2 and 4.6 it was clearly seen that an increase in ibuprofen concentration provided ODTs with worsening disintegration times, however the robustness of the dosage forms increased (Figure 4.3 and 4.7). The increased disintegration was expected as ibuprofen had low solubility and is also hydrophobic (Alvarez *et al.*, 2011, Rinaki *et al.*, 2004, Lowe *et al.*, 1999, Tang *et al.*, 2007), which resulted in ODTs that disintegrated more slowly. This was evident by the increased disintegration time when the drug concentration was increased from 10-50% w/w. This was possibly due to the tablet becoming more hydrophobic as the increasing levels of ibuprofen started to increase the overall hydrophobic portion of the tablet. This therefore reduced the wettability of the tablet and caused them to disintegrate more slowly. However as mentioned above, the utilisation of milled mannitol with 50% ibuprofen still provided very low disintegration times, considering the high drug load and absence of any superdisintegrant. It proved that milled mannitol was useful in providing tablets with low disintegration times, regardless of the high drug load, with the unmilled mannitol tablets taking

significantly longer to disintegrate ($p<0.05$), especially at a drug load of 30/50% w/w. However it appeared that as the ibuprofen concentration increased, the hardness of the dosage forms also increased along with a reduction in friability. This was unexpected as ibuprofen had been stated as having a poor compressibility (Patel and Bansal, 2011, More *et al*., 2013, Nokhodchi *et al*., 2015), which should have provided tablets with higher concentrations of ibuprofen giving weaker tablets. However this wasn't the case. The highly compressible nature of the preblends along with the high moisture content and cohesivity of ibuprofen, led to the higher concentrations of ibuprofen providing robust tablets. The MCC/milled mannitol was able to homogenously mix throughout the ibuprofen powder, therefore allowing a robust tablet to be formed, due to the high plastic deformability of the preblend. This would need to be investigated further to assess the compressibility of the premix blend as well as the grade of ibuprofen used.

4.3.4 MCC Blend Optimisation

4.3.4.1 Optimisation of Silica Concentration

This first step of preblend optimisation involved the concentration and mixing time/stage of the silica. In the previous investigation the silica was added alongside the milled mannitol and MCC in a one step process, however silica may have disrupted the coating efficiency of the milled mannitol on to the MCC host particles. To assess this affect, milled mannitol was mixed for 30 mins alongside MCC, and in a second mixing step silica was added to act as a glidant and improve the flow of the resulting powder. It was also a requirement to then optimise the concentration of silica to give the optimal powder flow, whilst providing acceptable tablets. Powder flow results are shown in Figure 4.9, which showed that adding silica at the end of mixing for 5 mins reduced powder flow and gave rise to a higher angle of repose (40.97°) compared to when silica was mixed in the bulk powder, with statistical analysis

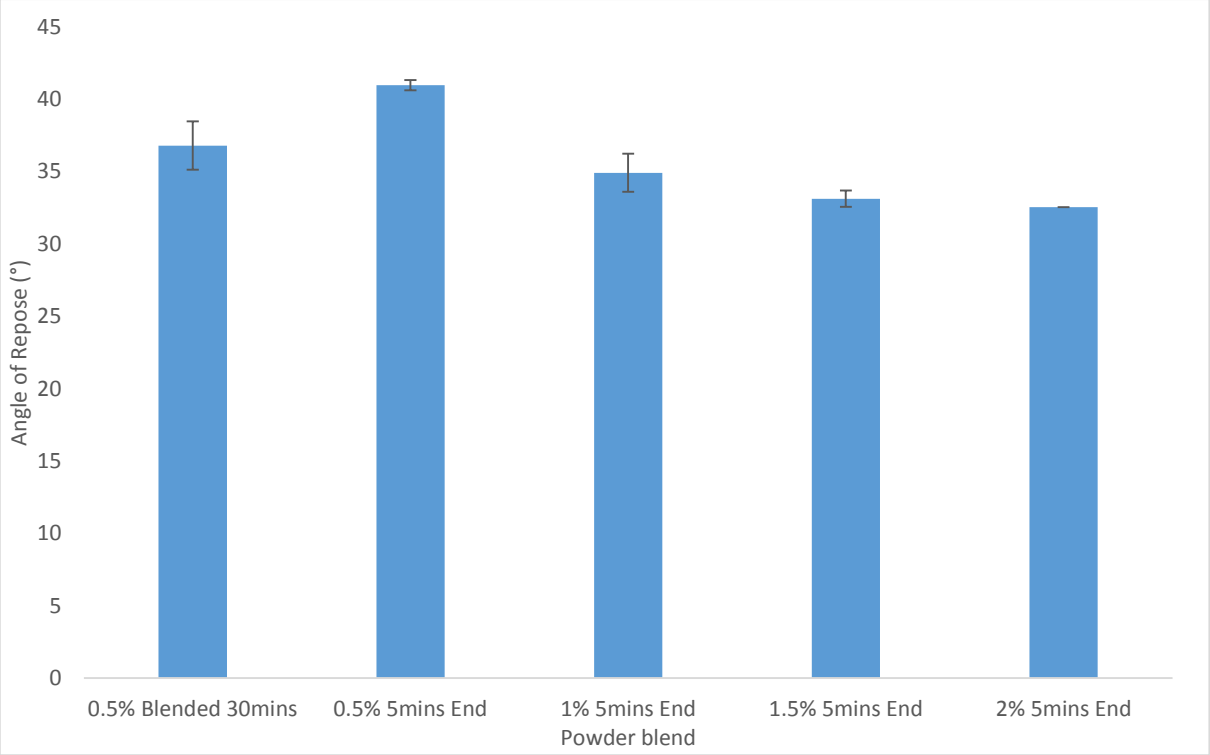

Figure 4.9: A graph showing the effect of silica concentration on the flow of the preblend powder through angle of repose. Significant differences were observed at 0.5%/1.5% and 2% compared to the blend where all of the excipients were mixed together (0.5% blended 30 mins). Was seen that after 1% of silica addition a flow category improvement was seen, from fair to good. (n=3, $p<0.05$ for all powder except 1% 5 mins end).

suggesting that this was a significant worsening in flow ($p<0.05$). This was expected as the silica was mixed for less time, meaning that it wasn't able to sufficiently deagglomerate and evenly distribute through the powder, whereas in the 30 min total mixed blend, it was able to coat a larger proportion of MCC and milled mannitol surfaces due to the increased mixing time of the blend. Another key observation was that as silica concentration was increased the flow of the powder improved, with the angle of repose coming down to 32.55° with 2% w/w silica. Figure 4.10 shows SEM images of the preblend particles (largely MCC and milled mannitol) coated with silica, with the three images indicating an increased silica concentration from A-C respectively. It was evident from the images that increasing the concentration of silica increased the coverage of the nano sized silica upon the MCC/milled mannitol, with 2%w/w silica showing the largest surface coverage, followed by 1% w/w and then 0.5% w/w. This resulted in an improved flow at 2% w/w silica compared to other concentrations, however it was not significant when compared to 1% w/w, with the flow remaining in the good category. It was visualised that an increased surface coating was present at 2% w/w, however

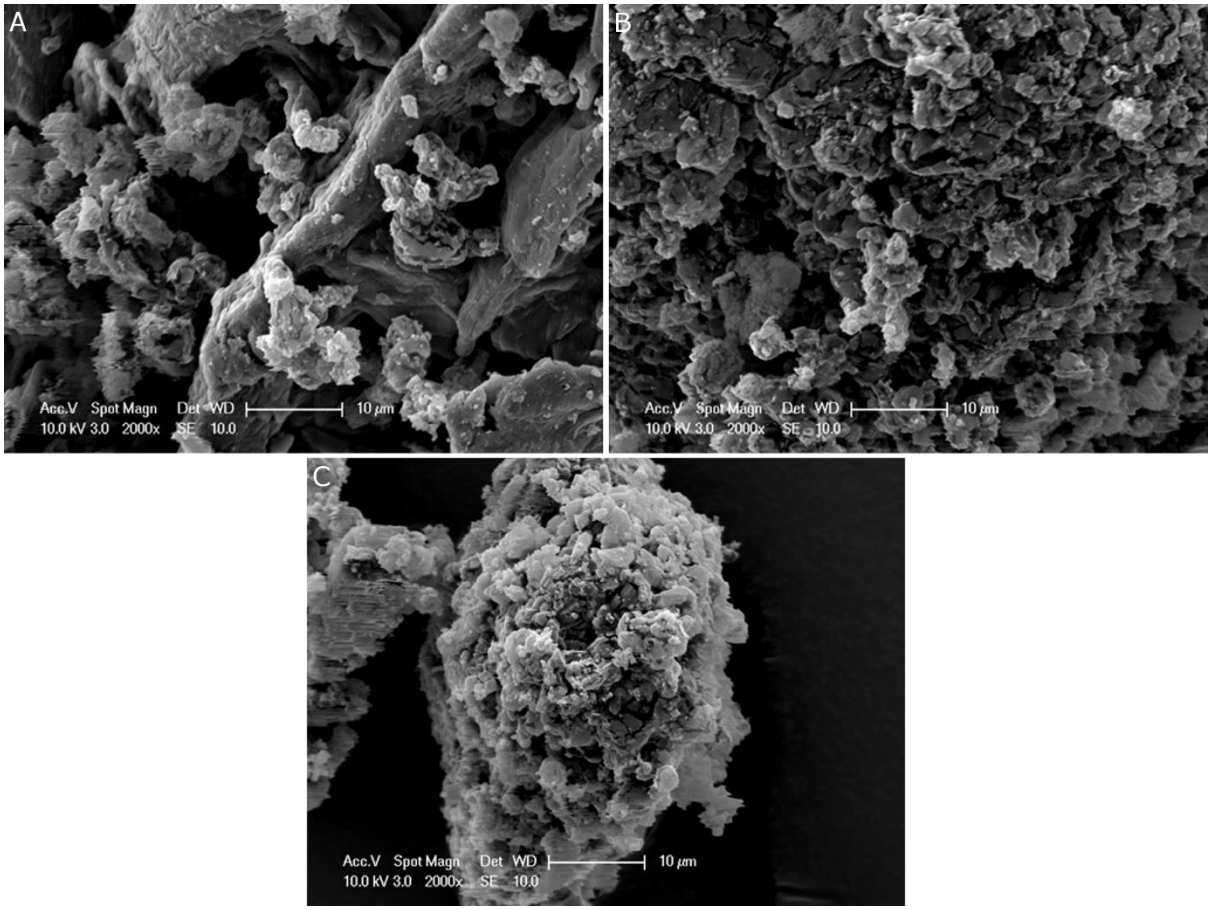

Figure 4.10: SEM images showing particles of: A – 0.5% silica blended for 30 mins alongside milled mannitol and MCC; B – 1% silica mixed for 5 mins after 30 min blend of milled mannitol and MCC; C – 2% silica mixed for 5mins after 30 min blend of milled mannitol and MCC. Images clearly show that increasing the concentration of silica increases the surface coverage of silica on the larger preblend particles, with 2% silica having the highest levels of surface adhered silica.

visibly the difference compared to 1% w/w was insignificant. The reduced loading efficiency of the silica within the 2% w/w blend meant that there was an increased amount of free silica present within the bulk powder blend. Also when employed in ODTs it is disadvantageous to use silica in high concentrations due to its insolubility in water, which results in a highly gritty texture in the mouth upon disintegration, decreasing the palatability of the dosage form (Rowe *et al*., 2012).

To assess tablet properties of the preblends with different concentrations of silica, powders were compacted with different amounts of the insoluble API ibuprofen (10, 30, 50% w/w) and the resulting compacts analysed for their disintegration time, porosity and mechanical strength. Hardness results

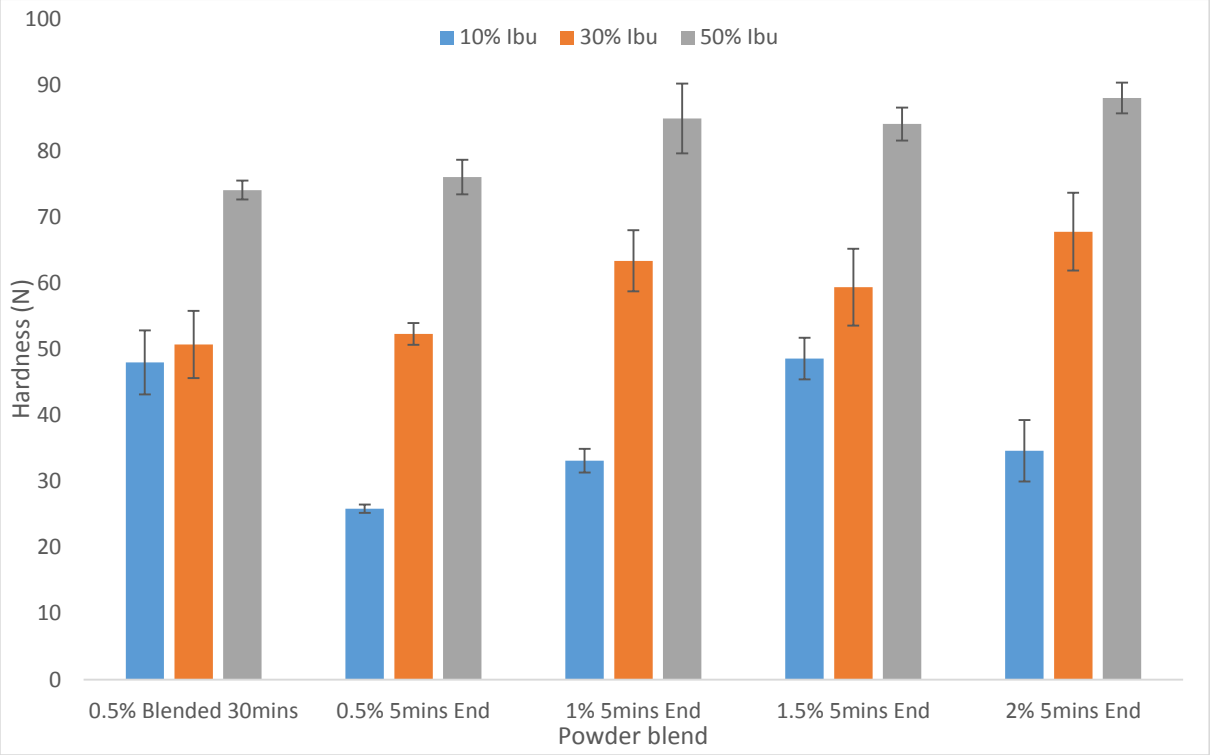

Figure 4.11: A graph showing hardness of the tablets produced from the preblends mixed with differing concentrations of ibuprofen. Results indicated that in general as the concentration of silica increased the hardness of the dosage form also increased. Significant differences were observed between several tablets, with 10% ibuprofen showing an improved hardness at 0.5% blended for 30 mins and 30%/50% ibuprofen showing improved hardness at 2% (n=3, $p<0.05$).

are illustrated in Figure 4.11. A general pattern was observed whereby increasing the concentration of silica tended to increase the mechanical strength of the tablets, with the 2% silica tending to have the highest hardness at 30/50% ibuprofen concentrations. The results generally indicated that at each increment of 0.5% w/w silica, a gradual increase in hardness was observed up to 2% w/w silica load. Statistical analysis showed that the 0.5% 30 min blend, alongside the 1.5% silica blend, had the highest hardness at 10% ibuprofen with 2% silica having significantly higher hardness at 30 and 50% ibuprofen concentration ($p<0.05$). These results were unexpected as it was thought that using increasing concentrations of silica to adhere to mannitol/MCC surfaces would result in reduced interparticle bonding, and therefore would negatively impact tablet strength. However it was identified in literature that when using mixtures of colloidal silicon dioxide with magnesium stearate in the tableting blend, compact strength would increase, due to the colloidal silica coating larger areas of the milled mannitol/MCC resulting in an improved tablet strength, with the lubricant sensitivity of MCC

also reduced (Bolhuis and Holzer, 1996, van Veen *et al*., 2005, Zuurman *et al*., 1999). This also explained the increased strength of the 30min premixed total blend over the 0.5% silica 5 min blend, as the total blend had a higher amount of time for the silica to evenly disperse through the mix and coat the larger host particles of MCC and milled mannitol. Therefore an increased level of stronger bonds were able to form between the mannitol and MCC during compaction. The hardness of the tablets appeared generally proportional to the disintegration time, with disintegration time results shown in Figure 4.12.

The disintegration time results showed that increasing the concentration of silica caused an increase in disintegration time, with very similar disintegration times seen between the two formulations containing 0.5% w/w silica, and a step wise increase in disintegration time as the proportion of silica

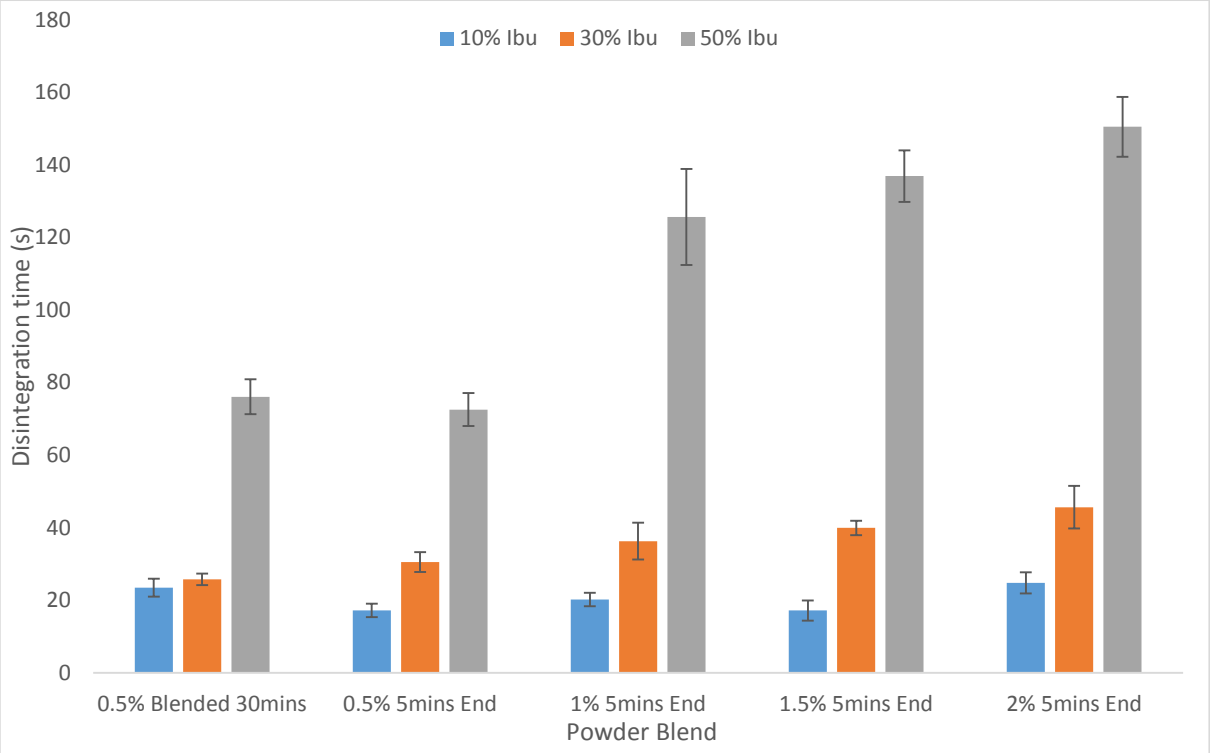

Figure 4.12: A graph showing the disintegration time of the tablets produced from the preblends mixed with differing concentrations of ibuprofen. Results gave a clear indication that as silica concentration increased the disintegration time of the tablet *al*so increased, which was especially evident at 30 and 50% ibuprofen concentration, with concentrations of 1% silica and above significantly different to the 0.5% total blend at 30% ibuprofen concentration and concentrations of 1% silica and above being significantly longer disintegrating than either of the 0.5% silica preblends at 50% ibuprofen concentration (n=3, $p<0.05$).

increased up to 2% w/w silica. The disintegration time at 10% w/w ibuprofen was very low for all formulations due to the low mechanical strength, therefore no statistical significance was observed. At 30% w/w ibuprofen, the increase in disintegration time with the increase in silica concentration became more obvious, with significant differences seen between the 0.5% w/w silica total blend and the higher concentrations of silica mixed at the end, and a significant difference observed between 0.5% w/w silica added at the end and the 2% w/w silica blend ($p<0.05$). At 50% w/w ibuprofen concentration statistical significance was observed between all formulations except the two 0.5% w/w silica formulations, which all gave a clear indication that the higher levels of silica were increasing the disintegration time. The increased disintegration time could have been due to two possible reasons, one being the reduced energy of interparticle separation due to the higher levels of silica present within the compact, and secondly the reduced porosity of the compacts with increased levels of silica (shown in Figure 4.13). From Figure 4.13 it was seen that the increasing concentrations of silica caused

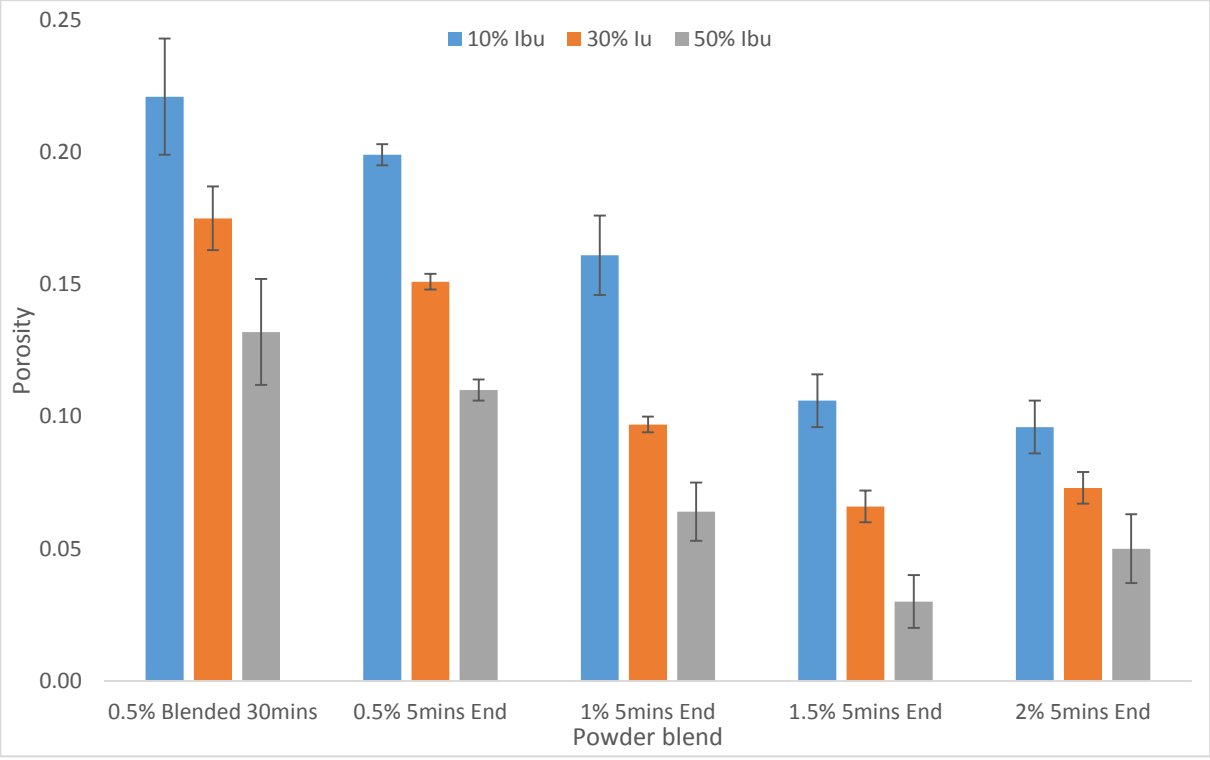

Figure 4.13: A graph showing the porosity of the tablets produced from the preblend powders containing different concentrations of silica at different ibuprofen drug loads. Results indicated that as the concentration of silica increased the porosity of the tablets decreased; at 10% ibuprofen load statistical significance was observed at all concentrations except when comparing the two 0.5% silica preblends and between 1.5% and 2% silica; and at 30% and 50% ibuprofen load significant differences were observed at all concentrations of silica except between the two 0.5% blends and between 1% and 2%/1.5% and 2% ($n=3$, $p<0.05$).

a reduction in porosity across all three ibuprofen drug loads, with the two 0.5% silica preblends showing no statistical significance at any of the ibuprofen loads. This was similar to previous findings where it was found that increasing levels of colloidal silica within powder blends up to 3% w/w caused a reduction in pore volume within the resulting compact (Gucluyildiz *et al*., 1977). The porosity of the tablets was a key factor in their resulting disintegration, as the reduced pore volume of the higher silica concentration tablets reduced water uptake into the tablet. Whereas, at the lower concentrations of 0.5% w/w, where the pore volume of the compact was much higher, the tablet was able to draw water into the pores more rapidly which allowed subsequent breakdown of the compact (Pabari and Ramtoola, 2012, Seager, 1998). Due to the absence of disintegrant in the preblend it was concluded that the disintegration of the tablets was primarily due to the porosity of the dosage form, which allowed water to penetrate and breakdown the structure. However it was also observed that the porosity of the tablets was inversely proportional to the pattern in hardness of the compacts. It was seen in previous findings that a more porous tablet structure did lead to a lower mechanical strength in the resulting compacts (Fukami *et al*., 2006), with similar results also seen in this study. This was explainable by the bonding area of the MCC and milled mannitol. The lower porosity of the compacts indicated that the MCC and milled mannitol formed a larger surface area of bonds during the compression cycle. This led to a higher tablet hardness, as the energy required to break the bonds was increased due to increased bonding surface area (Khomane and Bansal, 2013, Joiris *et al*., 1998). The friability of the tablets is shown in Figure 4.14, and although it could be said that the friability followed a similar pattern to the porosity, where friability decreased with increased silica concentration, this was only observed up to 1.5% w/w, with 2% w/w silica giving a higher friability at all three of the ibuprofen concentrations. It was interesting to see that the 0.5% w/w total blend had a fairly low friability compared to the other tablets tested, which was comparable to the 1.5% w/w silica 5 min mixed blend. This showed that mixing silica for a longer duration helped to lower the friability of the tablets. However in all cases it was seen that friability was above the 1%w/w

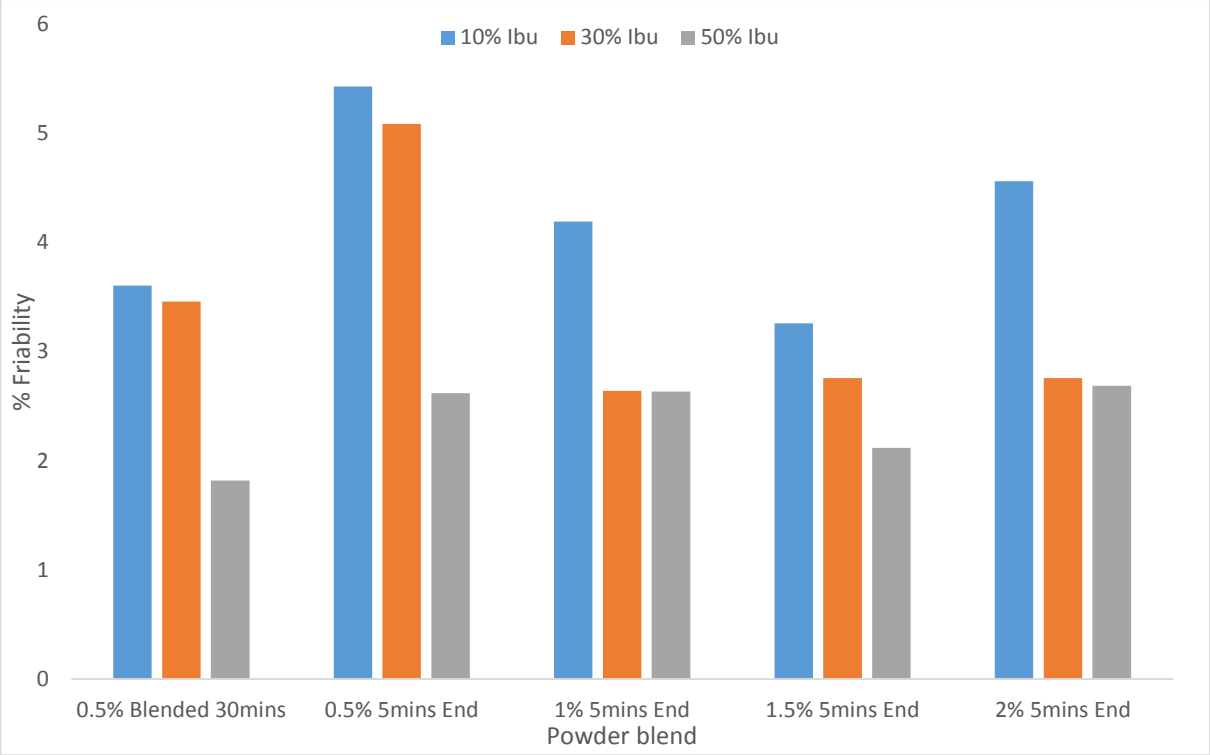

Figure 4.14: A graph showing the friability of the tablets made from preblends containing different concentrations of silica, at three different ibuprofen drug loads. It was gathered that no clear observable pattern was obtained, with the 30 min total blend having very good friability whereas 5 min mixed silica blends had higher friability. Could also be said that a general reduction in friability was seen as the silica concentration increased up to 1.5%.

acceptability threshold, but this was due to the low compression force used during tableting and the utilisation of milled mannitol.

The final step in optimising the silica addition was to find the most appropriate time for mixing. Figure 4.15 showed how the flow of the powder changed over time, up to a mixing time of 30 mins, through the angle of repose. A 1% w/w silica concentration was chosen as the flow was good with the 5 min mixing time, and it also gave disintegration times that weren't extremely high, as was seen with the 1.5 and 2% w/w blends, with the robustness of the dosage forms also being acceptable. Results indicated that an increased mixing time gave an improved flow up to 20 min blending, with the graph showing a clear plateau in the improvement of flow. Figure 4.15 showed that there was a huge difference between the angle of repose of the powder between a 5 and 10 min mixing time, with the angle dropping by around 8°, from the passable category to the good category (USP37, 2014c). A further enhancement in flow was seen at the 20min mixing time, although the drop wasn't as drastic,

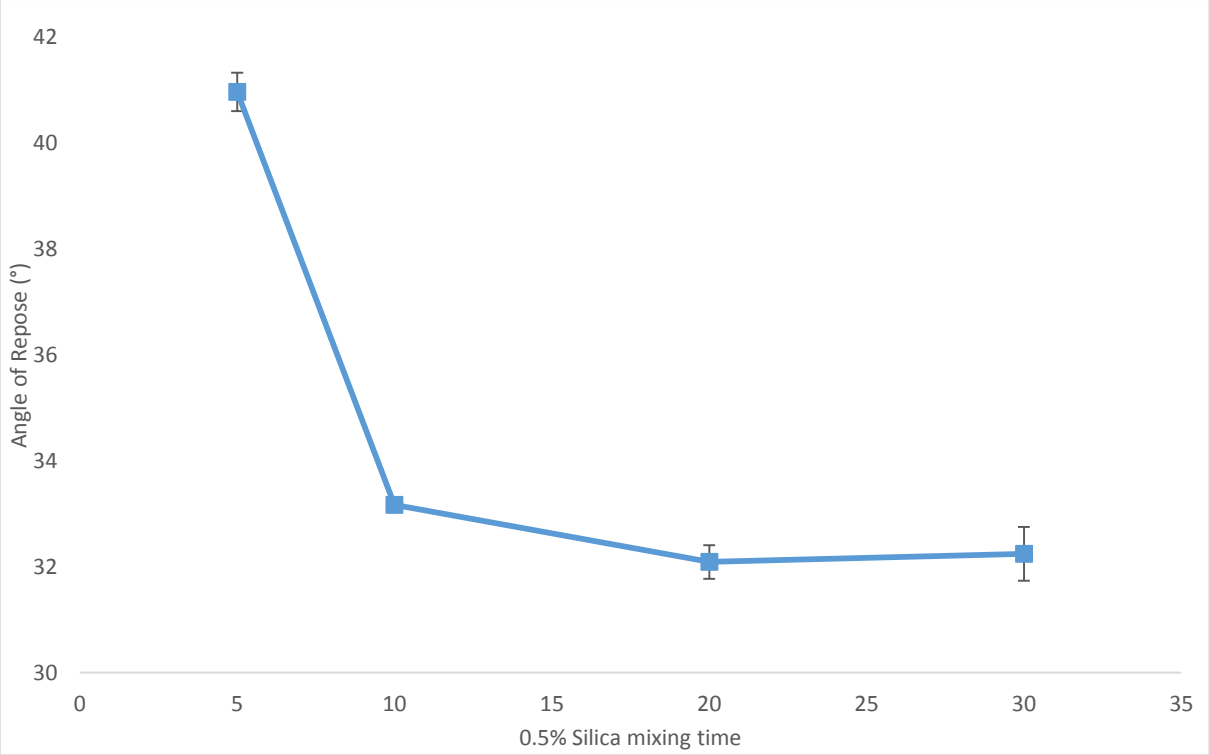

Figure 4.15: A graph showing the effect of silica mixing time on the flow of the preblend powder through angle of repose. Significant improvements in flow were observed after a 10 min mixing time compared to the 5 min silica mixed powder, with 20 and 30 min mixed powders also being significantly more flowable than powder mixed for 10mins (n=3, $p<0.05$).

with the flow improvement plateauing at 30 mins. The improved flow was because the dry coating device was able to deagglomerate a higher proportion of the silica particles, and allow them to coat on to the larger milled mannitol and MCC. The interparticle friction between the larger particles, especially the very small milled mannitol particles, was therefore reduced and the glidant effects of the silica were more prominent. Any further mixing of the silica post 20 mins resulted in no further enhancement in flow.

For further study the 1% silica concentration was chosen and mixed for 20 mins to form an optimally flowing powder, as the angle of repose represented a 'good' flowing powder with acceptable tablet characteristics.

4.3.4.2 Surface Coverage during Mixing

In this study the mannitol was added to the MCC and mixed in the dry coater in one step to produce the dry coated particles. Previous work conducted by Yang *et al*. (2005) found that the theoretical

concentration required for full surface coverage of the host particle could be calculated using the particle size and true densities of the host and guest particles for a particular mixture. It was hoped that if the milled mannitol and MCC coating was conducted in two or more steps, several layers of mannitol may have been observed coating the larger MCC particle. To further assess the preblend properties a smaller particle sized MCC was introduced as a comparison, with Avicel PH101 having particles around 50 µm compared to the 100 µm of the Avicel PH102. It was hoped that the larger surface area of the smaller sized particles would reduce the levels of free mannitol in the mixture and result in further enhancements in coating. Using the surface coverage equations proposed by Yang *et al*. (1997) it was found that the amount of milled mannitol required to theoretically coat the PH102 and PH101 MCC particles was 35.9% w/w and 57.8% w/w respectively. Therefore the first mixing step entailed a mixture of the respective amount of mannitol and MCC mixed for 30 mins, and then the remaining quantity of the milled mannitol required for the preblend was added in a second step for further mixing, before 1% w/w silica was added in the final step for 20 mins.

Figure 4.16 shows SEM images of the one step addition and surface coverage powders for the PH102 and PH101 grades of MCC. From the images it was seen that the milled mannitol and the silica were coating both grades of MCC to a large extent, with the surface appearing very rough due to the adherence of the small sized milled mannitol particles on to the MCC surface. This represented a clear difference between the dry coated blends and uncoated MCC, with the surface of uncoated MCC being much smoother, with no visible particles attached to the surface (Figure 4.16(A) and (B)). It was also seen that the nano-sized silica particles were coating on to the outside of the milled mannitol as well as the MCC. It was clearly visible that the particles of the PH101 grade were much smaller in comparison to the PH102 particles. For dry coating the order of magnitude of size difference between the guest and host particle needs to be at least two, with the strength of attraction increasing as the

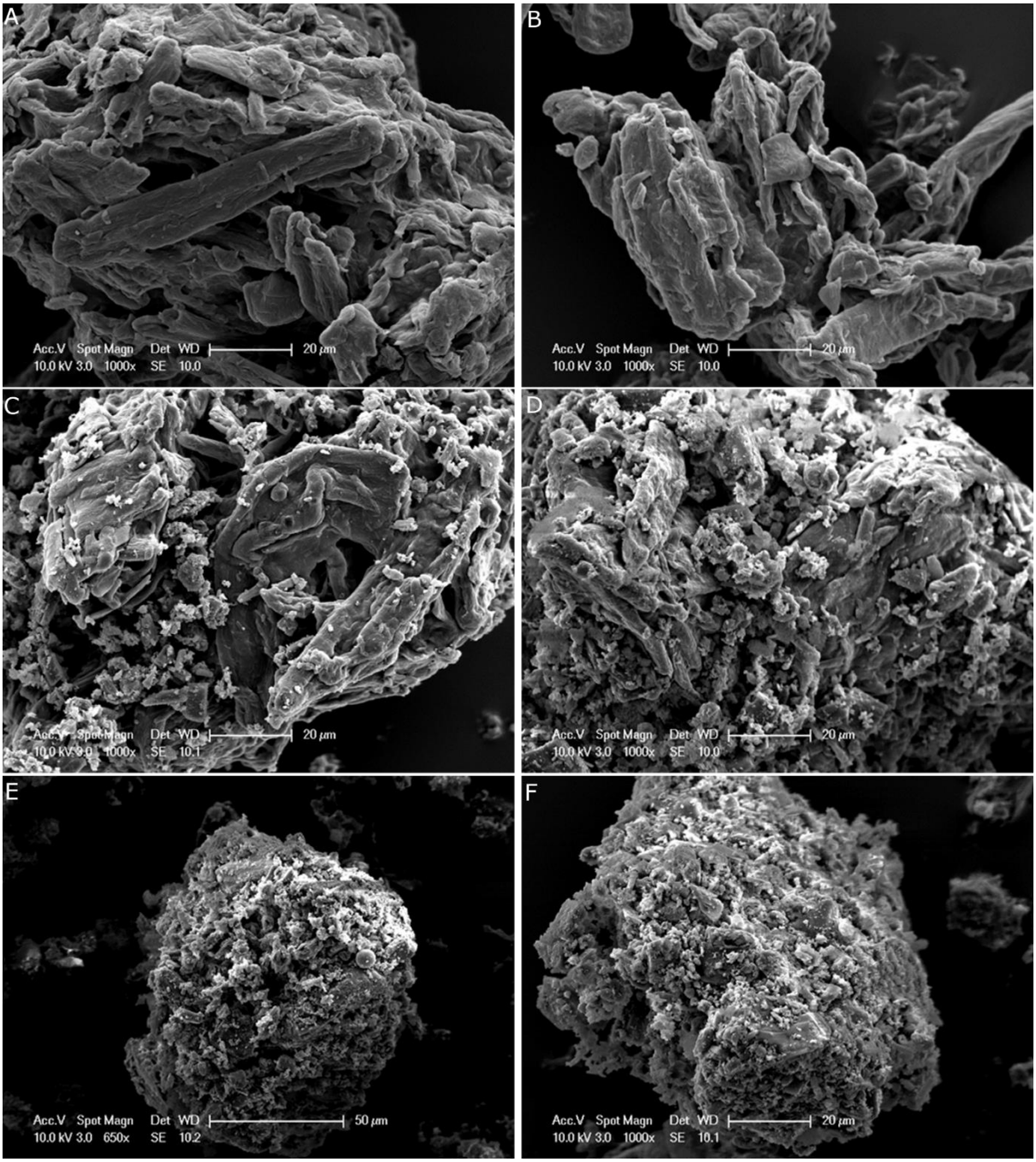

Figure 4.16: SEM images of the calculated surface coverage blends compared to the all in one mixtures with A- showing an uncoated particle of MCC PH102; B- showing an uncoated particle of MCC PH102; C - showing the all in one powder blend of PH102; D – the PH102 blend with calculated surface coverage; E – the all in one powder blend of PH101 and F – the PH101 blend with calculated surface coverage. Levels of coating appeared to be slightly higher on the calculated surface coverage blends for both PH102 and PH101, although the loading amount of the mannitol and silica was high in both cases.

size difference between the particles increases (Dahmash and Mohammed, 2015, Ishizaka *et al*., 1989, Honda *et al*., 1994, Alonso *et al*., 1990). Therefore it was expected that the PH101 would have some level of dry coating, as the size difference between the MCC and milled mannitol was around 5 orders of magnitude. The PH102 was expected to have higher levels of coating as the difference between the

host MCC and the guest milled mannitol was around 10 orders of magnitude, therefore the attraction forces were expected to be higher. However it appeared as though the PH101 particles had higher levels of surface coating than the PH102, as seen between Figure 4.21 (C) and (E), with higher levels of mannitol and silica observed in (E). This could have been due to the larger surface area available to coat with the 50 μm MCC. However the two particles that were visualised when using the surface coverage calculations (Figure 4.16(D) and (F)), the same difference was not seen, with surface coverage for both particles being very high and very little difference in coverage observed.

The main point of comparison here was the difference between the total blend and the surface coverage blend. The SEM images indicated that when surface coverage calculations were used, a larger proportion of the MCC was covered with milled mannitol, as was observed with the PH102 blend (Figure 4.16(C) and (D)). The increased levels of loading of mannitol on to PH102 with the surface coverage could have been explained by the increased coating upon the second addition of the mannitol, leading to an increased number of layers. In the first step enough mannitol was added to achieve a theoretical full surface coverage. This would have resulted in high levels of loading on to the MCC surface, with little of the mannitol left free within the powder blend. With an extra addition of the small sized mannitol after the first step, the extra mannitol was able to further coat on to the previously coated MCC particle. This could have been explained by the large size difference between the milled mannitol and the already coated MCC, which would have displayed a slightly enlarged particle size due to the layer of mannitol already surrounding the MCC. Such distinct differences were not seen with the PH101 total blend and surface coverage blend, with both blends displaying a very high adherence of the mannitol on the MCC surface. This may have been due to the smaller particle size of the PH101 grade, which after the first dry coating stage wasn't able to attract further mannitol as the electrostatic forces had been dampened by the mannitol already attached to the MCC.

Figure 4.17 shows a graph of the flow of the surface coverage blends compared to the blends where the powder was added in all at once, through the angle of repose. The data showed that the surface

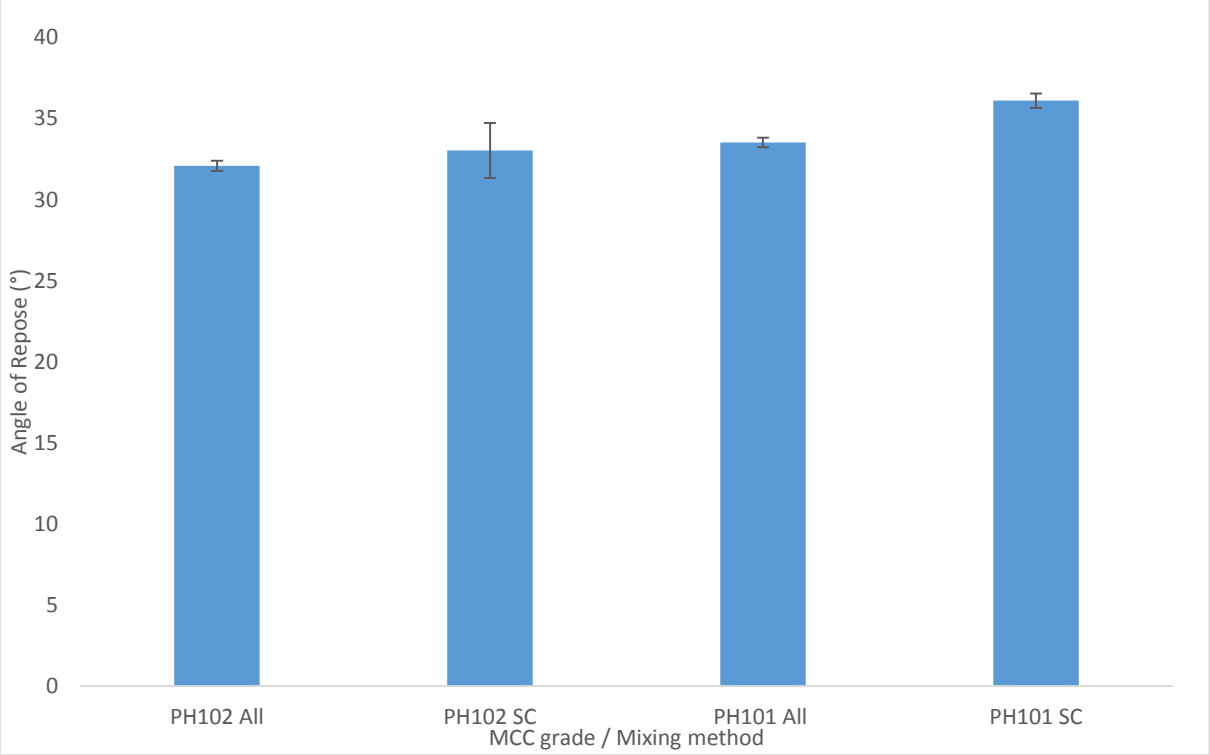

Figure 4.17: A graph showing the flow of the surface coverage calculated blends compared to the all in mixed blends for the two sizes of MCC investigated, through the angle of repose. The general pattern was that surface coverage resulted in a slight worsening in flow, with a statistically significant difference seen with the PH101 blends (n=3, $p<0.05$).

coverage blends did slightly worsen the flow of the powder, with a significant worsening seen with the PH101 blend, alongside a flow category worsening from good to fair. The PH102 blend remained fairly consistent with only a slight increase in the angle of repose.

This slight worsening in flow may have been due to the several addition steps of mannitol; in the first step most of the mannitol was coating the larger MCC particles leaving less space for further coating; the second step where more of the mannitol was added led to a slight increase in the coating levels, however the mannitol was in excess prior to the mixing step, therefore more of it would have aggregated together to reduce the overall powder flow (Westerberg and Nyström, 1993, Dahmash and Mohammed, 2015). With the total addition blend, mannitol would have had more space to attract to the MCC surface, and although still in excess there would have been less time for the mannitol to form aggregates, as this blend was only mixed for 30 mins, as opposed to the two 30 min mixing times for mannitol with the surface coverage blends. The flow wasn't hugely different between the two

methods as 1% silica was added as a final addition step and mixed for 20 mins, which acted to increase the flow of the powder blend.

Figures 4.18-4.20 shows the mechanical properties and the disintegration time of tablets produced from the surface coverage blends compared to the total addition blends. Figure 4.18 shows the hardness of the tablets; the data indicated that the hardness between the two mixing methods didn't display a clear pattern, with the only difference observed at 50% ibuprofen where the surface coverage blend was statistically significantly stronger than total addition blend ($p<0.05$). It appeared as though at 10% and 30% the total blends were more mechanically strong, however no statistical significance was observed, but at 50% the surface coverage blends came out significantly harder. There was no clear pattern to the mechanical strength, and the friability also reflected this (Figure 4.19), with the friability of the surface coverage blends being higher at 50% ibuprofen and no clear pattern observable at the other ibuprofen concentrations. The increased strength of the surface

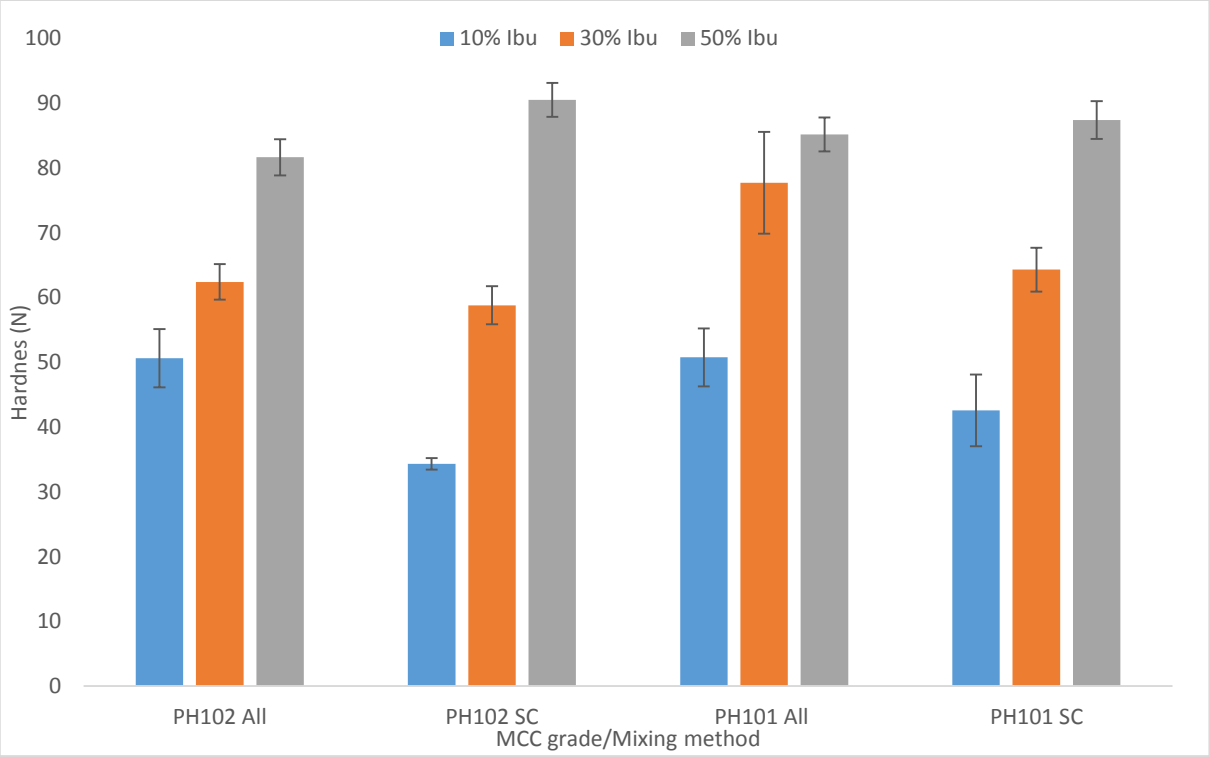

Figure 4.18: A graph showing the hardness of the surface coverage blends compared to the total addition of powder blends at three difference concentrations of ibuprofen. No observable pattern was seen in the results, however a significant increase in hardness was seen at 50% ibuprofen for both of the surface coverage blends compared to their total addition counterpart ($n=3$, $p<0.05$).

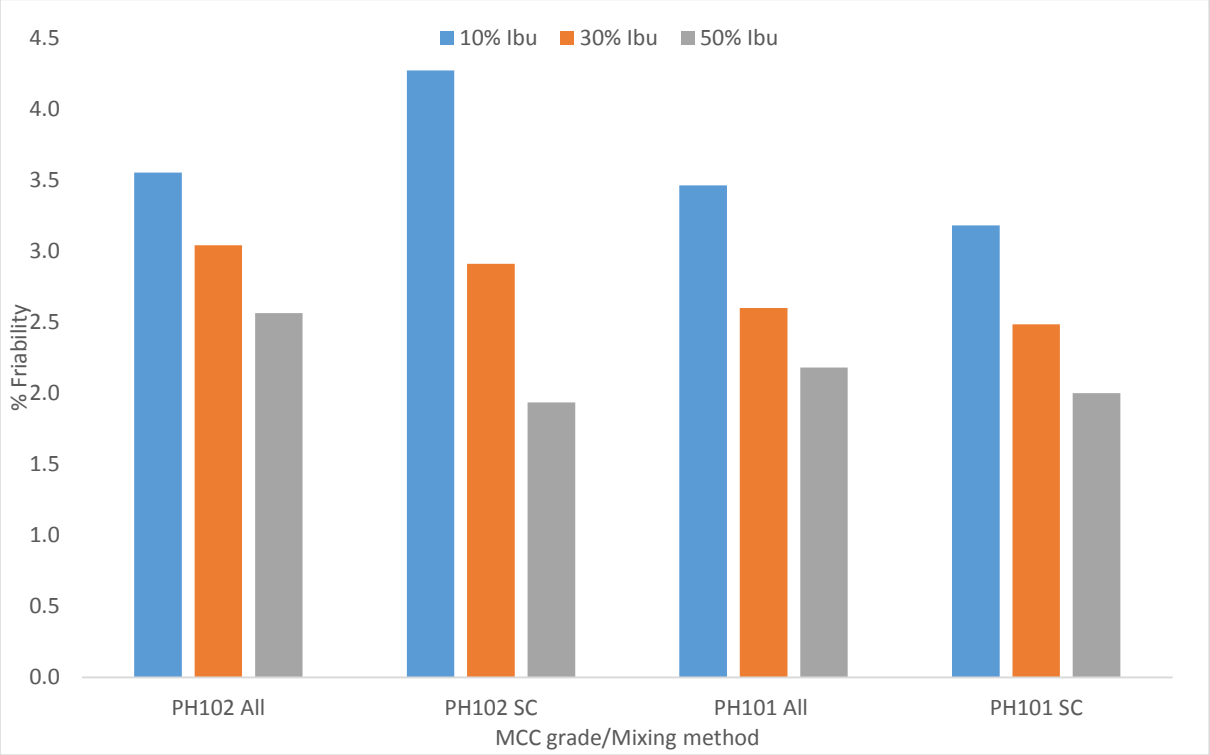

Figure 4.19: A graph showing the friability of the surface coverage blends compared to the total addition powder blends at three difference concentrations of ibuprofen. No observable pattern was seen when comparing the surface coverage blends to the total addition blends.

coverage blend at 50% ibuprofen was due to the increased levels of ibuprofen which lead to an overall higher mechanical strength as the ibuprofen used was very compressible due to its high cohesivity and moisture content. It could also be said that the agglomerates of mannitol were higher with the surface coverage blend, therefore the close interactions between the mannitol agglomerates were forming stronger bonds during the compression cycle. Disintegration time of the tablets was proportional to the hardness, as the hardness of the tablets increased the disintegration time also increased, due to the lower ability of water to penetrate and break up the compacts. Again with disintegration time no clear pattern in how the mixing methods were affecting the disintegration capability of the tablets was attainable. With the PH102 MCC, disintegration time of the surface coverage blends was lower than the total addition blend, however with PH101 the disintegration time of the surface coverage blend was higher (Figure 4.20). Disintegration time at 50% ibuprofen was high due to the increased hardness of the compacts, because the ibuprofen was highly compactable. However disintegration times at 10 and 30% w/w ibuprofen were acceptable for all the PH102 blends as opposed to the PH101.

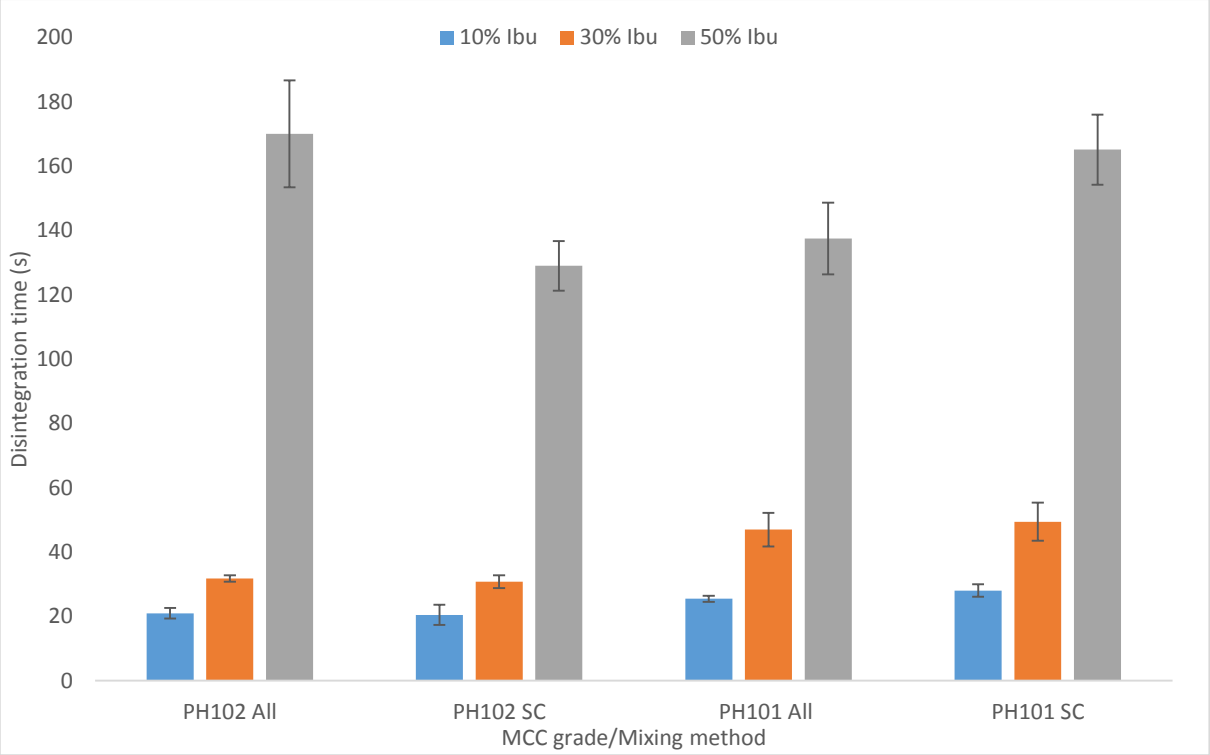

Figure 4.20: A graph showing the disintegration time of the surface coverage blends compared to the total addition of powder blends at three difference concentrations of ibuprofen. No observable pattern was seen in the results, with PH102 MCC showing lower disintegration with surface coverage blending, whereas PH101 showed lower disintegration with the total addition of the powder. Statistical significance was seen between 50% ibu for both PH101 and PH102 (n=3, $p<0.05$).

This was because of the smaller sized particles of MCC present in PH101, which would have been more compactable as they were able to fill smaller voids within the powder bed during compression.

Although flow was affected by the mixing method for the dry coated blend, with surface coverage powders being slightly less flowable than the total addition blends. No fixed pattern was observable with the tablet properties, as the mechanical strength and disintegration time varied depending on the particle size of MCC analysed. Visually, small differences in the particle surface morphology were seen, as surface coverage blends displayed a slightly increased loading of mannitol on the surface of MCC, especially with the PH102, due to the increased mixing time and possible dual layering on to the larger MCC particle.

4.3.4.3 Use of Glyceryl Behenate and Ethocel as an alternative to Silica

Colloidal silicon dioxide is the most common and well established glidant in the pharmaceutical industry due to its very small particle size, enabling it to coat larger particles and reduce interparticle

friction. However it has its disadvantages, whereby it causes lubricant sensitivity with certain excipients, such as MCC (Zuurman *et al*., 1999, Hoag *et al*., 2008), it can increase disintegration times of tablets as the concentration increases, as evidenced by results above, and due to its hydrophobic non-dissolving nature, when employed in ODTs can delay disintegration time. Glyceryl Behenate was chosen as a comparison as the manufacturer had stated that it can be employed as a lubricant in solid oral dosage forms, and can help keep disintegration times low as well as improve compressibility of the powder (Li and Wu, 2014, Jannin *et al*., 2003). It was therefore investigated as a flow improvement aid in this study. A small particle size grade of Ethocel (Ethocel HP®) was also used in a low concentration to see if the excipient had any use as a flow aid for dry powder formulations, and if it presented any improvements in tablet properties.

Figure 4.21 shows the important flowability results for the two newly investigated flow aids against silica. The results were very clear, showing that the silica flowed significantly better than both the glyceryl Behenate and Ethocel. This was because of its nanosized particles which were able to evenly

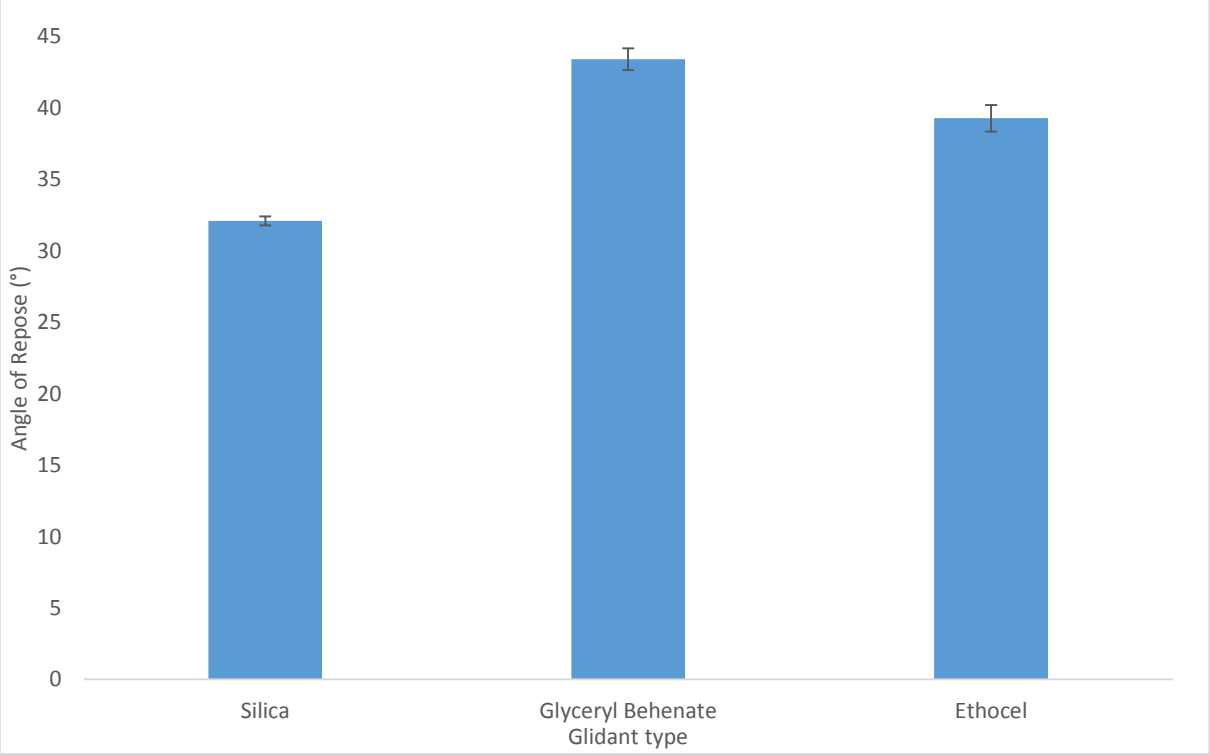

Figure 4.21: A graph showing the flow of glyceryl Behenate and Ethocel compared to Silica through angle of repose. Results indicated that powders containing silica flowed significantly better than powders containing the other two excipients. Ethocel flowed significantly better than glyceryl Behenate (n=3, $p<0.05$).

disperse through the dry coated powder blend and coat the larger MCC and milled mannitol particles, reducing the interparticle friction and allowing the powder to flow more homogenously. The particle sizes of the glyceryl behenate and Ethocel were much larger than the silica, so were not able to uniformly disperse throughout the blend. It was also evident that the Ethocel flowed better than the glyceryl behenate, with statistical analysis also showing this ($p<0.05$). The glyceryl behenate had a particle size of around 50 µm, which explained its poor flow aid capabilities, as only 1% w/w of the excipient was used. This would have meant that the powder was not able to uniformly disperse through the blend, and therefore had very little effect on the flowability of the dry coated milled mannitol powder. Ethocel however did have some improvement in the flow of the powder, down to an angle of repose of 39° as opposed to the 42° of the glyceryl behenate. The Ethocel had an average size of below 8 µm, this meant that adding 1% w/w of the excipient to the dry coated blend allowed some distribution and layering of the Ethocel on to the MCC and milled mannitol particles. This would have helped to reduce interparticle attraction/friction forces, and slightly improve the flow of the powder. Compared to the silica, the particle size of Ethocel was still fairly large, and therefore silica had a higher coating efficiency on to the host particles, and proved to be the better flow aid.

Figures 4.22 and 4.23 show the hardness and disintegration time of the tablets manufactured using the different flow aids at different ibuprofen concentrations. In terms of hardness no clear pattern was observable between the three. Silica appeared to have the better hardness at 10% w/w ibuprofen load, Ethocel had the better hardness at 30% w/w ibuprofen load and glyceryl behenate having a better hardness at 50% w/w ibuprofen load. It was therefore concluded that the interchanging of the flow aid wouldn't have a significant effect on the mechanical strength of the manufactured tablets. Ethocel did present an advantage over silica and the glyceryl behenate as it had high hardness at both 30 and 50% w/w ibuprofen loads. Ethylcellulose has been shown to increase the compressibility of powder blends, and including this at a small load had in fact improved the compressibility above that of silica at higher drug loads (Goswami *et al*., 2014). Glyceryl behenate in general provided tablets of

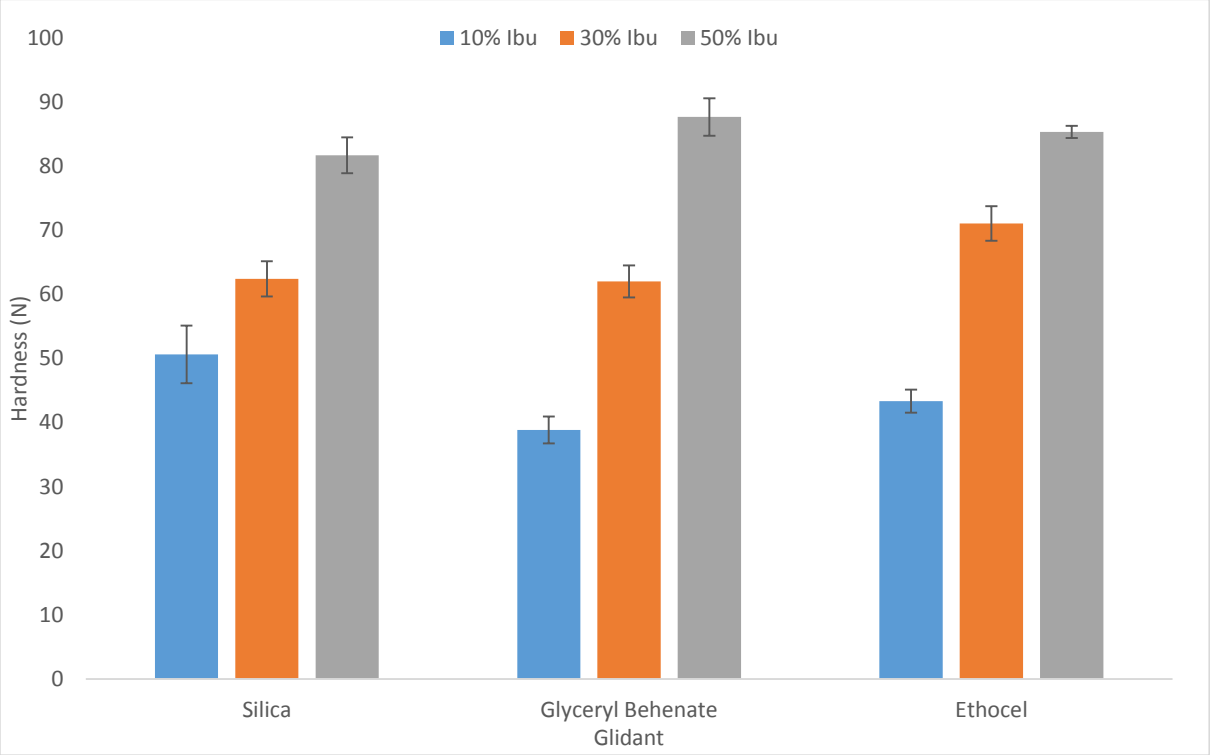

Figure 4.22: A graph showing the hardness of the tablets manufactured from the powders containing the two new investigated flow aids compared to silica, with different ibuprofen drug loads. The general pattern observed was that glyceryl behenate had the lowest hardness at 10 and 30%, with silica being significantly harder at 10% and Ethocel being significantly harder at 30% ibuprofen drug load. Glyceryl behenate was significantly harder than silica at 50% ibuprofen load (n=3, $p<0.05$).

lower mechanical strength, with only tablets at the higher ibuprofen load showing strength improvements. This was expected as literature had shown improvements in compressibility and hardness of tablets was observed when a glyceryl behenate concentration of 20% was used (Mužíková *et al*., 2015). Therefore due to the lower concentration of glyceryl behenate employed in this study, a significant mechanical strength improvement wasn't observed.

Figure 4.23 showed the disintegration times of the tablets produced from the powder blends containing the three different flow aids. It was seen that there were no significant differences between the flow aids, except at 50% w/w ibuprofen drug load where the Ethocel proved advantageous in having significantly lower disintegration times ($p<0.05$). This was because Ethocel was able to increase pore volume in the tablet, allowing a higher capillary action/water ingress into the dosage form, causing a subsequent faster disintegration of the tablet structure. This led to an overall improvement in the disintegration behaviour of the Ethocel containing powder blends.

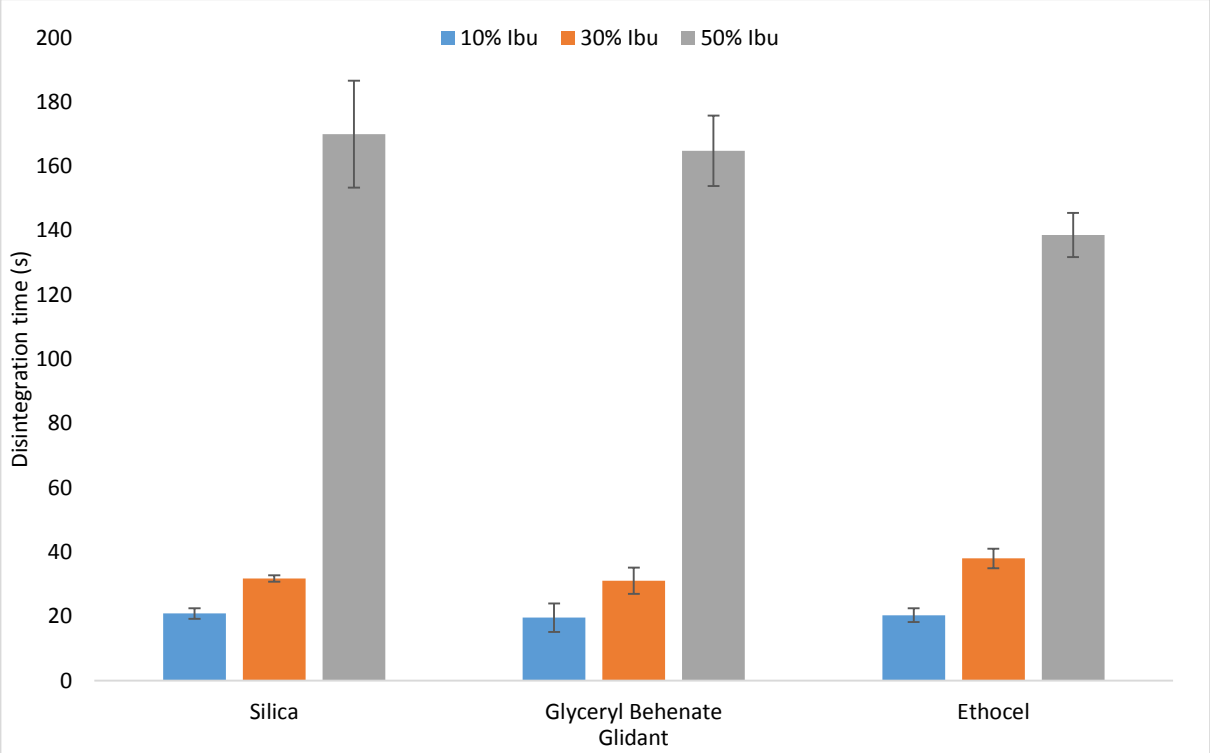

Figure 4.23: A graph showing the disintegration times of the tablets manufactured from the powders containing the two new investigated flow aids compared to silica, with different ibuprofen drug loads. The general pattern observed was that there was no clear difference in disintegration time at 10/30% ibuprofen load, however at 50% the Ethocel was faster disintegrating compared to the silica and glyceryl behenate (n=3, $p<0.05$).

Overall it was seen that the traditional flow aid silica was advantageous, especially for powder flow improvement. Tablet properties weren't hugely different between the three different flow aids tested. Disintegration and mechanical strength of the Ethocel containing powder was improved compared to the silica containing powder. Ethocel helped increase porosity within the tablet, which explained its faster disintegration properties, whilst the hardness was also improved at higher drug loads. This indicated the Ethocel could possibly be used as a flow aid in the pharmaceutical industry as it did give some promising results, and with further optimisation could provide compressible and flowable powders that disintegrate very quickly.

4.4 Conclusion

The aim of the study was to investigate a suitable mix of excipients that could be included in a preblend to add straight to an API and lubricant for ODT production. Milled mannitol was carried forward from previous work as it was found to be advantageous in producing more robust and faster disintegrating

tablets. When it was employed in the preblend and mixed with the model API ibuprofen, it was found to produce tablets of similar robustness to the unmilled alternative, with vastly improved disintegration times. This was a key advantage of the milled mannitol as it was more hydrophilic due to the exposure of the more hydrophilic crystal plane on the particle increasing the wettability of the ODT. Two mixing methods were also compared when producing the preblend. It was found that the novel composite mixer was advantageous in producing a better flowing powder due to its dry coating ability, particularly when milled mannitol was used in the preblend mix.

In terms of optimisation of the blend it was concluded that blending 1% silica for 20mins post mixing of the milled mannitol and MCC, provided an ideally flowing powder that would not adhere to storage containers and not hang up. Surface coverage calculations were undertaken, however this provided no clear advantage for the powder or resultant tablets. It was observed that increased coating of the host particle was achieved when surface coverage calculations were undertaken, however this did not materialise in clear advantages in the powder flow or to tablet properties. The final investigation involved comparing different excipients as flow aids, with Ethocel having potential in being used as a flow aid. It had a very small particle size and also helped tablet properties, with disintegration times being lower than silica and in some cases hardness also being improved. However it was concluded that the silica still provided the best option as a flow aid, as the primary purpose of this excipient was to increase the flowability of the powder, and silica was far better in lowering the angle of repose.

This chapter provided a comprehensive outline for the procedure of preblend production, alongside the idea proportion of the flow aid/mixing time to be used to improve the inherent poorly flowing nature of the milled mannitol. However further enhancement of the blends could be undertaken to prepare them more for commercial formulation.

Chapter 5

Utilisation of a Novel Dry Particle Coating Method to Develop an MCC/Silica Hybrid Powder to be employed in Directly Compressible Orally Disintegrating Tablets

5.1 Introduction

Microcrystalline cellulose (MCC) is an extensively used filler/binder within solid oral dosage forms, including tablets and capsules, due to its largely plastic deformability, high dilution potential and disintegrant properties (Rowe *et al*., 2012, Thoorens *et al*., 2014, Bhalekar *et al*., 2010, Bolhuis and Chowhan, 1996). It is a partially depolymerised cellulose prepared from α-cellulose and appears as a spray dried porous, white, tasteless, odourless crystalline powder, with some amorphous regions (Thoorens *et al*., 2014, Rowe *et al*., 2012). Its possesses excellent binding properties due to its highly plastic nature, low lubricant requirement and low die wall friction upon compression (Hwang and Peck, 2001, Thoorens *et al*., 2014). Primarily it is the plastic deformability of MCC that gives it its compaction behaviour, due to the large surface area available for interparticle bonding resulting from the slip planes and dislocation occurring during applied pressure. This allows strong hydrogen bonds to form between the closely interacting hydrogen groups on the cellulose particles, providing the resultant compact with high mechanical strength (Hüttenrauch, 1971, Bolhuis and Chowhan, 1996, Thoorens *et al*., 2014). It is marketed as Avicel by FMC Biopolymer (Philadelphia, USA) with the two most commonly used grades in solid oral dosage forms being Avicel PH101 and Avicel PH102, with particle sizes of around 50 µm and 100 µm respectively (FMC-Biolpolymer, 2016). MCC tends to have a low bulk density, with Avicel PH101 exhibiting poor flow due to the low bulk density, its matchstick/needle like shape, which would lead to interlocking during the bulk flow of the powder, and increased cohesion due to the small sized particles within the powder. Whereas the PH102 grade exhibits increased flowability behaviour due to the more uniform spherical particle shape, and larger particle size which results in lower friction and cohesive forces within the powder, however flow is inhibited by the low bulk density (Bolhuis, 2011, Staniforth and Aulton, 2007). Another disadvantage of MCC is its high lubricant sensitivity which results in weaker compacts, due to the inability of MCC to form new slip planes that are free of the lubricant, leading to a reduction in the hydrogen bonding between the adjacent cellulose particles (Zuurman *et al*., 1999, Hoag *et al*., 2008).

Due to these limitations a newly developed co-processed MCC was developed in combination with colloidal silicon dioxide, whereby MCC was spray dried alongside silicon dioxide to form particles, which , possessed an intimate association between the silicon dioxide and MCC (Sherwood *et al*., 1996). This product was commercialised under the brand Prosolv SMCC (silicified Microcrystalline Cellulose), and is currently marketed by JRS Pharma (Patterson, New York). Prosolv comes in two different grades, with Prosolv P50, the silicified equivalent to Avicel PH101 with a particle size of 50 µm, and Prosolv P90 which is equivalent to Avicel PH102, having a particle size of 90 µm. The SMCC was shown to have greater compressibility, superior flow, more resistant to wet granulation and less lubricant sensitivity over standard MCC, therefore the production of the more compressible MCC was seen as breakthrough in the manufacture of directly compressible tablet excipients (Sherwood *et al*., 1996, Edge *et al*., 1999, Edge *et al*., 2000, van Veen *et al*., 2005, Sherwood and Becker, 1998, Luukkonen *et al*., 1999). Therefore it was expected that the silification process had in fact altered the physical make-up of the excipient. However the mechanical and chemical nature of SMCC was observed to be very similar to the standard unsilicified MCC, tests conducted included compaction simulations, tensile strength tests, toughness tests, effective stiffness tests, with chemical modifications assessed using Fourier-transform infrared spectroscopy (FTIR), gas adsorption, x-ray diffraction, solid state NMR, Raman spectroscopy, and calorimetry (Buckton *et al*., 1996, Buckton *et al*., 1999, Edge *et al*., 1999, Edge *et al*., 2000, Tobyn *et al*., 1998). A physical difference observed was the presence of silicon dioxide, and the improvement in functionality of the excipient was related to the location of the silicon dioxide. A study by Edge *et al*. (1999) identified that the spray drying manufacturing method resulted in deagglomeration of the silicon particles, and therefore a uniform distribution of the silica over the surface of the MCC, giving particles of a far rougher surface and much larger surface area compared to unsilicified MCC (Luukkonen *et al*., 1999). It was highlighted that during processing, the silicon dioxide particles were actually present within the structure of MCC, as well as in the surface of the MCC (Luukkonen *et al*., 1999). The increase in compact strength compared to unsilicified MCC was explained by differences in interfacial interactions due to the presence of

silicon dioxide within the structure of MCC, where interfacial strength and interactions were higher with the silicified MCC grade. The presence of the silicon dioxide in the surface of MCC also led to improvements in the flow of SMCC, as silicon reduces friction and cohesive forces between adjacent particles, and provided the SMCC with less lubricant sensitivity (Edge *et al*., 1999, Edge *et al*., 2000).

Dry particle coating is becoming more thoroughly investigated currently due to its advantageous processing conditions compared to traditional manufacturing methods, whereby the powders are exposed to less chemical and physical modifications, providing powders with new functionalities (Dahmash and Mohammed, 2015). A patented composite blender developed in the laboratory has been shown to provide functionalised particles through an environmentally friendly mixing method whereby small guest particles are adhered to the surface of a larger host through cohesive forces, giving novel modified particles that have undergone no chemical alteration during processing, and are only physically attracted. The aim of this work was to assess if dry particle coating could provide a suitable alternative to the silicified MCC grade, Prosolv, whereby compressibility enhancement of dry coated powders was compared to the unmodified MCC, and disintegration times were compared to Prosolv, which was known to disintegrate slowly compared to unmodified MCC. The premise was that the environment experienced during the dry coating process was less harsh, with no pre-processing of the material required before mixing, and that dry coated powders were produced in a one stop, high yield manufacturing method, compared to spray drying of Prosolv.

5.2 Materials and Methods

5.2.1 Materials

MCC (Avicel PH101 and PH102) was obtained from FMC Biopolymer (Philadelphia, USA), Prosolv P50 and P90 were received from JRS Pharma (Patterson, USA) and colloidal silicon dioxide (Aerosil 200) was obtained from Evonik Industries (Essan, Germany). For tableting studies the magnesium stearate was obtained from Fischer Scientific (Loughborough, UK), D-mannitol was purchased from Sigma-

Aldrich (Dorset, UK) and Metformin Hydrochloride was purchased from Discovery Fine Chemicals (Dorset, UK). Powders were used as received.

Prosolv P50 and P90 were used as two powders under investigation and were the focal point of comparison for the developed dry coated blends in this study. Prosolv P50 has an average particle size of 50 µm and Prosolv P90 have a particle size of 90 µm.

5.2.2 Composite Blending

For the initial comparison, Avicel PH101 (particle size 50 µm) and Avicel PH102 (particle size 100 µm) were utilised as the host particles for silica. To establish the effect of silica loading on to the MCC particles, different concentrations of silica were initially used, ranging from 0.25-2% w/w. The Avicel PH101 dry coated powders were directly compared to Prosolv P50, with an uncoated PH101 powder used as a control; Avicel PH102 dry coated powders were directly compared to Prosolv P90, with an uncoated PH102 powder used as a control.

Dry coating was conducted in a novel composite blender that was developed within the laboratory. The mixing was conducted over a 30 minute time period with each of the proportions of MCC and silica. 1 bar of air pressure was introduced into the mixing chamber to aid the deagglomeration of the silica particles and increase shear forces to enhance the mixing and dry coating process.

5.2.3 Scanning Electron Microscopy (SEM)

SEM micrographs were obtained using a Phillips XL-30 FEG ESEM (Eindhoven, Netherlands) to allow an exploration of particle shape/size and evidence of dry coating upon the MCC particles. Approximately 1 mg of each sample was adhered to a double-sided adhesive strip and placed on to an aluminium stub. The samples were coated with a thin layer of platinum using an Emscope SC500 sputter coater (Quorum Technologies, Lewes, UK) at 20 mA for 1 minute. After platinum coating each sample was examined using SEM, with the acceleration voltage (kV) and magnification stated on each monograph.

5.2.4 Raman Spectroscopy

Raman microscopy was conducted using a Horiba XploRA Plus Raman Microscope (Kyoto, Japan), to allow molecular identification of the particles within the dry coated silica/MCC powder blends. This allowed a qualitative analysis of the presence of silica upon the surface of the MCC. The powders were investigated at 532 and 785 nm excitation, with 785 nm having a lower background noise. The 785 nm was used for further study, with 100 mW laser power utilised.

5.2.5 Investigation of Powder Flow

Angle of repose was used as the method of choice for assessing powder flow of the investigated powders. The method outlined in the USP monograph <1174> (USP37, 2014c) was followed, and the height and diameter of the pile measured. This was then added to the equation, $\tan(\Theta) = \text{height}/0.5\text{diameter}$, where Θ was the angle of repose. All values were analysed in triplicate and displayed as mean ± SD. This was conducted on all the powders to allow a comparison of the novel dry coated MCC/Silica hybrid to the commercially available Prosolv® preblends as well as the Avicel® control.

5.2.6 Thermogravimetric Analysis (TGA)

TGA was conducted to assess moisture content and loss on ignition of the powders evaluated in this study. A Pyris 1 TGA (Waltham, MA, USA) was utilised with 3-5 mg of sample measured for each run,. The method for the TGA was optimised using different end temperatures, heat ramps and hold times. The final optimised method that was utilised was as follows: The sample was ran from 50 °C to 100 °C at 10 °C/min and held for 5 mins; the sample was then heated from 100 °C to 150 °C at 10 °C/min and then from 150 °C to 700 °C at 20 °C/min and held for another 5 mins, the sample was then allowed to cool. The sample weight was measured throughout using the TGA balance. Moisture content was measured as the percentage loss in weight between 70-130 °C, as this was the range for moisture loss. For loss on ignition an initial MCC scan indicated that MCC degrades at around 350 °C, the sample was heated well above this to remove almost all traces of MCC from the sample pan. A silica control was

also ran and negligible amounts of silica degraded up to 700 °C therefore any residue left in the TGA pan was likely to be silica.

Avicel PH101 and PH102 were run as controls and any residual weight left In the TGA pan was subtracted from the Prosolv and dry coated blends to ascertain levels of silica present within the powders. Dry coated powders with 0.5, 1 and 2% silica were tested to observe whether loss of MCC indicated higher levels of silica present within each blend. The final percentage weight left in the pan at the end of each run was taken as a qualitative indication to the amount of silica present within each powder, and it allowed a comparison of silica levels within the blend. Each of the powders were analysed in triplicate and results are presented as mean ± SD.

5.2.7 Tableting and Tablet Properties

Tablets were prepared from each of the Prosolv powders and the dry coated MCC powders manufactured in this study, with the Avicel tablets used as a control. 500 mg portions of each of the powders were individually weighed out and compressed using a Specac semi-automatic hydraulic press (Slough, UK) equipped with 13 mm flat faced punches. The tablets were compressed at 75 MPa.

5.2.7.1 Hardness

Hardness of the tablets was measured using a Copley TBF 100 Hardness tester (Nottingham, UK). Tensile strength (σ) was then calculated using the equation:

$$\sigma = \frac{2\,H}{\pi\,D\,T} \qquad \text{(Eq. 5.1)}$$

Where H is the hardness, D is the diameter and T is the thickness of the tablet. All readings were taken in triplicate and displayed as mean ± SD.

5.2.7.2 Friability

The standard USP friability test was utilised for the assessment of the percentage friability of the manufactured tablets (USP37, 2014d). Six tablets were brushed off and weighed altogether for the initial weight, they were then inserted into a Sotax F2 Friabilitor (Allschwil, Switzerland). The test was

conducted for a total time of 4 minutes at 25 rpm, with 100 revolutions in total. The tablets were then de-dusted and reweighed to get the final weight. Percentage friability was calculated using the equation:

$$\%\ Friability = \frac{Initial\ weight - Final\ weight}{Intial\ weight} \times 100 \quad \text{(Eq. 5.2)}$$

5.2.7.3 Disintegration Time

The standard USP disintegration method was used to assess disintegration time of the tablets (USP37, 2014b). A Copley ZT41 disintegration apparatus (Nottingham, UK) was used, with a single tablet being tested at a time for accuracy. Each tablet was placed in the vessel (without a disk) and oscillated at 30 cycles per minute. Dissolution medium of 800 ml distilled water was maintained at 37 °C, and disintegration time measured when all of the fragments of tablet had passed through the mesh at the bottom of the vessel. All readings were taken in triplicate and represented as mean ± SD.

5.2.7.4 Porosity

Porosity of the tablets was assessed using a Quantachrome Helium Multipycnometer (Florida, USA). Diameter and thickness of the tablets was measured using a digital calliper, and the weight of individual tablets taken using an electronic balance. The bulk volume (V_B) and bulk density (ρ_{bulk}) of the tablets were then calculated using the following equations:

$$V_B = \frac{\pi R^2}{T} \quad \text{(Eq. 5.3)}$$

$$\rho_{bulk} = \frac{Tablet\ weight}{V_B} \quad \text{(Eq. 5.4)}$$

The true volume (V_t) of the tablet was calculated using the pycnometer, which applies the theory of gas displacement allowing the porous nature of the tablet to be assessed. The true volume was calculated using the equation:

$$V_t = V_c - V_r \left(\frac{P1}{P2} - 1\right) \quad \text{(Eq. 5.5)}$$

Where V_C is the volume of the sample cell, V_r is the volume of the reference cell, P1 and P2 are the atmospheric pressure and pressure change during the measurement respectively. The true volume was then used to calculate true density in the equation:

$$\rho_{true} = \frac{Tablet\ weight}{V_t} \quad \text{(Eq. 5.6)}$$

The final step to calculate porosity (ε) of the tablet used the following equation:

$$\varepsilon = 1 - \frac{\rho_{bulk}}{\rho_{true}} \quad \text{(Eq. 5.7)}$$

5.2.8 Powder Compression Profiling

To assess the compression profiles of the powder, three properties that affect the densification of the powder bed were assessed. Individual 500 mg portions of powder were weighed out and compressed at forces ranging from 75-150 MPa, and analysed for compressibility, compactability and tabletability.

5.2.8.1 Compressibility

Compressibility is a measure of the area of bonding occurring during the densification of the powder bed, and is measured by plotting the porosity of the tablet against the compression force used to compress it. Three tablets were prepared at each of the different compression forces and assessed for porosity to allow a compressibility profile to be built. The mean of the porosities at each of the compression forces was plotted.

5.2.8.2 Compactability

Compactability is a measure of the bonding strength of the bonds that form during powder compaction. It is measured by plotting the tensile strength of the tablet against the porosity of that tablet. Three tablets were prepared at each of the different compression forces and measured for their porosity and the subsequent tensile strength, then plotted on a graph. The mean of the tensile strength and porosity was plotted.

5.2.8.3 Tabletability

Tabletability is a measure of tensile strength of a tablet against the compaction force that the tablet was compressed at. It takes into account both compressibility and compactability of the tablet. Three tablets were measured for tensile strength at each compression force, and the mean of the tensile strength plotted to allow the tabletability profile to be generated.

5.2.9 Addition of a Non-Compressible API

To investigate the effects of utilising each of the blends in a typical dosage form, the non-compressible API metformin hydrochloride was used to assess how well the blends compacted alongside an API with inherent poor compression properties. As MCC was a large constituent of the preblend a non-compressible API was chosen as this presented the worst case scenario in terms of compaction of the powder. Two different ratios of preblend were investigated, with the compositions of the two types shown in Table 5.1. Magnesium stearate was used as a lubricant, and a crystalline grade of mannitol was added to blend 2 as an additional filler to assess the effect of the amount of preblend in the typical formulation. The tablets were compacted at 75 MPa using a Specac semi-automatic hydraulic press (Slough, UK), and assessed for the same tableting properties as the single preblend tablets above. Out of the dry coated blends manufactured above only AvicelPH101/1% and Avicel PH102/1% were taken forward to blend with the API, along with the two Prosolv grades and the two Avicel control powders. The dry coated powders were chosen for their favourable flow and tablet properties, and

Table 5.1: A table able showing the composition of the two different blends used to manufacture API loaded tablets allowing the effect of the proportion of preblend in the powder/tablet to be assessed alongside a non-compressible API.

Blend 1	**Blend 2**
40% Metformin	40% Metformin
59.5% Preblend	30% Mannitol
0.5% Magnesium Stearate	29.5% Preblend
-	0.5% Magnesium Stearate

increasing the concentration of silica beyond 1% lead to larger quantities of free silica being present in the blend, as was observed post mixing.

5.2.10 Statistical Analysis

One way ANOVA followed by a Tukey's multiple comparison post-hoc test, were performed using GraphPad Prism 7 software (California, USA). For statistical significance a p-value <0.05 was used, and all data was presented as mean ± standard deviation.

5.3 Results and Discussion

5.3.1 Effects of Silica Concentration during Dry Coating compared to Prosolv

Raman spectroscopy was conducted to ascertain if the chemical composition of the dry coated blend displayed any dual peaks from the constituent particles, or record absence/reduction of the MCC peaks due to the partial covering of the MCC surface with the silica. Figure 5.1 and 5.2 highlight the Raman Spectroscopy data for Avicel PH101 and PH102 respectively. Both the figures show a scan of the uncoated MCC grade alongside the silica scan with the dry coated blend represented at the top. The results indicated that uncoated MCC had large sharp peaks on the scan, with PH101 showing the largest peak at an intensity of around 11000 counts, and PH102 showing the largest peak at approximately 9000 counts. In terms of the silica scan the only characteristic peaks that were likely to appear in a dry coated blend were at a Raman shift clustered around 1600 cm^{-1}, as all other peaks were likely to be engulfed by MCC. The results showed that the dry coated powders with 2% silica were very similar for both grades of MCC, with the overall peak heights of the MCC peaks being reduced down to 8500 counts for PH101/2% and 4000 counts for PH102/2%, most likely due to the presence of silica upon MCC surface, therefore reducing the exposure of MCC and downsizing the intensity of the Raman peak. However the three small silica peaks around 1600 cm^{-1} were not detected, which indicated that the coating of silica was very thin, which was expected, as it was known that silica particles were very small in size, down in the nanometre range, therefore detection of these small particles using the Raman microscope would have been difficult in the dry coated blend.

However the overall peak reduction of the MCC represented a positive indication that the exposure of the MCC was reduced due to the presence of fine silica particles on the MCC surface, which was further supported using the SEM images. Figure 5.3 visualises the particles of each of the powders through SEM analysis, allowing the morphology of the particles to be observed. Dry coated powders were manufactured with a silica concentration increasing from 0.25-2% w/w, with SEM images highlighting the differences between the silica concentrations as shown in Figure 5.4. SEM images indicated that during dry coating there was a clear deposition of the silica upon the surface of the MCC, as observed in Figure 5.3 (E) and (F) and all of the SEM images in Figure 5.4, which correlated with the Raman spectroscopy data to highlight that silica was present upon the surface of the MCC, and partial coverage of MCC by silica was primarily responsible for the peak reduction observed on the Raman data, due to the lower exposure of MCC.

For Prosolv P50 (Figure 5.5), it was observed that the uncoated PH101 had a much higher angle of repose and therefore poorer flow compared to Prosolv, which was expected as previous findings

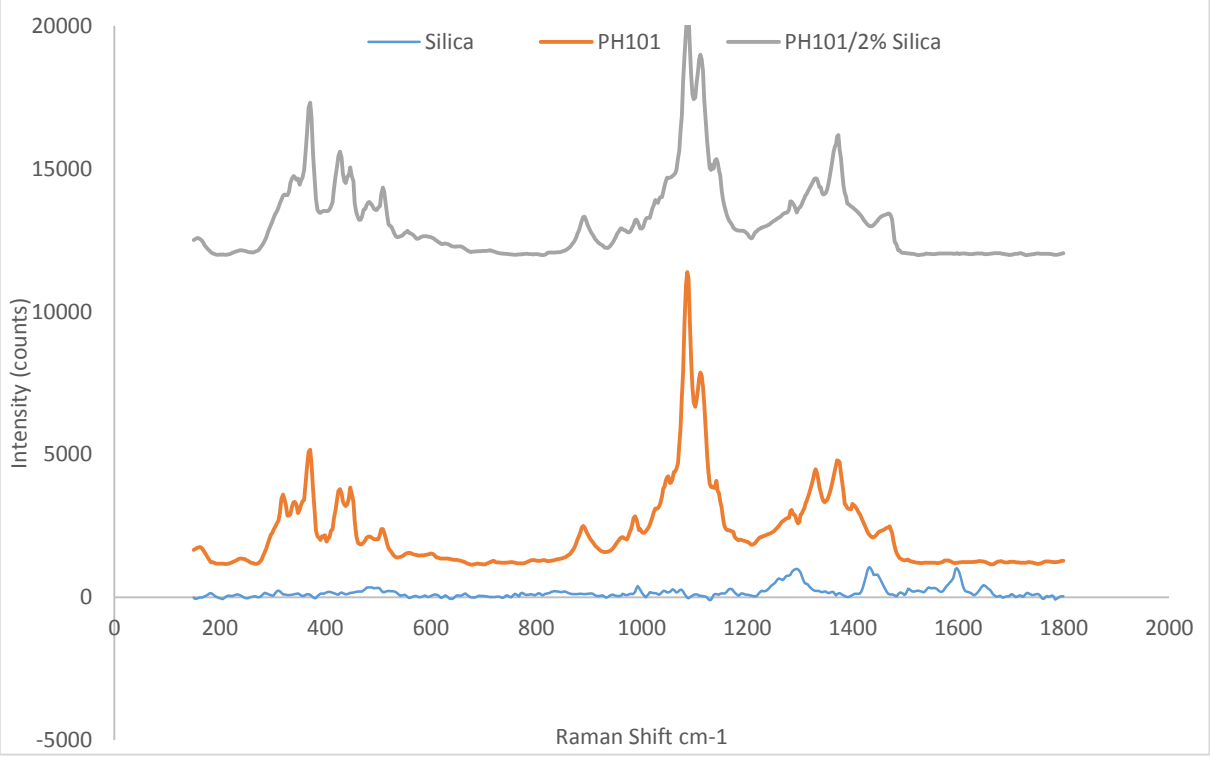

Figure 5.1: Raman spectroscopy data showing the Raman signature for silica, uncoated Avicel PH101 and dry coated Avicel PH101 with 2% silica loading. Raman signature shows MCC peak reduction post dry coating, indicating a lower MCC signal due to lower exposure of the MCC surface due to the presence of fine silica particles on the MCC surface.

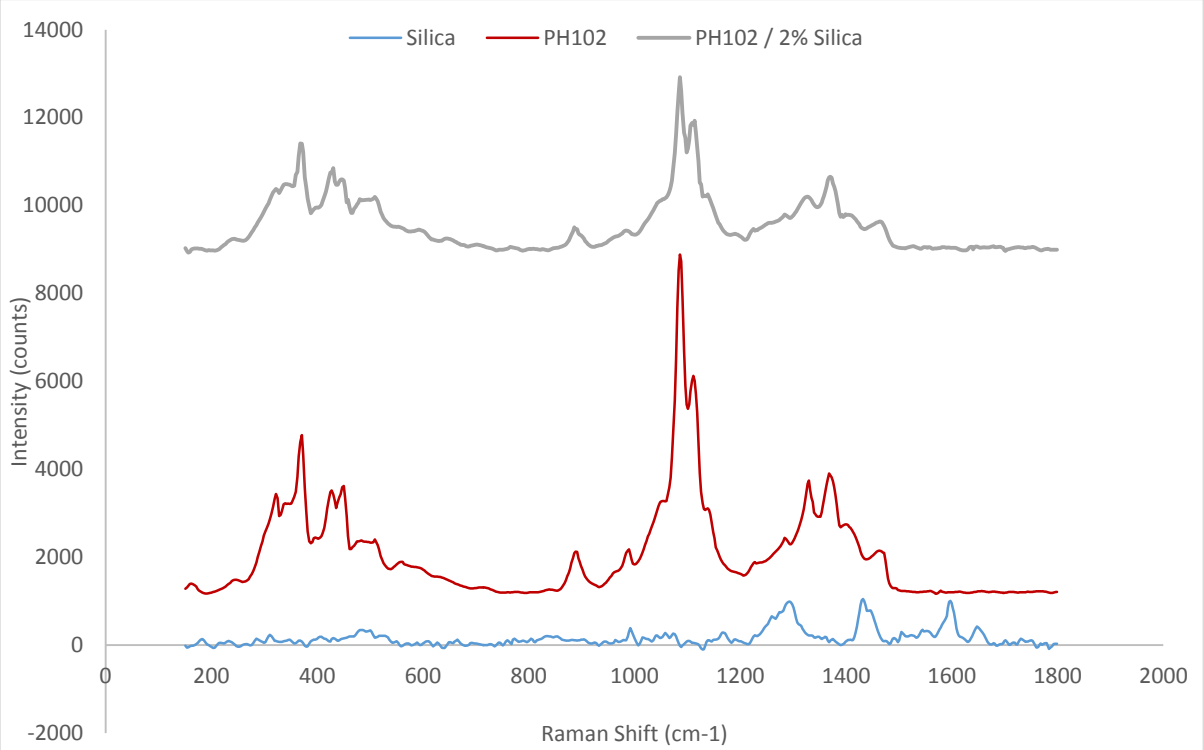

Figure 5.2: Raman spectroscopy data showing the Raman signature for silica, uncoated Avicel PH102 and dry coated Avicel PH102 with 2% silica loading. Raman signature shows MCC peak reduction post dry coating, indicating a lower MCC signal due to lower exposure of the MCC surface due to the presence of fine silica particles on the MCC surface.

stated that an advantage of the Prosolv grade was that it had an increased bulk density compared to unsilicified MCC, which resulted in the Prosolv having better flow properties. This increase in bulk density was attributed to the inclusion of silica within the pre-processed particle (van Veen *et al*., 2005). The Avicel PH101 also had a match stick like structure, as observed from Figure 5.3 (C), along with the relatively low particle size, which contributed to its poorly flowing nature (Bolhuis and Chowhan, 1996). Adding silica at a concentration of 0.25% improved the flow, and it was evident that increasing the concentration up to 2% continued to lower the angle of repose and improve the powder flow. It was seen that at higher concentrations, the angle of repose was starting to plateau, showing that the silica was reaching maximum loading capacity and flow improvement did not increase as expected. Also observed within the actual powder blend were higher levels of uncoated silica, as the concentration of silica was increased. This was a further indication that the loading capacity of silica upon MCC reached its maximum, and further increases in the levels of silica within the blend led to no further flow improvements of the powder. This was further evidenced on the SEM (Figure 5.4) as

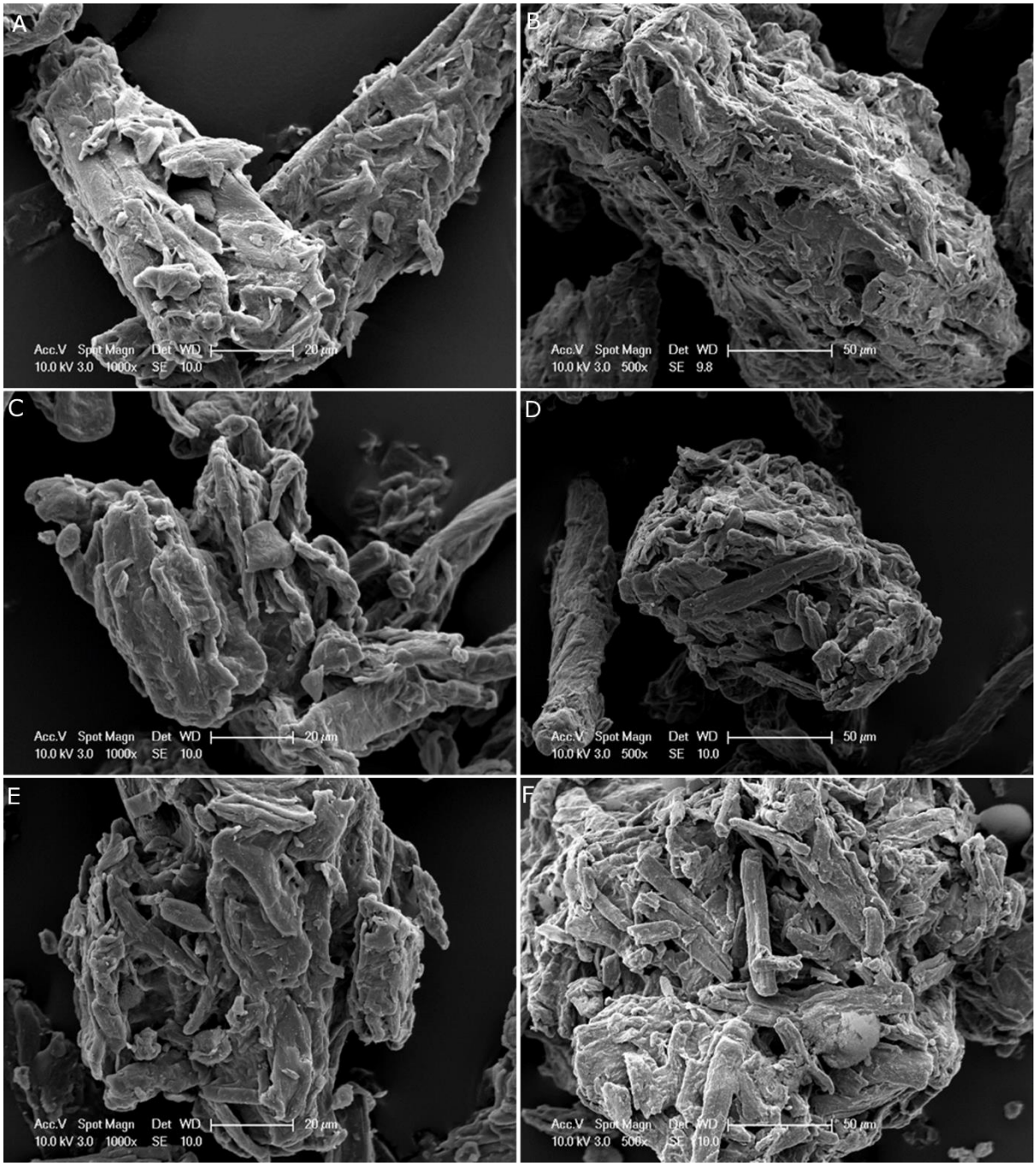

Figure 5.3: SEM images of the different powders investigated in this study, with A, C and E at 1000x magnification and B, D, F at 500x magnification; A – Prosolv P50 showing a rough particle surface, B – Prosolv P90 showing again a rough surface; C – Avicel PH101 showing a smoother particle surface compared to the Prosolv; D – Avicel PH102 showing a smoother particle surface compared to the Prosolv; E – Avicel PH101/1% silica dry coated blend, showing an MCC particle with a clear coating of silica upon the particle surface and F – Avicel PH102/1% silica dry coated blend with clear evidence of silica dry coated upon the MCC particle surface.

the monographs showed that when concentration was increased from 0.5 to 1%, an increase in silica loading upon the MCC was observed, with far more nano/micro sized silica coating the MCC.

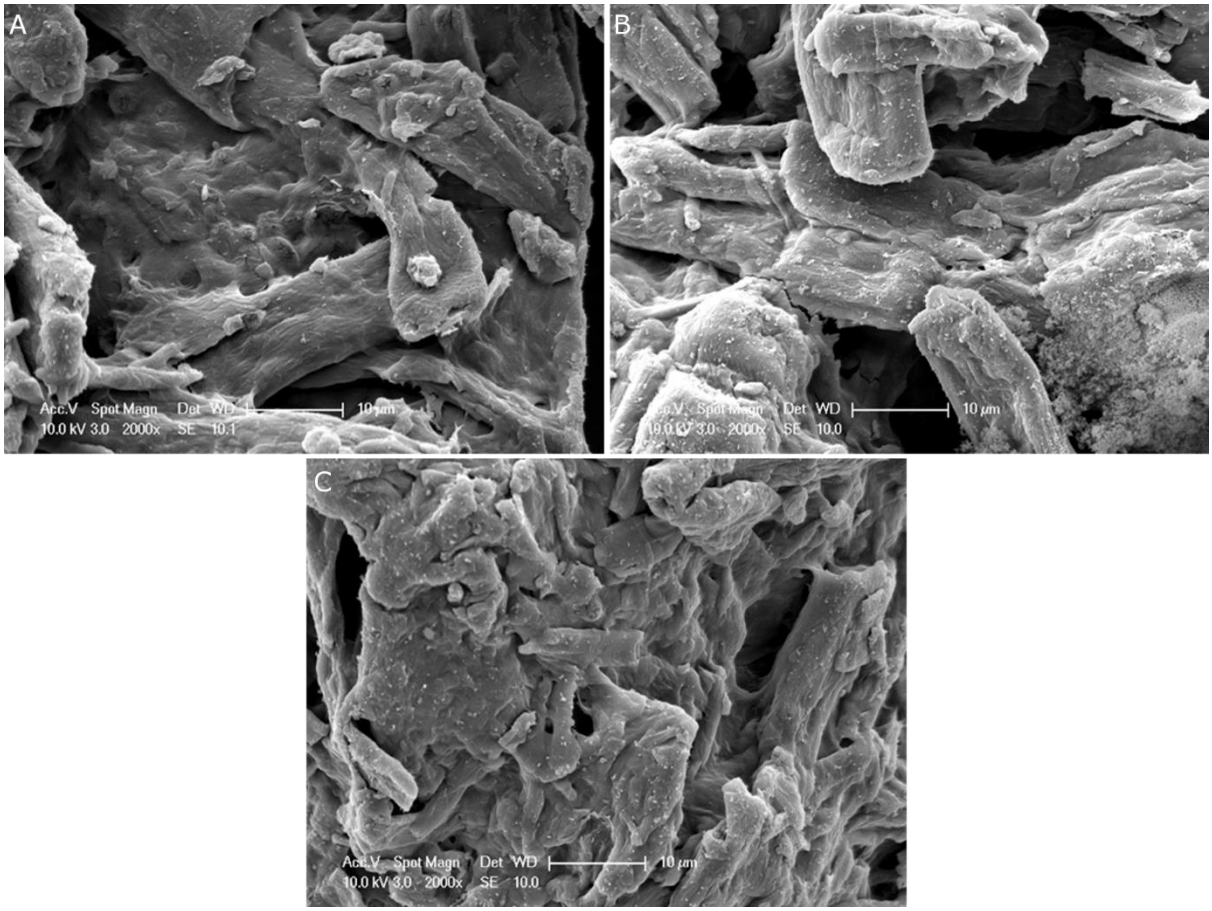

Figure 5.4: SEM images of the Avicel PH102 with different silica loading, with all images at 2000x magnification; A – 0.5% silica; B – 1% silica and C – 2% silica. Images indicate a large difference in silica loading between 0.5 and 1%, however when the concentration is increased up to 2% a significant difference in silica loading upon the MCC is not observed.

However when the concentration was doubled from 1 to 2% no significant increase in silica coating on the MCC was observed. This gave further indication that, along with flow results (Figure 5.5), increasing the silica concentration beyond 1% led to little enhancement in the loading efficiency of the silica upon MCC particles. Overall it was seen that the smaller particle sized MCC loaded with >1% silica had a very similar flow to Prosolv P50, which was a very well flowing excipient.

Loss on ignition was conducted to ascertain the level of silica within/dry coated on to the powders, with results shown in Table 5.2. For Prosolv P50 and the PH101 powders, it was seen that 0.5% silica loading had negligible levels of silica present within the blend, however upon increasing the concentration up to 1 and 2%, increasing concentrations, similar to that in Prosolv, were seen. At 0.5% silica load, flow results indicated an improvement, highlighting that silica was present in low concentrations, which couldn't be detected on the loss of ignition.

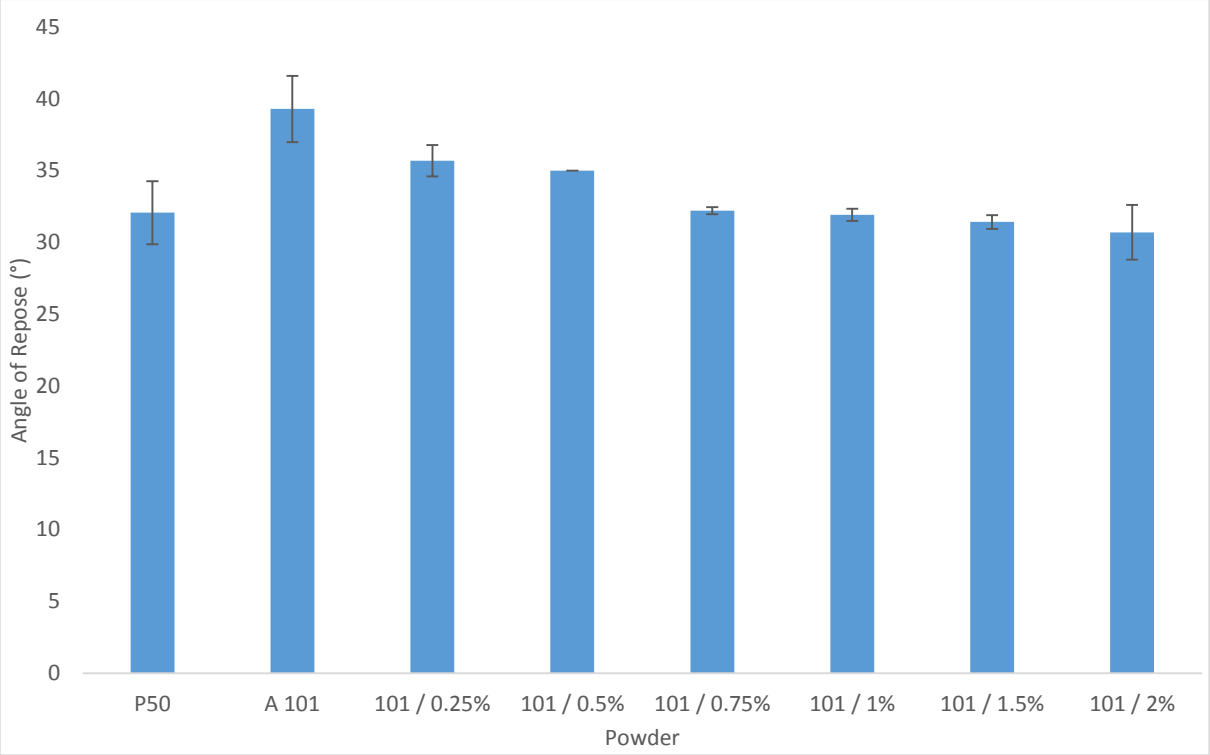

Figure 5.5: A graph showing the powder flow, through angle of repose, of the Prosolv P50 compared to the dry coated Avicel PH101 powders, with uncoated Avicel PH101 used as a control. No significant difference observed between the Prosolv and the dry coated powders (n=3, p>0.05).

Table 5.2: A table showing the silica content of the Prosolv and dry coated blends obtained through loss on ignition using TGA. For P50/PH101 there was an observable amount of silica present at 1 and 2% silica with 0.5% significantly lower than the three other powders. However with PH102 the amount of silica was similar for 0.5 and 1%, however 2% silica showed a significantly higher amount of silica presence. No significant difference in silica concentration between the dry coated powders and Prosolv were observed (except P50 and 101/0.5% P<0.05). Moisture content was similar for all blend with no significant difference observed. (n=3, p>0.05).

Powder	Silica Content (%)	Moisture content (%)
PH101	-	2.95 ± 0.20
P50	2.44 ± 0.19	2.66 ± 0.47
101/0.5%	0.00 ± 0.00*	3.31 ± 0.21
101/1%	2.33 ± 0.84	2.46 ± 0.77
101/2%	2.58 ± 0.21	3.17 ± 0.36
PH102	-	3.17 ± 0.27
P90	4.37 ± 0.47	3.23 ± 0.09
102/0.5%	3.66 ± 0.34	3.36 ± 0.41
102/1%	3.67 ± 0.11	2.74 ± 0.24
102/2%	5.33 ± 0.51	2.80 ± 0.34

However when concentration was increased up to 1 and 2% silica levels were detectable, and a clear coating of silica was present on the MCC, as observed on SEM, which correlated with the improvement in flow compared to the uncoated MCC. There was no statistical difference in silica levels between Prosolv P50 and PH101/1% and PH101/2%, indicating that silica levels were very similar between these three powders ($p>0.05$) A difference in silica loading was seen with PH102, with levels appearing higher than the PH101 powders. This was due to the dry coating phenomenon, where a larger difference in particle size between the guest and host resulted in more distinct coating. The higher levels of silica present on the PH102 powder was due to the particle size being 100 µm as opposed to the 50 µm of PH101, which would have resulted in stronger cohesive forces between the silica and MCC in PH102, and therefore a stronger and improved coating would have been produced. The pattern with PH102 powders was slightly different, although it was observed that silica concentration increased as the amount in the dry coated powder was increased, the difference between 0.5 and 1% was negligible, at 3.66 and 3.67% respectively, however 102/2% had a significantly higher proportion of silica at 5.33%. This therefore indicated that at 2% a higher level of silica was attaching itself to the MCC, and that loading had increased, however it was not statistically different when compared to Prosolv P90 ($p>0.05$).

Prosolv P90 was the larger particle size grade of Prosolv, and it had a clear flow improvement over Prosolv P50 due to the larger particle size, which reduced interparticle cohesive, electrostatic and Van der Waals forces (Liu *et al*., 2008, Staniforth and Aulton, 2007). It was observed again that the uncoated PH102 had a worse flow behaviour compared to Prosolv, as expected, due to the absence of silica within the particle itself, which resulted in a lower bulk density of the regular MCC (van Veen *et al*., 2005). Upon dry coating of the silica on to the surface of the PH102 powders it could be seen that a clear improvement in flow was observed (Figure 5.6) from 28.13° with Prosolv to 24.54° with PH102/1% silica, with statistical significance observed amongst all dry coated formulations. The excellent flow properties of the Prosolv (both grades) was attributed to the fact that the silica within

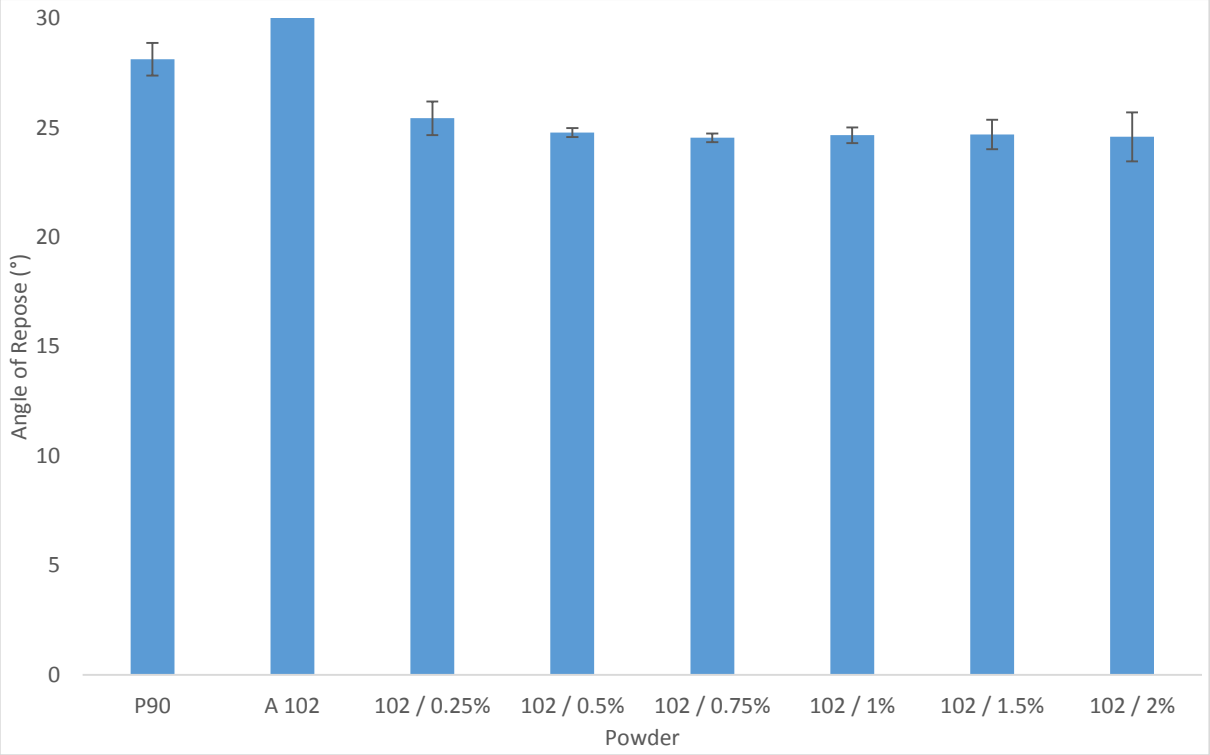

Figure 5.6: A graph showing the powder flow, through angle of repose, of the Prosolv P90 compared to the dry coated Avicel PH102 powders, with uncoated Avicel PH102 used as a control. Significant difference was observed between the Prosolv and all of the dry coated powders, with dry coated powders providing a more flowable powder (n=3, $p<0.05$).

the particles was mainly adhered at the surface of MCC, however some of the silica also formed part of the internal structure due to the production process (Edge *et al*., 1999). However for the PH102 dry coated powders, silica was completely at the surface of the particles. This meant that silica acted to reduce interparticulate friction by coating the main constituent particles within the blend, and any free silica within the dry coated powder also acted to further enhance the flow (Chattoraj *et al*., 2011). Moisture content was also analysed, as shown in Table 5.2, to assess if moisture levels had an impact on flow, as a previous study by Alyami *et al*. (2016b) found that dry particle coating could be utilised for moisture optimisation within powders. However the results in the study indicated that no statistical difference in moisture content was observed, and that moisture levels remained around 2-3.5% w/w.

Results in this study showed that improvement in flow properties was dependent on the concentration of silica. As with PH101, the PH102 powders beyond 1% tended to have some amount of free silica within the blend that didn't coat the MCC particles, which was also observed on the

SEM images shown in Figure 5.4. Loss on ignition results clearly indicated an increased silica presence with 102/2%, however even with the increased silica load no increase in powder flow was obtained. This gave a clear indication that beyond a certain concentration of silica, levels of dry coating were reaching their optimum level and no significant increase in silica loading on to MCC was occurring and thus led to a higher proportion of free silica within the powder. Therefore in this study the optimum concentration of silica was observed to be 1% w/w to achieve optimum dry coating and flow improvement.

In terms of tablet properties, hardness and disintegration times of the Prosolv and the Avicel/Silica dry coated powders are shown in Figures 5.7 and 5.8, with porosity and friability shown in Table 5.3. From these results it was clear that the mechanical strength for Prosolv tablets for both the P50 and P90 (Figure 5.7 and 5.8 respectively) was higher than all of the dry coated tablets, with statistical

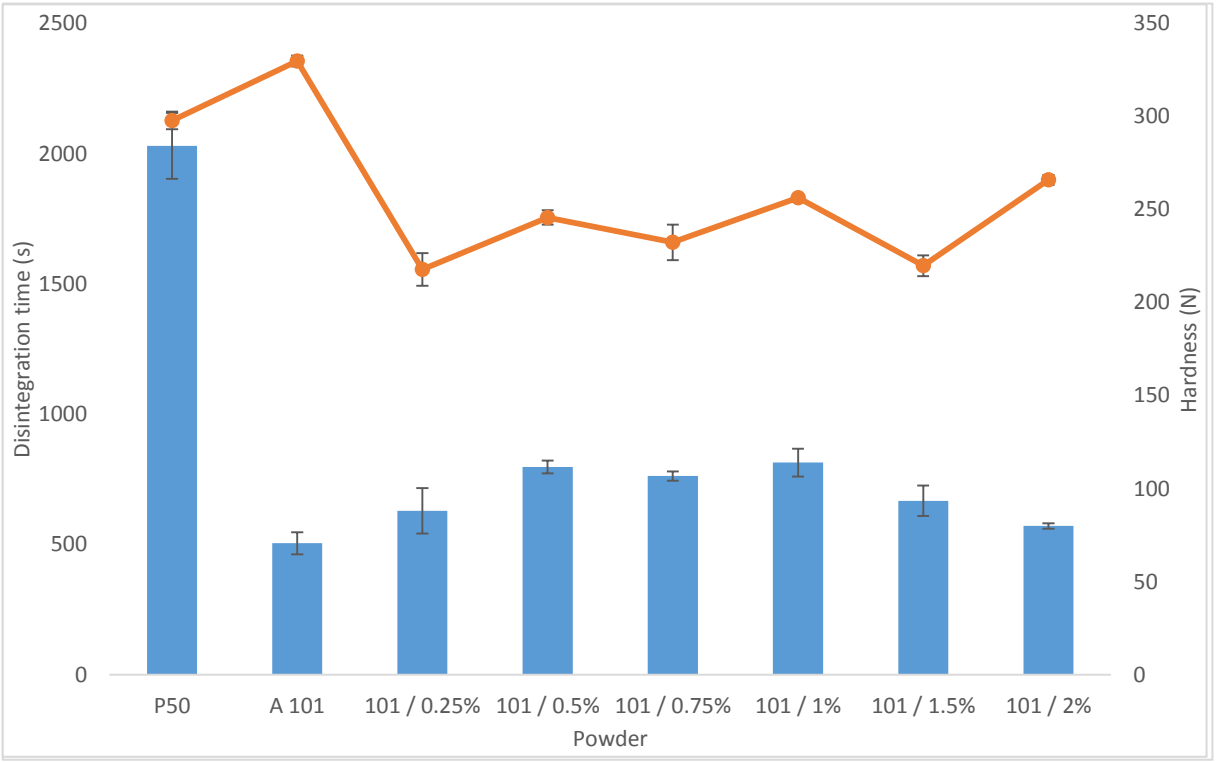

Figure 5.7: A graph showing the hardness and disintegration time of the tablets compressed at 75 MPa of the Prosolv P50 and Avicel PH101 dry coated tablets/control, with different proportion of silica, with hardness represented by the line and disintegration time by the bars. Results indicated that Prosolv displayed advantageous mechanical strength compared to dry coated grades (n=3 $p<0.05$), however disintegration time was significantly improved with the dry coated grades, even though mechanical strength was still very high (n=3, $p<0.05$).

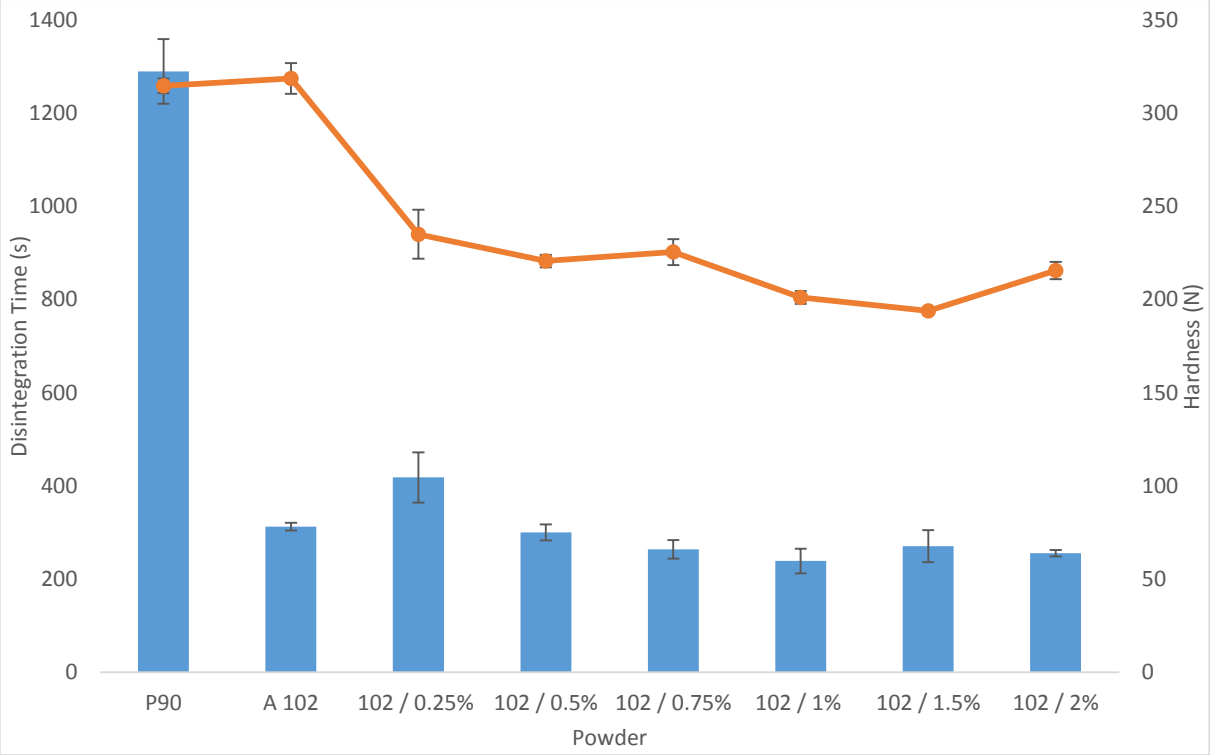

Figure 5.8: A graph showing the hardness and disintegration time of the tablets compressed at 75 MPa of the Prosolv P90 and Avicel PH102 dry coated tablets/control, with different proportion of silica, with hardness represented by the line and disintegration time by the bars. Results indicated that Prosolv displayed advantageous mechanical strength compared to dry coated grades (n=3 $p<0.05$), however disintegration time was significantly improved with the dry coated grades, even though mechanical strength was still very high (n=3, $p<0.05$).

significance observed. It was seen that the uncoated Avicel also displayed similar hardness to the Prosolv at both particle sizes, which indicated that the dry coating process was affecting the binding efficiency of MCC, due to the addition of silica to the outer surface of the particle. The similarities between Prosolv and uncoated Avicel were due to the silica being processed along with the MCC in Prosolv. This allowed strong bonds to form between adjacent MCC particles, as silica was present within the particle, whilst also being present to some extent at the particle surface. This resulted in very little interruption to the hydrogen bonding mechanism, whereas the presence of silica on the surface of MCC in the dry coated blends interrupted MCC-MCC bonding. However due to the presence of silica at the particle surface the levels of interparticle bonding may have been reduced, leading to a lower overall hardness of the tablets (van Veen *et al.*, 2005). Due to the high mechanical strength, the friability of all the tablets analysed in this study was very low and

Table 5.3: A table showing the friability and porosity of the tablets manufactured from the different powders tested in this study. Results indicated that in terms of friability all tablets (both the Prosolv P50/Avicel PH101 compared powders and Prosolv P90/Avicel PH102 compared powders) passed the test with friability being below the designated 1% threshold and no clear pattern observed. Porosity results also displayed no significant differences and no clear pattern, indicating friability and porosity of the dry coated tablets were very similar to the Prosolv and the Avicel control (n=3, p>0.05).

Powder	Friability (%)	Porosity	True Density
Prosolv P50	0.102	0.291 ± 0.019	1.656 ± 0.048
Avicel PH101	0.014	0.261 ± 0.021	1.570 ± 0.049
Avicel PH101 / 0.25%	0.135	0.266 ± 0.015	1.569 ± 0.029
Avicel PH101 / 0.5%	0.168	0.277 ± 0.014	1.586 ± 0.030
Avicel PH101 / 0.75%	0.2	0.308 ± 0.019	1.595 ± 0.042
Avicel PH101 / 1%	0.033	0.277 ± 0.005	1.545 ± 0.009
Avicel PH101 / 1.5%	0.033	0.278 ± 0.016	1.563 ± 0.038
Avicel PH101 / 2%	0.033	0.282 ± 0.022	1.564 ± 0.041
Prosolv P90	0.102	0.269 ± 0.009	1.604 ± 0.019
Avicel PH102	0.216	0.255 ± 0.014	1.572 ± 0.032
Avicel PH102 / 0.25%	0.066	0.244 ± 0.021	1.497 ± 0.038
Avicel PH102 / 0.5%	0.132	0.244 ± 0.010	1.480 ± 0.022
Avicel PH102 / 0.75%	0.099	0.264 ± 0.023	1.512 ± 0.045
Avicel PH102 / 1%	0.099	0.243 ± 0.021	1.468 ± 0.035
Avicel PH102 / 1.5%	0.066	0.242 ± 0.024	1.451 ± 0.041
Avicel PH102 2%	0.198	0.253 ± 0.024	1.467 ± 0.044

well within acceptable limits (friability below <0.2%) as shown in Table 5.3, with no impact from silica concentration. However it was seen that disintegration time with the dry coated formulations was significantly better than Prosolv. The reduction in disintegration time could be attributed to the reduced mechanical strength of the dry coated formulations, but it could also be said that including the silica during the production process of Prosolv was negatively affecting the disintegrating ability of the MCC as the control uncoated version disintegrated rapidly even though it had comparable hardness. Previous work had indicated that the silicified MCC grades (Prosolv) were more resistant to

disintegration than unsilicified grades of MCC (Kachrimanis *et al*., 2003). It was hypothesised that the co-processing of silica with MCC in Prosolv, whereby silica was present within the MCC structure and at the surface (Edge *et al*., 1999), acted as a barrier to the wetting of the particles. The adsorbed moisture acted to reduce the energies involved in interparticle separation and therefore led to prolonged disintegration times (Kachrimanis *et al*., 2003). It was also observed by Luukkonen *et al*. (1999) that Prosolv tended to adsorb more moisture within its structure leading to a lower liquid saturation, whereas Avicel tended to have higher levels of liquid within the particle, which would have led to a faster disintegration with Avicel based tablets as the increased water within the tablet would aid breakdown and disintegration of the structure. Therefore the dry coated MCC presented a far better option in terms of enhancing disintegration of the tablets as it retained properties similar to the uncoated MCC, with powders retaining very similar disintegration times to the uncoated powder. MCC has been shown to exhibit good disintegrating properties, as it forms swellable, porous tablets which promote water uptake through capillary action (Bhalekar *et al*., 2010, Thoorens *et al*., 2014, Bolhuis and Chowhan, 1996). Therefore the reduction in disintegration capability of the Prosolv indicated that the inclusion of silica within the co-processed MCC reduced the disintegrating properties of the SMCC, whereas dry coating the MCC with silica preserved MCC's inherent fast disintegrating properties. The reduced disintegration capability of the Prosolv couldn't be attributed to the porosity as it was seen that porosity across the small particle sized MCC and large particle sized MCC, as shown in table 5.2, were very similar, ranging from 0.5 to 0.3. This was low due to the highly plastic nature of MCC, meaning it had a very good compressibility leading to a less porous particle being produced (Thoorens *et al*., 2014, Almaya and Aburub, 2008).

5.3.2 Compression Properties of the powder

Figures 5.9-5.11 and 5.12-5.14 show profiles for the compressibility, compactability and tabletability comparisons for Prosolv P50 against the dry coated PH101 powders and Prosolv P90 against the dry coated PH102 powders respectively. The tablets were compressed from a compaction force range of between 75-150 MPa, as the mechanical strength beyond 150 MPa was not measurable by the tablet

hardness tester. With both particle sizes of dry coated powders a very similar pattern emerged where compressibility of the dry coated blends was very similar to the Prosolv and uncoated Avicel, however compactability and tabletability was reduced.

The compressibility profiles indicated the materials ability to reduce in volume during the application of a compaction pressure, and displayed the relative bonding area that had occurred during the compaction of the material (Khomane and Bansal, 2013, Joiris *et al*., 1998). The results in this study, as shown in Figure 5.9 and 5.12 for Prosolv P50/Avicel PH101 and Prosolv P90/Avicel PH102 respectively, indicated that dry coating did not affect the compressibility of the material, with the bonding area during compaction remaining very similar. This meant that silica as an additional layer on the outside of the MCC particles was not significantly affecting the proportion of bonds forming between adjacent MCC particles, as MCC is a highly plastic material which forms a large number of bonds during applied pressure. Very similar results were observed for both particle sizes tested with no significant differences observed between the Prosolv and Avicel for either size, which indicated that the dry coating did not affect the compressibility of the material irrespective of the particle size.

However it was observed that compactability and tabletability of the dry coated blends were reduced compared to Prosolv and Avicel control. In terms of compactability (Figure 5.10/Figure 5.12 for Prosolv P50/Avicel PH101 and Prosolv P90/Avicel PH102 respectively), which was a measure of the interparticulate bonding strength, displayed as porosity against tensile strength; therefore a high tensile strength at a higher porosity would indicate an increased bonding strength for that particular material (Khomane and Bansal, 2013, Joiris *et al*., 1998). The results presented in the study revealed that although the bonding area for the dry coated material remained the same, the strength of the bonds was reduced, due to the reduction in tensile strength of the tablets at a given porosity.

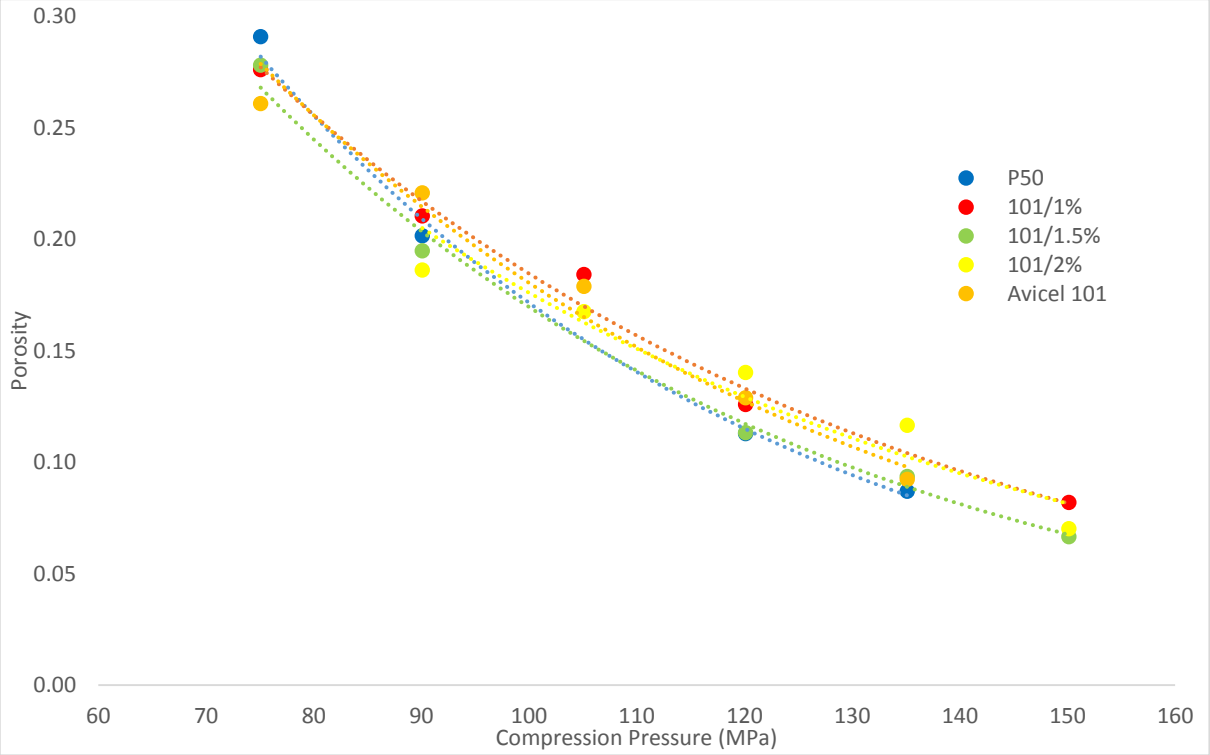

Figure 5.9: A graph showing the compressibility profile of the Prosolv P50 and Avicel PH101 dry coated powders, with results displaying a very similar compressibility profile between all powders, this indicated bonding area was very similar amongst all powders.

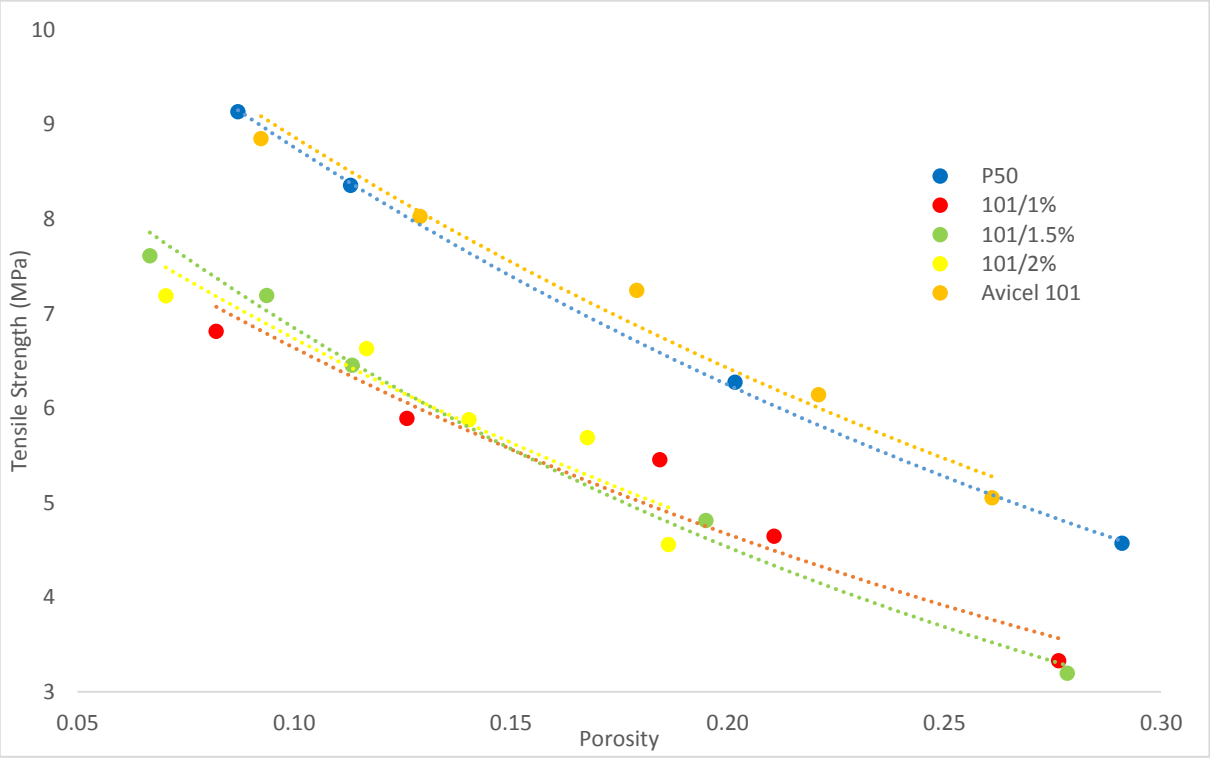

Figure 5.10: A graph showing the compactability profile of the Prosolv P50 and Avicel PH101 dry coated powders, with results showing Prosolv and the Avicel control had superior compactability, and therefore bond strength compared to dry coated powders.

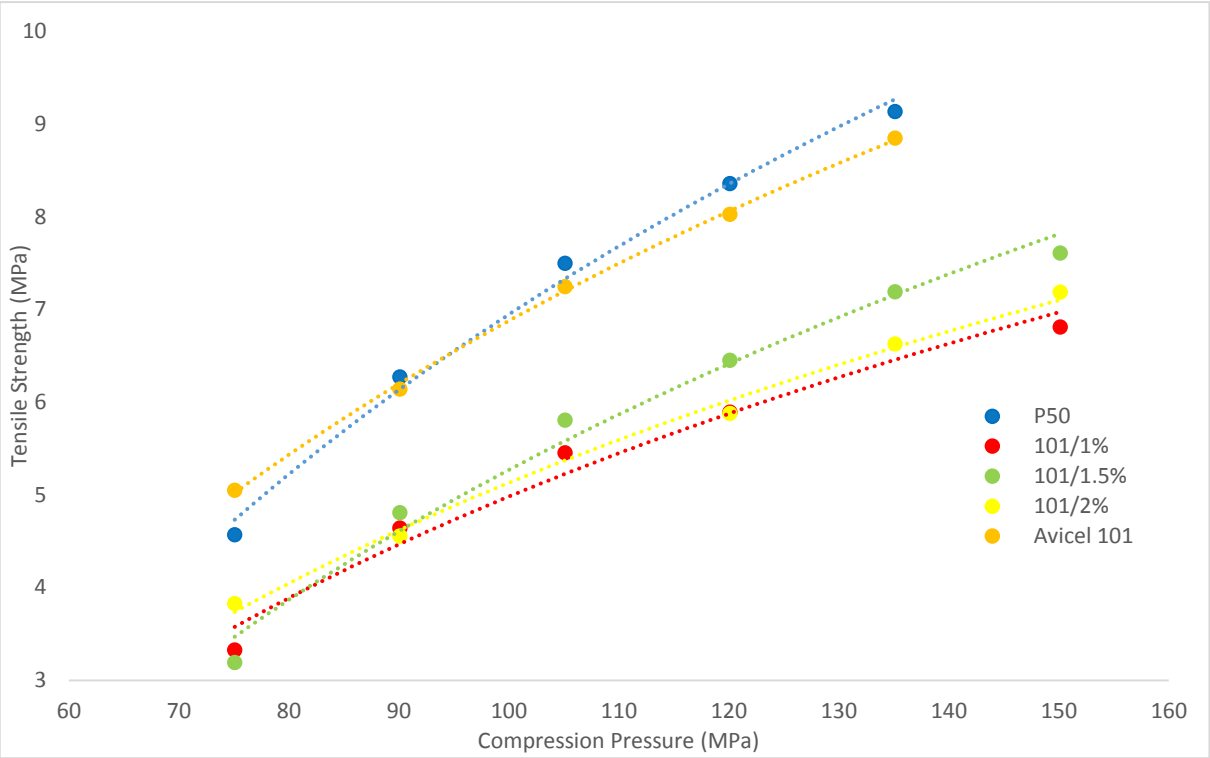

Figure 5.11: A graph showing the tabletability profile of the Prosolv P50 and Avicel PH101 dry coated powders, with results showing Prosolv and the Avicel control had increased tabletability, due to the increased compactability of the powders compared to the dry coated powder.

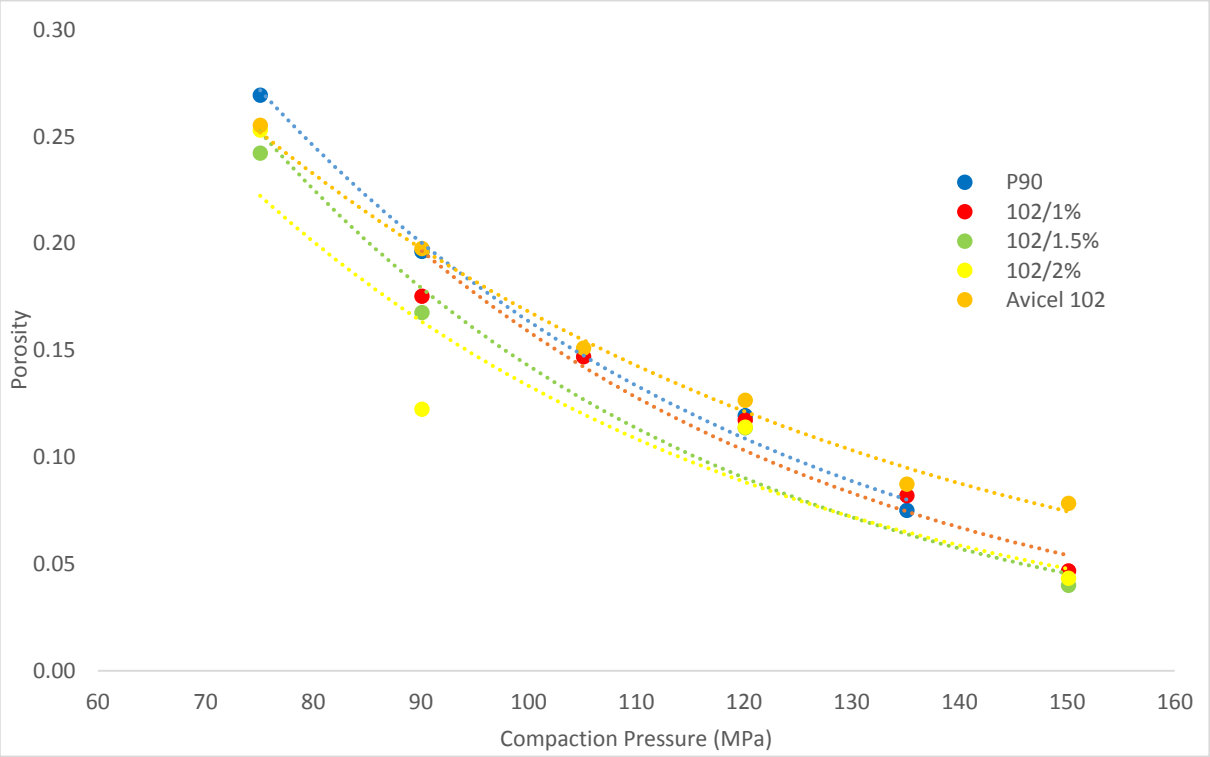

Figure 5.12: A graph showing the compressibility profile of the Prosolv P90 and Avicel PH102 dry coated powders, with results displaying a very similar compressibility profile between all powders, this indicated bonding area was very similar amongst all powders.

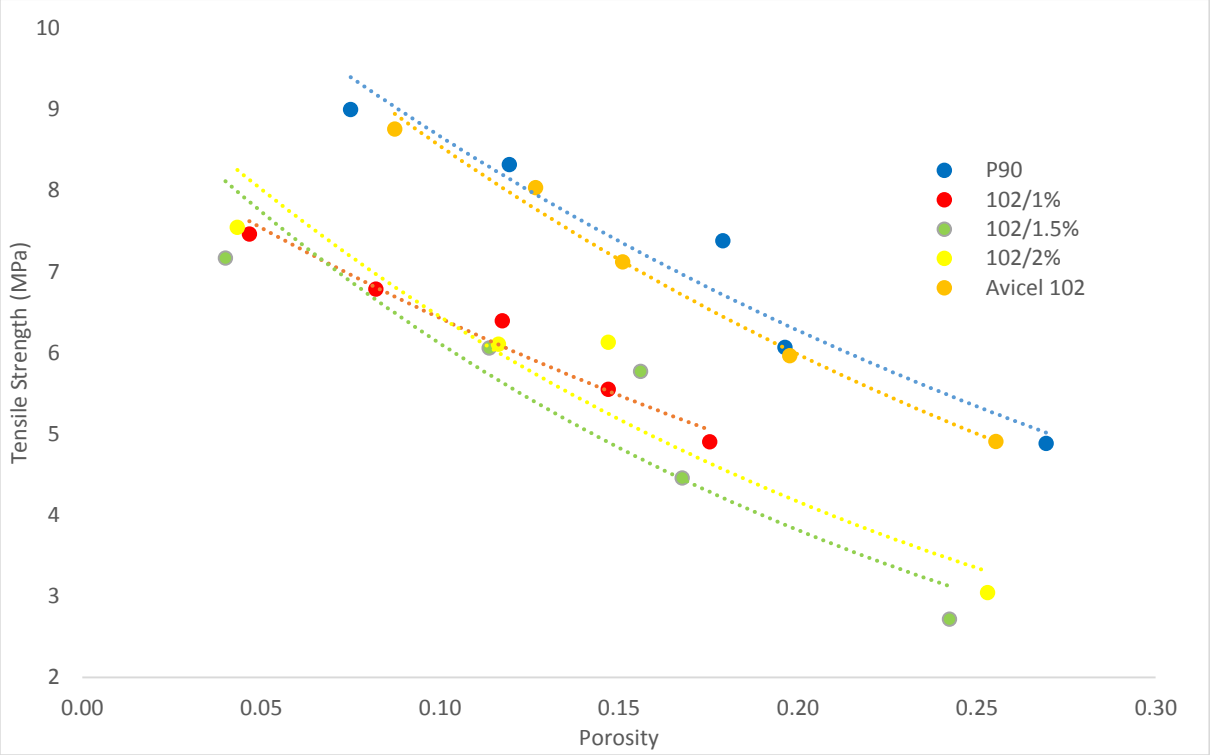

Figure 5.13: A graph showing the compactability profile of the Prosolv P90 and Avicel PH102 dry coated powders, with results showing Prosolv and the Avicel control had superior compactability, and therefore bond strength compared to dry coated powders.

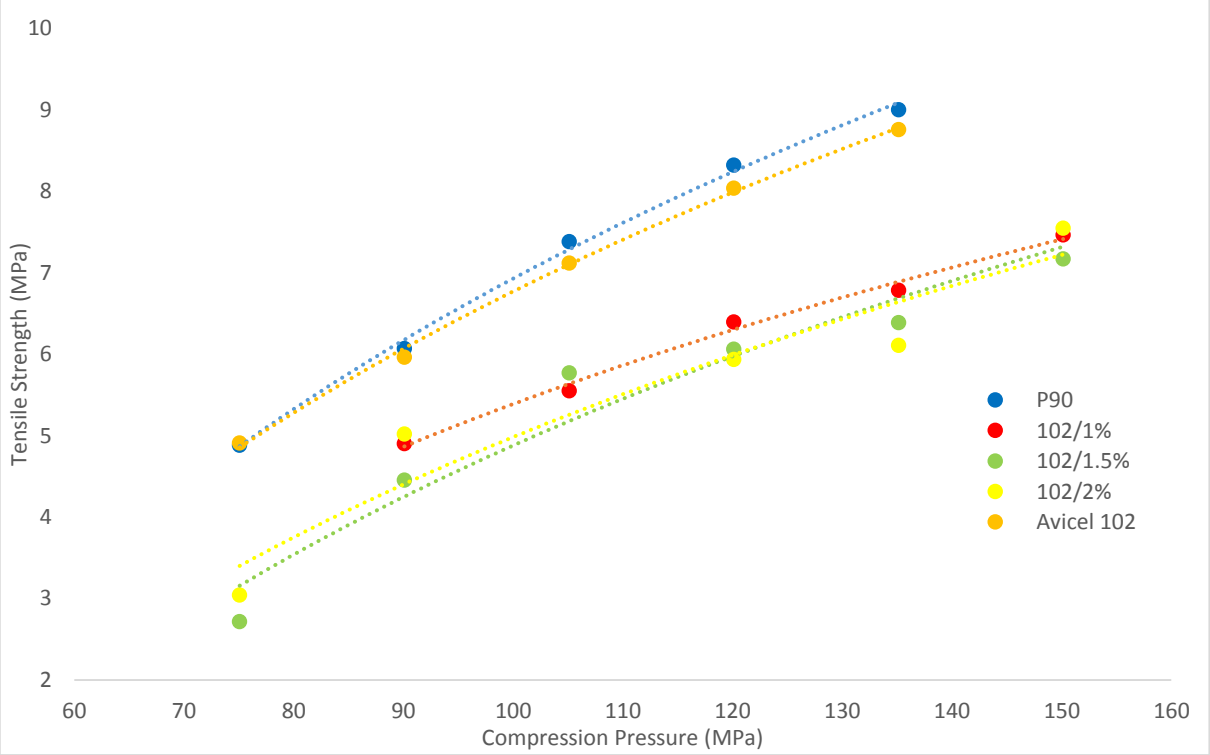

Figure 5.14: A graph showing the tabletability profile of the Prosolv P90 and Avicel PH102 dry coated powders, with results showing Prosolv and the Avicel control had increased tabletability, due to the increased compactability of the powders compared to the dry coated powder.

This indicated that the addition of silica to the surface of the MCC affected the materials ability to form strong bonds. Although it has to be understood that the tensile strength of the dry coated tablets was still very high for the given compaction pressure, with tablets compressed at 150 MPa having a tensile strength of 7.189 and 7.548 MPa for PH101 and PH102 with 2% silica respectively. With Avicel and Prosolv displaying very similar results for both particle sizes it indicated that adding the silica alongside the MCC during the spray drying process resulted in the MCC being able to retain its ability to form strong bonds. A previous study had also indicated that at slow compaction speeds, as used in the single tablet press used in this study, compactability of the Prosolv had remained very similar to the unsilicified MCC (Edge *et al*., 2000). The alteration of the surface characteristics of the MCC, due to adsorbed silica to the MCC particle surface during dry coating, affected this ability and in fact reduced the bonding strength of MCC. Silica possibly acted by reducing interparticle friction, therefore this could have been a primary reason for the reduction in strength of the bonds, as this may have reduced the ability of MCC to mechanically interlock, thus reducing the strength of bonds formed between the adjacent particles (Al-khattawi *et al*., 2014). This may have been due to the increased surface area of the silicified Prosolv grades, as shown in Figure 5.3, possessed a fairly rough surface, which would have increased the levels of interlocking between adjacent particles, and promoted strong bond formation (Al-khattawi *et al*., 2014). The concentration of silica didn't affect the bonding strength, as all three powders and both particle sizes indicated very similar compactabilities, which resulted in the assumption that it was primarily the presence of silica reducing the bonding strength of the material and was independent of concentration. It was observed in the above results that at a concentration of 1%w/w silica loading on to the particle surface of MCC was optimal, whereby further increasing the silica led to a higher proportion of free silica within the powder mix. Therefore these results again supported that the MCC particles were coated with a large proportion of silica.

Tabletability was also reduced for both the PH101 and PH102 dry coated powders in a very similar magnitude to that of the reduction observed in the compactability. Tabletability is the ability of the powder to be manufactured into a tablet of certain strength with the application of a compaction

pressure (Khomane and Bansal, 2013, Joiris *et al*., 1998), and is indicated by Figures 5.11 and 5.14 for Prosolv P50/Avicel PH101 and Prosolv P90/Avicel PH102 respectively. The tabletability of a material is dependent on its compressibility, compactability and true density (Khomane and Bansal, 2013). True density of the Prosolv was always higher than the dry coated blends, which gave an indication that a higher true density provided an improved tabletability with the investigated powders (Table 5.3). The results indicated again that the dry coated powders had a lower tabletability than the Prosolv and the Avicel controls used. As tabletability is a measure of both the compressibility and compactability of the material, it was expected that the tabletability would have been reduced as a consequence of the reduced bonding strength of the dry coated powders. As mentioned above, this reduction in bonding strength wasn't a major issue as the tablets that were being produced still had a mechanical strength of a very high magnitude at low compaction forces for both particle sizes investigated. However it was seen that the addition of the silica to the surface of the MCC did produce a notable reduction in the tabletability of the dry coated powders, as the tensile strength of the compacts for both Prosolv and the Avicel control were higher at each of the compaction pressures used.

5.3.3 Effect of the Addition of the non-compressible API Metformin Hydrochloride

In this section the effect of the addition of 40% of the non-compressible API metformin was assessed, alongside two different loads of the MCC/silica preblends. The first preblend load of 59.5% w/w (displayed as blue bars throughout the results below) assessed effect of the MCC/silica alone on tablet properties of an API loaded tablet and the second preblend load of 29.5% w/w, alongside 30% w/w of mannitol, allowed assessment of the preblend in a powder with not only a non-compressible API, but also a brittle fragmenting excipient.

In terms of the flow of the API loaded powders, it was observed that a similar pattern to the 100% preblend formulations was obtained. The PH101 dry coated powder had a very similar flow to Prosolv, however the PH102 dry coated powder with the metformin produced a more flowable preblend (as shown in Figure 5.15 and 5.16 respectively). Although the flow did worsen with the addition of API, it

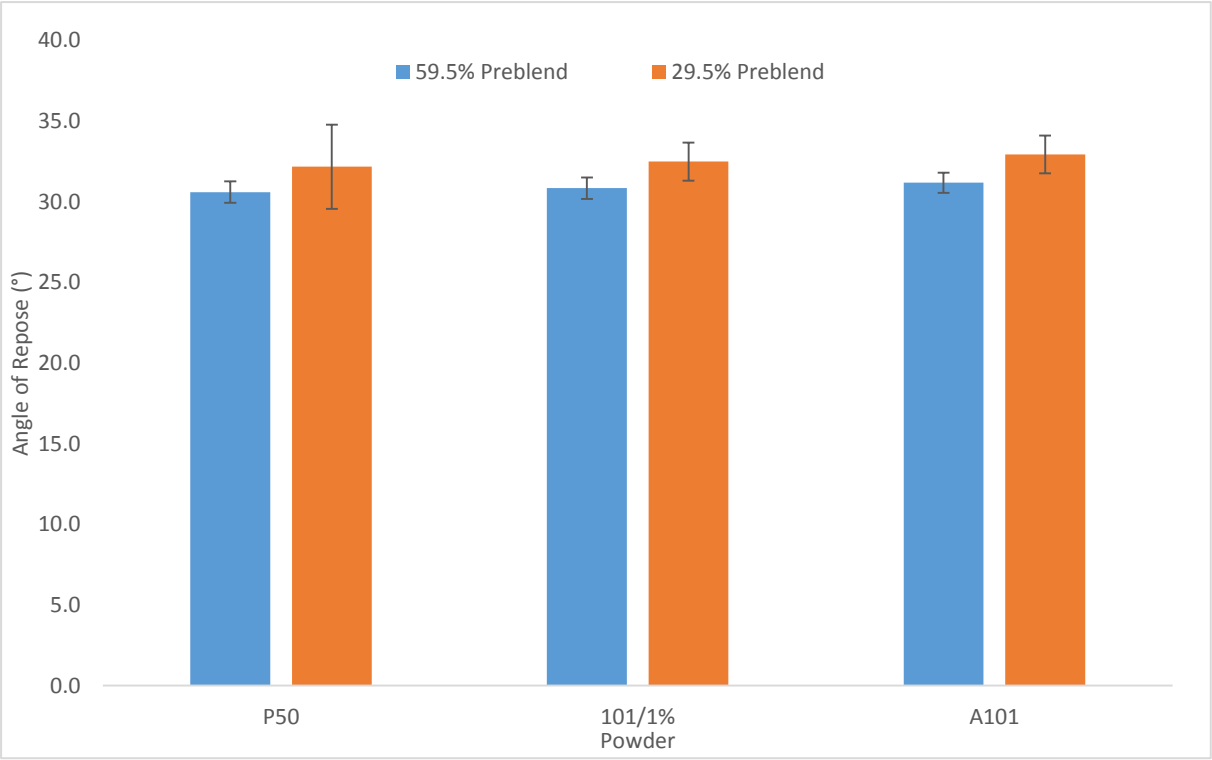

Figure 5.15: A graph showing the powder flow through angle of repose of the API loaded Prosolv P50 and Avicel PH101 dry coated powders/control, with very little difference observed between the flow of the powders at both preblend loads (n=3, p>0.05).

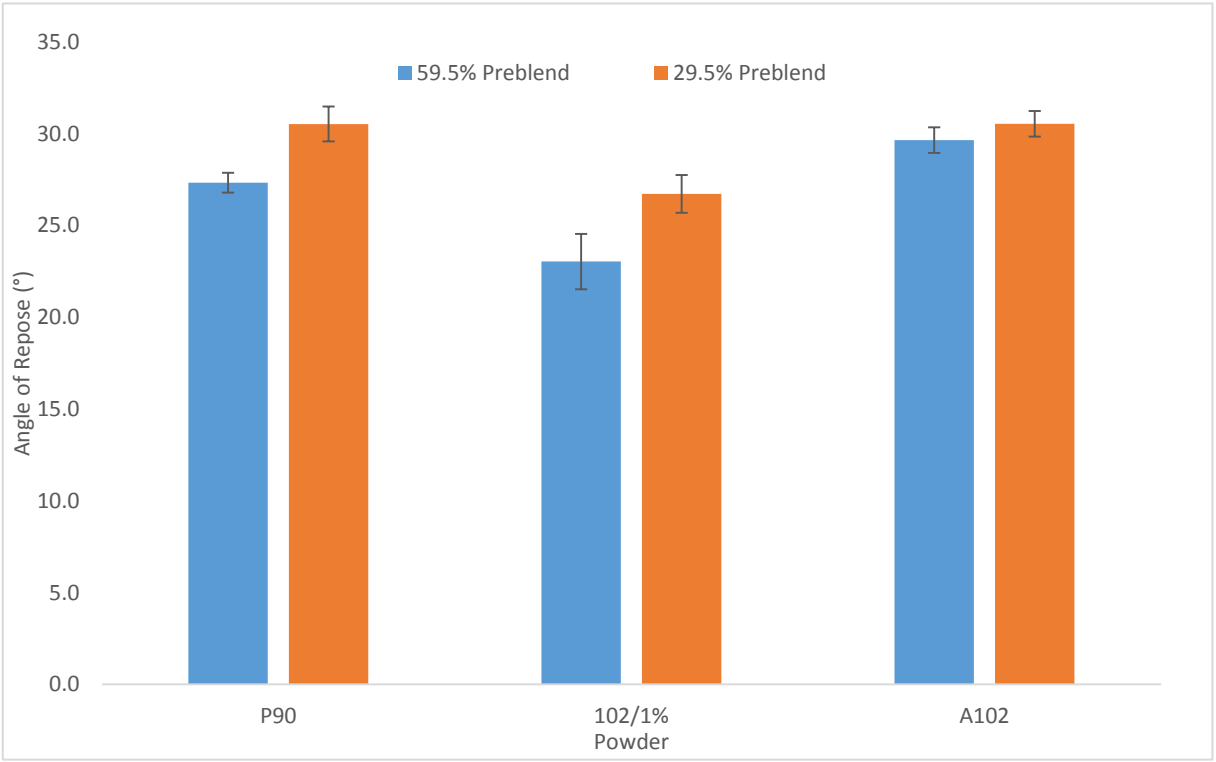

Figure 5.16: A graph showing the powder flow through angle of repose of the API loaded Prosolv P90 and Avicel PH102 dry coated powders/control, dry coated Avicel PH102 showing an improvement in flow compared to both the Prosolv P90 and Avicel control for both preblend loads (n=3, p<0.05).

still remained within a very flowable range and would pass the flowability test for production on a large scale. It was observed that the addition of mannitol to the powder blend worsened the flow in all cases. This was expected as mannitol is a needle shaped particle that had a tendency to interlock and segregate, which negatively impacted the flowing nature of the powder. However in all cases the powder flowed well, and would have been acceptable to scale up in terms of its flowability.

Figures 5.17-5.18 display the hardness and disintegration time of tablets compressed at 75 MPa, with Table 5.4 showing friability and porosity results from the drug loaded preblends investigated in this study. Result patterns were again very similar to the unloaded preblends that were investigated, with the hardness being significantly higher with Prosolv (both grades) especially at the 59.5% preblend load, with little difference observed between the tablets manufactured with the 29.5% preblend,

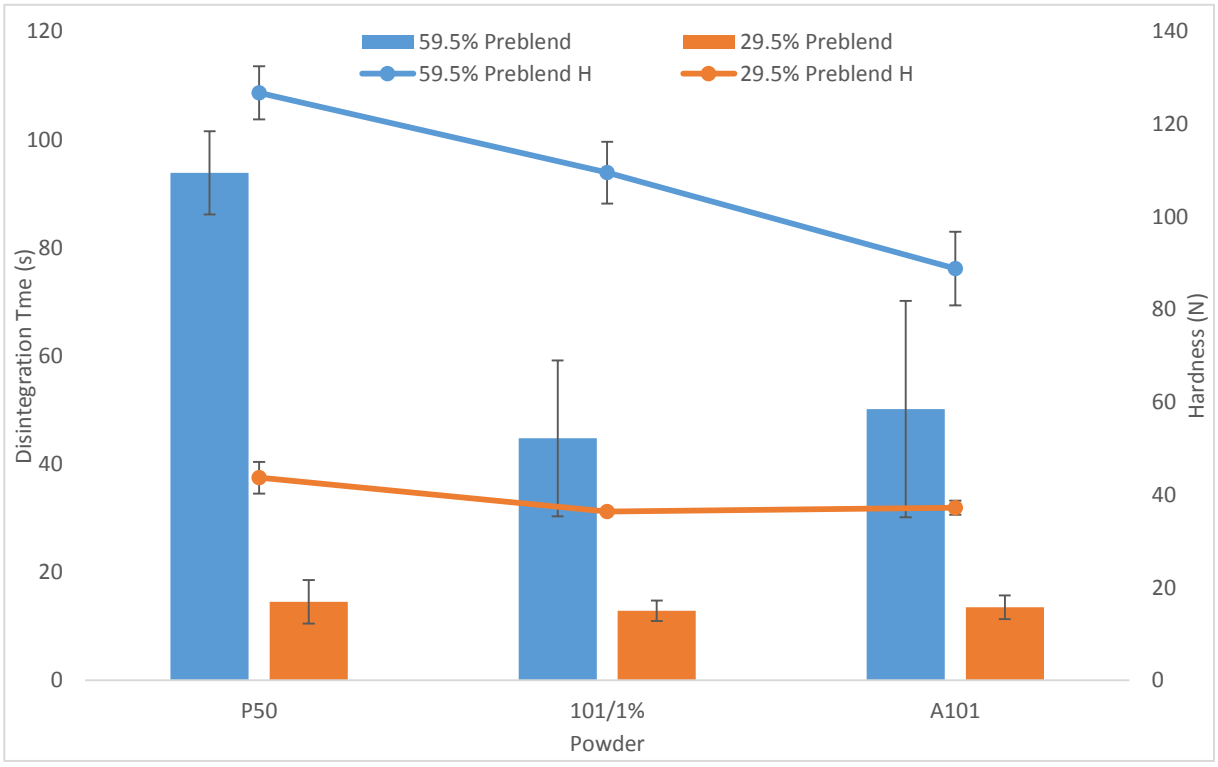

Figure 5.17: A graph showing the disintegration time and hardness of tablets compressed at 75 MPa produced from the API loaded Prosolv P50/Avicel PH101 dry coated powders investigated in this study, with disintegration time displayed on the bars and hardness on the line. Results indicated that hardness for Prosolv was improved over the Avicel PH101 dry coated powder and control ($n=3$, $p<0.05$) at 59.5% preblend load, with little difference observed at 29.5% preblend load ($n=3$, $p>0.05$). However disintegration time was markedly improved for the dry coated powder over the Prosolv ($n=3$, $p<0.05$) at the 59.5% preblend load, again with little difference seen at the 29.5% preblend load ($n=3$, $p>0.05$).

load, with little difference observed between the tablets manufactured with the 29.5% preblend, whereby the mechanical strength was quite low, due to the inclusion of mannitol which fragments during compression, causing high die wall interactions and therefore weak bonding within the tablet structure (Koner *et al*., 2015). The higher hardness of the Prosolv grades was partly attributed to its higher bulk density leading to improved packing properties of the particles and therefore the ability to form stronger bonds (Luukkonen *et al*., 1999, van Veen *et al*., 2005). Another key factor observed here was that Prosolv was much harder than the Avicel uncoated grades, as well as the dry coated grades. The difference for the dry coated blends was that the silica film around the particles possibly reduced the levels of interparticle bonding, whereas for Prosolv the silica was embedded into the surface, and therefore tablets of a lower hardness were manufactured. However in terms of the big difference between the uncoated MCC and Prosolv, this was far more evident with API than the tablets

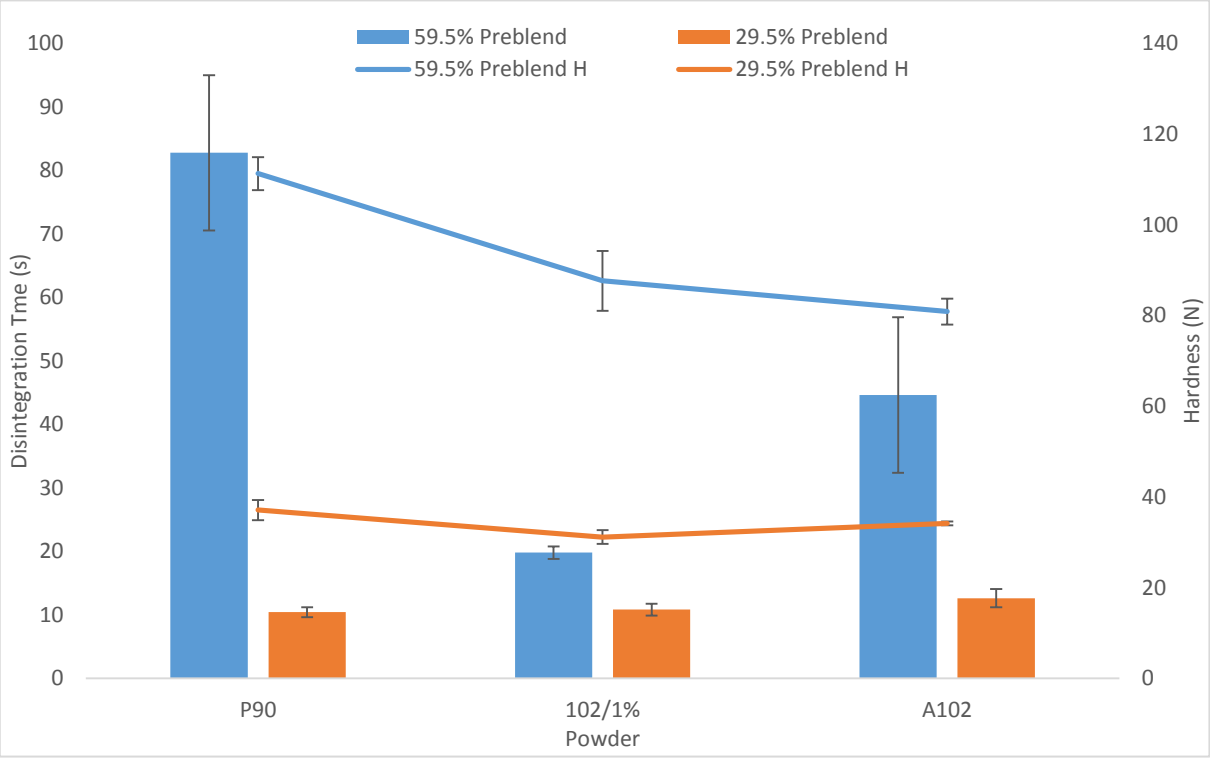

Figure 5.18: A graph showing the disintegration time and hardness of tablets compressed at 75 MPa produced from the API loaded Prosolv P90/Avicel PH102 dry coated powders investigated in this study, with disintegration time displayed on the bars and hardness on the line. Results indicated that hardness for Prosolv was improved over the Avicel PH102 dry coated powder and control (n=3, $p<0.05$) at 59.5% preblend load, with little difference observed at 29.5% preblend load (n=3, $p>0.05$). However disintegration time was markedly improved for the dry coated powder over the Prosolv (n=3, $p<0.05$) at the 59.5% preblend load, again with little difference seen at the 29.5% preblend load (n=3, $p>0.05$).

Table 5.4: A table showing the friability and porosity results for the API loaded powders of Prosolv and the respective Avicel dry coated powders, with friability being similar with the Prosolv P50 and PH101 results at 59.5% preblend load, however PH102 dry coated tablets have higher friability compared to Prosolv P90 at 59.5% preblend load. Friability is well above threshold for the 29.5% preblend loaded powders, due to low mechanical strength of tablets. Porosity results indicated no significant differences between the Prosolv grades for either particle size compared to the dry coated powders, however compared to the Avicel controls for each of the powders the porosity of the dry coated powder tended to be higher. Data significantly different is marked with an asterisk (*) (n=3, $p<0.05$).

Powder	Friability (%)		Porosity	
	59.5% Preblend	29.5% Preblend	59.5% Preblend	29.5% Preblend
Prosolv P50	0.890	3.574	0.174 ± 0.014	0.178 ± 0.019
Avicel PH101 / 1%	0.788	4.803	0.183 ± 0.031	0.174 ± 0.017
Avicel PH101	1.465	4.808	0.150 ± 0.015	0.113 ± 0.015*
Prosolv P90	1.125	5.218	0.183 ± 0.007	0.156 ± 0.001
Avicel PH102 / 1%	2.280	3.248	0.157 ± 0.010	0.143 ± 0.027
Avicel PH102	2.026	5.035	0.109 ± 0.010*	0.109 ± 0.010

without API. This was attributed to the fact that unsilicified MCC was known to be lubricant sensitive (Zuurman *et al*., 1999). Also visualised on the SEM images (Figure 5.3) was the Prosolv grades having a far rougher particle surface, which was also observed in previous studies where the Prosolv grades had a specific surface area about 5 times greater than Avicel (Luukkonen *et al*., 1999). This surface roughness was attributed to texturisation of the MCC by the silica, occurring during the pre-processing of the excipient (Tobyn *et al*., 1998). This led to increased levels of mechanical interlocking between adjacent Prosolv particles leading to strong interparticle attraction, which resulted in low levels of tablet relaxation during compression and therefore tablets of a higher hardness being produced (Al-khattawi *et al*., 2014, van der Voort Maarschalk *et al*., 1996). The study by van Veen *et al*. (2005) also demonstrated that in the presence of magnesium stearate, the hardness of tablets containing unsilicified MCC was much lower than the Prosolv grades, due to the increased relaxation time after compression, which was the same pattern observed with the uncoated Avicel as well as the dry coated

MCC. This resulted in an overall lower hardness of the tablets containing Avicel compared to Prosolv. The reduction in strength of the uncoated Avicel compared to the Prosolv was advantageous for the dry coated blend. It had been observed in previous work that uncoated MCC was lubricant sensitive (Zuurman *et al*., 1999), highlighted by the massive reduction in hardness compared to Prosolv from the blend manufactured with 100% preblend (Figures 5.7 and 5.8) compared to blends containing magnesium stearate and the API (Figures 5.17 and 5.18). The dry coated MCC maintained a similar difference to Prosolv, and at a preblend load of 59.5% had a higher hardness than the uncoated MCC for both particle sizes. This showed that the dry coated powders had reduced in lubricant sensitivity, and possessed this advantage over the uncoated MCC, as hardness of the compacts was not reduced as significantly in the presence of lubricant.

Disintegration time was observed to be better with the dry coated preblend tablets, similar to the results above for the blends without API. This was particularly evident with PH102 tablets, where the disintegration time of the tablets at a 59.5% preblend load was as low as 20 s, indicating that the dry coated powder provided clear benefits in terms of disintegration. At the low preblend load of 29.5% across both grades, no statistically different disintegration data was observed ($p>0.05$). Interestingly with the inclusion of API the porosity of the uncoated MCC dropped below that of the dry coated powder with both PH101 and PH102 (shown in Table 5.4), which explained the improved disintegration time of the tablets manufactured from the dry coated powder. The reduced disintegration time of the tablets containing the unsilicifed MCC (Avicel) was due to the Prosolv having slow disintegrating properties, due to the silica acting as a barrier to water uptake into the tablet, as was seen with the blends with the absence of API (Kachrimanis *et al*., 2003).

5.4 Conclusion

From the results in this study it can be concluded that dry coated composite particles of silica and MCC provided positive results giving a free flowing powder with high mechanical strength and faster disintegration time. Although tablet hardness, both with and without API was reduced compared to Prosolv, it still remained very compressible even at very low compression forces. It was less lubricant sensitive than the uncoated Avicel, and therefore provided powders that remained highly compressible after mixing with magnesium stearate and API. A fairly high drug load of the non-compressible API metformin was used, and using a preblend concentration of 59.5% provided tablets of a sufficient mechanical strength. However the key advantage of the dry coated particles was that it retained the very good disintegrating properties of the uncoated MCC. Disintegration times were significantly lower than the Prosolv grades at both sizes, showing that the tablets were disintegrating more rapidly with dry coated powders compared to the pre-processed Prosolv. Flow was also improved for the dry coated particles, particularly with the PH102 MCC compared to the Prosolv P90, due to the surface coverage of the silica resulting in a higher reduction in the frictional forces between particles, giving a better bulk flow of the powder. Compression profiles of the powder also indicated that although bond strength did decrease when dry coating MCC, this wasn't an issue as the resulting hardness of the tablets was still very high. More importantly compressibility of the MCC was retained, with compressibility remaining very similar between dry coated MCC and the Prosolv/Avicel control for both particle sizes investigated.

Therefore it can be established that the dry coated powders provide an alternative advantage over Prosolv. Disintegration of the dry coated powders was rapid, very similar to uncoated MCC, whilst having an improved powder flow and reduced lubricant sensitivity compared to the Avicel control. Dry coating provided a suitable alternative to Prosolv, whilst being produced in a one stop environmentally friendly processing condition, whereby MCC and silica were not exposed to any chemicals or physical alteration.

Chapter 6

Conceptualisation, Development and Fabrication of a Novel Disintegration Tester Designed Specifically for Orally Disintegrating Tablets

6.1 Introduction

To ensure an ODT is fit for purpose the undertaking of characterisation assessments is vital. Among the assessments conducted, disintegration time is one of the most essential testing methods to ensure that the ODT disintegrates within the recommended FDA time of 30 seconds (FDA, 2008) or European Pharmacopoeia time of 3 minutes (Ph.Eur, 2013), with the dosage form designed to disperse/disintegrate on the tongue.

The currently recommended ODT disintegration test is the US FDA standard disintegration test for solid oral dosage forms, as shown in Figure 6.1. This test consists of a basket rack attached to a rod which oscillates vertically and a beaker filled with disintegration medium, which is placed beneath the basket assembly and kept at 37 °C. The basket is immersed into the disintegration medium at a frequency of between 29-32 cycles per minute through a distance of around 53 mm to allow tablet disintegration to take place. The basket is made up of 6 disintegration vessels with a wire mesh at the bottom (with holes of between 1.8 mm-2.2 mm), and disintegration time is measured once all

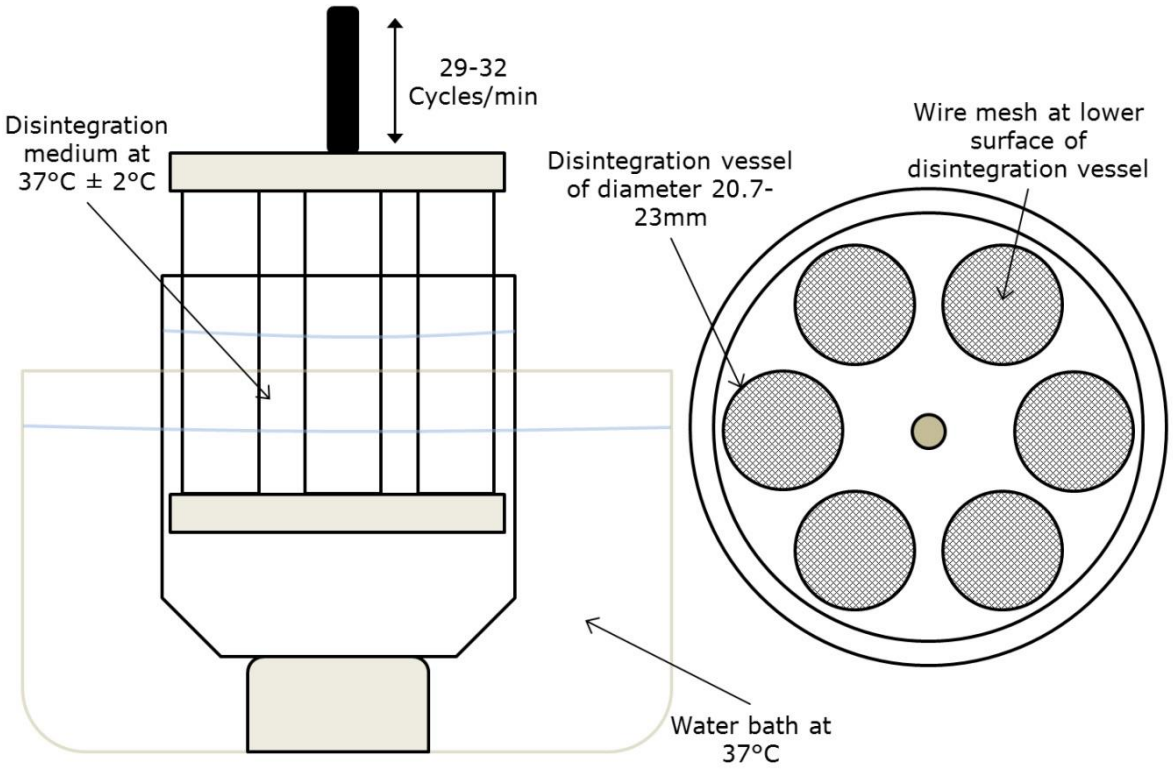

Figure 6.1: A diagram illustrating a typical set up for the standard USP disintegration test for solid oral dosage forms, that is utilised for ODT disintegration testing. It shows how the basket would typically by placed within the beaker/water bath, and how the dissolution vessels are arranged within the basket.

fragments of the oral dosage form have passed through the wire mesh. A disk can be placed on top of the oral dosage form, but for ODT testing this is not usually utilised (USP, 2008).

However *In Vivo*, an ODT would be placed on to the tongue of the patient and then subsequently disperse/disintegrate through interaction with the saliva present within the oral cavity. As the tablet is placed in the mouth, and the mouth closed, there would be interactions between the ODT and the upper palate, as well as a controlled temperature of around 37 °C (Moore *et al*., 1999), and relative humidity of around 90-95% (Mathias *et al*., 2010). These conditions would aid in the disintegration of the ODT, as the high humidity and temperature would promote further moisture uptake into the tablet and the pressing of the upper palate would aid in the breakdown of the tablet.

The process of taking an ODT requires no water to be consumed as the dosage form disintegration within the mouth allowing it to be swallowed easily. Having examined the *In Vivo* conditions, it can be seen that the current recommended USP disintegration test does not bare resemblance to the *In Vivo* conditions. The standard test uses a large volume of disintegration medium, and the dosage form disintegrates within the oscillating vessel, which would be similar/correlate more to the disintegration of a conventional tablet that is swallowed with water and disintegrates within the stomach. Also the time taken for disintegration is measured when the last fragment of the tablet has passed through the wire mesh at the bottom of the vessel, which does not necessarily relate to the time taken for the ODT to disintegrate within the oral cavity, and is subsequently ready to swallow.

This highlights a significant gap in the market regarding a disintegration test specifically for ODT's. The USP guidance for "ODTs in industry" specifies that an improvised test can be developed and used for measuring the disintegration time of the ODT providing results are equivalent to the USP method as well as correlating with *In Vivo* conditions (FDA, 2008). Previous efforts have been made at conducting an *In Vivo* relevant/correlating test, with methods ranging from the fabrication of tailored equipment (Yoshita *et al*., 2013, Harada *et al*., 2006, Uchida *et al*., 2013, Hermes, 2012), to improvised methods that are developed using currently available lab equipment (Kakutani *et al*., 2010, Bi *et al*., 1996, Dor

and Fix, 2000, el-Arini and Clas, 2002, Abdelbary *et al*., 2005, Park *et al*., 2008, Morita *et al*., 2002, Kondo *et al*., 2012) . However tests that have been developed use conditions that are still not entirely representative of *In Vivo* conditions (refer to Table 1.2 in Chapter 1), with methods using varying conditions to achieve ODT disintegration. The previous work, although successful in providing new methods of ODT disintegration time data gathering, has limited data regarding *In Vitro In Vivo* Correlation, and therefore further support is needed to assess the validity of the tests in representing real ODT disintegration time.

This study was therefore designed to develop and conceptualise a new ODT disintegration test which was not only representative of *In Vivo* conditions, but also correlated with *In Vivo* results. Various phases of development of the tester were conducted, and results from the final design were compared to an *In Vivo* ODT disintegration time study to assess whether the proposed ODT disintegration test was a valid and true in representation of real ODT disintegration times.

6.1.1 Proposed Design

The method for disintegration time was developed throughout three phases. Distance/time plots were able to distinguish between different types of ODTs, as well as not allowing a standard release tablet to disintegrate. The thorough literature review had highlighted key areas that were needed to obtain a tester that gave conditions that were representative of the oral cavity. These were:

- Temperature of 37 °C
- Humidity of 90-95%
- Disintegration medium flow of up to 10 ml/min
- Minor manipulation of the tablet bed representing contact and manoeuvring of the tablet by the upper palate

A proposed design for the disintegration tester was drawn up, as shown in Figure 6.2. The chamber was designed to maintain a constant temperature and humidity according to the conditions above. The silicon tubing was designed with perforations in the zone where the tablet would make contact, this would allow the disintegration medium to flow from underneath and spread over the surface. The

tablet probe would start outside the chamber and the tablet would be attached to the probe. The probe would enter the chamber at a predetermined speed and come into contact with the silicon tubing, where the predefined force would be applied on to the tablet and chamber would move laterally, mimicking the action of the upper palate. The probe would be attached to software that would draw the distance time plot required for defining the disintegration time. An area for collection of the disintegrating fragments from the tablet could also be added, and assayed, possibly in line, to assess the leakage of the drug in the oral cavity.

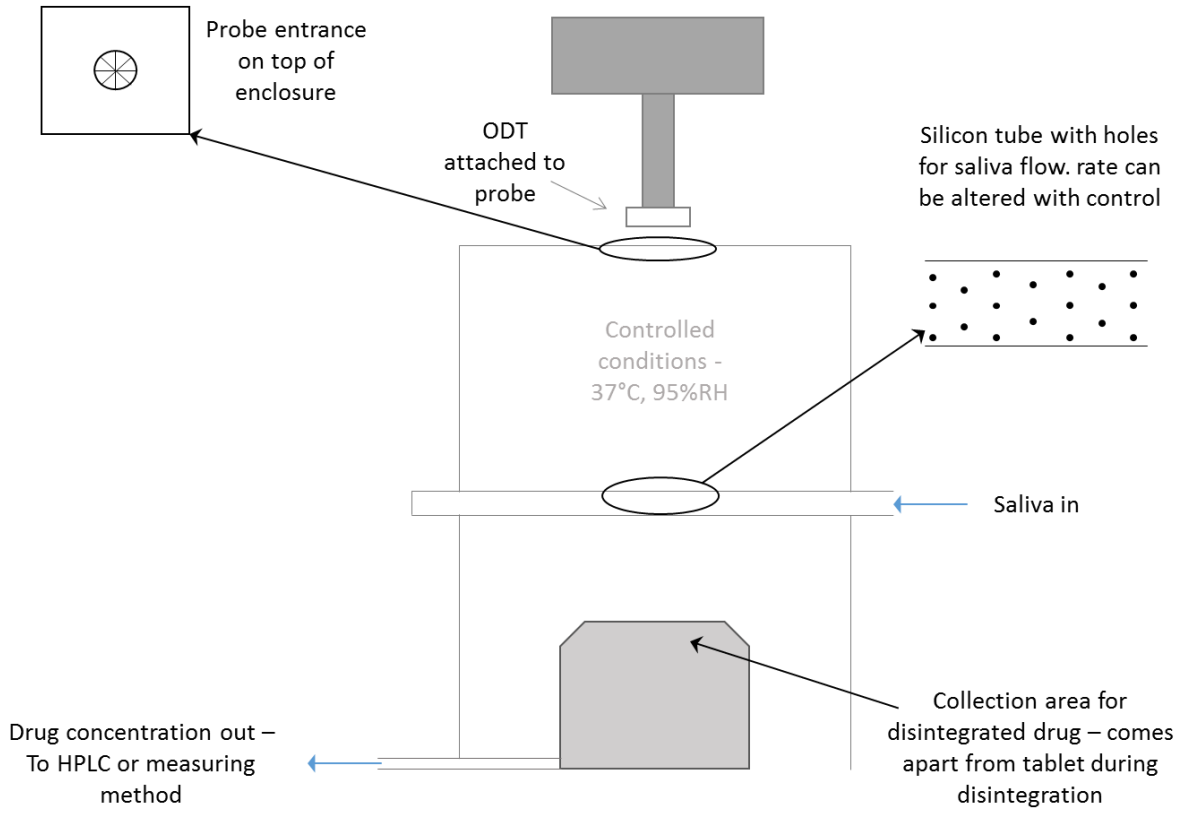

Figure 6.2: A schematic diagram showing the proposed design of the specific disintegration tester for ODTs, comprising of conditions representative of the oral cavity, including temperature/humidity, disintegration medium flow rate and applied pressure on the tablet. An area for collection of the disintegrating fragments from the tablet could also be added to assess drug leakage/absorption in the mouth.

6.2 Materials and Methods

This study was split into two different stages: 1 – Testing of the new disintegration tester, comparing results from tablet properties to the standard USP test; 2 – An *In Vivo* study to gather a correlation of *In Vivo* results to be compared against the newly developed tester and the standard USP test.

6.2.1 Materials

Nurofen Meltlets, from Reckitt Benckiser (Slough, UK) were utilised as a commercially available ODT and standard release paracetamol, from Wockhardt (Wrexham, UK), was also used for disintegration testing.

Materials for ODT preparation included D-mannitol (Sigma-Aldrich, Dorset, UK), MCC (Avicel PH102, FMC Biopolymer, Philadelphia, USA), Starch 1500® (Colorcon Inc., Harleysville, USA), crospovidone (Kollidon CL, BASF, Ludwigshafen, Germany), Pearlitol Flash® (Roquette, Lestrem France), sodium stearyl fumarate (Alubra®, FMC Biopolymer, Philadelphia, USA) and magnesium stearate (Fischer Scientific, Loughborough, UK). Additionally, HPMC (Methocel K100M, Colorcon Inc., Harleysville, USA) was used for matrix tablet production.

6.2.2 Validation of Disintegration using Newly Developed Disintegration Tester

Several different tablets were tested in this stage. Two commercially available tablets were tested, an ODT formulation, Nurofen Meltlet® and a standard release paracetamol were used as GMP tablets in the tester. Five sets of tablets were manufactured in the laboratory to test time sensitivity within the newly developed disintegration tester, four ODTs compacted at different compression forces and a controlled release matrix tablet were manufactured.

6.2.2.1 Tablet Preparation

The lab based ODTs tested in this study were composed of 60% D-mannitol, 35% MCC, 4% crospovidone as the main tablet excipients and 1% magnesium stearate as a lubricant. All excipients, except magnesium stearate were manually blended for 10 mins to achieve a uniform powder blend, and then magnesium stearate added and mixed for a further minute. Individual 500 mg portions of

powder were weighed and compressed using a Specac semi-automatic hydraulic press (Slough, UK) equipped with 13 mm flat faced punches. Four compression forces were chosen to allow the sensitivity of the disintegration tester to be analysed, these ranged from 75 MPa to 300 MPa.

The controlled release matrix tablets were composed of 40% HPMC, 40% MCC, 19% d-mannitol and 1% magnesium stearate. All the excipients, except magnesium stearate, were manually blended for 10 mins to achieve a uniform powder blend, and then the magnesium stearate was added and mixed for a further minute. The powders were individually weighed to 500 mg, and tableted using the Specac semi-automatic hydraulic press (Slough, UK), with the same 13 mm flat faced punches as above. These were compressed at a compression force of 225 MPa.

6.2.2.2 New Disintegration Test

A new disintegration test apparatus was developed in the laboratory, according to the proposed drawing in Figure 6.2, which was designed to mimic conditions encountered in the oral cavity, and intended to be a more representative measure of ODT disintegration time, shown in Figure 6.3.The test housing is placed on top of a hot plate, which is set to an optimised temperature designed to achieve a constant temperature of 37±1 °C within the compartment, similar to *In Vivo* conditions (Moore *et al*., 1999). The test housing contains a specific amount of potassium chloride (Sigma-Aldrich,

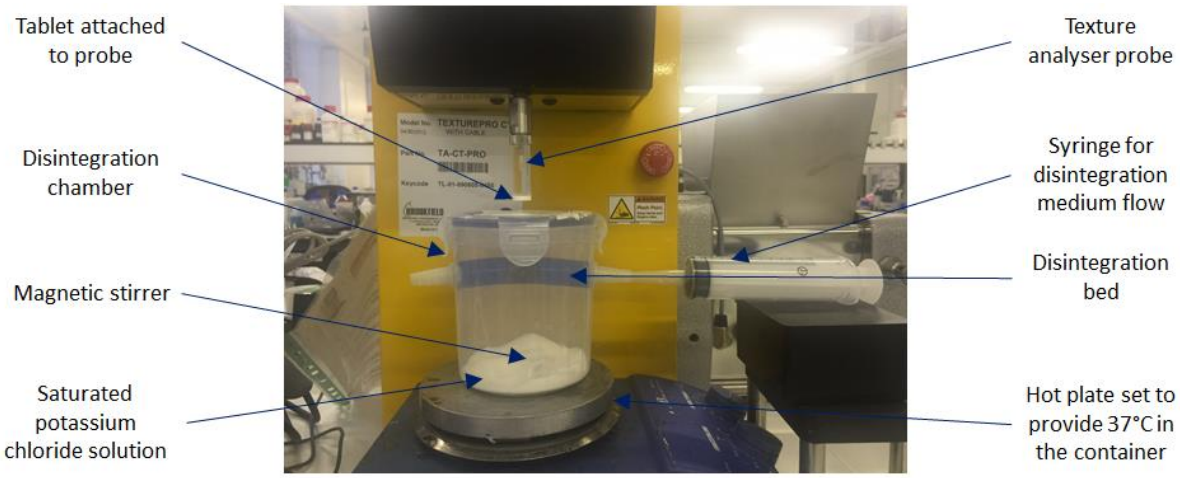

Figure 6.3: Diagram of the setup of the new disintegration tester, highlight all key components of the equipment. The texture analyser probe comes through an entrance at the top of the container which has been cut out and covered with silicon sheeting to allow humidity and temperature to be retained but still allow the probe to enter without triggering the texture analyser probe.

Dorset, UK) which is used to form a saturated salt solution, and gives a relative humidity of approximately 93±3% in the enclosed container, similar to those conditions encountered in the oral cavity (Saraiva *et al*., 2015). The disintegration bed was a silicone pipe that had been slightly flattened, with an area under where the tablet would disintegrate having small 4 mm holes embedded to allow water/saliva to flow through. This flow of saliva would interact with the tablet and cause subsequent disintegration alongside the simulated *In Vivo* conditions. The chosen flow rate of saliva was 10 ml/min, as previous work had shown that this amount of liquid allowed a consistent disintegration of the tablet.

The disintegration compartment was placed under the probe of a texture analyser (Brookfield Engineering's CT3 Texture Analyser, Harlow, UK), set at speed of 2 mm/s. The tablet was adhered to the probe with double sided sticky tape. Once the tablet came into contact with the disintegration bed, the probe was set to apply a fixed 50 g weight for a set amount of time, similar to texture analyser methods described previously (Abdelbary *et al*., 2005, el-Arini and Clas, 2002). A distance against time plot would be drawn up and allow disintegration time to be calculated based on the plot plateauing when the tablet came into contact with the disintegration bed. All tablets in this stage were tested eight times and analysed using Brookfield's Texture Pro CT (Brookfield Engineering, Harlow, UK), and data presented as mean ± SD.

6.2.2.3 USP Disintegration Test

The standard USP disintegration method was also used to assess disintegration time of the tablets to allow a comparison to the newly developed test (USP37, 2014b). A Copley ZT41 disintegration apparatus (Nottingham, UK) was used, with a single tablet being tested each time for accuracy. Each tablet was placed in the vessel (without a disk) and oscillated at 30 cycles per minute. A dissolution medium of 800 ml distilled water was maintained at 37°C, and disintegration time measured when all of the fragments of tablet had passed through the mesh at the bottom of the vessel. All readings were taken in triplicate and represented as mean ± SD.

6.2.2.4 Hardness

Hardness of the all the tablets was measured using a Copley TBF 100 Hardness tester (Nottingham, UK). Tensile strength (σ) was then calculated using the equation:

$$\sigma = \frac{2\,H}{\pi\,D\,T} \qquad \text{(Eq. 6.1)}$$

Where H is the hardness, D is the diameter and T is the thickness of the tablet. All readings were taken in triplicate and displayed as mean ± SD.

6.2.2.5 Porosity

Porosity of the tablets was assessed using a Quantachrome Helium Multipycnometer (Florida, USA). Diameter and thickness of the ODT's was measured using a digital calliper, and the weight of individual ODT's taken using an electronic balance. The bulk volume (V_B) and bulk density (ρ_{bulk}) of the tablets were then calculated using the following equations:

$$V_B = \frac{\pi\,R^2}{T} \qquad \text{(Eq .6.2)}$$

$$\rho_{bulk} = \frac{Tablet\ weight}{V_B} \qquad \text{(Eq . 6.3)}$$

The true volume (V_t) of the tablet was calculated using the pycnometer, which applies the theory of gas displacement allowing the porous nature of the tablet to be assessed. The true volume was calculated using the equation:

$$V_t = V_c - V_r\left(\frac{P1}{P2} - 1\right) \qquad \text{(Eq. 6.4)}$$

Where V_C is the volume of the sample cell, V_r is the volume of the reference cell, P1 and P2 are the atmospheric pressure and pressure change during the measurement respectively. The true volume was then used to calculate true density in the equation:

$$\rho_{true} = \frac{Tablet\ weight}{V_t} \quad \text{(Eq. 6.5)}$$

The final step to calculate porosity (ε) of the ODT used the following equation:

$$\varepsilon = 1 - \frac{\rho_{bulk}}{\rho_{true}} \quad \text{(Eq. 6.6)}$$

6.2.3 In Vivo In Vitro Correlation

6.2.3.1 In Vivo Disintegration Time Assessment

In Vivo disintegration time was investigated using nine different types of tablets across 35 participants. The study design is detailed below.

6.2.3.2 Study Design

The study was subject to Ethics approval from the Aston University Ethics Committee, and gained a favourable opinion letter for commencement of the study based on the Research Protocol, Patient Information Sheet and Patient Consent form. The lead investigator, Jasdip Koner, was also certified in Good Clinical Practice through the NHS.

The study was designed as a single blind study whereby participants were not aware of what tablet they were taking. Each participant was assigned a participant number according to their chosen seat in the study room, which was used by the researchers to assign what tablets they were taking. Participants were required to take a total of six tablets per scheduled study, this involved the participant taking two different tablet formulations in triplicate, however the participant was not privy to this information. Participants followed a set of instructions set out by the research team. The tablets were taken in the defined order set out by the researchers, and times recorded from when the tablet entered the oral cavity to when the participant felt the tablet had disintegrated. Participants were briefed on when end of disintegration should be/feel like. Prior to taking the first tablet participants had to rinse the oral cavity, as well as rinsing at the end of each tablet disintegration and before the start of each test. A wait time of 1-2 mins was advised to allow oral conditions to return to resting state before moving on to the next tablet. Participants measured their own disintegration time using

stop watches, and recorded the time next to which number tablet was taken. The study involved no swallowing of the tablet, with participants informed that all residue was to be removed from the oral cavity. Once all studies had been completed results were collated. No patient demographic data was collected and there was also no patient identifiable data, as participants chose their own number/seat at the study.

6.2.3.3 Participant Recruitment

A total of 35 participants were utilised for the *In Vivo* disintegration time study. Participants were required to commit up to 60 mins for the study. Participants were recruited from Aston University staff, and were subject to inclusion and exclusion criteria to determine eligibility for the study. The volunteers were sent participant information sheets and consent forms prior to the study and allowed to make their own informed decision on whether to take part. All completed consent forms were given to the research team to provide the participants informed consent. Patients were under no obligation to take part and were allowed to withdraw at any time, and also remove their results from the study prior to collection by the research team.

6.2.3.4 Manufacture of Tablets

A total of five different formulations were manufactured, with four formulations compressed at two different compression forces and the final formulation compressed at just one force, the tablet details are highlighted in Table 6.1. Tablets were manufactured with GMP excipients as to ensure safety, although the participants were informed to remove all residue from the mouth after each test. Tablets were composed of Pearlitol Flash (Roquette, Lestrem, France), Starch 1500 (Colorcon Inc., Harleysville, USA) and Magnesium stearate (Fischer Scientific, Loughborough, UK), with compositions also highlighted in Table 6.1. Excipient concentration and compression force was varied to obtain tablets of differing disintegration times, allowing a wide range of times to be compared between the *In Vivo* disintegration times and the times obtained for the *In Vitro* methods.

Table 6.1: Table highlighting tablet formulation details for the 9 batches of tablets utilised in the *In Vivo* disintegration study. Each formulation, except formulation 5, was compressed at two different compression forces to provide tablets of different disintegration times.

Formulation	Batch	Pearlitol Flash (%)	Starch 1500 (%)	Magnesium Stearate (%)	Compression Force (KN)
Formulation 1	B1	99.5	-	0.5	4
	B2				9.5
Formulation 2	B3	89	10	1	9.5
	B4				22
Formulation 3	B5	79	20	1	20
	B5				46
Formulation 4	B7	49.5	49.5	1	26
	B8				57
Formulation 5	B9	24.5	74.5	1	32

Data Analysis

Each tablet batch was assessed 21 times, with seven participants taking a particular tablet batch in triplicate. This was to gather not only inter-person variability but also intra-person variability, whilst also providing a very robust mean value. The data was collated and analysed according to participant means, with outliers highlighted and removed. Data was presented as mean ± SD.

6.2.3.5 In Vitro Tablet Disintegration Time Assessment

The tablet formulations outlined in Table 6.1 were also tested *In Vitro* to allow a comparison to the *In Vivo* disintegration times. The newly developed tester was set up as described above, with the temperature maintained at 37 °C with around 95% humidity. The saliva flow was 10 ml/min and the probe was set to maintain a 50 g load at a speed of 2 mm/s. The tablet was adhered to the probe with double sided sticky tape. The distance against time plot was utilised for the disintegration time. The USP test for disintegration was also conducted, with 800 ml of disintegration medium, maintained at 37 °C used. Each tablet was placed in the vessel (without a disk) and oscillated at 30 cycles per minute. A dissolution medium of 800 ml distilled water was maintained at 37 °C, and disintegration time measured when all of the fragments of tablet had passed through the mesh at the bottom of the vessel. Each tablet batch was repeated in triplicate for each test and data presented as mean ± SD.

6.2.4 Statistical Analysis

One way and two way ANOVA followed by Tukey's and Sidak's multiple comparison post-hoc tests were performed in this study, using GraphPad Prism 6 software (California, USA). For statistical significance a p-value <0.05 was used, and all data was presented as mean ± standard deviation.

6.3 Results and Discussion

6.3.1 Method Development

The fabrication of the final disintegration test set up was developed through several stages, with the initial stages highlighted below.

6.3.1.1 Phase One

An initial design was drawn up and set up as shown in Figure 6.4. This design incorporates a texture analyser (Brookfield CT3, Brookfield Engineering Laboratories, Massachusetts, USA) to apply a load up to 50 g and hold for 60 s. The speed of the probe was set to 1mm/s. Distilled water was used as disintegration medium, and was kept at a constant temperature of 37 ± 2 °C using a hot plate. The disintegration medium was pushed through a peristaltic pump at a flow rate of 2 ml/min to simulate saliva flow. The tubes of the pump were attached to a plate, which contained bovine tongue as a disintegration bed. The plate containing the tongue was placed on top of a heating block maintained at 37 ± 2 °C, and contained 10ml of distilled water to simulate saliva present in the mouth. For this initial test, commercial ODTs, Nurofen Meltlets® (Reckitt Benckiser, Slough, UK), were used, as they have been shown to have a disintegration time around 20 s *In Vivo* (Gryczke *et al*., 2011). The ODT was placed on to the tongue and the texture analyser activated to allow the distance over time plot to be drawn up. This test was repeated in triplicate to gather initial data to relate to literature values. From the results obtained it was seen that there is a clear area where disintegration had occurred and

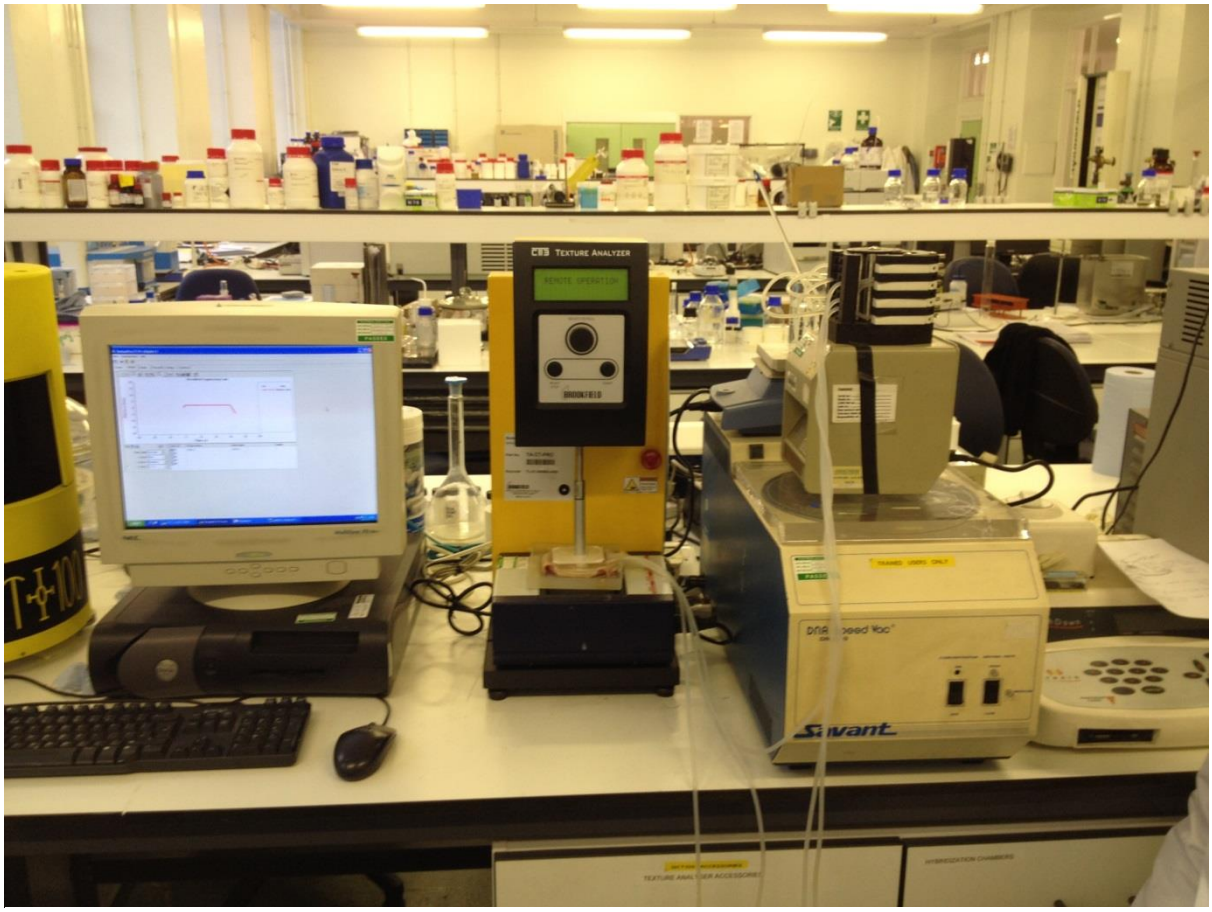

Figure 6.4: An image of Phase One of the modified disintegration test being developed. It shows the texture analyser probe using a large upper palate pressing down on to an ODT which is placed upon the bovine tongue. The heating block maintains tongue temperature at 37 °C, and a hot plate placed behind the peristaltic pump is used to keep saliva at 37 °C.

finished. However the time for disintegration from these results indicated that disintegration was around 3 s, which does not relate to the actual disintegration time of the Nurofen Meltlets®. This showed that the ODT was disintegrating too quickly before the texture analyser came into contact, and in fact the disintegration of the tablet had already occurred before collecting the results. Also another issue with this phase of the equipment was the tongue. When the ODT disintegrated on the tongue, it left a large amount of residue on the surface, which had to be cleaned after each test, and with ongoing tests the residue tended to build up and was more difficult to clean.

However this first test demonstrated that the texture analyser was capable of gathering disintegration time results, and further optimisation was needed.

6.3.1.2 Phase Two

From phase one there were two main developments for phase two of testing. The first change involved the plate and tongue utilised as the disintegration bed; Instead a watch glass containing 10 ml of water was used as the base of the mouth, with filter paper acting as the tongue in this test, as when the paper came into contact with the water it proceeded to get moistened and as the texture analyser pressed down, the water beneath the paper came through and interacted with the side of the tablet which aided disintegration. The other development was regarding the placement of the ODT. Double sided sticky tape was used to attach the tablet to the probe of the texture analyser, as this allowed a start time for disintegration to be established as when the tablet came into contact with the disintegration bed, it would allow full distance/time plot to be drawn up (Figure 6.5). Initial data gathered using this set up ran into complications, as the software for this particular texture analyser

Figure 6.5: An image of Phase Two of the modified disintegration test being developed. It shows the texture analyser probe with an ODT attached by double sided sticky tape. The disintegration bed is a watch glass with 10 ml of water with a piece of filter paper placed on top to simulate the tongue. The heating block maintains temperature at 37 °C, and a hot plate placed behind the peristaltic pump is used to keep saliva at 37 °C**.**

used a target load value, and once that target was reached the hold time started and no further load from the probe was applied, and no further distance data was able to be gathered. This meant that if the ODT was slow disintegrating, a 50 g load was reached very quickly (as the tablet had not had enough time to reach partial/full wetting), and the reading stopped. To overcome this, slower speeds of the probe were used as this would have given the tablet enough time to wet and thus allowed a suitable disintegration plot to be drawn up. An optimum speed of 0.2 mm/s was used in this phase of the test. The Nurofen Meltlets® were again used in this test, as well as some fast disintegrating ODTs manufactured in the laboratory (MCC 40%, Mannitol 55% Crospovidone 4% Magnesium Stearate 1%), all results were taken in triplicate and presented as mean ± SD. Figures 6.6 and 6.7 show the results for these two tablets respectively. For the Nurofen Meltlets® a time of 12.53 ± 5.59 s was obtained clearly showing large deviations. Although the readings for disintegration time became more accurate,

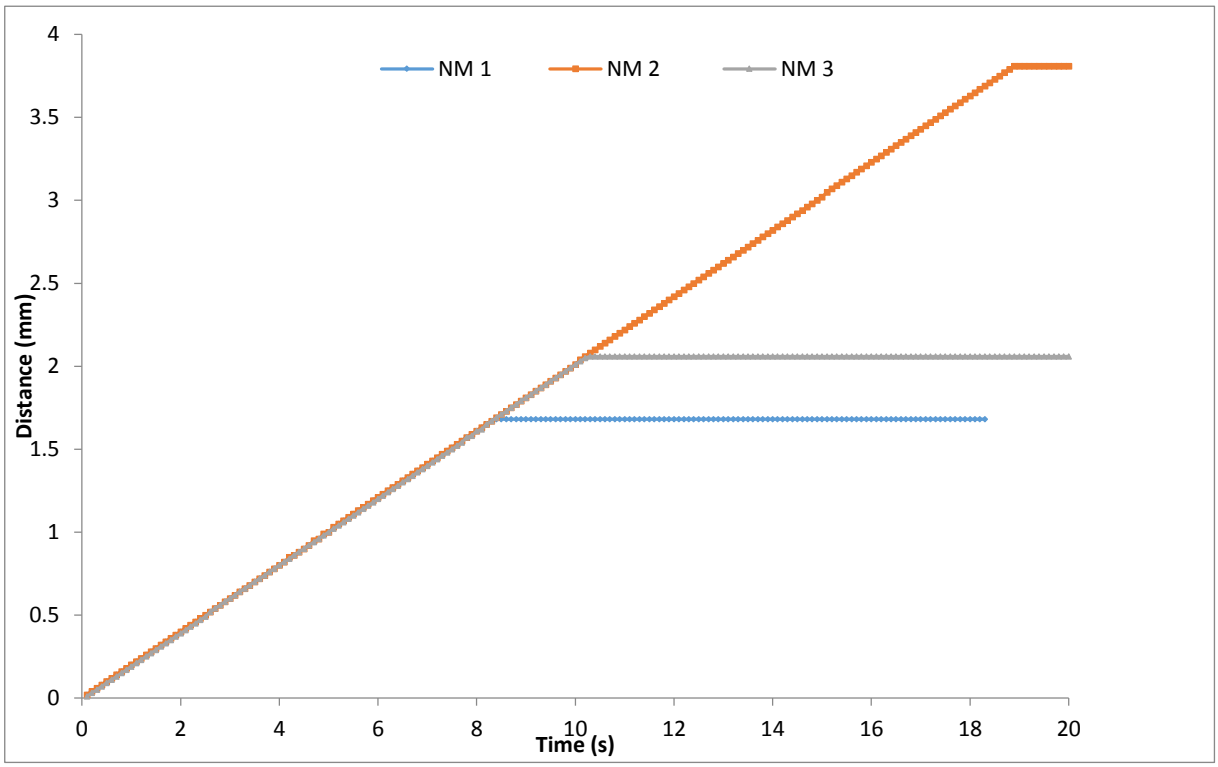

Figure 6.6: A distance versus time plot of the disintegration time of Nurofen Meltlet® tablets obtained using the Phase 2 modified disintegration test (n=3), the plateau represents the end of disintegration.

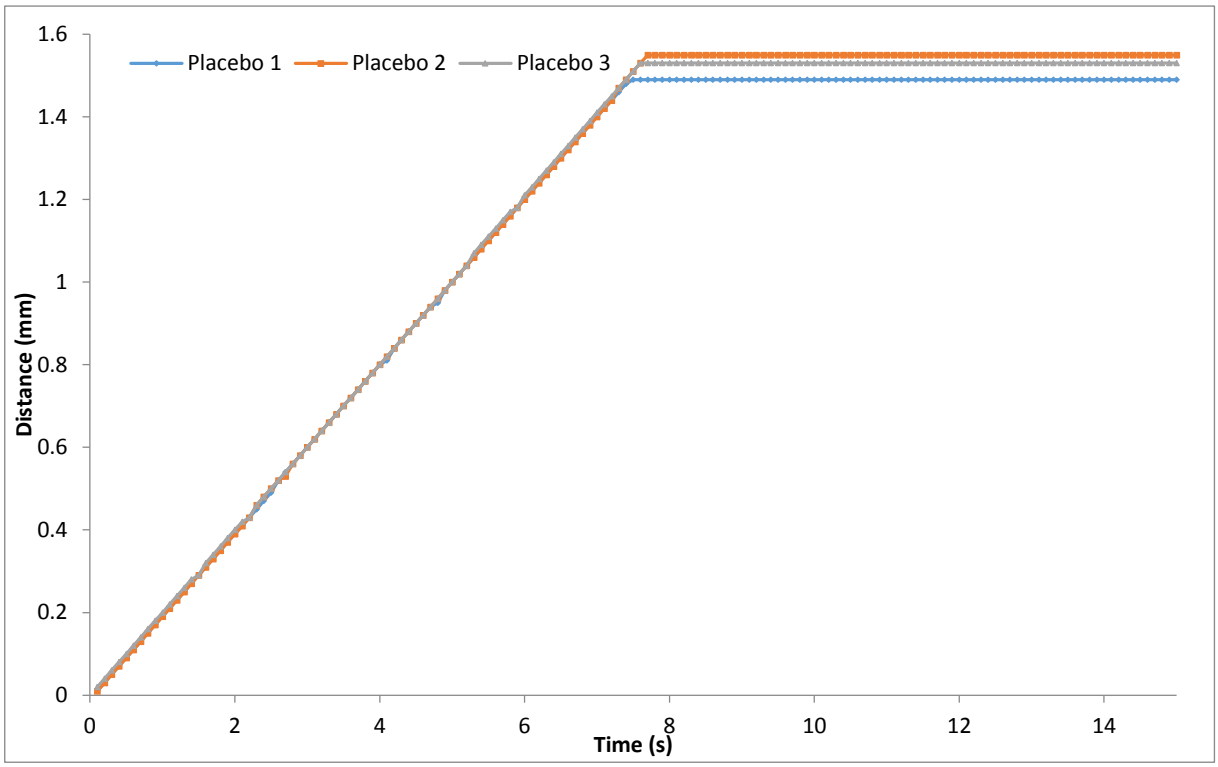

Figure 6.7: A distance versus time plot of the disintegration time of the laboratory manufactured tablets obtained using the Phase 2 modified disintegration test (n=3), the plateau represents the end of disintegration.

as they were closer to the results from the previous study by Gryczke (2011), the test however needed further optimisation for slower disintegration tablets to reduce the deviation as well as provide more accurate results.

6.3.1.3 Phase Three

Before the manufacture of the compartment and development of the design, initial results were obtained using a mechanical tester, MicoTest 5848 (Instron, Buckinghamshire, UK), which was operated using Bluehill 2 software. This work was undertaken to analyse how accurate the distance against time plots were at assessing disintegration time on a very accurate and sensitive machine. This test used a force of 1 N / 100g, which was applied over a predetermined time, which depended on the disintegration of ODT. In the preliminary results, three tablets were tested, a placebo ODT that was rapidly disintegrating and developed in the lab (Pearlitol Flash® 95%, Crospovidone 3.5%, and Alubra® 1.5%), Nurofen® Meltlets and a standard paracetamol tablet. These tablets were chosen to assess the sensitivity of the apparatus and to see how the disintegration times of the tablets affected the resultant plots. The disintegration bed was taken from phase two, with a petri dish which had 10 ml

of water placed in it, a filter paper was placed on top to act as the tongue/bed for disintegration; the filter paper was damp after contact with the water. The results are shown in Figures 6.8-6.10. The disintegration plot on this software had four distinct areas for ODTs. Part 1 of the line was where disintegration started, here the tablet had made contact with the disintegration bed and the load increased from 0 to 1 N. Also the ODT was still hard and had just begun wetting, so the line displayed a reduction in extension as the probe applied constant load and the tablet was not soft enough for the probe to push the distance further. Part 2 of the plot was where water began to ingress into the tablet, so the tablet started to disintegrate and become softer, therefore applying the load of 1 N caused the probe to extend towards the disintegration bed due to the structure of the tablet breaking down and disintegrating. Part 3 of the plot was where the line plateaued, here disintegration of the tablet ended as the probe could not extend past the disintegration bed, therefore the load of 1 N was applied to the petri dish and there was no further movement with the probe. The end of disintegration

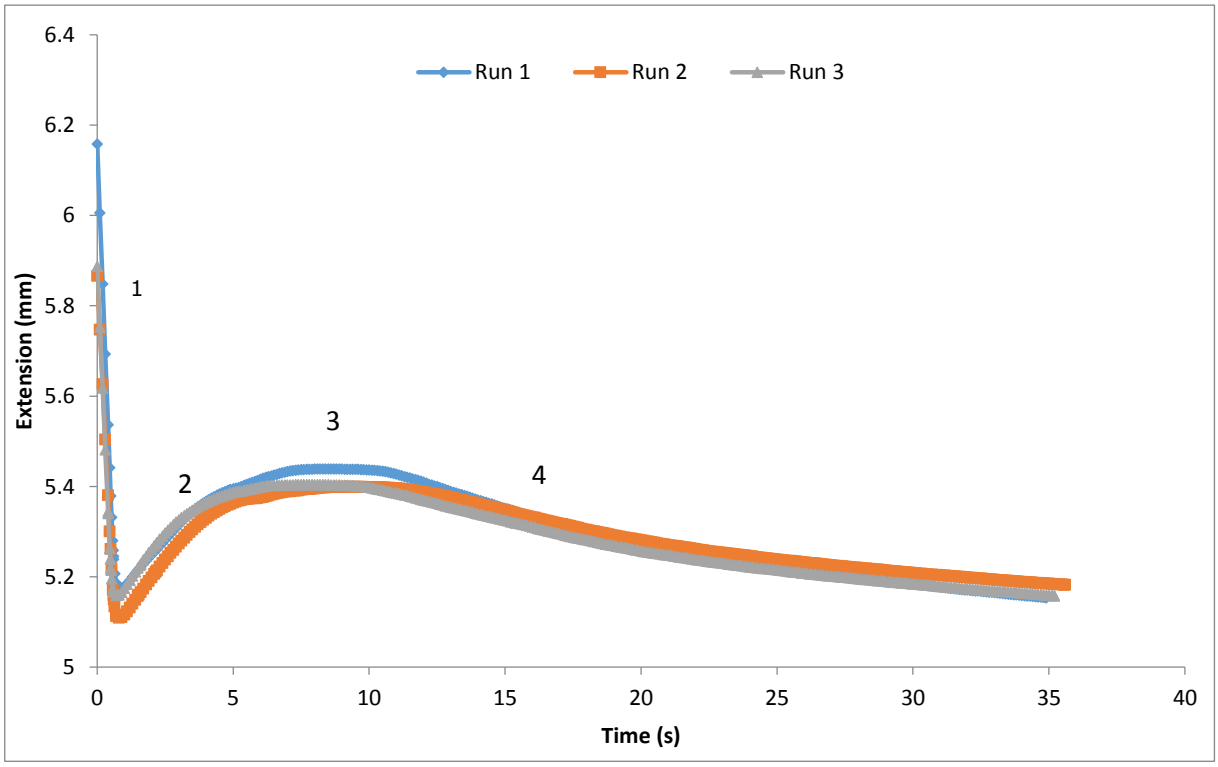

Figure 6.8: Distance against time plot representing disintegration time of placebo ODTs manufactured in the lab (n=3) measured from time 0 to when plot plateaus and starts reducing in extension. Areas 1-4 highlight the different disintegration phases of ODT disintegration.

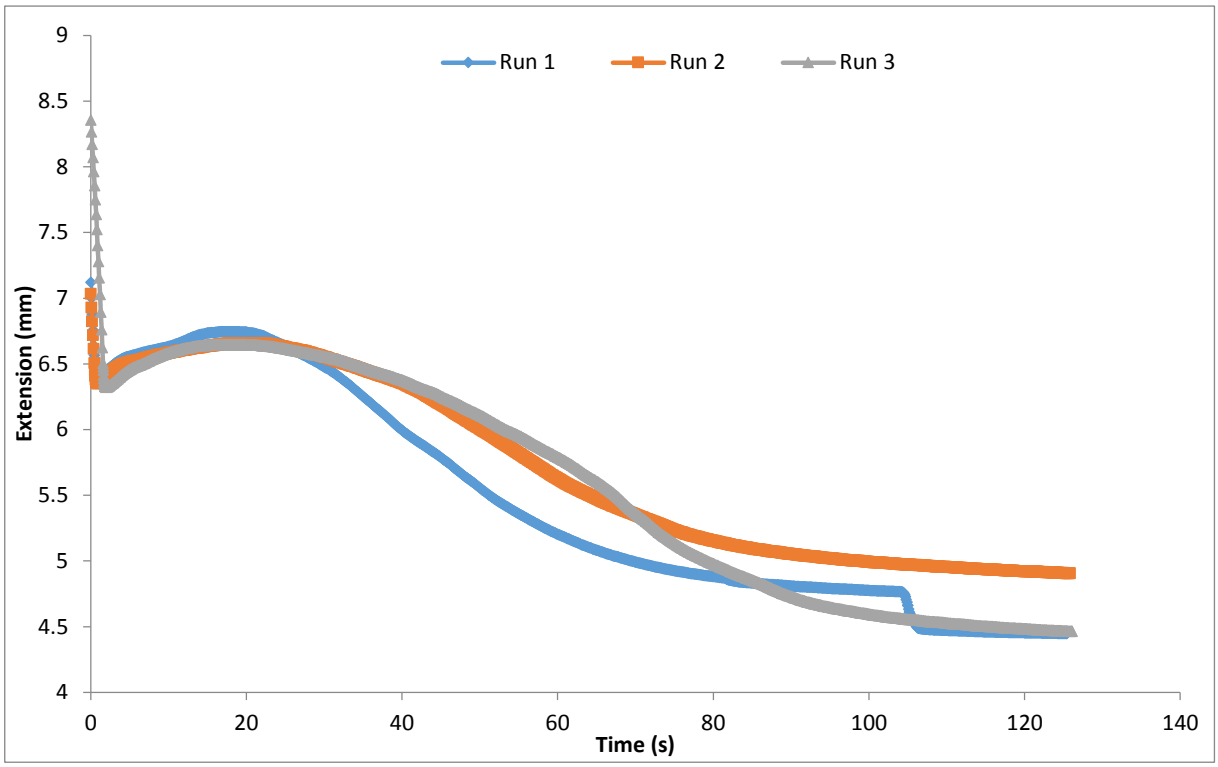

Figure 6.9: Distance against time plot representing disintegration time of Nurofen® Meltlet ODTs (n=3) measured from time 0 to when plot plateaus and starts reducing in extension.

was taken as the last point before the extension started to reduce again after the plateau region. Part 4 represented the region when the probe was at equilibrium and the extension was reduced due to the probe not moving any further distance. These four areas are seen clearly when ODTs were used (Figures 6.8 and 6.9), however when standard paracetamol was used (Figure 6.10) it could be seen that only regions 1 and 2 were present. This indicated that the paracetamol tablet did not disintegrate during this test, and this was also evident when the test had ended, as the tablet remained very hard and only small parts of the tablet had disintegrated during the allotted 180 s. This showed that this test was not be suitable for standard release tablets, but also gave confirmation that the plot represented disintegration time for ODTs at the plateau region. This was because the ODTs had clearly disintegrated visually, whereas the paracetamol tablet visually wasn't close to disintegrating, as the areas that were absent from the plot were regions 3 and 4. This shows that these areas were where the end of disintegration had occurred.

A comparison of the three tablets showed how different the plots were for three types of tablets, which had different disintegration times. It was seen that, as expected, the placebo tablets were much

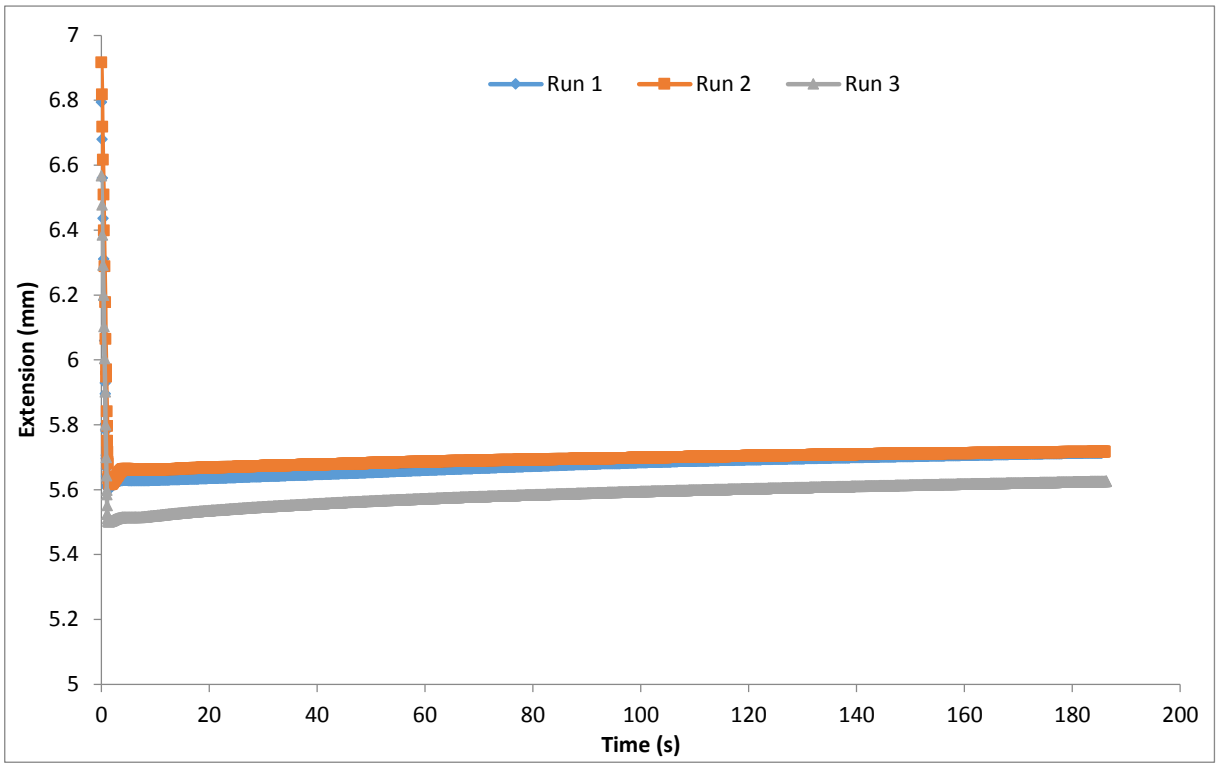

Figure 6.10: Distance against time plot representing disintegration time of standard Paracetamol tablets that are not designed to disintegrate within the oral cavity (n=3) measured from time 0 to when plot plateaus and starts reducing in extension.

faster disintegrating (9.00 ± 0.66 s) than the Nurofen® Meltlet (18.57 ± 16 s) and the standard paracetamol (>180.00 s). The standard paracetamol didn't have a defined disintegration time using this test as this tablet was not designed to disintegrate within the oral cavity. The graphs showed that the Nurofen Meltlet® is the intermediate disintegrating tablet, and the disintegration profile appeared very similar to the placebo tablets, although it was elongated due to the slower disintegration. In comparison to literature values the Nurofen® Meltlet was close to what was specified, as it has been shown to disintegrate *In Vivo* at around 20 s (Gryczke *et al*., 2011), and the value obtained in this study was very similar, showing that this test method provided a valid model for disintegration testing of ODTs.

6.3.2 Validation of Disintegration using Newly Developed Disintegration Tester

6.3.2.1 Disintegration times using the new tester

The disintegration tester was conceptualised on the basis that no validated test currently exists that mimics oral *In Vivo* conditions encountered by an ODT during disintegration. Although several

attempts have been made to design a test that is more specific to ODTs (Yoshita *et al*., 2013, Harada *et al*., 2006, Harada *et al*., 2010a, Narazaki *et al*., 2004, Haraguchi *et al*., 2014, Uchida *et al*., 2013, Park *et al*., 2008, Kakutani *et al*., 2010, Abdelbary *et al*., 2005, el-Arini and Clas, 2002, Bi *et al*., 1996, Bi *et al*., 1999, Morita *et al*., 2002, Kondo *et al*., 2012, Segado, 2003, Ohta *et al*., 2001, Desai *et al*., 2013, Szakonyi and Zelkó, 2013), no test has reached approval specifically for ODT disintegration testing. Disintegration times for the seven formulations are shown in Table 6.2.

Figure 6.11 shows the disintegration times of the tablets from the new disintegration test method singularly, and allows a comparison between each of the tablets tested. For the manufactured ODTs a compression force range of 75-300 MPa was chosen to establish the sensitivity of the test to assess disintegration times for tablets. Hardness and porosity values for each of the tablets are also shown in Table 6.2. It was seen that as the compression force increased the disintegration time of the ODTs

Table 6.2: Table showing tableting results for all tablets tested in this study. All data is presented as mean ± SD, with data marked with an asterisk (*) showing the maximum time for the disintegration test, and therefore shows this tablet had not disintegrated within the stated time and was still left as a solid dosage form.

Formulation	Disintegration Time (s)	USP Disintegration Time (s)	Hardness (N)	Tensile strength (N/mm^2)	Porosity
75MPa	22.51 ± 3.2	13.83 ± 0.25	58.67 ± 2.95	0.899 ± 0.076	0.399 ± 0.005
150MPa	28.11 ± 2.5	14.47 ± 1.42	121.37 ± 7.60	2.120 ± 0.133	0.320 ± 0.010
225MPa	35.27 ± 2.07	22.70 ± 2.00	154.87 ± 3.80	2.766 ± 0.062	0.314 ± 0.10
300MPa	42.15 ± 2.07	28.60 ± 1.31	177.33 ± 6.12	3.267 ± 0.109	0.292 ± 0.011
Nurofen Melt	38.77 ± 3.96	15.80 ± 0.10	44.37 ± 2.41	0.447 ± 0.024	0.368 ± 0.004
Matrix	Did not disintegrate	Did not disintegrate	173.70 ± 20.87	3.290 ± 0.575	0.300 ± 0.022
Paracetamol	Did not disintegrate	97.60 ± 5.99	144.80 ± 10.20	1.875 ± 0.137	0.270 ± 0.013

as expected, and with each increase in 75 MPa there was around a 7 second increase in disintegration time. As the compression force was increased the subsequent tablet hardness also increased. This increased tablet hardness caused a higher disintegration time, as the harder tablet was less prone to moisture and water uptake, and therefore reduced wicking into the tablet. This was due to the particles in the compact interacting more closely and being bound tightly during the compression cycle, due to the high content of MCC which is plastically deforming (Thoorens *et al*., 2014). The key finding here was that the disintegration tester was able to distinguish between tablets of different mechanical strength and also showed the expected pattern of increased disintegration time with the harder tablets. The test also appeared sensitive enough to be able to detect small differences in time (as here the difference was a little as 7 seconds). An important investigation in this study was to see whether this test would be able to differentiate between an ODT and a standard release/controlled release tablet that would not disintegrate within the oral cavity. Table 6.2 and Figure 6.11, show that both the matrix tablet and standard release paracetamol had not disintegrated with the 180 s limit

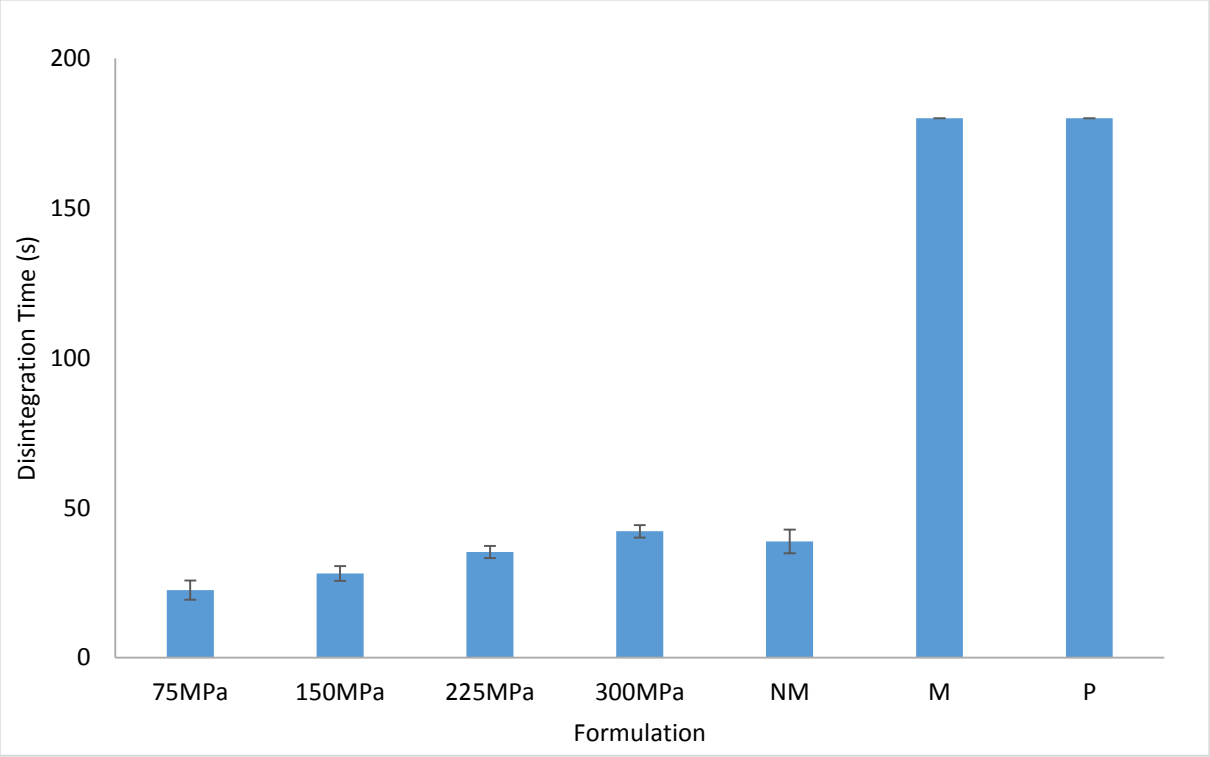

Figure 6.11: A graph showing the disintegration times of the various tablets tested in the new disintegration testing equipment. Values for the matrix tablet and paracetamol tablet are at the maximum time of 180 s of the disintegration tester and represent a tablet that did not disintegrate during the test. All data is presented as mean ± SD (n=8, $p<0.0001$).

set for the test, and on visual analysis it was seen that the matrix tablet was almost fully intact with a thin hydrated layer at the bottom of the tablet. Similarly the paracetamol tablet was also intact, however a larger proportion of the tablet had disintegrated and broke off the main structure. Figure 6.12 illustrates the differences between the disintegration pathways of the ODTs tested and the matrix controlled release system/the standard release paracetamol. It was deduced that all the ODTs follow a similar pathway, there was an initial small flat region, where water and humidity started to ingress into the tablet to break down the structure, as the tablet wasn't fully wet and still retained some mechanical strength, followed by a sharp increase in distance as the tablet was breaking down and falling apart from the main structure and away from the disintegration bed. This caused the probe to press further into the tablet, as there was very little resistance from the soft wet tablet. The final stage was when the probe had pushed through the ODT and on to the surface of the disintegration bed, whereby the plot came to a plateau as the probe exerted its maximum 50 g force. The plots also showed that there was a difference between the disintegration times of the ODTs manufactured at different compression forces ($p<0.05$). The lines for the tablets showed that there was a difference in

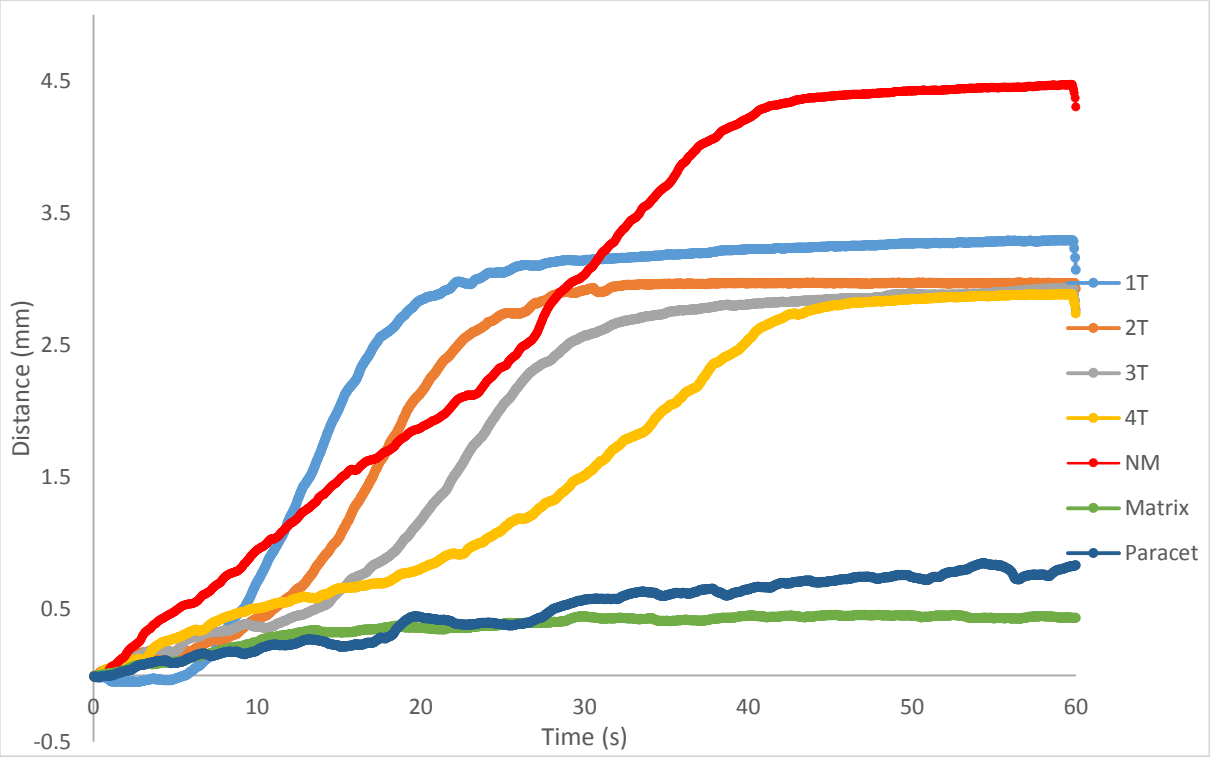

Figure 6.12: Disintegration profiles (Distance vs time plots) of the seven formulations tested within this study, showing marked differences between disintegration pathways for ODTs and standard/controlled release formulations, with statistical significance observed (n=8, $p<0.05$).

thickness of the tablets compressed at different forces, as the final distance for the tablets compressed at higher forces was smaller than those compressed at smaller forces. This supported the theory that the test was sensitive enough to pick up small differences in disintegration time due to differences in compression force, mechanical strength and porosity. However for the controlled release matrix tablet and the standard release paracetamol it was observed that the disintegration pathway was very different, with neither tablet undergoing significant disintegration. Here the final distance moved by the probe was very small, with the paracetamol disintegrating a little more than the matrix tablet. Both of these tablets are designed to be swallowed whole and enter the GI tract, whereby the tablet would subsequently disintegrate in a large volume of fluid. The paracetamol tablet was an immediate release dosage form so would disintegrate in the stomach in a fairly quick time, whereas the matrix tablet was a controlled release system that would slowly swell and erode layer by layer to provide a sustained release of a drug. The disintegration profile for both was similar at the start, where the water from underneath the tablet had come into contact whilst the tablet also interacted with the humidity in the chamber, providing a small increase in distance. However after this initial movement, it was seen there was very little further distance moved by the probe. This was because the tablet remained hard, as the small level of water flow and humidity weren't able to ingress into the tablets and cause a breakdown of the structure, resulting in the probe applying its maximum set weight of 50 g throughout most of the test. However the matrix tablet provided very little movement throughout the test and remained very flat, as the tablet was designed to undergo controlled release in a large volume of fluid. The comparison between ODTs and standard/controlled release tablets was essential as the results would have indicated whether the tester was able to clearly distinguish between different types of tablets, and more so allow an ODT to disintegrate but keep the other types of tablets intact, as they were manufactured to disintegrate in larger volumes of fluid as opposed to within the oral cavity.

6.3.2.2 Comparison to the USP test

It was established that the newly developed disintegration test was able to successfully determine different disintegration times and profiles between ODTs and standard release/matrix tablets, whilst also being able to provide different disintegration time between ODTs manufactured at different compression forces. The next important investigation was to analyse how the test compared to the standard USP disintegration test, especially for those ODTs manufactured in the lab. Figure 6.13 shows a comparison graph of the disintegration time for all the tablets tested between the new and the USP test.

The values for the four lab manufactured ODTs and the Nurofen Meltlets® appeared to be lower when tested in the USP test rather than the new test. This was expected as the conditions in the USP test, submerging the tablet in 800 ml of disintegration medium and oscillating it through the medium, would most probably cause rapid disintegration of the dosage form. This was due to the tablet being

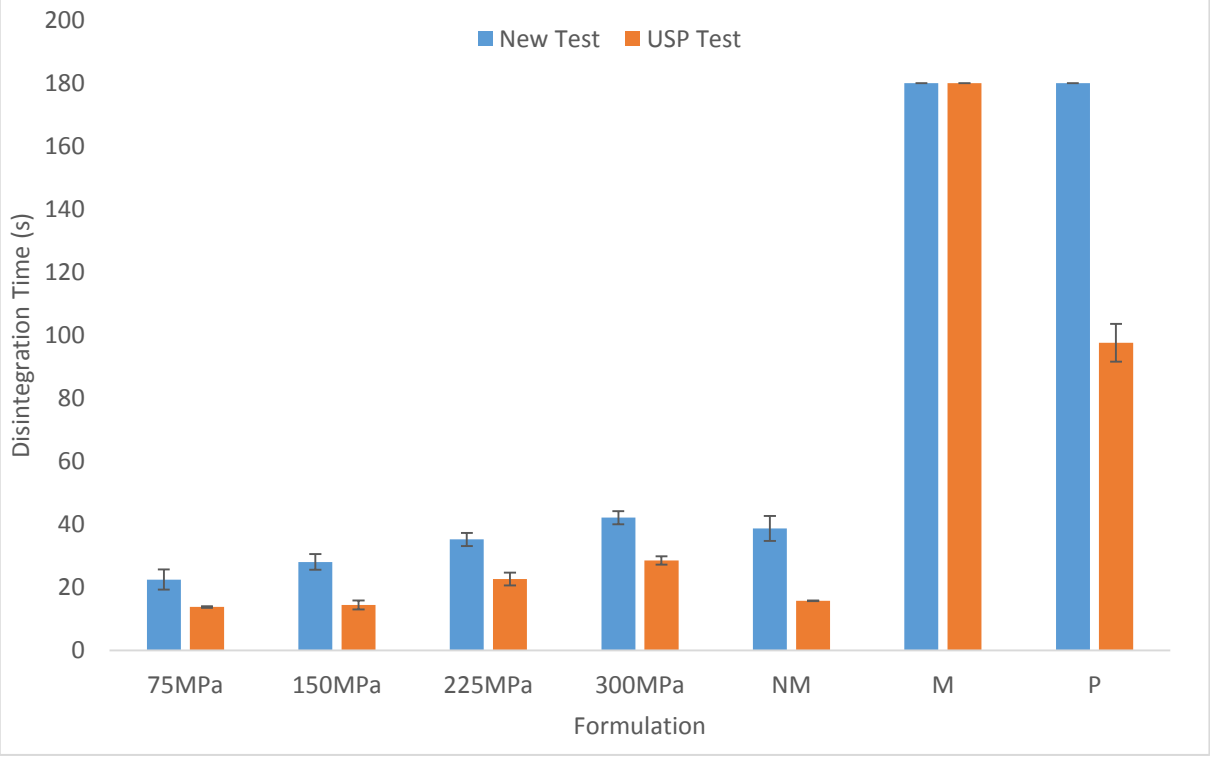

Figure 6.13: A graph comparing disintegration times for the new ODT specific disintegration test and the standard USP test, showing that for ODTs the USP test provides much lower disintegration times than the new test. Both values for the matrix tablet and the disintegration time for the paracetamol both reach the maximum time of 180 s in the new test and 1800 s for matrix in the USP test, so values have been set at 180 s to represent maximum. Data is presented as mean ± SD (n=8 for new test and n=3 for the USP test, $p<0.0001$ between tests indicating results are significantly different between the two tests).

completely surrounded by the disintegration medium, which led to a rapid ingress of water into the ODT and subsequent swelling and breakdown of the structure. This, alongside the mechanical agitation the tablet underwent during the oscillations, caused a rapid disintegration of the dosage form, much faster than would be expected if the tablet was in the oral cavity (Abdelbary *et al*., 2005, Bi *et al*., 1996, Szakonyi and Zelkó, 2013, Harada *et al*., 2006, Brniak *et al*., 2015). Whereas the new test only provided a saliva flow underneath the tablet, the water would then be required to wick through the dosage form to get access to the whole of the structure. However the utilisation of a relative humidity was a novel addition to this test that previous tests did not attempt. The mouth has a high relative high humidity and this is an important factor in helping the ODT disintegrate within the oral cavity, as this also provides moisture to help the tablet disintegrate. The use of relative humidity in this test helped attach small amounts of moisture to the outer surface of the tablet that wasn't in contact with the disintegration bed, so would therefore have aided in the disintegration of the tablets. The moisture levels wouldn't be significant enough to fully submerge the tablet, as in the USP test, however would aid in wetting of the outer surfaces of the tablet, and therefore would be more representative of *In Vivo* conditions rather than the USP test.

It was seen that the standard release paracetamol and matrix tablet experienced very little disintegration during the new test, and the results represented as the maximum time of 180 s in Figure 6.13. The matrix tabl*et al*so experienced very little disintegration during the standard USP test, and at 30mins the dosage form was intact. However the standard release paracetamol clearly disintegrated during the standard USP at around 97 s, which was almost half the maximum time set during for the new disintegration test. This big difference showed that the standard release tablets didn't experience significant disintegration during the new test, however did disintegrate rapidly during the USP test, which is similar to the conditions the standard release would experience during *In Vivo* disintegration. Upon visual analysis, and the analysis of the disintegration profile (Figure 6.12) it was seen that the paracetamol underwent very little disintegration during the new test due to the small volume of

disintegration fluid in contact with the dosage form, and the humidity in the container having very little effect upon the tablet.

Figures 6.14-6.17 show the correlations for hardness, tensile strength, porosity and compression force against disintegration time respectively, for both the newly developed test and the USP test. For this analysis only the four laboratory manufactured tablets were compared as these formulations were kept constant with only the compression force changing, which would allow a correlation to be observed between the various tablet properties. The standard release and matrix tablets were excluded as the test was ODT specific and did not provide any disintegration times for these dosage forms in the new tester. From all figures it was seen that the new tester provided higher correlations, with the R^2 values for hardness, tensile strength, porosity and compression force being 0.92, 0.93, 0.77 and 0.99 respectively, compared to the lower values of 0.78, 0.77, 0.56 and 0.92 respectively from the USP test. This showed that the new tester provided consistent disintegration times that were based more on the other tablet properties compared to the USP test. The correlations between hardness

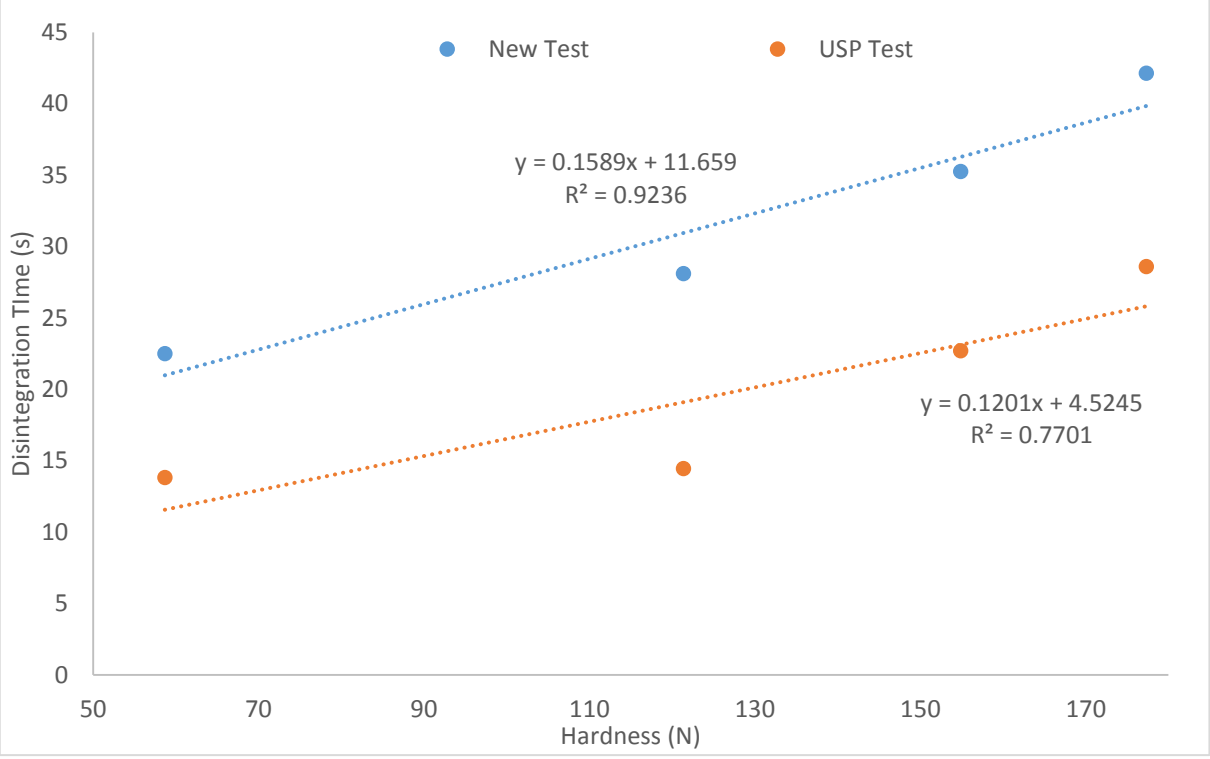

Figure 6.14: A graph comparing the correlation between hardness and disintegration time data for both the new disintegration test and the standard USP test, with results indicating a better correlation with the newly developed disintegration test.

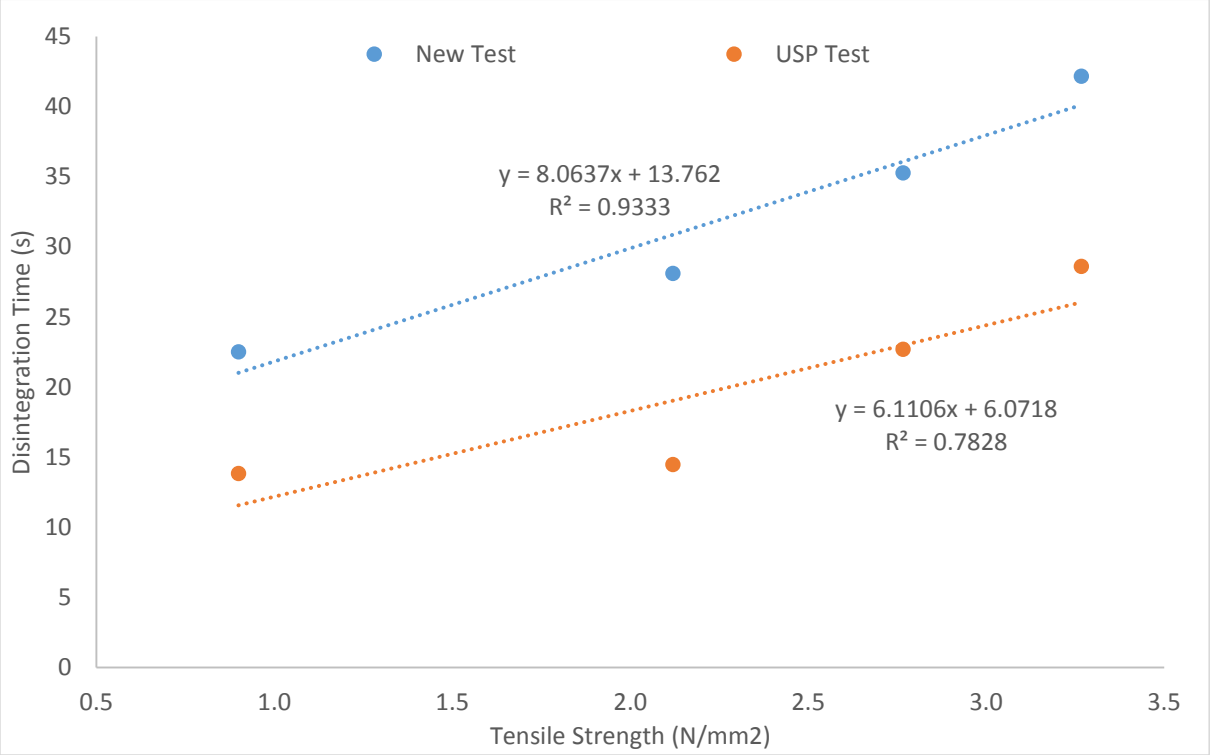

Figure 6.15: A graph comparing the correlation between tensile strength and disintegration time data for both the new disintegration test and the standard USP test, with results indicating a better correlation with the newly developed disintegration test.

and tensile strength (Figure 6.14 and 6.16 respectively) seem to be very high for the new tester, with the USP tester correlation falling far below this. This showed that in terms of disintegration time, mechanical strength played an important part, particularly in the case of the new tester, during the formulation of ODTs to ensure that the tablet disintegrated rapidly in *In Vivo* conditions. In terms of the porosity of the tablet (Figure 6.16), the new tester demonstrated a strong positive correlation, with an R^2 of 0.77, showing that porosity also plays a key part in the disintegration time of ODTs. Whereas the correlation for the USP test indicated a weaker correlation between the disintegration time and porosity, suggesting that disintegration time is less dependent on porosity. The final investigation compared the compression force used during tableting to the disintegration times, shown in Figure 6.17. Here the correlation between the compression force and the disintegration time in the new tester had an R^2 of 0.997, compared to the lower value for the USP test of 0.921, showing again the disintegration time of the ODTs was strongly dependant on the compression force. The correlations were analysed to see how the disintegration times achieved in each of the tests were affected by other tablet and process parameters.

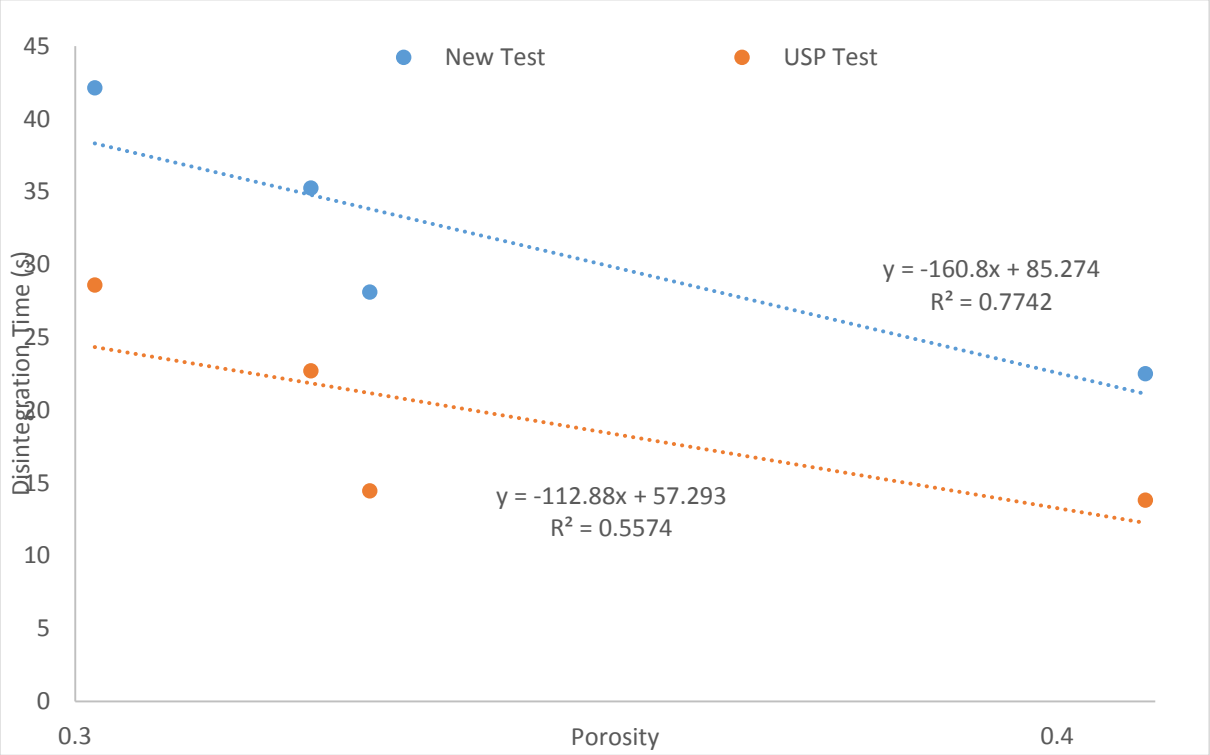

Figure 6.16: A graph comparing the correlation between porosity and disintegration time data for both the new disintegration test and the standard USP test, with results indicating a better correlation with the newly developed disintegration test.

Overall the results gathered in this study showed that the new tester was a suitable tool for gathering disintegration time data for ODTs, as it provided more representative conditions to those encountered *In Vivo*, and also provided much stronger correlations than the standard USP test when comparing tablet properties. This meant the data obtained for the tablet properties was more strongly related and provided more of a rationale to differences in disintegration times, compared to the USP test. As mentioned above, the USP test provided much lower disintegration times, due to the high volume of liquid used in the test, and therefore the correlations achieved may have been skewed based on the unnatural disintegration conditions encountered by the tablet that was designed to disintegrate in the oral cavity.

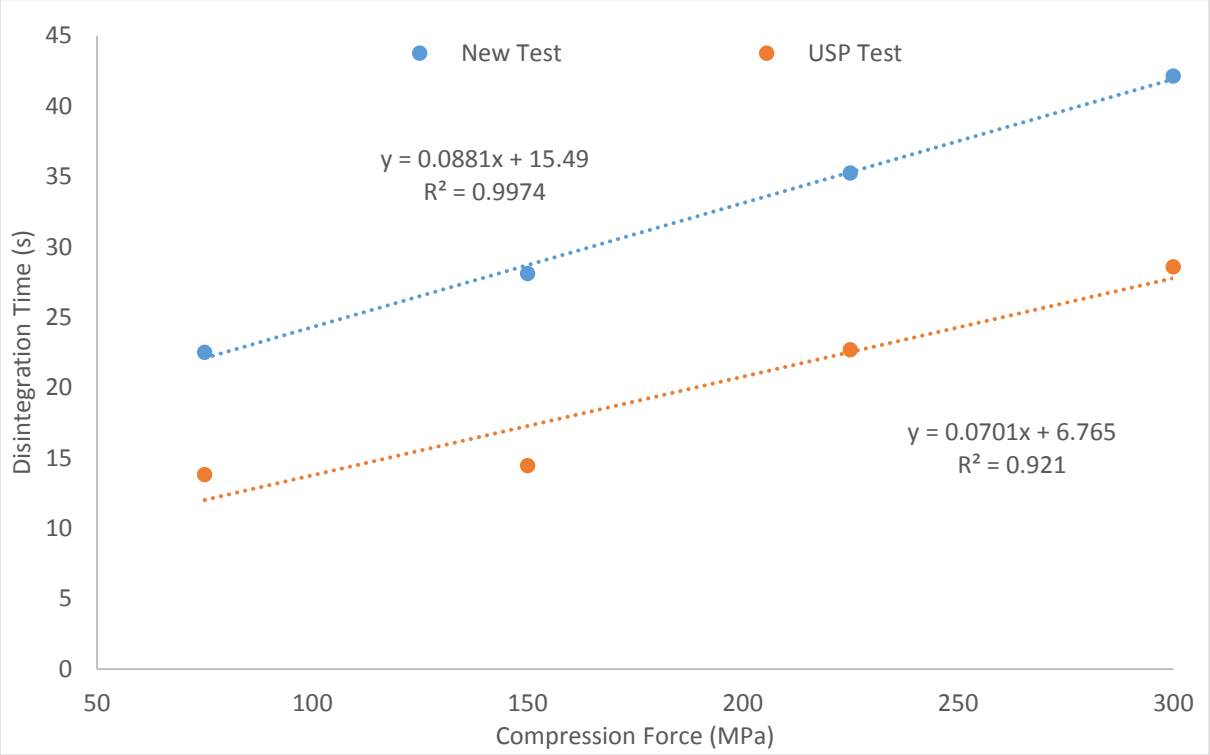

Figure 6.17: A graph comparing the correlation between compression force of the tablet press and disintegration time data for both the new disintegration test and the standard USP test, with results indicating a better correlation with the newly developed disintegration test.

6.3.3 In Vivo In Vitro Correlation

The *In Vivo* disintegration times for all batches were compared and correlated with results from the newly developed disintegration tester, as well as with the USP tester, these results are shown in Figure 6.18. The collection of 21 individual results for the *In Vivo* study allowed a wide representation of disintegration times and was key to obtaining an accurate reading for ODT disintegration. This was because each individual is subjective as to when they perceive the end of disintegration to be, the blinded nature of the study meant that participants were not aware that they were taking two sets of tablets in triplicate. To supplement this, results from seven participants were taken to then calculate the mean for that particular tablet. This therefore allowed an accurate representation of the disintegration time for each batch of tablets tested in the study, by having both inter and intra person variability. The tablets were manufactured so that the disintegration time would span a timeframe from 10s to 150s; this allowed a wide range of times to be correlated and to see if there was any large

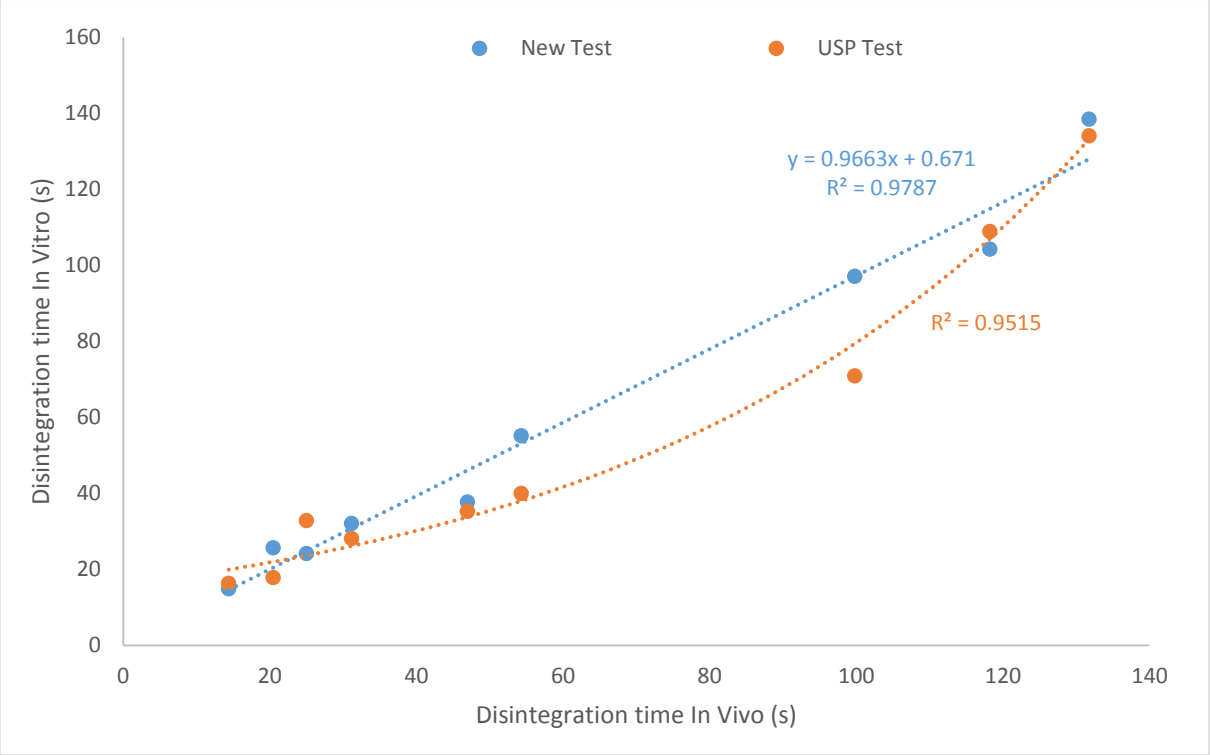

Figure 6.18: A graph showing the IVIVC of the newly developed disintegration tester compared to the standard USP disintegration test. Results show that the newly developed tester has a linear correlation for the In Vivo In Vitro disintegration times whereas the USP tester appears to show a curved data set therefore indicating a direct correlation is not observable with the USP tester.

differences between a correlation of results accepted by the EU regulations (180s) (Ph.Eur, 2013) or the regulations recommended by the FDA (30s) (FDA, 2008).

Figure 6.18 shows the IVIVC for tablets spanning both the acceptable range for the EU and FDA regulations, with the time going up to 180 s. Results indicated that the newly developed disintegration tester had a very good linear correlation with the *In Vivo* results, with a correlation value of 0.98. Also it was observed that the gradient of the line was almost 1, at 0.97, indicating that a direct correlation was obtained, whereby if the disintegration time *In Vivo* was increasing by 1 second, then the disintegration time observed on the newly developed tester was also increasing by 1 second. This represented a very positive result, as it was indicating that the values obtained from the newly developed disintegration tester were almost a direct representation of the *In Vivo* times. However, in comparison the results obtained for the USP tester were not linear, with a curved dataset observed and a strong R^2 value of 0.95 for the curve, indicating that the USP test did not provide a direct representation of the disintegration time for ODTs *In Vivo*. The two IVIVC results therefore showed

that the new disintegration test developed in this study was superior in generating accurate *In Vitro* ODT disintegration times. This result was expected as the conditions encountered within the new tester were far more representative of those encountered in the oral cavity, with the high humidity, fixed temperature, flow rate and interaction of the tablet with the probe/upper palate. This therefore allowed the tablets to disintegrate in a similar manner during *In Vitro* testing as well as *In Vivo* testing. However the USP tester provided an environment that was not similar to that of the oral cavity and therefore the disintegration times were far more varied, resulting in the curved dataset observed.

As the results in the validation indicated, ODTs have particular characteristics that allow them to disintegrate rapidly but also correlate with the ODT disintegration time. The newly designed tester proved that it can correlate not only the tablet characteristics to the disintegration time, but also has a very strong correlation to *In Vivo* results, with USP test results lagging behind in both cases. The *In Vivo* test took into account both inter and intra person variability, accounting for the subjective nature as to when people perceive the end point of disintegration to be, which therefore provided an accurate basis to allow a comparison to the *In Vitro* methods. The newly developed tester provided more accurate results for ODT disintegration, with times being more representative compared to the standard USP method. This was due to the tablet in the new tester undergoing a disintegration pattern similar to what the tablet would experience in the oral cavity, whereby temperature and humidity were controlled similar to *In Vivo* conditions, and applied pressures/manipulations were also experienced by the tablet, similar to the conditions encountered during disintegration in the mouth. The USP tester used a large volume of 800 ml, with the oscillating basket apparatus, and therefore conditions were vastly different to the oral cavity environment, which led to different disintegration pattern with the tablets, and therefore the correlation was lower and not representative of *In Vivo* disintegration.

6.4 Conclusion

The objective of this study was to assess whether the newly developed prototype disintegration tester would be a suitable alternative for testing ODT disintegration time compared to the currently recommended USP method. Disintegration data was compared to the standard USP test and correlations between various tablet properties against disintegration time were also analysed.

It was concluded that the newly developed prototype was successful at distinguishing between ODTs manufactured at different compression forces, showing sensitivity at picking up subtle changes in disintegration time when compression force was changed by 75 MPa, with around a 7 s difference observed between each step. Differences were clearly observed on the disintegration profiles drawn up by the texture analyser software, where the probe with attached ODT travelling the full thickness of the tablet to come into contact with the disintegration bed, whereas for the standard/controlled release tablets the probe travelled a very small distance due to the tablet still being intact and attached to the probe. The new tester was also able to achieve higher correlations when comparing tablet properties to the disintegration times achieved, showing that times gathered in the new test were more dependent on the properties of the tablet, possibly due to the ODTs undergoing a more representative disintegration pathway rather than the different pattern achieved in the USP test.

The *In Vivo* study was crucial to demonstrating real applicability of the new tester as an IVIVC comparison of the two tests highlighted whether the new test was actually providing an improvement on the current USP test. IVIVC results indicated that the new tester provided a linear correlation for disintegration times, with a very strong correlation of 0.97 observed. In comparison the USP test was less accurate in predicting *In Vivo* disintegration times as the results showed a curved data set, therefore showing the USP test was not representative of *In Vivo* ODT disintegration. This was a key result which highlighted that the newly developed tester provided a suitable alternative to the current USP test for ODT disintegration, and could therefore be used to gather more accurate *In Vitro* disintegration times for all ODTs tested.

Chapter 7

General Discussion and Future Work

General Discussion

Direct compression manufacture of ODTs is increasing in popularity due to its cost effectiveness and ease of manufacture. However the mechanistic properties of the materials constituting the powder blend become vital in ensuring the flowability of the powder is consistent, allowing the formation of uniform dosage forms, whilst being compressible enough to form robust, mechanically strong tablets that disintegrate within acceptable time limits. Mannitol is a key filler in ODT manufacture due to its high palatability and non-hygroscopic nature, however its poor compression behaviour, due to its fragmentation under pressure, results in mechanically weak tablets. The purpose of this thesis was to study the fragmentation behaviour of mannitol, whilst establishing whether the utilisation of dry coated powders could result in the formation of suitable ODTs.

Ball milling was utilised as a comminution method to study how high levels of energy fragmented the individual mannitol crystals. The primary plane of fracture for the mannitol crystal during the milling process was the (011) plane, as visualised on the SEM images and the subsequent evaluation of surface energies and disintegration time profiles. This fragmenting method could therefore be related to the fragmentation of the mannitol crystal during tableting, whereby the crystal would be expected to primarily fracture at the (011) plane during applied pressure. It was observed that the inclusion of fractured mannitol during tableting resulted in an improvement in the compressibility of the excipient, as more of the compaction energy was utilised in bonding of the compact as opposed to fragmentation of the excipient, whereby energy was expelled through high die wall interaction. ODT properties of the milled mannitol compacts were also improved, with disintegration times being lower compared to unmilled mannitol, as the mannitol particles had increased wettability due to the exposure of the hydrophilic (011) plane. The hardness of the ODTs also improved due to the increased compressibility of mannitol, with Heckel analysis showing a reduction in the fragmenting behaviour of mannitol, with a higher plastic deformability observed.

Milled mannitol was also successfully scaled up with dry particle coating, alongside MCC, producing a flowable powder that was capable of being compressed in an auto tablet press. Compared to conventional cube mixing, dry coating provided a far superior powder, as the poorly flowing nature of the milled mannitol resulted in cube blending producing unacceptable, non-uniform tablets. However dry coating produced uniform tablets that were mechanically sound and disintegrated rapidly, as the powder flowed well into the dies during auto-compression, as the dry coating process utilised the cohesive nature of the milled mannitol to produce a more homogenous powder blend.

To assess the viability of milled mannitol as a commercial entity, a comparison study was conducted to evaluate the effectiveness of current commercial mannitol grades employed in ODTs. The study found that spray dried mannitol had the most desirable properties for utilisation as a binder within ODTs. Results indicated that it formed ODT's with good mechanical properties, whilst also providing the lowest overall disintegration times of all the commercial grades tested. This was due to the presence of the alpha polymorph, which is the most compressible of all the mannitol polymorphs. The granulated forms however didn't display any significant improvements in tablet properties, due to the lack of α-mannitol within the powder, however powder flowability was seen as a key advantage of the granulated mannitol. In comparison, the key advantage of the milled mannitol was its very low disintegration time, due to the increased wettability of the powder, providing ODTs that rapidly disintegrated, much faster than any of the commercial grades. Although mechanical strength and the friability of the milled mannitol ODT's was lower than the spray dried grades, the vast improvement in disintegration time provided a key advantage compared to the commercial powders, especially for employment in ODTs. The poor flowability of the milled mannitol was its main disadvantage, however as mentioned above, dry coating was capable of enhancing flow to suitable levels. Therefore the milling of mannitol provided a suitable alternative to the commercial grades for the production of ODTs.

The next stage in the development of milled mannitol was to investigate a suitable mix of excipients that could be included in a preblend for ODT production. The results indicated that employing milled mannitol with the model poorly soluble API Ibuprofen, formed tablets of similar robustness to the unmilled alternative at 150 MPa compaction force, with vastly improved disintegration times, even at high drug loads of 50%, due to the more hydrophilic nature of the milled mannitol. A comparison of dry coating and conventional cube mixing was also conducted for producing the preblend. Dry coating was again advantageous in producing better flowing powder, particularly when milled mannitol was used in the preblend. The optimisation of the powder blend found that mixing 1% silica for 20 mins post mixing of the milled mannitol and MCC provided an ideally flowing powder, which produced ODTs with desirable properties. The preblends were optimised to ensure that milled mannitol remained in high quantities to utilise its key advantages in producing ODTs with rapid disintegration, without the use of superdisintegrants in the powder blend. Silica also proved to be the ideal flow aid compared to glyceryl behenate and Ethocel, whilst powders manufactured using multi-layering/surface coverage calculations didn't provide any major advantage. The optimised powders from the study indicated that milled mannitol produced preblends with a high dilution potential, whereby high drug concentrations could be included, and the key advantage was the potential for using high load drugs in ODTs, as ODTs have a limited maximum weight of 500 mg. Furthermore the milled mannitol/MCC dry coated preblends highlighted that dry particle coating could provide powders with enhanced functionalities for use in ODTs.

Silicified MCC, manufactured using spray drying, provided enhanced MCC powders with the inclusion of silica within the MCC particle, giving an enhanced flow and compressibility of the MCC. Dry coating of silica with MCC was designed to assess whether dry particle coating could provide similar enhancements in MCC properties for employment into ODTs. Results indicated that the dry coated particles of silica and MCC provided a free flowing powder that once compacted gave tablets that disintegrated, rapidly with a high mechanical strength. Although tablet hardness, both with and without the non-compressible API Metformin, was reduced compared to the silicified MCC Prosolv, it

still remained very compressible even at very low compression forces. When the dry coated MCC/silica was employed in typical ODT formulations, it was less lubricant sensitive than the uncoated Avicel control, and therefore provided powders that remained highly compressible, even when high drug loads of metformin were incorporated. However the key advantage of the dry coated particles was that it retained the very good disintegrating properties of the uncoated MCC, with disintegration times significantly lower than both of the Prosolv grades. Flow was also improved for the dry coated particles, particularly with the PH102 MCC compared to the Prosolv P90, due to the surface coverage of the silica resulting in reduction of the frictional forces between particles. Compression profiling also indicated that although bond strength did decrease when dry coating MCC, this wasn't an issue as the resulting hardness of the tablets was still very high, whilst compressibility of the MCC was retained. It was therefore established that, although the dry coated powders weren't as compactible as the Prosolv, they provided a key advantage over Prosolv for employment in ODTs. Disintegration of ODTs manufactured using dry coated powders was rapid, whilst having an improved powder flow and reduced lubricant sensitivity compared to the Avicel control. Consequently this study highlighted that dry particle coating provided MCC powders with enhanced functionalities, particularly for enhancing compression of poorly compressible APIs, whilst retaining an acceptable disintegration profile.

Throughout the study period several ODT tests were conducted to assess the properties of the tablets. Disintegration time was a vital characteristic tested, with a target disintegration time of 30s. However the testing conditions encountered by the ODT in the currently recommended USP test were not entirely representative of the conditions the ODT would encounter in the oral cavity. It was highlighted that there was an opportunity to develop a more relevant ODT disintegration test, as USP guidelines indicated modified tests could be used, providing the method generated similar and representative disintegration times. Literature had highlighted several tests that were developed to produce modified ODT disintegration tests, however none had incorporated the vast majority of conditions encountered in the mouth. Over the course of this work efforts were applied to developing a novel disintegration test that provided conditions which were similar to those encountered in the oral cavity,

and as a consequence assess whether the newly developed prototype disintegration tester would be a suitable alternative for testing ODT disintegration time. A new modified disintegration tester was designed, incorporating a housing where conditions were tightly controlled, similar to those in the oral cavity, whilst a texture analyser was used introduce the tablet to the housing and to apply the necessary force on the tablet. It was established that the newly developed prototype was sensitive at picking up subtle changes in disintegration time, whilst being successful at distinguishing between ODTs manufactured at different compression forces. The tester was able to successfully determine which dosage forms were designed to disintegrate within the oral cavity and those that were not, with standard/modified release tablets not exhibiting disintegration within the new tester. The texture analyser was also able to draw up disintegration time profiles, as well as highlighting the end point of disintegration. Correlations between the disintegration time of the ODTs and other tablet properties were higher for the new disintegration tester compared to the USP tester, highlighting that the new test was providing positive results because tablet properties such as hardness and porosity were highly related to the disintegration time of that particular tablet. A key aspect in the development of the new tester was the undertaking of an *In Vivo* study to provide a correlation to the *In Vitro* results in both the new disintegration tester and the standard USP test. IVIVC provided crucial results that confirmed the new tester delivered a higher correlation to *In Vivo* times compared to the USP tester, with a massive improvement seen. The new tester was able to provide a strong linear correlation compared to the curved nature of the results generated by the USP tester. The IVIVC results were vital and highlighted that the newly developed tester provided a suitable and superior alternative to the current USP test for ODT disintegration, and was therefore an acceptable test for gathering more representative disintegration times.

Future Work and Direction

The establishment of milled mannitol as a suitable filler binder provides a platform for further work, especially with regards to the employment of the excipient within ODTs. Results obtained in this thesis showed that milled mannitol was able to produce mechanically robust tablets, through lower

fragmentation on compression, with the clear advantage being its improvement in disintegration, due to the increased wettability of the excipient. Scale up work also indicated that mannitol could be tableted on a high throughput scale. Further work would need to be conducted to ascertain the suitability of milled mannitol in conventional mixing methods, as this thesis primarily used dry particle coating as the mixing method of choice, due to the superior processing allowing production of more flowable powder. However this technique is very unique to our laboratory. During dry particle coating adjuvant excipient levels of the MCC were kept as low as possible to produce viable ODTs with desired high quantities of mannitol. Future work with milled mannitol could be conducted whereby adjuvant excipient concentrations were optimised to levels that not only helped to improve the flow of mannitol in conventional mixing, but also keep the integral low disintegration time. Compaction pressure of the tablets could also be optimised, as Chapter 2 indicated that using higher compaction forces resulted in the milled mannitol providing more robust dosage forms compared to the unmilled mannitol. This could then allow the utilisation of milled mannitol in conventional solid dosage forms as the high dilution potential of the milled mannitol, alongside the larger weight limits with conventional tablets would allow the formation of compressible powders that contain high loads of API, whilst also disintegrating within USP limits.

The successful development of the novel disintegration tester was a key outcome from this thesis. This work highlighted that the new disintegration tester provided a superior correlation to *In Vivo* ODT disintegration times compared to the USP tester. The initial development work highlighted the ideal set up of the housing, which maintained conditions similar to the oral cavity, whilst the texture analyser applied the required pressure and drew the distance/time plot, allowing the end of disintegration to be quantified. As per the original design, a section could be added underneath the silicon pipe where the tablet disintegrates, which would collect the tablet residue over the disintegration period. This could then be extracted and analysed through HPLC to ascertain what levels of the API could be potentially absorbed in the mouth/oesophagus. Further work to the housing could lead to the development of an improved mechanism to ascertain the end point of disintegration. A

complete equipment could be designed whereby the housing would be taken forward and upgraded to maintain the temperature and humidity of the oral cavity. The silicon pipe/disintegration bed section could have a conductive sponge, so when the tablet probe makes contact, post disintegration of the attached tablet, it would indicate the end of disintegration time on an automatic timer that would start when the tablet makes contact with the disintegration bed. Additional features could also be added whereby dosage forms like orally disintegrating films could be assessed.

This future directions section highlights the additional work that could be conducted to further the two main findings of this thesis. The milled mannitol and disintegration tester work provided a strong basis for potential commercialisation, with milled mannitol being a possible filler/binder for solid oral dosage forms, and the novel disintegration test method being an alternative to the USP disintegration test for ODTs.

References

Abdel-Hamid, S. & Betz, G. (2011). Study of radial die-wall pressure changes during pharmaceutical powder compaction. *Drug Development and Industrial Pharmacy,* 37**,** 387-95.

Abdelbary, G., Eouani, C., Prinderre, P., Joachim, J., Reynier, J. & Piccerelle, P. (2005). Determination of the in vitro disintegration profile of rapidly disintegrating tablets and correlation with oral disintegration. *International Journal of Pharmaceutics,* 292**,** 29-41.

Abdellaoui, M. & Gaffet, E. (1994). A mathematical and experimental dynamical phase diagram for ball-milled Ni10Zr7. *Journal of Alloys and Compounds,* 209**,** 351-361.

Abdellaoui, M. & Gaffet, E. (1995). The physics of mechanical alloying in a planetary ball mill: Mathematical treatment. *Acta Metallurgica et Materialia,* 43**,** 1087-1098.

Abe, H., Yasui, S., Kuwata, A. & Takeuchi, H. (2009). Improving powder flow properties of a direct ticalcompression formulation using a two-step glidant mixing process. *Chemical and Pharmaceur Bulletin (Tokyo),* 57**,** 647-52.

Al-Khattawi, A., Aly, A., Perrie, Y., Rue, P. & Mohammed, A. R. (2012). Multi Stage Strategy to Reduce Friability of Directly Compressed Orally Disintegrating Tablets. *Drug Delivery Letters,* 2**,** 195-201.

Al-khattawi, A., Alyami, H., Townsend, B., Ma, X. & Mohammed, A. R. (2014). Evidence-Based Nanoscopic and Molecular Framework for Excipient Functionality in Compressed Orally Disintegrating Tablets. *PLoS ONE,* 9**,** e101369.

Al-Khattawi, A., Koner, J., Rue, P., Kirby, D., Perrie, Y., Rajabi-Siahboomi, A. & Mohammed, A. R. (2015). A pragmatic approach for engineering porous mannitol and mechanistic evaluation of particle performance. *European Journal of Pharmaceutics and Biopharmaceutics,* 94**,** 1-10.

Al-khattawi, A. & Mohammed, A. R. (2013). Compressed orally disintegrating tablets: excipients evolution and formulation strategies. *Expert Opinion on Drug Delivery,* 10**,** 651-663.

AlHusban, F. A., El-Shaer, A. M., Jones, R. J. & Mohammed, A. R. (2010). Recent patents and trends in orally disintegrating tablets. *Recent Patents on Drug Delivery & Formulation,* 4**,** 178-97.

Almaya, A. & Aburub, A. (2008). Effect of Particle Size on Compaction of Materials with Different Deformation Mechanisms with and without Lubricants. *AAPS PharmSciTech,* 9**,** 414-418.

Alonso, M., Satoh, M. & Miyanami, K. (1990). The effect of random positioning on the packing of particles adhering to the surface of a central particle. *Powder Technology,* 62**,** 35-40.

Alvarez, C., Nunez, I., Torrado, J. J., Gordon, J., Potthast, H. & Garcia-Arieta, A. (2011). Investigation on the possibility of biowaivers for ibuprofen. *Journal of Pharmaceutical Sciences,* 100**,** 2343-9.

Alyami, H., Dahmash, E., Alyami, F., Dahmash, D., Huynh, C., Terry, D. & Mohammed, A. R. (2016a). Dosage form preference consultation study in children and young adults: paving the way for patient-centred and patient-informed dosage form development. *European Journal of Hospital Pharmacy*.

Alyami, H., Koner, J., Dahmash, E. Z., Bowen, J., Terry, D. & Mohammed, A. R. (2016b). Microparticle surface layering through dry coating: impact of moisture content and process parameters on the properties of orally disintegrating tablets. *Journal of Pharmacy and Pharmacology*.

Aulton, M. E. (2007). Drying. *In:* AULTON, M. E. (ed.) *Pharmaceutics: The Design and Manufacture of Medicines.* Philadelphia, USA: Elsevier Health Sciences.

Baerlocher, C. & McCusker, L. B. (1994). Practical Aspects of Powder Diffraction Data Analysis. *In:* JANSEN, J. C., STOCKER, M., KARGE, H. G. & WEITKAMP, J. (eds.) *Advanced Zeolite Science and Applications* Amsterdam, The Netherlands: Elsevier Science.

Balaz, P. (2008). High Energy Milling. *In:* BALAZ, P. (ed.) *Mechanochemistry in Nanoscience and Minerals Engineering.* Springer.

Barra, J., Lescure, F. & Doelker, E. (1999). Taste masking as a consequence of the organisation of powder mixes. *Pharmaceutica Acta Helvetiae,* 74**,** 37-42.

Beach, L. E. (2011). *Effect of Dry Particle Coating on the Properties of Cohesive Pharmaceutical Powders.* Doctor of Philosophy in Chemical Engineering, New Jersey Institute of Technology.

Benedetti, C., Abatzoglou, N., Simard, J. S., McDermott, L., Léonard, G. & Cartilier, L. (2007). Cohesive, multicomponent, dense powder flow characterization by NIR. *International Journal of Pharmaceutics,* 336**,** 292-301.

Bhalekar, M. R., Desale, S. S. & Madgulkar, A. R. (2010). Synthesis of MCC–PEG Conjugate and Its Evaluation as a Superdisintegrant. *AAPS PharmSciTech,* 11**,** 1171-1178.

Bi, Y., Sunada, H., Yonezawa, Y., Danjo, K., Otsuka, A. & Iida, K. (1996). Preparation and evaluation of a compressed tablet rapidly disintegrating in the oral cavity. *Chemical and Pharmaceutical Bulletin (Tokyo),* 44**,** 2121-7.

Bi, Y. X., Sunada, H., Yonezawa, Y. & Danjo, K. (1999). Evaluation of rapidly disintegrating tablets prepared by a direct compression method. *Drug Development and Industrial Pharmacy,* 25**,** 571-81.

Bolhuis, G. K. (2011). Compaction Properties of Directly Compressible Materials. *In:* ÇELIK, M. (ed.) *Pharmaceutical Powder Compaction Technology, Second Edition.* Second ed. Florida, USA: CRC Press.

Bolhuis, G. K. & Chowhan, Z. T. (1996). Materials for Direct Compaction. *In:* ALDERBORN, G. & NYSTRÖM, C. (eds.) *Pharmaceutical Powder Compaction Technology.* New York: Marcel Dekker.

Bolhuis, G. K. & Holzer, A. W. (1996). Lubricant Sensitivity. *In:* ALDERBORN, G. & NYSTRÖM, C. (eds.) *Pharmaceutical Powder Compaction Technology.* New York: Marcel Dekker.

Bowen, J., Cheneler, D., Walliman, D., Arkless, S. G., Zhang, Z., Ward, M. C. L. & Adams, M. J. (2010). On the calibration of rectangular atomic force microscope cantilevers modified by particle attachment and lamination. *Measurement Science and Technology,* 21**,** 115106.

BP. (2015). *Appendix XII C. Consistency of Formulated Preparations* [Online]. London: Stationery Office. Available: https://www.pharmacopoeia.com/bp-2016/appendices/appendix-12/appendix-xii-c--consistency-of-formulated-preparations.html?published-date=2015-08-03 [Accessed 24/09/2015 2015].

Brniak, W., Jachowicz, R. & Pelka, P. (2015). The practical approach to the evaluation of methods used to determine the disintegration time of orally disintegrating tablets (ODTs). *Saudi Pharmaceutical Journal,* 23**,** 437-443.

Brunauer, S., Emmett, P. H. & Teller, E. (1938). Adsorption of Gases in Multimolecular Layers. *Journal of the American Chemical Society,* 60**,** 309-319.

Buck, M. L. (2013). Alternative Forms of Oral Drug Delivery for Pediatric Patients. *Pediatric Pharmacotherapy,* 19.

Buckton, G., Darcy, P. & Sherwood, B. (1996). Caloric and gravimetric water sorption profiles of silicified microcrystalline cellulose (SMCC). *Pharmaceutical Research,* 13**,** S199-S198.

Buckton, G., Yonemochi, E., Yoon, W. L. & Moffat, A. C. (1999). Water sorption and near IR spectroscopy to study the differences between microcrystalline cellulose and silicified microcrystalline cellulose before and after wet granulation. *International Journal of Pharmaceutics,* 181**,** 41-7.

Burger, A., Henck, J. O., Hetz, S., Rollinger, J. M., Weissnicht, A. A. & Stottner, H. (2000). Energy/temperature diagram and compression behavior of the polymorphs of D-mannitol. *Journal of Pharmaceutical Sciences,* 89**,** 457-68.

Burgio, N., Iasonna, A., Magini, M., Martelli, S. & Padella, F. (1991). Mechanical alloying of the Fe−Zr system. Correlation between input energy and end products. *Il Nuovo Cimento D,* 13**,** 459-476.

Campbell Roberts, S. N., Williams, A. C., Grimsey, I. M. & Booth, S. W. (2002). Quantitative analysis of mannitol polymorphs. X-ray powder diffractometry—exploring preferred orientation effects. *Journal of Pharmaceutical and Biomedical Analysis,* 28**,** 1149-1159.

Carlin, B. A. C. (2008). Direct Compression and the Role of Filler-binders. *In:* AUGSBERGER, L. L. & STEPHEN, H. W. (eds.) *Pharmaceutical Dosage Forms: Tablets.* New York: Informa Healthcare.

Carlson, G. T. & Hancock, B. C. (2006). A Comparison of Physical and Mechanical Properties of Common Tabletting Diluents. *In:* ASHOK KATDARE, M. C. (ed.) *Excipient Development for Pharmaceutical, Biotechnology, and Drug Delivery Systems.* New York: Informa Healthcare.

Carter, J. C. (2001). *The Role of Lubricants in Solid Oral Dosage Manufacturing* [Online]. Keswick: Carter Pharmaceutical Consulting. [Accessed 26 March 2014].

Castricum, H. L., Yang, H., Bakker, H. & Deursen, J. H. V. (1997). A Study of Milling of Pure Polymers and a Structural Transformation of Polyethylene. *Materials Science Forum,* 1**,** 211-216.

Chattoraj, S., Shi, L. & Sun, C. C. (2011). Profoundly improving flow properties of a cohesive cellulose powder by surface coating with nano-silica through comilling. *Journal of Pharmaceutical Sciences,* 100**,** 4943-52.

Childress, A. & Sallee, F. R. (2013). The use of methylphenidate hydrochloride extended-release oral suspension for the treatment of ADHD. *Expert Review of Neurotherapeutics,* 13**,** 979-88.

Chowhan, Z. T. & Yang, I. C. (1983). Powder flow studies IV. Tensile strength and orifice flow rate relationships of binary mixtures. *International Journal of Pharmaceutics,* 14**,** 231-242.

Coffin-Beach, D. P. & Gary Hollenbeck, R. (1983). Determination of the energy of tablet formation during compression of selected pharmaceutical powders. *International Journal of Pharmaceutics,* 17**,** 313-324.

Colorcon (2005). Lactose Replacement with Starch 1500® in a Direct Compression Formula *In:* INC., C. (ed.) *Starch 1500®.* Harleysville, USA.

Cuna, M., Vila Jato, J. L. & Torres, D. (2000). Controlled-release liquid suspensions based on ion-exchange particles entrapped within acrylic microcapsules. *International Journal of Pharmaceutics,* 199**,** 151-8.

Dahiya, R. J., Jalwal, P. & Singh, B. (2015). Chewable Tablets: A Comprehensive Review. *The Pharma Innovation Journal,* 4**,** 100-105.

Dahmash, E. (2016). *Development of a Novel Dry Coating Device for Pharmaceutical Application.* Doctor of Philosphy, Aston University.

Dahmash, E. Z. & Mohammed, A. R. (2015). Functionalised particles using dry powder coating in pharmaceutical drug delivery: promises and challenges. *Expert Opinion Drug Delivery***,** 1-13.

de Villiers, M. M. (1997). Description of the kinetics of the deagglomeration of drug particle agglomerates during powder mixing. *International Journal of Pharmaceutics,* 151**,** 1-6.

Desai, P. M., Liew, C. V. & Heng, P. W. (2012). Understanding disintegrant action by visualization. *Journal Pharmaceutical Sciences,* 101**,** 2155-64.

Desai, P. M., Liew, C. V. & Heng, P. W. S. (2013). Assessment of disintegration of rapidly disintegrating tablets by a visiometric liquid jet-mediated disintegration apparatus. *International Journal of Pharmaceutics,* 442**,** 65-73.

Descamps, M., Willart, J. F., Dudognon, E. & Caron, V. (2007). Transformation of pharmaceutical compounds upon milling and comilling: the role of T(g). *Journal of Pharmaceutical Sciences,* 96**,** 1398-407.

Dor, P. J. & Fix, J. A. (2000). In vitro determination of disintegration time of quick-dissolve tablets using a new method. *Pharmaceutical Development and Technology,* 5**,** 575-7.

Edge, S., Potter, U. J., Steele, D. F., Tobyn, M. J., Chen, A. & Staniforth, J. N. (1999). The Location of Silicon Dioxide in Silicified Microcrystalline Cellulose. *Pharmacy and Pharmacology Communications,* 5**,** 371-376.

Edge, S., Steele, D. F., Chen, A., Tobyn, M. J. & Staniforth, J. N. (2000). The mechanical properties of compacts of microcrystalline cellulose and silicified microcrystalline cellulose. *International Journal of Pharmaceutics,* 200**,** 67-72.

Eiche, F. E. & Kudehinbu, A. O. (2009). Effect of Particle size of Granules on some Mechanical Properties of Paracetamol Tablets. *African Journal of Biotechnology,* 8**,** 5913-5916.

el-Arini, S. K. & Clas, S. D. (2002). Evaluation of disintegration testing of different fast dissolving tablets using the texture analyzer. *Pharmaceutical Develeopment and Technology,* 7**,** 361-71.

EMA (2006). Reflection Paper: Formulations of choice for the Paediatric Population. *In:* (CHMP), C. F. M. P. F. H. U. (ed.) *Pre-authorisation Evaluation of Medicines for Human Use.* London: European Medicines Agency.

EU. (2006). *The European Parliament and the Council of the European Union. Regulation EC No. 1901/2006 Medicinal Products for Paediatric Use.* [Online]. EU. [Accessed January 9th 2017].

FDA. (Year) Published. US Food and Drug Administration Amendments Act of 2007. Proceedings of the 110th Congress of the United States of America, January 4th 2007 2007 Washington, DC.

FDA. (2008). *Guidance for Industry Orally Disintegrating Tablets* [Online]. New Hampshire, MD: United States Food and Drug Administration. Available: http://www.fda.gov/downloads/Drugs/GuidanceComplianceRegulatoryInformation/Guidances/ucm070578.pdf [Accessed 15/10/2014 2014].

Flament, M.-P., Leterme, P. & Gayot, A. (2004). The influence of carrier roughness on adhesion, content uniformity and the in vitro deposition of terbutaline sulphate from dry powder inhalers. *International Journal of Pharmaceutics,* 275**,** 201-209.

FMC-Biolpolymer. (2016). *Avicel® for Solid Dose Forms* [Online]. Philadelphia, USA: FMC Biopolymer. [Accessed 09th September 2016 2016].

Fu, Y., Jeong, S. H., Callihan, J., Kim, J. & Park, K. (2006). Preparation of Fast-Dissolving Tablets Based on Mannose. *Polymeric Drug Delivery II.* American Chemical Society.

Fu, Y., Yang, S., Jeong, S. H., Kimura, S. & Park, K. (2004). Orally fast disintegrating tablets: developments, technologies, taste-masking and clinical studies. *Critical Reveiws in Therapeutic Drug Carrier Systems,* 21**,** 433-76.

Fukami, J., Yonemochi, E., Yoshihashi, Y. & Terada, K. (2006). Evaluation of rapidly disintegrating tablets containing glycine and carboxymethylcellulose. *International Journal of Pharmaceutics,* 310**,** 101-109.

Gharaibeh, S. F. & Aburub, A. (2013). Use of First Derivative of Displacement vs. Force Profiles to Determine Deformation Behaviour of Compressed Powders. *AAPS PharmSciTech,* 14**,** 398-401.

Gohel, M. (2009). Manufacturing Methods of Tablets. *In:* GOHEL, M. (ed.) *Tablet: The Ruling Dosafe form since Years.* Ahmedabad: Pharmainfo.

Goswami, K., Khurana, G., Marwaha, R. K. & Gupta, M. (2014). Development and Evaluation of Extended Release Ethylcellulose based Matrix Tablet of Diclofenac Sodium. *International Journal of Pharmacy and Pharmaceutical Science,* 6**,** 296-301.

Gryczke, A., Schminke, S., Maniruzzaman, M., Beck, J. & Douroumis, D. (2011). Development and evaluation of orally disintegrating tablets (ODTs) containing Ibuprofen granules prepared by hot melt extrusion. *Colloids and Surfaces B: Biointerfaces,* 86**,** 275-284.

Gucluyildiz, H., Banker, G. S. & Peck, G. E. (1977). Determination of Porosity and Pore-Size Distribution of Aspirin Tablets Relevant to Drug Stability. *Journal of Pharmaceutical Sciences,* 66**,** 407-414.

Gupta, P., Nachaegari, S. K. & Bansal, A. K. (2006). Improved Excipient Functionality by Coprocessing. *Excipient Development for Pharmaceutical, Biotechnology, and Drug Delivery Systems.*

Han, X., Ghoroi, C. & Davé, R. (2013). Dry coating of micronized API powders for improved dissolution of directly compacted tablets with high drug loading. *International Journal of Pharmaceutics,* 442**,** 74-85.

Harada, T., Narazaki, R., Nagira, S., Ohwaki, T., Aoki, S. & Iwamoto, K. (2006). Evaluation of the disintegration properties of commercial famotidine 20 mg orally disintegrating tablets using a simple new test and human sensory test. *Chemical and Pharmaceutical Bulletin (Tokyo),* 54**,** 1072-5.

Harada, T., Narazaki, R., T.Ohwaki & Uhida, T. (2010a). Effect of Physical Properties of Orally Disintegrating Tablets on Disintegration Time as Determined by New Apparatus. *Journal of Drug Delivery Science and Technology,* 20**,** 377-383.

Harada, T., Uchida, T., Yoshida, M., Kobayashi, Y., Narazaki, R. & Ohwaki, T. (2010b). A new method for evaluating the bitterness of medicines in development using a taste sensor and a disintegration testing apparatus. *Chemical and Pharm Buletinl (Tokyo),* 58**,** 1009-14.

Haraguchi, T., Yoshida, M. & Uchida, T. (2014). Evaluation of ebastine-loaded orally disintegrating tablets using new apparatus of detecting disintegration time and e-tongue system. *Journal of Drug Delivery Science and Technology,* 24**,** 684-688.

Harmon, T. M. (2007). Orally disintegrating tablets a valuable life cycle management strategy. *Pharmaceutical Commerce.*

He, X., Han, X., Ladyzhynsky, N. & Deanne, R. (2013). Assessing powder segregation potential by near infrared (NIR) spectroscopy and correlating segregation tendency to tabletting performance. *Powder Technology,* 236**,** 85-99.

Heckel, R. W. (1961a). Density-Pressure Relationships in Powder Compaction. *Transactions of the Mettallurgical Society of AIME,* 221**,** 1961-1967.

Hermes, M. F. K. (2012). *Kindgerechte, niedrigdosierte Zubereitungen mit Enalaprilmaleat.* Doctoral Degree of Mathematics and Natural Sciences, Heinrich-Heine University.

Hersey, J. A., Cole, E. T. & Rees, J. E. (1973). *Proceedings of the first International Conference on the Compaction and Consolidation of Particulate Matter,* Brighton, Powder Advisory Centre London.

Hirani, J. J., Rathod, D. A. & Vadalia, K. R. (2009). Orally Disintegrating Tablets: A Review. *Tropical Journal of Pharmaceutical Research,* 8**,** 161-172.

Ho, R., Hinder, S. J., Watts, J. F., Dilworth, S. E., Williams, D. R. & Heng, J. Y. Y. (2010). Determination of surface heterogeneity of d-mannitol by sessile drop contact angle and finite concentration inverse gas chromatography. *International Journal of Pharmaceutics,* 387**,** 79-86.

Ho, R., Naderi, M., Heng, J. Y., Williams, D. R., Thielmann, F., Bouza, P., Keith, A. R., Thiele, G. & Burnett, D. J. (2012). Effect of milling on particle shape and surface energy heterogeneity of needle-shaped crystals. *Pharmaceutical Research,* 29**,** 2806-16.

Ho, R., Wilson, D. A. & Heng, J. Y. Y. (2009). Crystal Habits and the Variation in Surface Energy Heterogeneity. *Crystal Growth & Design,* 9**,** 4907-4911.

Hoag, S. W., Dave, V. S. & Moolchandani, V. (2008). Compression and Compaction. *In:* AUGSBURGER, L. L., HOAG, S. W. & HOAG, S. W. (eds.) *Pharmaceutical Dosage Forms: Tablets.* London: Informa.

Honda, H., Kimura, M., Honda, F., Matsuno, T. & Koishi, M. (1994). Preparation of monolayer particle coated powder by the dry impact blending process utilizing mechanochemical treatment. *Colloids and Surfaces A: Physicochemical and Engineering Aspects,* 82**,** 117-128.

Hong, Y., Liu, G. & Gu, Z. (2016). Recent advances of starch-based excipients used in extended-release tablets: a review. *Drug Delivery,* 23**,** 12-20.

Hulse, W. L., Forbes, R. T., Bonner, M. C. & Getrost, M. (2009). The characterization and comparison of spray-dried mannitol samples. *Drug Development and Industrial Pharmacy,* 35**,** 712-8.

Hüttenrauch, R. (1971). Identification of hydrogen bonds by means of deuterium exchange demonstration of binding forces in compressed cellulose forms. *Pharmazie,* 26**,** 645-646.

Hwang, R.-C. & Peck, G. R. (2001). A systematic evaluation of the compression and tablet characteristics of various types of microcrystalline cellulose. *Pharmaceutical Technology,* 25**,** 112-132.

ICH (2003). Guidance for Industry: Stability Testing of New Drug Substances and Products. *Q1A(R2).* Rockville, MD: U.S. Department of Health and Human Services, Food and Drug Administration.

Ingram, J. T. & Lowenthal, W. (1968). Mechanism of action of starch as a tablet disintegrant. 3. Factors affecting starch grain damage and their effect on swelling of starch grains and disintegration of tablets at 37 degrees. *Journal of Pharmaceutical Sciences,* 57**,** 393-8.

Irfan, M., Rabel, S., Bukhtar, Q., Qadir, M. I., Jabeen, F. & Khan, A. (2016). Orally disintegrating films: A modern expansion in drug delivery system. *Saudi Pharmaceutical Journal,* 24**,** 537-546.

Ishizaka, T., Honda, H., Ikawa, K., Kizu, N., Yano, K. & Koishi, M. (1988). Complexation of aspirin with potato starch and improvement of dissolution rate by dry mixing. *Chemical and Pharmaceutical Bulletin (Tokyo),* 36**,** 2562-9.

Ishizaka, T., Honda, H., Kikuchi, Y., Ono, K., Katano, T. & Koishi, M. (1989). Preparation of drug-diluent hybrid powders by dry processing. *Journal of Pharmacy and Pharmacology,* 41**,** 361-8.

Ivanovska, V., Rademaker, C. M. A., Dijk, L. v. & Mantel-Teeuwisse, A. K. (2014). Pediatric Drug Formulations: A Review of Challenges and Progress. *Pediatrics,* 134**,** 361-372.

Jannin, V., Berard, V., N'Diaye, A., Andres, C. & Pourcelot, Y. (2003). Comparative study of the lubricant performance of Compritol 888 ATO either used by blending or by hot melt coating. *Internatipnal Journal of Pharmaceutics,* 262**,** 39-45.

Jensen, J. L., Karatsaidis, A. & Brodin, P. (1998). Salivary secretion, stimulatory effects of chewing-gum versus paraffin tablets. *European Journal of Oral Sciences,* 106**,** 892-896.

Jivraj, M., Martini, L. G. & Thomson, C. M. (2000). An overview of the different excipients useful for the direct compression of tablets. *Pharmaceutical Science & Technology Today,* 3**,** 58-63.

Joiris, E., Martino, P. D., Berneron, C., Guyot-Hermann, A.-M. & Guyot, J.-C. (1998). Compression Behavior of Orthorhombic Paracetamol. *Pharmaceutical Research,* 15**,** 1122-1130.

Jones, R. J., Rajabi-Siahboomi, A., Levina, M., Perrie, Y. & Mohammed, A. R. (2011). The influence of formulation and manufacturing process parameters on the characteristics of lyophilized orally disintegrating tablets. *Pharmaceutics,* 3**,** 440-57.

Jung, S. Y., Kim, D. W., Seo, Y. G., Woo, J. S., Yong, C. S. & Choi, H. G. (2012). Development of sildenafil-loaded orally disintegrating tablet with new lactate salt. *Drug Development and Industrial Pharmacy,* 38**,** 635-41.

Kachrimanis, K., Nikolakakis, I. & Malamataris, S. (2003). Tensile strength and disintegration of tableted silicified microcrystalline cellulose: Influences of interparticle bonding. *Journal of Pharmaceutical Sciences,* 92**,** 1489-1501.

Kakutani, R., Muro, H. & Makino, T. (2010). Development of a new disintegration method for orally disintegrating tablets. *Chemical and Pharmaceutical Bulletin (Tokyo),* 58**,** 885-90.

Kale, K., Hapgood, K. & Stewart, P. (2009). Drug agglomeration and dissolution – What is the influence of powder mixing? *European Journal of Pharmaceutics and Biopharmaceutics,* 72**,** 156-164.

Kaminsky, W. & Glazer, A. M. (1997). Crystal Optics of D-mannitol, C6H14O6: Crystal Growth, Structure, Basic Physical Properties, Birefringence, Optical Activity, Faraday Effect, Electro-optic Effects and Model Calculations}. *Zeitschrift fur Kristallographie,* 212**,** 283-296.

Katsuno, E., Tahara, K., Takeuchi, Y. & Takeuchi, H. (2013). Orally disintegrating tablets prepared by a co-processed mixture of micronized crospovidone and mannitol using a ball mill to improve compactibility and tablet stability. *Powder Technology,* 241**,** 60-66.

Kellie, S. J. & Howard, S. C. (2008). Global child health priorities: what role for paediatric oncologists? *European Journal of Cancer,* 44**,** 2388-96.

Kerr, A. C. (1961). *The Physiological Regulation of Salivary Secretions in Man,* New York, Pergamon Press.

Khomane, K. S. & Bansal, A. K. (2013). Effect of Particle Size on In-die and Out-of-die Compaction Behavior of Ranitidine Hydrochloride Polymorphs. *AAPS PharmSciTech,* 14**,** 1169-1177.

Kim, A. I., Akers, M. J. & Nail, S. L. (1998). The physical state of mannitol after freeze-drying: Effects of mannitol concentration, freezing rate, and a noncrystallizing cosolute. *Journal of Pharmaceutical Sciences,* 87**,** 931-935.

Klevan, I., Nordström, J., Tho, I. & Alderborn, G. (2010). A statistical approach to evaluate the potential use of compression parameters for classification of pharmaceutical powder materials. *European Journal of Pharmaceutics and Biopharmaceutics,* 75**,** 425-435.

Kojima, T. & Elliott, J. A. (2013). Effect of silica nanoparticles on the bulk flow properties of fine cohesive powders. *Chemical Engineering Science,* 101**,** 315-328.

Kondo, K., Niwa, T. & Danjo, K. (2012). Evaluation of disintegration properties of orally rapidly disintegrating tablets using a novel disintegration tester. *Chemical and Pharmaceutical Bulletin (Tokyo),* 60**,** 1240-8.

Koner, J. S., Rajabi-Siahboomi, A., Bowen, J., Perrie, Y., Kirby, D. & Mohammed, A. R. (2015). A Holistic Multi Evidence Approach to Study the Fragmentation Behaviour of Crystalline Mannitol. *Scientific Reports,* 5**,** 16352.

Kuno, Y., Kojima, M., Ando, S. & Nakagami, H. (2008). Effect of preparation method on properties of orally disintegrating tablets made by phase transition. *International Journal of Pharmaceutics,* 355**,** 87-92.

Le, V. N., Hoang Thi, T. H., Robins, E. & Flament, M. P. (2012). Dry powder inhalers: study of the parameters influencing adhesion and dispersion of fluticasone propionate. *AAPS PharmSciTech,* 13**,** 477-84.

Lee, Y.-Y., Wu, J. X., Yang, M., Young, P. M., van den Berg, F. & Rantanen, J. (2011). Particle size dependence of polymorphism in spray-dried mannitol. *European Journal of Pharmaceutical Sciences,* 44**,** 41-48.

Lerk, C. F., Andreae, A. C., De Boer, A. H., Bolhuis, G. K., Zuurman, K., de Hoog, P., Kussendrager, K. & van Leverink, J. (1983). Increased binding capacity and flowability of α-lactose monohydrate after dehydration. *Journal of Pharmacy and Pharmacology,* 35**,** 747-748.

Levina, M. & Rajabi-Siahboomi, A. R. (2004). The influence of excipients on drug release from hydroxypropyl methylcellulose matrices. *Journal of Pharmaceutical Sciences,* 93**,** 2746-54.

Li, J. & Wu, Y. (2014). Lubricants in Pharmaceutical Solid Dosage Forms. *Lubricants,* 2**,** 21-43.

Limwong, V., Sutanthavibul, N. & Kulvanich, P. (2004). Spherical composite particles of rice starch and microcrystalline cellulose: A new coprocessed excipient for direct compression. *AAPS PharmSciTech,* 5**,** 40-49.

Littringer, E. M., Mescher, A., Eckhard, S., Schröttner, H., Langes, C., Fries, M., Griesser, U., Walzel, P. & Urbanetz, N. A. (2011). Spray Drying of Mannitol as a Drug Carrier—The Impact of Process Parameters on Product Properties. *Drying Technology,* 30**,** 114-124.

Liu, L. X., Marziano, I., Bentham, A. C., Litster, J. D., E.T.White & Howes, T. (2008). Effect of particle properties on the flowability of ibuprofen powders. *International Journal of Pharmaceutics,* 362**,** 109-117.

Lopez, F. L., Ernest, T. B., Tuleu, C. & Gul, M. O. (2015). Formulation approaches to pediatric oral drug delivery: benefits and limitations of current platforms. *Expert Opinion on Drug Delivery,* 12**,** 1727-1740.

Lowe, T. L., Tenhu, H. & Tylli, H. (1999). Effect of hydrophobicity of a drug on its release from hydrogels with different topological structures. *Journal of Applied Polymer Science,* 73**,** 1031-1039.

Lutterotti, L. (2010). Total pattern fitting for the combined size–strain–stress–texture determination in thin film diffraction. *Nuclear Instruments and Methods in Physics Research Section B: Beam Interactions with Materials and Atoms,* 268**,** 334-340.

Luukkonen, P., Schæfer, T., Hellén, L., Juppo, A. M. & Yliruusi, J. (1999). Rheological characterization of microcrystalline cellulose and silicified microcrystalline cellulose wet masses using a mixer torque rheometer. *International Journal of Pharmaceutics,* 188**,** 181-192.

Mathias, P., Rocha, V., Saraiva, L., Cavalcanti, A. N., Azevedo, J. F. & Paulillo, L. A. (2010). Intraoral environment conditions and their influence on marginal leakage in composite resin restorations. *Acta Odontol Latinoam,* 23**,** 105-10.

Mattsson, S. (2000). *Pharmaceutical Binders and Their Function in Directly Compressed Tablets.* Doctor of Pharmacy, Uppsala University.

Maurice, D. R. & Courtney, T. H. (1990). The physics of mechanical alloying: A first report. *Metallurgical Transactions A,* 21**,** 289-303.

McCormick, D. (2005). Evolutions in Direct Compression. *Pharmaceutical Technology,* April**,** 52-62.

McLaughlin, R., Banbury, S. & Crowley, K. (2009). Orally Disintegrating Tablets: The Effect of Recent FDA Guidance on ODT Technologies and Applications. *Pharmaceutical Technology,* 2009**,** 1-7.

Mennella, J. A., Spector, A. C., Reed, D. R. & Coldwell, S. E. (2013). The Bad Taste of Medicines: Overview of Basic Research on Bitter Taste. *Clinical Therapeutics,* 35**,** 1225-1246.

Mishra, D. N., Bindal, M., Singh, S. K., Gurusamy, S. & Kumar, V. (2006). Spray Dried Excipient Base: A Novel Technique for the Formulation of Orally Disintegrating Tablets. *Chemical & Pharmaceutical Buletin,* 54**,** 99-102.

Mohamed, M. B., Talhari, M. K., Tripathy, M. & Majeed, A. B. A. (2012). Pharmaceutical Applications of Crospovidone: A review. *Internation Journal of Drug Formulation and Research,* 3**,** 13-28.

Monov, V., Sokolov, B. & Stoenchev, S. (2012). Grinding in Ball Mills: Modeling and Process Control. *Cybernetics and Information Technologies,* 12**,** 51-68.

Moore, R., Watts, J., Hood, J. & Burritt, D. (1999). Intra-oral temperature variation over 24 hours. *The European Journal of Orthodontics,* 21**,** 249-261.

More, P. K., Khomane, K. S. & Bansal, A. K. (2013). Flow and compaction behaviour of ultrafine coated ibuprofen. *International Journal of Pharmaceutics,* 441**,** 527-534.

Morita, Y., Tsushima, Y., Yasui, M., Termoz, R., Ajioka, J. & Takayama, K. (2002). Evaluation of the disintegration time of rapidly disintegrating tablets via a novel method utilizing a CCD camera. *Chemical and Pharmaceutical Bulletin (Tokyo),* 50**,** 1181-6.

Mullarney, M. P. & Leyva, N. (2009). Modeling Pharmaceutical Powder-Flow Performance Using Particle-Size Distribution Data. *Pharmaceutical Technology,* 33**,** 126-135.

Mužíková, J., Muchová, S., Komersová, A. & Lochař, V. (2015). Compressibility of tableting materials and properties of tablets with glyceryl behenate. *Acta Pharmacologica Sinica,* 65**,** 91-98.

Nada, A., Mueller, B. W. & Al-Saidan, S. M. (2005). Improving the Physical and Chemical Properties of Ibuprofen. *Pharmaceutical Technology,* 29**,** 90-101.

Narazaki, R., Harada, T., Takami, N., Kato, Y. & Ohwaki, T. (2004). A new method for disintegration studies of rapid disintegrating tablet. *Chemical and Pharmaceutical Bulletin (Tokyo),* 52**,** 704-7.

Navarro, V. (2010). Improving medication compliance in patients with depression: Use of orodispersible tablets. *Advances in Thereapy,* 27**,** 785-95.

Nokhodchi, A., Homayouni, A., Araya, R., Kaialy, W., Obeidatf, W. & Asare-Addog, K. (2015). Crystal engineering of ibuprofen using starch derivatives in crystallization medium to produce promising ibuprofen with improved pharmaceutical performance. *RSC Advances,* 5**,** 46119-46131.

Nunn, T. & Williams, J. (2005). Formulation of medicines for children. *British Journal of Clinical Pharmacology,* 59**,** 674-676.

Ohta, K. M., Fuji, M., Takei, T. & Chikazawa, M. (2003). Effect of geometric structure and surface wettability of glidant on tablet hardness. *International Journal of Pharmaceutics,* 262**,** 75-82.

Ohta, M., Hayakawa, E., Ito, K., Tokuno, S., Morimoto, K. & Watanabe, Y. (2001). *A tablet comprising; sugar alcohol or saccaride selected from mannitol and lactose, each having an average particle diameter of not more than 30 mu m, an active ingredient, and crosscarmellose sodium, crosspovidone etc. as disintegrant*. US 09/147,374.

Pabari, R. M. & Ramtoola, Z. (2012). Effect of a Disintegration Mechanism on Wetting, Water Absorption, and Disintegration Time of Orodispersible Tablets. *Journal of Young Pharmacists : JYP,* 4**,** 157-163.

Park, J. H., Holman, K. M., Bish, G. A., Krieger, D. G., Ramlose, D. S., Herman, C. J. & Wu, S. H. (2008). An Alternative to the USP Disintegration Test for Orally Disintegrating Tablets. *Pharmaceutical Technology,* 32**,** 54-58.

Parkash, V., Maan, S., Deepika, Yadav, S. K., Hemlata & Jogpal, V. (2011). Fast disintegrating tablets: Opportunity in drug delivery system. *Journal of Advanced Pharmaceutical Technology & Research,* 2**,** 223-35.

Paronen, P. & Ilka, J. (1996). Porosity - Pressure Functions. *In:* ALDERBORN, G. & NYSTRÖM, C. (eds.) *Pharmaceutical Powder Compaction Technology.* New York: Marcel Dekker.

Patel, S. & Bansal, A. K. (2011). Prediction of mechanical properties of compacted binary mixtures containing high-dose poorly compressible drug. *International Journal of Pharmaceutics,* 403**,** 109-114.

Ph.Eur (2013). *European Pharmacopoeia Version 8*.

Rao, J. B., Catherin, G. J., Murthy, I. N., Rao, D. V. & Raju, B. N. (2011). Production of nano structured silicon carbide by high energy ball milling. *International Journal of Engineering, Science and Technology,* 3**,** 82-88.

Rasenack, N. & Müller, B. W. (2002). Crystal habit and tableting behavior. *International Journal of Pharmaceutics,* 244**,** 45-57.

Rinaki, E., Dokoumetzidis, A., Valsami, G. & Macheras, P. (2004). Identification of Biowaivers Among Class II Drugs: Theoretical Justification and Practical Examples. *Pharmaceutical Research,* 21**,** 1567-1572.

Roberts, R. J. & Rowe, R. C. (1985). The effect of punch velocity on the compaction of a variety of materials. *Journal of Pharmacy and Pharmacology,* 37**,** 377-384.

Roberts, R. J. & Rowe, R. C. (1986). The effect of the relationship between punch velocity and particle size on the compaction behaviour of materials with varying deformation mechanisms. *Journal of Pharmacy and Pharmacology,* 38**,** 567-71.

Rowe, R. C., Sheskey, P. J. & Quinn, M. E. (2012). *Handbook of Pharaceutical Excipients,* London, Pharmaceutical Press.

S Velmurugan & Vinushitha, S. (2010). Oral Disintegrating Tablets: An Overview. *International Journal of Chemical and Pharmaceutical Sciences,* 1**,** 1-12.

Sandler, N., Reiche, K., Heinamaki, J. & Yliruusi, J. (2010). Effect of Moisture on Powder Flow Properties of Theopylline. *Pharmaceutics,* 2**,** 275-290.

Santl, M., Ilic, I., Vrecer, F. & Baumgartner, S. (2012). A compressibility and compactibility study of real tableting mixtures: the effect of granule particle size. *Acta Pharmaceutica,* 62**,** 325-40.

Saraiva, L. O., Aguiar, T. R., Costa, L., Cavalcanti, A. N., Giannini, M. & Mathias, P. (2015). Influence of Intraoral Temperature and Relative Humidity on the Dentin Bond Strength: An in Situ Study. *Journal of Esthetic and Restorative Dentistry,* 27**,** 92-99.

Sastry, S. V., Nyshadham, J. R. & Fix, J. A. (2000). Recent technological advances in oral drug delivery – a review. *Pharmaceutical Science & Technology Today,* 3**,** 138-145.

Scardi, P. & Leoni, M. (2001). Diffraction line profiles from polydisperse crystalline systems. *Acta Crystallographica Section A,* 57**,** 604-13.

Seager, H. (1998). Drug-delivery products and the Zydis fast-dissolving dosage form. *Journal of Pharmacy and Pharmacology,* 50**,** 375-82.

Segado, J., S. (2003). *Orally disintegrating tablets and process for obtaining them*. Spain patent application WO 2003103629 A1.

Shabir, A., Alhusban, F., Perrie, Y. & Mohammed, A. R. (2011). Effects of ball-milling on PLGA polymer and its implication on lansoprazole-loaded nanoparticles. *Journal of Basic and Clinical Pharmacy,* 2**,** 71-82.

Shanmugam, S. (2015). Granulation techniques and technologies: recent progresses. *BioImpacts : BI,* 5**,** 55-63.

Sherwood, B. E. & Becker, J. (1998). A new class of high functionality excipients: silicified microcrystalline cellulose. *Pharmaceutical Technology,* 22**,** 183-194.

Sherwood, B. E., Hunter, E. A. & Staniforth, J. H. (1996). *Pharmaceutical excipient having improved compressability*. USA patent application US 08/370,576.

Shu, T., Suzuki, H. & Ito, K. (2002). Studies of Rapidly Disintegrating Tablets in the Oral Cavity Using Co-ground Mixtures of Mannitol with Crospovidone. *Chemical & Pharmaceutical Buletin,* 50**,** 193-198.

Singh, M. N., Hemant, K. S. Y., Ram, M. & Shivakumar, H. G. (2010). Microencapsulation: A promising technique for controlled drug delivery. *Research in Pharmaceutical Sciences,* 5**,** 65-77.

Sosnik, A. & Seremeta, K. P. (2015). Advantages and challenges of the spray-drying technology for the production of pure drug particles and drug-loaded polymeric carriers. *Advances in Colloid and Interface Science,* 223**,** 40-54.

SPI-Pharma (2012). Mannogem Mannitol: The Perfect Formulation Tool. *In:* PHARMA, S. (ed.) *Mannogem Mannitols.* Wilmington, Delaware: SPI Pharma.

Spomer, N., Klingmann, V., Stoltenberg, I., Lerch, C., Meissner, T. & Breitkreutz, J. (2012). Acceptance of uncoated mini-tablets in young children: results from a prospective exploratory cross-over study. *Archive of Disease in Childhood,* 97**,** 283-6.

Srikar, G., Gouthamib, K. S., Manasac, B. & Sirishad, A. S. (2013). Formulation optimization and characterization of amlodipine oral disintegrating tablets prepared by co-grinding technique. *Der Pharmacia Lettre,* 5**,** 335-343.

Staniforth, J. N. & Aulton, M. E. (2007). Powder Flow. *In:* AULTON, M. E. (ed.) *Pharmaceutics: The Design and Manufacture of Medicines.* Philadelphia, USA: Churchill Livingstone.

Summers, M. P. & Aulton, M. E. (2007). Granulation. *In:* AULTON, M. E. (ed.) *Pharmaceutics: The Design and Manufacture of Medicines.* Philadelphia, USA: Elsevier Health Sciences

Sun, C. C. (2010). Setting the bar for powder flow properties in successful high speed tableting. *Powder Technology,* 201**,** 106-108.

Szakonyi, G. & Zelkó, R. (2013). Prediction of oral disintegration time of fast disintegrating tablets using texture analyzer and computational optimization. *International Journal of Pharmaceutics,* 448**,** 346-353.

Tan, K.-H., Johan, M. R., Ahmad, R., Kadri, N. A., Zain, N. M. & Arof, A. K. (2012). Mechanical Analysis of the Effects of Different Mechanical Alloying Periods on Ni3Al Intermetallic Compound Fabrication Quality *Internation Journal of Electrochemical Science,* 7**,** 3765-3772.

Tang, Y.-D., Venkatraman, S. S., Boey, F. Y. C. & Wang, L.-W. (2007). Sustained release of hydrophobic and hydrophilic drugs from a floating dosage form. *International Journal of Pharmaceutics,* 336**,** 159-165.

Thoorens, G., Krier, F., Leclercq, B., Carlin, B. & Evrard, B. (2014). Microcrystalline cellulose, a direct compression binder in a quality by design environment—A review. *International Journal of Pharmaceutics,* 473**,** 64-72.

Tobyn, M. J., McCarthy, G. P., Staniforth, J. N. & Edge, S. (1998). Physicochemical comparison between microcrystalline cellulose and silicified microcrystalline cellulose. *International Journal of Pharmaceutics,* 169**,** 183-194.

Tong, B., Liu, R.-B., Meng, C.-G., Yu, F.-Y., Ji, S.-H. & Tan, Z.-C. (2010). Heat Capacities and Nonisothermal Thermal Decomposition Reaction Kinetics of d-Mannitol. *Journal of Chemical & Engineering Data,* 55**,** 119-124.

Turner, M. A., Catapano, M., Hirschfeld, S. & Giaquinto, C. (2014). Paediatric drug development: The impact of evolving regulations. *Advanced Drug Delivery Reviews,* 73**,** 2-13.

Uchida, T., Yoshida, M., Hazekawa, M., Haraguchi, T., Furuno, H., Teraoka, M. & Ikezaki, H. (2013). Evaluation of palatability of 10 commercial amlodipine orally disintegrating tablets by gustatory sensation testing, OD-mate as a new disintegration apparatus and the artificial taste sensor. *Journal of Pharmacy and Pharmacology,* 65**,** 1312-20.

USP37. (2014a). *<616> Bulk and Tapped Density* [Online]. Rockville, MD: The United States Pharmacopeia Convention. Available: http://www.usp.org/sites/default/files/usp_pdf/EN/USPNF/revisions/m99375-bulk_density_and_tapped_density_of_powders.pdf [Accessed 23/09/2015 2015].

USP37. (2014b). *<701> Disintegration* [Online]. Rockville, MD: The United States Pharmacopeia Convention Available: http://www.usp.org/sites/default/files/usp_pdf/EN/USPNF/generalChapter701.pdf [Accessed 23/09/2015 2015].

USP37. (2014c). *<1174> Powder Flow* [Online]. Rockville, MD: The United States Pharmacopeia Convention. Available: http://www.pharmacopeia.cn/v29240/usp29nf24s0_c1174.html [Accessed 23/09/2015 2015].

USP37. (2014d). *<1216> Friability* [Online]. Rockville, MD: The United States Pharmacopeia Convention. Available: http://www.pharmacopeia.cn/v29240/usp29nf24s0_c1216.html [Accessed 25/09/20115 2015].

van der Voort Maarschalk, K., Zuurman, K., Vromans, H., Bolhuis, G. K. & Lerk, C. F. (1996). Porosity expansion of tablets as a result of bonding and deformation of particulate solids. *International Journal of Pharmaceutics,* 140**,** 185-193.

van Riet-Nales, D. A., de Neef, B. J., Schobben, A. F. A. M., Ferreira, J. A., Egberts, T. C. G. & Rademaker, C. M. A. (2013). Acceptability of different oral formulations in infants and preschool children. *Archives of Disease in Childhood,* 98**,** 725-731.

van Veen, B., Bolhuis, G. K., Wu, Y. S., Zuurman, K. & Frijlink, H. W. (2005). Compaction mechanism and tablet strength of unlubricated and lubricated (silicified) microcrystalline cellulose. *European Journal of Pharmaceutics and Biopharmaceutics,* 59**,** 133-138.

Vega, J. A., Ochoa, P. S. & Holder, P. (2014). Introduction to Parenteral Preparations. *In:* OCHOA, P. S. (ed.) *Concepts in Sterile Preparations and Aseptic Technique.* Burlington, MA: Jones & Bartlett Learning.

Vehring, R. (2008). Pharmaceutical Particle Engineering via Spray Drying. *Pharmaceutical Research,* 25**,** 999-1022.

Vromans, H., Bolhuis, G. K., Lerk, C. F., van de Biggelaar, H. & Bosch, H. (1987). Studies on tableting properties of lactose. VII. The effect of variations in primary particle size and percentage of amorphous lactose in spray dried lactose products. *International Journal of Pharmaceutics,* 35**,** 29-37.

Vromans, H., De Boer, A. H., Bolhuis, G. K., Lerk, C. F., Kussendrager, K. D. & Bosch, H. (1985). Studies on tableting properties of lactose. Part 2. Consolidation and compaction of different types of crystalline lactose. *Pharmaceutisch Weekblad Scientific Edition,* 7**,** 186-93.

Westerberg, M. & Nyström, C. (1993). Physicochemical aspects of drug release XVII. The effect of drug surface area coverage to carrier materials on drug dissolution from ordered mixtures. *International Journal of Pharmaceutics,* 90**,** 1-17.

Westermarck, S., Juppo, A. M., Kervinen, L. & Yliruusi, J. (1998). Pore structure and surface area of mannitol powder, granules and tablets determined with mercury porosimetry and nitrogen adsorption. *European Journal of Pharmaceutics and Biopharmaceutics,* 46**,** 61-68.

Willart, J. F., Caron, V. & Descamps, M. (2007). Transformations of crystalline sugars upon milling. *Journal of Thermal Analysis and Calorimetry,* 90**,** 125-130.

Wisniewski, R. (Year) Published. Spray Drying Tecnology Review. 45th International Conference on Environmental Systems 2015 Bellevue, Washington. 1-46.

Yadav, G., Kapoor, A. & Bhargava, S. (2012). Fast Dissolving Tablets Recent Advantages: A Review. *International Journal of Pharmaceutical Sciences and Research,* 3**,** 728-736.

Yang, J., Sliva, A., Banerjee, A., Dave, R. N. & Pfeffer, R. (2005). Dry particle coating for improving the flowability of cohesive powders. *Powder Technology,* 158**,** 21-33.

Yokoyama, T., Urayama, K., Naito, M., Kato, M. & Yokoyama, T. (1987). The angmill mechanofusion system and its applications. *KONA Powder and Particle Journal,* 5**,** 59-68.

Yoshinari, T., Forbes, R. T., York, P. & Kawashima, Y. (2002). Moisture induced polymorphic transition of mannitol and its morphological transformation. *International Journal of Pharmaceutics,* 247**,** 69-77.

Yoshita, T., Uchida, S. & Namiki, N. (2013). Clinical disintegration time of orally disintegrating tablets clinically available in Japan in healthy volunteers. *Biological and Pharmaceutical Bulletin,* 36**,** 1488-93.

Yu, L., Mishra, D. S. & Rigsbee, D. R. (1998). Determination of the Glass Properties of D-Mannitol using Sorbitol as an Impurity. *Journal of Pharmaceutical Sciences,* 87**,** 774-777.

Zámostný, P., Petrů, J. & Majerová, D. (2012). Effect of Maize Starch Excipient Properties on Drug Release Rate. *Procedia Engineering,* 42**,** 482-488.

Zhang, Y., Law, Y. & Chakrabarti, S. (2003). Physical Properties and Compact Analysis of Commonly Used Direct Compression Binders. *AAPS PharmSciTech,* 4**,** 1-11.

Zhou, Q., Armstrong, B., Larson, I., Stewart, P. J. & Morton, D. A. V. (2010). Improving powder flow properties of a cohesive lactose monohydrate powder by intensive mechanical dry coating. *Journal of Pharmaceutical Sciences,* 99**,** 969-981.

Zimmermann, I., Eber, M. & Meyer, K. (2004). Nanomaterials as Flow Regulators in Dry Powders. *Zeitschrift für Physikalische Chemie,* 218**,** 51-102.

Zuurman, K., Van der Voort Maarschalk, K. & Bolhuis, G. K. (1999). Effect of magnesium stearate on bonding and porosity expansion of tablets produced from materials with different consolidation properties. *International Journal of Pharmaceutics,* 179**,** 107-115.